Characterization of Lung Adenocarcinoma in Transgenic Mice Overexpressing Calreticulin under Control of the *Tie-2* Promoter

by

Behzad Yeganeh

A Thesis submitted to the Faculty of Graduate Studies of

The University of Manitoba

in partial fulfilment of the requirements of the degree of

DOCTOR OF PHILOSOPHY

Department of Biochemistry and Medical Genetics

Faculty of Medicine

University of Manitoba

Winnipeg

Abstract

Calreticulin (CRT) is a multifunctional Ca^{2+} dependent chaperone protein, which is localized to the endoplasmic reticulum and plays many important biological roles. In addition to its critical role in cardiovascular development, CRT has been reported to be important for cell migration, adhesion and apoptosis. Several studies have also postulated different roles for exogenous CRT in angiogenesis and tumor growth. However no direct evidence for the role of endogenous CRT in these processes is available. To study the *in vivo* role of CRT in angiogenesis and vascular development, our lab generated a transgenic mouse overexpressing CRT under the control of the *Tie2* promoter (referred to as *Tie2-CRT*), which is active in both endothelial cells and hematopoietic stem cells (HSCs).

The most striking phenotype of these mice is an increased incidence of lung tumors. These tumors have been characterized according to their histochemical properties as being adenocarcinoma with a Surfactant Protein-C positive ($SP\text{-}C^{Pos}$) and Clara Cell Protein negative ($CC10^{Neg}$) phenotype suggesting an alveolar origin for these tumors. We observed that during the early stages of tumor formation, the lungs show signs of increased inflammation as evident by congestion, reddish discoloration and the accumulation of inflammatory cells. Using histological analyses, we showed that the lung tumors of *Tie2-CRT* mice are comprised of a heterogeneous population of tumor cells with different immunophenotypic characteristics including $SP\text{-}C^{Pos}$ cells and a novel cell type which is positive for expression of HSC markers (CD34, c-kit and Sca-1) and exogenous CRT, but negative for expression of SP-C and CC10. Based

on these observations we hypothesized that overexpression of CRT in endothelial cells and HSCs results in an inflammatory response that facilitates the recruitment of HSCs to the lungs. Eventually, this high rate of inflammation in the lungs leads to malignant transformation of the recruited HSCs and tumor formation.

We have identified that the early stage tumors contain cells that express exogenous CRT and HSC markers including CD133, Sca-1, and c-Kit. As the tumor progresses to a fully developed adenocarcinoma, these cells lose the expression of exogenous CRT and HSCs markers and gain an alveolar type II phenotype (SP-C^{Pos}). *In vitro* evaluation of tumor cell phenotype following isolation and characterization of lung tumor cells from *Tie2-CRT* mice demonstrated a differentiation dependent expression of HSC markers by tumor cells supporting our hypothesis that HSCs might be the cells of origin for the lung tumors observed in *Tie2-CRT* mice. We also demonstrated that HSC mobilization is increased in *Tie2-CRT* mice as compared to *wt* controls and that HSCs of *Tie2-CRT* mice are more proliferative and potentially tumorigenic as they are able to form colonies under anchorage independent growth conditions.

We also studied the A549 human lung adenocarcinoma cell line and demonstrated that undifferentiated masses of these cells express CRT and HSC markers and expression of these markers was down regulated upon differentiation. Furthermore, immunohistochemistry with anti-CRT antibody on a human lung adenocarcinoma tissue microarray showed a significantly lower levels of CRT expression in the tumor region as compared to the adjacent normal lung tissue suggesting a possible role for CRT expression in lung tumor development.

The results from this study provide evidence that lung tumors from the *Tie2-CRT* mice are non-epithelial in origin and that undifferentiated populations of tumor cells have HSC characteristics. After differentiation, these cells lose their HSC phenotype and acquire a more epithelial phenotype. This study is the first to examine the potential link between CRT and lung cancer development.

Acknowledgments

I am deeply grateful to my supervisor Dr. Nasrin Mesaeli for her patience and encouragement that carried me on through difficult times and for her insights and suggestions that helped to shape my research skills. Without her, this dissertation would not have been possible.

I also thank my thesis committee members: Dr. Jeffrey Wigle, Dr. Leigh Murphy and Dr. Yvonne Myal. Their valuable feedback helped me to improve the dissertation in many ways. I would also like to thank my external examiner Dr. Michal Opas for the critical review of my thesis.

I am deeply grateful to a number of other people for their assistance and support for the fulfillment of this thesis. Thanks to all of the Mesaeli and Wigle lab members past and present especially; Shahrzad Jalali, Anton Uvarov, Maliheh Aghasi, Josette Douville, David Cheung, Ezgi Ogutcen and Mehdi Eshraghi. I am deeply grateful to all of them for their support and friendship that enabled me to complete my study. An especial thank to Shannon Baxter for reading the last draft of the manuscript. My sincere gratitude goes to those people who have written, published and distributed the books, journals and thesis, I have referenced from.

I would also like to acknowledge Melanie Durston and Michael Wiwchar for establishing the *Tie2-CRT* mouse colonies and initial histopathologic analysis of these mice. I also would like to thank the Genetic Model Centre of the University of Manitoba for generation of *Tie2-CRT* mice. A special thanks to all the staff of animal unit at St. Boniface Research Centre for taking care of the animals and helping me during my Ph.D work.

I am also thankful to Canadian Institutes of Health Research, Manitoba Health Research Council, Institute of Cardiovascular Sciences and Manitoba Medical College Foundation for funding my project with studentship awards.

I would also like to thank to the members of the support staff of the Department of Biochemistry and Medical Genetics: Tuntun Sarkar, Jan Middleton and Gerhard Dyck. I am thankful to Mr. Monro Chan for flow cytometry analyzing, Dr. George Skliris and Mrs. Anne Blanchard for helping me in tissue microarray analysis.

Most of all my love, sincerest admiration, concern and apologies go to my son "Omid" and my wife "Azadeh" who is also my best friend. I thank her for supporting me through all these years. Lastly and most importantly, I would like to thank my Mom and Dad for their continuing support and love. Their encouragement and sacrifice allowed me to get an education and achieve anything I have achieved in my life. I dedicate this thesis to my wife, son and parents.

TABLE OF CONTENTS

Page

LIST OF TABLES

LIST OF FIGURES

LIST OF ABBREVIATIONS

2-DE	Two-Dimensional Gel Electreopheresis
AAH	Atypical Adenomatose Hyperplasia
AFP	α-Fetoprotein
Ang	Angiopoietin receptor
BASC	Bronchoalveolar stem cell
BM	Bone Marrow
BMDC	Bone marrow-derived cell
BrdU	5-bromodeoxyuridine
CASPASE	Cysteine-Dependent Aspartyl-Specific Protease
CC10	Clara Cell 10 kDa Protein
CCSP	Clara Cell Secretory Protein
CML	Chronic Myelogenous Leukemia
CO2	Carbon Dioxide
COPD	Chronic Obstructive Pulmonary Disease
CRT	Calreticulin
CXCL12	Chemokine (CXC motif) Ligand 12
ddH_2O	Double Distilled Buffer
DMEM	Dulbecco's Modified Eagle Medium
ECL	Enhanced Chemiluminescence
ECM	Extra Cellular Matrix
EDTA	Ethylene Diamine Tetraacetic Acid
EGF	Epidermal Growth Factor
EGFP	Enhanced Green Fluorescent Protein
EGTA	Ethylene Glycol Tetraacetic acid
ELISA	Enzyme-Linked Immunosorbent Assay
EMT	Epithelial-Mesenchymal Transition
ER/SR	Endoplasmic/Sarcoplasmic Reticulum
ESC	Embryonic Stem Cell
FBS	Fetal Bovine Serum

FGF	Fibroblast Growth Factor
FISH	Fluorescence In Situ Hybridization
FITC	Fluorescein Isothiocyanate
GFP	Green Fluorescent Protein
H&E	Hematoxylin and Eosin
HGF	Hepatocyte Growth Factor
HRP	Horseradish Peroxidase
HSC	Hematopoietic Stem Cells
IF	Immunofluorescence
IHC	Immunohistochemistry
IL	Interleukin
IM	Idiopathic myelofibrosis
LCC	Large Cell Carcinoma
LCNEC	Large Cell Neuroendocrine Carcinoma
LDL	Low-Density Lipoprotein
LRP	LDL receptor-related protein
MAPK	Mitogen-Activated Protein Kinase
MBL	Mannose Binding Lectin
Mdm-2	Murine Double Minute
MEF	Mouse Embryonic Fibroblasts
MMPs	Matrix Metalloproteinase
MPO	Myeloperoxidase
mRNA	Messenger Ribonucleic Acid
NaCl	Sodium Chloride
Naf	Sodium Floride
NFAT	Nuclear Factor Activated T-Cells
NFκB	Nuclear factor Kappa-light-chain-enhancer of activated B cell
NMBCU	N-nitrosomethyl-bis-chloroethylurea
NSCLC	Non-Small-Cell Lung Cancer
NTCU	N-nitroso-trischloroethylurea
ORO	Oil Red O

Pen/Strep	Penicillin/streptomycin
PBS	Phosphate Buffered Saline
PCR	Polymerase Chain Reaction
PI3K	Phosphoinositide 3-kinase
PMSF	Phenylmethylsulphonyl fluoride
PTEN	Phosphatase and Tension homologe
Rb	Retinoblastoma
ROS	Reactive Oxygen Species
RT-PCR	Reverse Transcriptase-PCR
SCC	Squamous Cell Carcinoma
SCLC	Small-Cell Lung Cancer
SDF-1	Stromal cell-Derived Factor-1
SDS	Sodium Dodecyl Sulfate
SIRP	Signal Regulatory Protein
SP-C	Surfactant Protein-C
TGF	Transforming Growth Factor
TMA	Tissue Microarray
TSP1	Thrombospondin-1
UV	Ultraviolet
VEGF	Vascular Endothelial Growth Factor
vWF	Von Willebrand factor
WB	Western Blotting
wt	Wild-type

Measurements

°C	Degree Celsius
bP	Base pare
cm	Centimeter
g	Gram
kDa	Kilodalton
kb	Kilo base pare
ml	Millimeter

mM	Millimolar
mm	Millimeter
nm	Nanometer
ppm	part per million
rpm	Revolutions per minute
sec	Seconds
v/v	Volume/volume
w/v	Weight/volume

CHAPTER I: INTRODUCTION

1.1. Calreticulin

Calreticulin (CRT) is a ubiquitous eukaryotic protein localized in the lumen of the endoplasmic/sarcoplasmic reticulum (ER/SR) (Milner *et al.* 1991). It is composed of 400 amino acids with a predicted molecular weight of 46 kDa. The protein has three putative domains classified based on their biological functions and amino acid sequence: **1)** a globular and hydrophobic amino terminal region known as the N-domain, **2)** a proline-rich domain in the middle of the protein which is referred to as the P-domain and **3)** an acidic carboxyl end of protein called the C-domain (Figure 1).

The N-domain of CRT spans residues 1-180 and forms a globular structure composed of eight antiparallel β-strands which are crucial for CRT's chaperone function (Michalak *et al.* 2002; Gelebart *et al.* 2005). The N-domain contains both the polypeptide and carbohydrate-binding sites (Kapoor *et al.* 2004; Leach *et al.* 2004), as well as a high affinity Zinc (Zn^{2+}) binding site (Baksh *et al.* 1995). Two cysteine residues in the N-domain have been shown to form a disulfide bridge (Andrin *et al.* 2000). This domain also contains several histidine residues, one of which (His^{153}) is essential for the chaperone function of CRT (Guo *et al.* 2003).

The P-domain extends from residues 181-290 (Baksh *et al.* 1991) and shares a high degree of homology with calnexin, another ER lectin-like chaperone (Schrag *et al.* 2001). Nuclear Magnetic Resonance (NMR) spectroscopy studies have revealed that the P-domain of CRT contains an extended arm-structure which is stabilized by three antiparallel β-sheets (Ellgaard *et al.* 2001). *In vitro* analyses indicate that the P-

domain also contains a high affinity (K_d=1μM), low capacity Ca^{2+} binding site (1 mol of Ca^{2+} per mol of protein for P-domains) (Baksh *et al.* 1991).

The third functional domain of CRT, known as the C-domain, covers amino acids 291-400 and contains a large number of negatively charged amino acids that are responsible for the calcium (Ca^{2+}) buffering capacity of the protein (Nakamura *et al.* 2001). The C-domain of CRT binds over 50% of ER luminal Ca^{2+} with high capacity (25 mol of Ca^{2+} per mol of CRT protein) and low affinity (K_d=2mM) (Nakamura *et al.* 2001). Since the C-domain of calnexin is shown to play an important role in the regulation of protein-protein interactions via phosphorylation, (Delom *et al.* 2006) a similar function for the C-domain of CRT is suspected. The C-terminal of CRT ends with the conserved KDEL (Lys-Asp-Glu-Leu) sequence, a known ER retention motif (Pelham 1988) which is responsible for targeting and recycling CRT to the ER lumen.

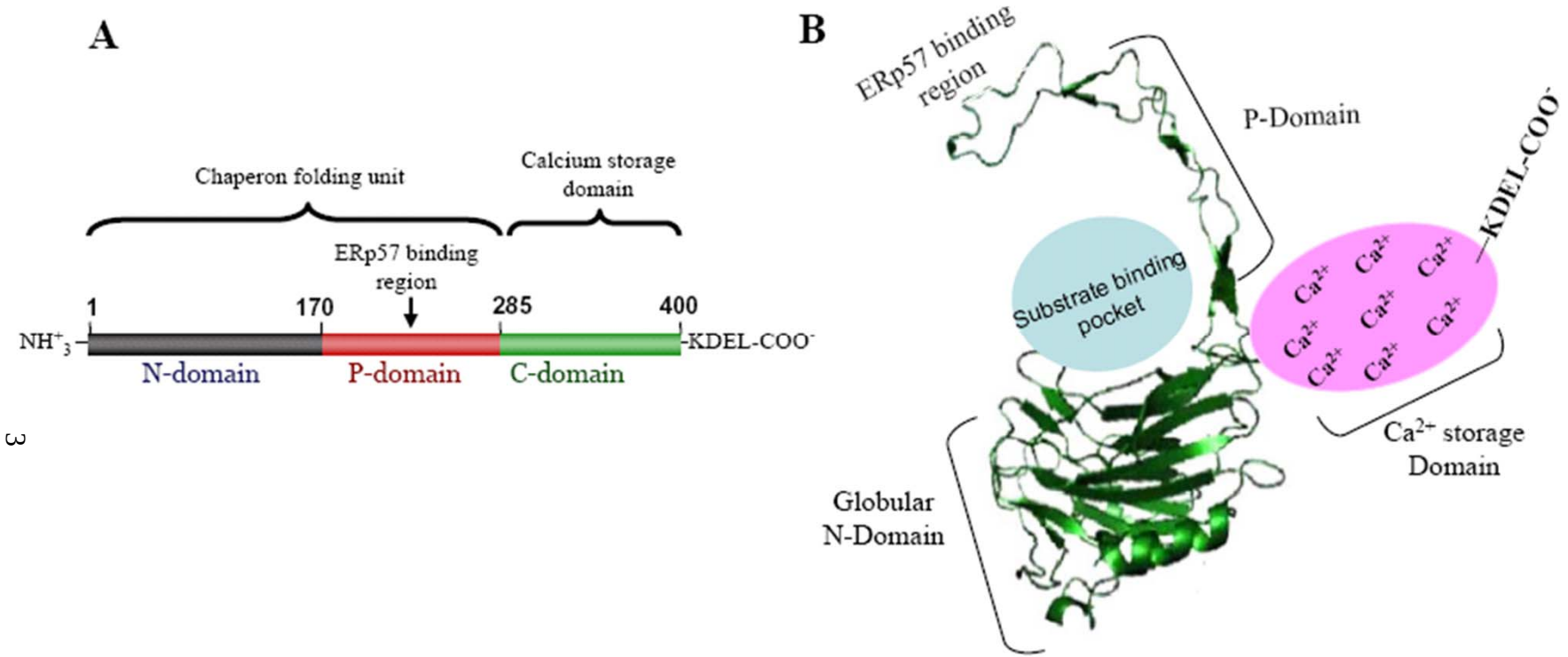

Figure 1. Schematic linear and three-dimensional structure of calreticulin (CRT). (A) Linear representation of CRT protein. This protein is composed of 400 amino acids with three putative domains, classified according to their biological functions and amino acid sequence as an N-domain or the amino-terminal (black box), P-domain (red box), C-domain (green box) which terminates with the ER retention sequence, KDEL. (B) A model of the three-dimensional structure of CRT. Based on NMR studies, it is predicted that the N-domain of CRT is globular and contains a carbohydrate binding pocket and a disulfide bridge. The P-domain is a proline-rich P-domain which is predicted to form an extended arm structure. The globular N-domain together with the extended arm P-domain of CRT are responsible for the chaperone function of the protein. The C-terminal region of CRT contains a large number of negatively charged amino acids and is involved in Ca^{2+} storage (with high capacity) in the lumen of the ER. The ERp57-binding site is also shown in this picture.

1.2. Biological functions of CRT

1.2.1. Chaperone function of CRT

In the ER lumen, molecular chaperones facilitate the proper folding of newly synthesized proteins including glycosylated, secreted or integral membrane proteins that enter the ER after synthesis (Saito *et al.* 1999). If protein folding fails, the aberrant products are degraded via the proteasomal degradation pathway. CRT and calnexin are two major ER chaperone proteins involved in correct protein folding and quality control of newly synthesized glycosylated and non-glycosylated proteins (Saito *et al.* 1999; Schrag *et al.* 2001). Other ER chaperones including grp94, ERp72, and Bip are also involved in the correct folding of non-glycosylated proteins (Nicchitta 1998; Gething 1999).

The extended arm together with the N-domain of CRT generate a pocket in which glycoproteins can enter for proper folding (Ellgaard *et al.* 2001; Martin *et al.* 2006). CRT and calnexin bind monoglycosylated carbohydrates attached to newly synthesized glycoproteins which ensure their proper folding. Carbohydrate moieties of newly synthesized glycoproteins consists of two N-acetylglucosamines, nine mannose residues and three terminal glucose residues in which the terminal glucose residue can be removed by the activity of glucosidase II and replaced by the activity of UDP-glucose: glycoprotein transferase (UGGT) in the lumen of the ER (Michalak *et al.* 1999; Michalak *et al.* 2002). Monoglycosylation serves as a signal to indicate unfolded substrates, resulting in association of the protein with CRT and/or calnexin (Michalak *et al.* 2002). This deglycosylation-glycosylation cycle may be repeated several times until the newly synthesized glycoprotein is properly folded. Once the terminal glucose

is removed, the protein dissociates from CRT/calnexin chaperones. CRT together with calnexin play a crucial role in the correct protein folding, assembly and maturation of many proteins including the human insulin receptor (Bass *et al.* 1998) and MHC class I proteins (Harris *et al.* 1998). CRT has also been shown to function as a chaperone and play an important role in the correct folding of myeloperoxidase (MPO) (Nauseef *et al.* 1995) and the bradykinin receptor (Nakamura *et al.* 2001).

The interaction of substrates with CRT recruits ERp57 (a PDI-like thiol oxidoreductase) for that rearranges the disulfide bonds in the newly synthesized proteins (Van der Wal *et al.* 1998; Oliver *et al.* 1999). The interaction of the P-domain of CRT with ERp57 has also been reported recently (Frickel *et al.* 2002; Trombetta 2003). The P-domain of CRT harbors two tryptophan residues (Trp^{302} and Trp^{244}) which are essential for the chaperone function of CRT (Martin *et al.* 2006). It has been shown that mutations of Glu^{239}, Asp^{241}, Glu^{243} and Trp^{244} in the tip of the P-domain disrupt the chaperone function of the P-domain as well as the interaction of CRT with ERp57 (Martin *et al.* 2006).

1.2.2. CRT and calcium homeostasis

CRT was initially discovered as a Ca^{2+} binding protein by Ostwald and MacLennan in 1974 (Ostwald *et al.* 1974) and was shown to have two Ca^{2+} binding sites: a high affinity, low capacity site and a low capacity, high affinity site (Ostwald *et al.* 1974; Milner *et al.* 1991). CRT-deficient cells as well as CRT overexpresing cells have been used to study the role of this protein in regulating Ca^{2+} homeostasis. Overexpression of CRT in HeLa and L fibroblast cells was shown to increase the concentration of intracellular Ca^{2+} without affecting cytosolic free calcium ($[Ca^{2+}]_c$)

concentration (Bastianutto *et al.* 1995; Mery *et al.* 1996). However, in rat cardiomyoblast cells, overexpression of CRT elevated the free cytosolic calcium concentration ($[Ca^{2+}]_c$) (Kageyama *et al.* 2002).

Coppolino and colleagues (Coppolino *et al.* 1997) showed that deletion of CRT did not alter the Ca^{2+} storage capacity of the ER in embryonic stem (ES) cells, but resulting defective integrin mediated Ca^{2+} signaling. This suggests an essential role for CRT in the modulation of both integrin adhesive functions and integrin-initiated signaling in ES cells. CRT-deficient mouse embryonic fibroblast cells, on the other hand, show reduced ER Ca^{2+} storage capacity with no change in the free ER luminal Ca^{2+} ($[Ca^{2+}]_{ER}$) (Nakamura *et al.* 2001).

Ca^{2+} concentration in the ER lumen regulates proper protein folding (Lodish *et al.* 1990; Corbett *et al.* 2000). Ca^{2+} signaling also governs many signaling pathways in the cells involved in cell survival, apoptosis, proliferation and differentiation (Berridge 2002; Orrenius *et al.* 2003; Lipskaia *et al.* 2004). For instance, activation of the GATA family of transcription factors, a key element in cardiac muscle differentiation, is regulated through a calcineurin/Nuclear Factor of Activated T-cells (NFAT) dependent manner (Morkin 2000). Calcineurin activity is also regulated through the binding of its regulatory subunits to calmodulin (a Ca^{2+} binding protein) and Ca^{2+}, respectively (Hemenway *et al.* 1999). It has been shown that a sustained increase of cytosolic Ca^{2+} level leads to activation of calcineurin (Cahalan *et al.* 1990) and subsequently, dephosphorylation and nuclear translocation of NFAT (Timmerman *et al.* 1996; Beals *et al.* 1997). NFAT, in cooperation with other transcription factors, enhances the transcription of a variety of genes, including the genes essential for cardiac development and hypertrophy (Crabtree 2001) and apoptosis (Chai *et al.* 2008).

Inhibition of NFAT translocation to the nucleus in CRT-deficient cells (Mesaeli *et al.* 1999) suggests that CRT modulates the calcineurin/NFAT pathway which leads to defects in heart development as seen in CRT knockout mice (Mesaeli *et al.* 1999).

Ca^{2+} is also involved in signaling pathways associated with apoptosis and cancer cell growth (Orrenius *et al.* 2003; Mamaeva *et al.* 2009). Mamaeva and colleagues (Mamaeva *et al.* 2009) have shown regulation of the Notch-1 signaling pathway in prostate cancer cells through Ca^{2+}/calmodulin-dependent kinase II, a kinase associated with osteoblastogenesis of human mesenchymal stem cells (Shin *et al.* 2008). High levels of NFAT expression in non-small cell lung cancer has recently been reported (Zhang *et al.* 2007). Using corticosterone-treated mouse Leydig tumor cells, Chai and colleagues (Chai *et al.* 2008) illustrated that NFAT directly stimulates the transcription of Fas Ligand, an important mediator of apoptosis.

1.2.3. Role of CRT in cell adhesion and migration

CRT has been shown to affect cell adhesion by the regulation of the adhesion-specific cytoskeletal proteins vinculin and N-cadherin (Opas *et al.* 1996; Fadel *et al.* 2001) as well as through modulating tyrosine phosphorylation of various focal adhesion proteins (Fadel *et al.* 1999; Fadel *et al.* 2001). The CRT N-domain was shown to interact with a highly conserved amino acid sequence (KXGFFKR) found in the cytoplasmic domain of α-integrins *in vitro* (Rojiani *et al.* 1991). Impaired integrin-mediated attachment and spreading of Jurkat cells upon downregulation of CRT using antisense oligonucleotides has also been reported (Leung-Hagesteijn *et al.* 1994). More recently, Szabo and colleagues (Szabo *et al.* 2009) investigated the adhesive properties of CRT-deficient Embryonic Stem Cells (ESCs). They showed that CRT-

deficient ESCs are highly adipogenic, poorly adhesive, and have increased calmodulin/CaMKII signaling as compared to wild-type ESCs. These authors concluded that adipogenesis of ESCs is directly controlled by the adhesive status of the cells which is modulated by CRT (Szabo *et al.* 2009). Additionally, loss of CRT function in the ESCs was shown to result in a disorganized cytoskeleton and a decreased level of focal adhesion-related proteins, such as vinculin, paxillin, and phosphorylated focal adhesion kinase resulting in limited focal adhesion formation and limited fibronectin deposition (Szabo *et al.* 2009).

Overexpression of CRT has been shown to decrease cell motility of L fibroblasts by increasing vinculin mRNA and protein expression, while downregulation of CRT has the opposite effects (Opas *et al.* 1996). Furthermore, overexpression of CRT in fibroblast cells resulted in increased expression of N-cadherin, that mediates Ca^{2+}-dependent adhesion (Fadel *et al.* 2001). These cells also exhibit diminished phosphorylation of β-catenin, a member of the *Wnt* signaling pathway involved in linking adherens-type junctional components to the actin cytoskeleton (Fadel *et al.* 2001). More recently, Hayashida *et al*. have reported a higher expression of N-cadherin and fibronectin in conjunction with decreased expression of E-cadherin in epithelial kidney cells overexpressing CRT (Hayashida *et al.* 2006). In contrast to fibroblasts, increased CRT expression in Madin-Darby canine kidney cells enhanced cell migration *in vitro* (Hayashida *et al.* 2006). In esophageal squamous cell carcinoma, knockdown of CRT was shown to impair cell migration, invasion and resistance to anoikis (cell death that is induced by loss of cell adhesion or inappropriate cell adhesion and cell-matrix interactions) (Du *et al.* 2009). Altogether,

these findings show that changes in CRT expression alters cell adhesion and migration although effects are cell type dependent.

The effect of CRT on cell proliferation of gastric cancer cell lines has been recently examined (Chen *et al.* 2007). Using the MTT assay (a colorimetric assay system which measures the reduction of a tetrazolium salt into an insoluble formazan product by the mitochondria of viable cells), a higher rate of proliferation was observed in CRT overexpressing cells whereas CRT-deficient cells displayed decreased proliferation. Moreover, CRT overexpressing cells had enhanced wound healing properties, a process that involves both cell proliferation and migration (Chen *et al.* 2007). Topical application of CRT in mammalian wound healing assays has previously been shown to increase cell migration to the injury site (Gold *et al.* 2006). These studies collectively show the effect of both endogenous and exogenous CRT in cell migration.

Overexpression of CRT was shown to increase fibronectin expression, cell spreading and up-regulation of the cytoskeletal proteins in focal adhesion contacts leading to an increase in cell adhesion (Opas *et al.* 1996; Humphries *et al.* 2007; Papp *et al.* 2007; Papp *et al.* 2008). Cardiac specific overexpression of CRT in mice has been shown to reduce connexin 40 and 43 expression and result in complete heart block and sudden death in these animals (Nakamura *et al.* 2001). This indicates that in addition to cell adhesion, CRT influences intracellular communication through gap junction proteins. Cell adhesion is believed to be regulated by CRT localized in the ER, (Opas *et al.* 1996) however, other important functions including migration and phagocytosis have also been demonstrated to be modulated by extracellular or cell

surface localized CRT (Goicoechea *et al.* 2000; Goicoechea *et al.* 2002; Orr *et al.* 2003; Orr *et al.* 2003; Gardai *et al.* 2005).

Although CRT generally resides in the ER and the nuclear envelope, it has also been detected at the cell surface (Johnson *et al.* 2001). Cell surface CRT has been detected in many types of mammalian cells, including platelets, fibroblasts, apoptotic cells and endothelial cells (Goicoechea *et al.* 2000; Elton *et al.* 2002; Orr *et al.* 2003) and has been suggested to play a role in cell adhesion, cell-cell communication, and apoptosis. CRT has been identified as a cell surface receptor for both thrombospondin-1 (TSP-1) and C1q, a component of the complement complex protein (Goicoechea *et al.* 2002; McGreal *et al.* 2002; Ghiran *et al.* 2003). TSP-1 is a multifunctional glycoprotein that has been shown to play key roles in interactions between human cells and components of the extracellular matrix (Chung *et al.* 1997). TSP-1 stimulates focal adhesion disassembly through a sequence known as the hep I peptide located in its heparin-binding domain (Greenwood *et al.* 1998; Goicoechea *et al.* 2000). A number of studies demonstrated that cell surface CRT interacts with the heparin-binding domain I of TSP-1 and Low-Density Lipoprotein (LDL) receptor-related protein (LRP) to mediate focal adhesion disassembly required for migration (Goicoechea *et al.* 2000; Pallero *et al.* 2008). The binding site in CRT that interacts with the heparin binding domain I has been localized to amino-acid residues 19–36 in the N-terminus of CRT (Goicoechea *et al.* 2002). Cell surface CRT also binds to the carbohydrate constituent of cell adhesion and basement membrane proteins such as laminin through integrin binding (White *et al.* 1995; McDonnell *et al.* 1996).

1.2.4. Role of CRT in apoptosis

Programmed cell death I or apoptosis (Krysko *et al.* 2008) is part of the normal physiological properties of a cell, and plays a major role in tissue homeostasis (Marsden *et al.* 2002). As such, cells that do not receive appropriate survival signals from the microenvironment undergo apoptosis. The apoptotic pathway, particularly the intrinsic pathway, is mediated by the mitochondria and the ER, thus any change in the ER luminal milieu can alter the susceptibility of cells to apoptotic signals (Srinivasan *et al.* 2005; Mao *et al.* 2007). CRT, as an ER resident chaperone, could affect several signaling pathways involved in cell survival and apoptosis. Expression of CRT has been proposed to modulate apoptosis through different signaling pathways. A study using the rat cardiomyoblast H9c2 cells revealed that overexpression of CRT increases differentiation-associated apoptosis of cardiac cells via suppression of Akt activity which is a downstream effector of the PI3K signaling pathway (Kageyama *et al.* 2002; Jalali *et al.* 2008).

Changes in protein phosphatase 2A (PP2Acα) expression and suppression of Akt activity were also reported upon overexpression of CRT in malignant glioma cells (Okunaga *et al.* 2006). CRT overexpression in H9c2 cardiomyoblast cells and glioma cells was shown to augment the cellular responses to apoptotic signals such as oxidative stress and ultraviolet (UV) radiation, which could be due to changes in Ca^{2+} homeostasis caused by CRT overexpression (Ihara *et al.* 2006). Furthermore, overexpression of CRT in HeLa cells was shown to increase their sensitivity to staurosporine-induced apoptosis (Nakamura *et al.* 2000). Conversely, loss of CRT function in Mouse Embryonic Fibroblasts (MEF cells) increases their resistance to drug and UV-induced apoptosis (Nakamura *et al.* 2000; Mesaeli *et al.* 2004). The

increased resistance to UV-induced apoptosis could be explained by decreased levels of p53 expression and function (Mesaeli *et al.* 2004). Diminished p53 in CRT-deficient cells is the result of increased degradation of p53 (Uvarov *et al.* 2008), which is mediated by activation and nuclear translocation of murine double minute (Mdm-2) (Mesaeli *et al.* 2004). Translocation of Mdm-2 to the nucleus was shown to ubiquitinate p53 cause it to be exported out of the nucleus where it is degraded by the ubiquitin-proteasome pathway (Haupt *et al.* 1997; Jabbur *et al.* 2002).

1.2.5. Role of CRT in the clearance of apoptotic cells

One of the features of apoptosis that differs from necrosis is the lack of an inflammatory response (Waterhouse *et al.* 2007). Apoptosis is generally associated with rapid condensation of the cytoplasm and nuclear chromatin, followed by DNA fragmentation and blebbing of the plasma membrane (Kerr *et al.* 1972). The resulting apoptotic bodies, which contain nuclear and cytoplasm material, are readily engulfed by neighboring cells or phagocytic cells recruited to the site of apoptosis (Lauber *et al.* 2003).

One hypothesis for the removal of apoptotic cells is that apoptotic cells release chemotactic factors that recruit phagocytic cells to sites of apoptosis (Lauber *et al.* 2003). This group identified lysophosphatidylcholine, which is produced via caspase-3-mediated activation of Ca^{2+}-independent phospholipase A2, as the chemotactic signal secreted by apoptotic cells (Lauber *et al.* 2003). Another hypothesis proposes that it is the initiation of electrical signals due to changes in the membrane composition of apoptotic cells that attract phagocytes (Zhao *et al.* 2006). Weihua and colleagues (Weihua *et al.* 2005) showed that a disruption in membrane composition of

apoptotic cells generates a negative surface charge, which has been shown to induce movement of endothelial cells toward the dying cells by a mechanism that involves endothelial cell membrane hyperpolarization and cytoskeleton reorganization.

Whether the clearance of apoptotic cells is directed via chemokines or electrical signals, there is mounting evidence that efficient removal of apoptotic cells is crucial both in suppressing inflammatory responses at sites of apoptosis and in maintaining an adaptive immune tolerance (Taylor *et al.* 2000). Indeed, the defective clearance of apoptotic cells has been shown to cause autoimmune and inflammatory diseases (Taylor *et al.* 2000). This indicates that effective discrimination between viable cells and dead or dying cells is crucial for the specific and efficient removal of apoptotic cells. Removal of apoptotic cells is a multiple-step process consisting of: the accumulation of phagocytes at the site of apoptosis, the recognition of dying cells through a number of receptors, engulfment by a unique uptake process, and processing of engulfed cells within phagocytes (Ogden *et al.* 2001; Gardai *et al.* 2005; Obeid *et al.* 2007; Waterhouse *et al.* 2007). Ogden *et al*. (Ogden *et al.* 2001) shed new light on the process of recognition and phagocytic uptake of the apoptotic cell by showing that C1q and mannose binding lectin bind to apoptotic cells and stimulate the ingestion of apoptotic cells by binding to CRT on the surface of phagocytic cells. The translocation of CRT to the cell surface may be due to the ability of CRT to escape the KDEL receptor-mediated salvage pathway (Afshar *et al.* 2005).

The chemotherapeutic agent anthracycline was demonstrated to induce translocation of CRT to the surfaces of mouse colon carcinoma (CT26 cell line) (Obeid *et al.* 2007). This translocation triggers a cascade of events which eventually lead to the activation of the immunogenic response and the removal of tumor cells by

dentritic cells. This observation suggests that CRT exposure at the cell surface of the apoptotic cells provides a signal that promotes phagocytosis of these cells (Gardai *et al.* 2005; Obeid *et al.* 2007). The level of CRT expression at the cell surface has been shown to correlate with the percentage of phagocytosis by dendritic cells (Obeid *et al.* 2007). More recently, Panaretakis and colleagues (Panaretakis *et al.* 2009) investigated pathways that mediate pre-apoptotic CRT exposure in immunogenic cell death in response to several immunogenic anticancer agents. They illustrated that following early activation of a complex of cascades including the ER kinase (PERK), caspase-8, BAP31, Bax and Bak, CRT transited the Golgi apparatus and was then secreted through a SNARE-dependent exocytosis (Panaretakis *et al.* 2009).

Viable cells normally express CD47 (Integrin-associated protein/IAP) protein on the cell surface which binds to Signal Regulatory Protein-alpha (SIRP-α) on macrophages (Gardai *et al.* 2005; Takizawa *et al.* 2007). Interaction of CD47 macrophage SIRP-α prevents clearance and phagocytosis of IgG opsonized viable cells (Gardai *et al.* 2005; Takizawa *et al.* 2007). Cell surface CD31 is another molecule presented on viable cells that has been shown to prevent the engulfment of healthy cells by circulating phagocytes (Brown *et al.* 2002). The precise mechanism of action of these molecules that discriminate against removal of viable cells is not yet fully defined. However, it has been shown that CRT clustering at the cell surface is largely coordinated with a decrease in the expression of CD47, a phenomenon that usually occurs in the early stage of apoptosis and functions as a signal to discriminate between viable cells and apoptotic cells (Gardai *et al.* 2005; Kuraishi *et al.* 2007). Using an antibody against the extracellular, but not the intracellular domain of LDL receptor-related protein (LRP), Gardai *et al*. (Gardai *et al.* 2005) showed that recognition of the

apoptotic cell requires exposure of CRT on the surface of apoptotic cells. Surface CRT will then stimulate phagocytosis upon binding with LRP/CD91 on phagocytes (Gardai *et al.* 2005). Clearance of apoptotic cells opsonized by C1q, or the collectins MBL, surfactant Protein A and D (SP-A, and SP-D), is through a similar mechanism involving CRT and LRP (Vandivier *et al.* 2002; Gardai *et al.* 2005). This is not surprising since CRT is a sticky protein interacting with the soluble proteins TSP-1 and C1q which are two important elements that may serve as bridges to facilitate the recognition of CRT by phagocytes (Ogden *et al.* 2001).

Adiponectin, a protein hormone that modulates a number of metabolic processes, is structurally similar to C1q and surfactant proteins (Takemura *et al.* 2007). Based on the structural similarity between adiponectin and these molecules, Takemura *et al*. recently elucidated that adiponectin also mediates the *in vivo* clearance of apoptotic cells (Takemura *et al.* 2007). This study revealed that CRT and CD91 are essential for adiponectin-stimulated uptake of apoptotic cells. CRT knockdown using siRNA blocks adiponectin-dependent phagocytosis of apoptotic Jurkat T cells (Takemura *et al.* 2007) suggesting that the interaction of adiponectin with CRT on both the macrophage and the apoptotic cell surface is critical for the clearance of apoptotic cells.

1.2.6. Role of CRT in angiogenesis

Growth of solid tumors and their ability to metastasize are generally dependent on the existence of a sufficient blood supply vessels. This requires the development of new blood vessels through a process known as angiogenesis (Folkman 1982; Hanahan *et al.* 1996). Angiogenesis is also essential for organ growth and repair. The

observation that increased angiogenesis occurs around tumors was first documented over 100 years ago (Goldman 1907). Alteration in CRT expression has been shown to regulate angiogenesis through different pathways (Pike *et al.* 1998; Liu *et al.* 2008). For example, Liu *et al*. (Liu *et al.* 2008) investigated the role of CRT in FGF-2 (Fibroblast Growth Factor-2)-induced angiogenesis in the ischemic myocardium and showed that down regulation of CRT is linked with FGF-2-induced angiogenesis through the calcineurin pathway. Furthermore, overexpression of CRT was shown to block FGF-2-induced microvascular endothelial cell proliferation (Liu *et al.* 2008).

Changes in CRT expression may also alter matrix metalloproteinase (MMPs) activities (Wu *et al.* 2007). MMPs are a family of zinc-containing endopeptidases that degrade numerous components of the extra cellular matrix (ECM) and have been strongly implicated in multiple stages of cancer progression including cancer cell growth, differentiation, migration, invasion, and the regulation of tumor angiogenesis (Vu *et al.* 1998; Sounni *et al.* 2002). MMPs contribute to tumor angiogenesis not only by degrading the basement membrane, which facilitates endothelial cell detachment and migration into new tissue, but also by releasing pro-angiogenic factors such as vascular endothelial growth factor (VEGF) from the ECM (Hawinkels *et al.* 2008). Furthermore, metastasis, a multi-step process that begins with the detachment of tumor cells from the original solid tumor and invasion through and into the basement membrane, requires the activity of different MMPs (Egeblad *et al.* 2002). As an ER resident chaperone, any alteration in CRT production may alter MMP activity. A recent study from our laboratory demonstrated a significant reduction in MMP-9 activity in CRT-deficient fibroblast cells which was accompanied by an increase in MMP-2 activity and an overall decrease in gelatinolytic properties (Wu *et al.* 2007).

The N-terminal fragment of CRT, also known as vasostatin, has been reported to inhibit angiogenesis and prevent endothelial cell proliferation both *in vivo* and *in vitro* (Pike *et al.* 1998). Furthermore, exogenously added full length CRT also inhibits angiogenesis and prevents endothelial cell proliferation (Lin *et al.* 1997; Pike *et al.* 1999). Yao *et al*. (Yao *et al.* 2002) demonstrated that binding of vasostatin to the ECM protein laminin inhibits endothelial cell attachment to ECM thus affecting their subsequent growth (Yao *et al.* 2002). The small size and solubility of vasostatin makes it a potential angiogenesis inhibitor (Pike *et al.* 1998). Inhibition of angiogenesis has been a key target in controlling tumor growth (D'Andrea *et al.* 2005; Goldberg *et al.* 2005). Targeting angiogenesis for example, through the VEGF pathway is a clinical strategy currently in use to treat a variety of types of cancer (D'Andrea *et al.* 2005; Goldberg *et al.* 2005).

The anti-angiogenic role of vasostatin (or CRT) was further examined using an *in vivo* assay to measure tumor growth. Xiao *et al.* showed that administration of a cDNA encoding vasostatin into the muscle of mice with lung tumors prevents angiogenesis and tumor progression (Xiao *et al.* 2002). These investigators showed that intramuscularly injected vasostatin cDNA can produce vasostatin which is released into the circulation (Xiao *et al.* 2002). Based on their data, Xiao *et al.* suggested that this method could be used to interfere with the progression of several types of cancer. More recently, adenoviral-mediated gene transfer of vasostatin was also reported to suppress tumor progression in pancreatic cancer (Li *et al.* 2006). However, other studies showed increased malignant behavior of the cells after vasostatin or CRT overexpression. For example, overexpression of vasostatin in neuroendocrine tumor cells enhanced their malignant properties and induced faster

tumor development when these cells are transplanted into mice (Liu *et al.* 2005). In addition, overexpression of CRT in colon cancer cell lines also increased aggressiveness of these cells *in vivo* (Hayashi *et al.* 2005).

Conclusion:

CRT is a multifunctional ER Ca^{2+} binding protein that functions as a Ca^{2+} buffer and chaperone protein. In this section, important roles of CRT in different cell functions including the regulation of cell adhesion and migration, angiogenesis, apoptosis, and cancer cell growth have been summarized. Furthermore, the role of Ca^{2+} as a key modulator of signaling pathways associated with apoptosis and cancer cell growth has been discussed. Considering all of these facts, any alteration in CRT levels may directly or indirectly impact many cellular functions and cell behavior, resulting in a pathological condition. In the next section, I will summarize the current knowledge regarding changes in CRT expression in different cancer subtypes.

1.3. Alteration of CRT expression in tumor cells

Early diagnosis of cancer is positively correlated with increased rates of survival (Jemal *et al.* 2009). Therefore, the development of proteomic technologies that enable the discovery of specific biomarkers is essential in the clinical setting to facilitate early diagnosis and to increase survival rates. Using proteomic techniques, several investigators reported differential expression of CRT in various types of tumors (Zhu *et al.* 1999; Brunagel *et al.* 2003; Kageyama *et al.* 2004; Toquet *et al.* 2007; Vougas *et al.* 2008; Alur *et al.* 2009). Furthermore, altered CRT expression levels have also been correlated with different stages of carcinogenesis in certain neoplasias such as gastric and esophageal cancers (Chen *et al.* 2007; Du *et al.* 2009). As such, CRT was proposed to be a marker that may be useful for early diagnosis of cancer (Kageyama *et al.* 2004; Chen *et al.* 2009; Kageyama *et al.* 2009). To date, little is known about the mechanisms underlying the observed changes in CRT expression in cancer cells. Whether fluctuations of the levels of CRT are a cause or a consequence of tumorigenecity needs further investigation. Table 1 lists the published reports on CRT expression in specific types of cancers, and a brief summary is described below.

1.3.1. CRT expression in bladder cancer

Kageyama and colleagues (Kageyama *et al.* 2004) measured the levels of several proteins in tissues obtained from bladder cancer patients using proteomic analysis. They found that the expression of CRT and nine other candidate proteins were not only increased in tumor tissue, but also detected CRT in urine samples of these patients (Kageyama *et al.* 2004). More recently, the same group (Kageyama *et*

al. 2009) developed an enzyme-linked immunosorbent assay (ELISA) procedure using commercially available anti-CRT antibodies to evaluate the potential utility of CRT as a urinary biomarker for bladder cancer. They measured the concentration of urinary CRT in a cohort of patients with histologically confirmed bladder urothelial carcinoma (n=109) and non-urological patients (n=40) and found that the urinary CRT concentration of patients with urothelial carcinoma was significantly higher than non-urological patients (Kageyama *et al.* 2009). Autoantibodies against CRT in the biological fluids of bladder cancer patients has also been reported which may suggest a potential application for CRT detection as a tumor marker for early diagnosis (Kageyama *et al.* 2004). Similarly, Hong, *et al*. (Hong *et al.* 2004) have identified CRT autoantibodies in the sera of pancreatic cancer patients.

Table 1: Expression profile of CRT in different types of human cancers as compared to normal tissues.

Type of cancer	Total Case Numbers	Method	Result	Reference
Bladder cancer	251	2-DE	+	(Kageyama *et al.* 2004)
Colon cancer	58	S.Q. IHC	-	(Toquet *et al.* 2007)
Colon cancer	10	2-DE	+	(Brunagel *et al.* 2003)
Colon cancer	92	SELDI	N/A	(Ward *et al.* 2006)
Esophagus	45	2-DE	+	(Jazii *et al.* 2006)
Esophagus	41	2-DE	+	(Du *et al.* 2007)
Liver cancer	11	2-DE	+	(Yoon *et al.* 2000)
Hepatoma cell line	N/A	2-DE	+	(Yu *et al.* 2000)
Breast cancer	12	2-DE	+	(Franzen *et al.* 1996)
Breast cancer	10	2-DE	+	(Bini *et al.* 1997)
Neuroblastoma	68	IHC, RT-PCR	+	(Hsu *et al.* 2005)

Note: +, increased; and –, decreased

S.Q: Semi-quantitative 2-DE: two-dimentional gel electreopheresis

SELDI: Surface enhanced laser desorption/ionization

1.3.2. CRT expression in breast cancer

Protein expression profiles of benign and malignant human breast tissue and the MCF-7 breast cancer cell line have been examined by several groups (Franzen *et al.* 1996; Bini *et al.* 1997; Sarvaiya *et al.* 2006). Using two-dimensional gel electrophoresis (2-DE), Bini *et al*. (Bini *et al.* 1997) compared the protein expression profiles of human breast ductal carcinoma to histologically normal breast tissue. Thirty-two spots, including CRT, were found to be highly expressed in all carcinoma specimens. Proteomic analysis (2-DE and mass spectrometry) of the MCF-7 breast cancer cell line showed altered expression of over 2000 proteins (Sarvaiya *et al.* 2006) including CRT. Furthermore, a positive correlation between CRT overexpression and metastasis in breast cancer patients has recently been reported (Eric *et al.* 2009).

1.3.3. CRT expression in colon cancer

Reports on alterations in CRT expression in colon cancer have been conflicting. Ward, *et al*. (Ward *et al.* 2006) investigated the proteomic profile of serum samples from colorectal cancer patients and healthy subjects and detected changes in the expression of several proteins but CRT was not present in this pool. In contrast, Toquet and colleagues (Toquet *et al.* 2007) analyzed the expression of CRT and CD91 in human colon adenocarcinomas using a semi-quantitative immunohistochemical method, and reported a lower expression of CRT and CD91 in 48% of human colon adenocarcinomas as compared to the normal tissue. Conversely, Brunagel, *et al.* (Brunagel *et al.* 2003), used 2-DE to evaluate the composition of nuclear matrix proteins in ten colon cancers, adjacent normal tissues, normal donor tissues, and two colon cancer cell lines and demonstrated increased expression of CRT in the nuclear

matrix of human colon cancer as compared to both the normal adjacent tissue and normal donor colon tissues. Similarly, higher expression of CRT in multiple intestinal neoplasias isolated from a mouse model of colon cancer has been previously reported (Cole *et al.* 2000). The discrepancy between the expression levels of CRT observed in these studies could be due to the type of tissue and the techniques used. Further studies are necessary to resolve these discrepancies.

1.3.4. CRT expression in esophageal cancer

The proteomic profile of esophageal carcinoma has been evaluated by several investigators (Zhou *et al.* 2005; Jazii *et al.* 2006; Du *et al.* 2007; Breton *et al.* 2008). In esophageal squamous cell carcinoma, CRT was among several other proteins which were significantly overexpressed (Jazii *et al.* 2006; Du *et al.* 2007). However, no changes in CRT expression were detected in esophageal adenocarcinoma (Breton *et al.* 2008). Further, studies are required to decipher the role of CRT in these two different subtypes of esophageal cancer.

1.3.5. CRT expression in liver cancer

Using a 2-DE technique, Yoon, *et al*. (Yoon *et al.* 2000) analyzed the nuclear matrix protein profiles of human hepatocyte cell carcinoma obtained from 11 partial hepatectomy specimens, and compared them with corresponding healthy liver tissue. A number of proteins including CRT were present predominantly in the nuclear matrix of carcinoma cells as compared to non-malignant liver tissues. Furthermore, a comparative proteomic expression profile of a human hepatoma cell line and normal liver cells showed higher expression of CRT in this cell line (Yu *et al.* 2000).

1.3.6. CRT expression in neuroblastoma

Expression of CRT on the surface of neuroblastoma cell lines has been reported (Xiao *et al.* 1999; Xiao *et al.* 1999) suggesting a possible role for CRT in neurite formation during cell differentiation. Similarly, CRT has also been shown to be crucial for neural development in mice (Rauch *et al.* 2000). In contrast, differentiation of neuroblastoma cells with dibutyryl c-AMP has been shown to significantly increase the stability and expression of CRT due to a large increase in the turnover time of CRT in differentiated cells (Johnson *et al.* 1998).

Hsu and colleagues (Hsu *et al.* 2005) examined CRT expression in neuroblastoma tumor cells using immunohistochemistry (IHC), reverse transcriptase PCR (RT-PCR) and western blot. Results obtained from this study demonstrated a positive correlation between CRT expression and a differentiated histology and better outcome of the disease. This highlights the potential for CRT to be used as an independent prognostic factor for the survival of neuroblastoma patients. It also implies that CRT may affect the differentiation of neuroblastoma cells, and could therefore have a role in mediating the behavior of this cancer.

Conclusion:

Changes in CRT expression have been reported in different types of tumors primarily through proteomic analyses including 2DE and mass-spectrometry. In most tumor types CRT expression was increased, however, one report showed decreased CRT expression in colon cancers using IHC analysis (Toquet *et al.* 2007). Despite evidence that indicate alteration of CRT expression in various cancer cells, the role of

CRT in tumorigenecity remains unknown. Some published reports show that increased CRT expression is correlated with poor prognosis such as in esophageal squamous cell carcinoma (Du *et al.* 2007), enhances the aggressive behavior of tumor cells such as in colon cancer (Hayashi *et al.* 2005) and correlates with metastasis as has been demonstrated with breast cancer patients (Eric *et al.* 2009). Alternatively, overexpression of CRT was shown to inhibit tumor growth and metastasis in a prostate cancer model (Alur *et al.* 2009). Overall, further research is needed to elucidate whether changes in CRT expression can cause malignant behavior in normal cells or if the observed changes are the consequence of the ensued cell stress during the tumorigenic process.

1.4. Tie2 receptor tyrosine kinase

1.4.1. Role of Tie2 in angiogenesis

The receptor tyrosine kinases are a family of receptors that have an intrinsic protein-tyrosine kinase activity. In 1990, Partanen and colleagues (Partanen *et al.* 1990) identified a gene encoding a transmembrane tyrosine kinase which they classified as an unknown tyrosine kinase-homologous to a cDNA fragment from human leukemia cells. They further characterized this gene and its encoded protein as a type of angiopoietin receptor (Ang) and renamed it Tie, which is an abbreviation for Tyrosine kinase with Ig and EGF (Epidermal Growth Factor) homology domains (Partanen *et al.* 1992; Sato *et al.* 1993). The Tie receptor has been shown to be expressed predominantly in endothelial cells, their precursors, and primitive hematopoietic stem cells (HSCs) (Dumont *et al.* 1992; Iwama *et al.* 1993; Sato *et al.* 1993).

Tie2 (also termed Tek) and Tie1 are structurally related receptors that constitute the Tie receptor family. Tie2 expression is detected in endothelial cells throughout development, and is also expressed in virtually all adult endothelial cells (Sato *et al.* 1993). Schlaeger and colleagues (Schlaeger *et al.* 1997) studied the role of Tie2 in rodent models using a transgenic mouse model when the LacZ reporter gene is driven by the *Tie2* promoter and showed that Tie2 is expressed during embryonic vessel development and in the quiescent adult vasculature suggesting a role for Tie2 in mouse vascular development. The structure of the Tie2 receptor is comprised of Ig-like, EGF and fibronectin-like-3 repeats, a single transmembrane domain, and an intracellular kinase domain (Jones *et al.* 2001). The Tie2 sequence is highly conserved

among vertebrate species, with the greatest amino acid identity occurring in its kinase domain (Jones *et al.* 2001).

The endogenous ligands of the Tie2 receptor include four members of the angiopoietin family of growth factors, all of which bind to Tie2 via a carboxy-terminal fibrinogen homology domain. These four members include Ang1 (angiopoietin-1), Ang2, and interspecies orthologs Ang3 (mouse) and Ang4 (human) (Davis *et al.* 1996; Maisonpierre *et al.* 1997; Valenzuela *et al.* 1999). Ang1 and Ang4, activate the Tie2 receptor, whereas Ang2 and Ang3 inhibit Ang1-induced Tie2 phosphorylation (Maisonpierre *et al.* 1997).

The mechanism of Tie2/Ang1 signaling has been studied primarily in endothelial cells. Binding of Ang1 to the Tie2 extracellular domain results in receptor dimerization, a process that leads to autophosphorylation of different tyrosine residues in the intracellular kinase domain. This domain acts as a docking site for many effectors of cytoplasmic signaling pathways including MAPK, p21-activated kinase and PI3-K/Akt (Kim *et al.* 2000; Jones *et al.* 2001; Shiojima *et al.* 2002). Tie2 dependent signaling regulates the survival and apoptosis of endothelial cells, controls vascular permeability, and regulates the capillary sprouting that occurs during normal angiogenesis (Kim *et al.* 2000; Jones *et al.* 2001; Shiojima *et al.* 2002). In many situations this occurs in coordination with the potent pro-angiogenic growth factor VEGF.

Tie2 and angiopoietins have been extensively studied *in vivo* using genetically modified animal models. These studies have provided valuable information regarding the physiological role of the Tie2 receptor and its ligands particularly highlighting their role in normal blood vessel development (Dumont *et al.* 1994; Sato *et al.* 1995).

Dumont and colleagues showed that Tie2-deficient mice die *in utero* due to severe vascular abnormalities (Dumont *et al.* 1994). Interestingly, *Ang1* knockout mice, are also embryonic lethal due to vascular defects closely resembling those seen in *Tie2* knockout mice (Suri *et al.* 1996). Sato and colleagues (Sato *et al.* 1993) also analyzed mouse embryos deficient in *Tie2* and demonstrated that endothelial cell expression of Tie2 plays a crucial role in angiogenesis, particularly during vascular network formation. Although these findings suggest that Tie2 and its downstream signaling events are critical for the normal maintenance of endothelial cells and the development of the cardiovascular system, the requirement for Tie2 signaling in endocardial development may be restricted to an early development phase, as Jones *et al.* (Jones *et al.* 2001) have demonstrated that normal heart development doesn't require Tie2 signaling.

1.4.2. Role of Tie2 in hematopoiesis

Hematopoiesis involves the continuous production of different mature blood cell types from HSCs which reside in the bone cavity or bone marrow (BM) (Fliedner 1998). HSCs are rounded cells with rounded nuclei, very similar to lymphocytes (Fliedner 1998) which makes it difficult to identify them in a microscope with regular staining procedure such as Giemsa staining. Therefore, HSCs are primarily identified by expression of various antigenic markers on their surface such as CD34, CD45, Sca-1, c-kit, CD133 and lack of lineage markers (Yin *et al.* 1997; Lagasse *et al.* 2000; Sata *et al.* 2002). Like many other stem cels, HSCs are also defined by their ability to form multiple cell types and their ability to self-renew (Fliedner 1998).

Interaction of HSCs with their particular microenvironments, known as stem cell niches, is essential for proper adult hematopoiesis in the BM (Fliedner 1998). At least 2 different niches for HSCs have been identified in the BM: the osteoblastic niche, a microenvironment close to the inner bone surface next to the osteoblasts (Calvi 2003; Zhang *et al.* 2003) and the vascular niche, an endothelial cell containing vascular zone of sinusoidal vessels (Kiel *et al.* 2005; Kopp *et al.* 2005). Osteoblasts are bone forming cells derived from mesenchymal stem cells (Calvi 2003) and have been shown to be an important component of the stem cell niche for adult HSCs (Calvi 2003; Zhang *et al.* 2003). These cells produce receptor activator for NF-kB ligand (RANKL) and release factors such as macrophage-colony stimulating factor (M-CSF) that induce the differentiation of osteoblasts from HSCs (Yasuda *et al.* 1998). HSCs were shown to interact not only with osteoblasts but also with other stromal cells, including sinusoidal endothelial cells (Li *et al.* 2004) suggesting an alternative niche created by endothelial cells termed as vascular niche (Kiel *et al.* 2005; Kopp *et al.* 2005).

The quiescent state is believed to be an essential property for the maintenance of HSCs in the BM (Calvi 2003). Indeed, 5-bromodeoxyuridine (BrdU) labeling of stem cells from the epidermis and hair revealed that in their normal state, stem cells are slow-cycling cells, however, when stem cells enter a proliferative state, they differentiate to replace damaged and senescent cells (Taylor *et al.* 2000). Several signaling molecules have been studied and suggested to be involved in niche regulation including SCF/c-Kit, Jagged/Notch, Tie2/Ang1, and Ca^{2+}-sensing receptor (Heissig 2002; Calvi 2003; Arai *et al.* 2004; Adams *et al.* 2006).

The Tie2/Ang1 signaling pathway has been shown to play an important role in maintaining the long-term population and quiescent status of HSCs in the BM niche (Cheng *et al.* 2000). Ang1 is expressed in osteoblasts, while Tie2, is expressed in HSCs osteoblastic niche and endothelial cells (Arai *et al.* 2004). Furthermore, in the osteoblastic niche, Ang1 is secreted by osteoblasts and activates Tie2 in HSCs, resulting in tighter adhesion of the HSCs to the osteoblasts via integrin β1 and N-cadherin and maintenance of HSCs in a quiescent and anti-apoptotic state (Arai *et al.* 2004). Circulation of HSC involves HSCs leaving the BM, entering the vascular system (mobilization), and returning to the BM (homing) and it has been postulated that this process is dependent on various factors including specific molecular recognition, cell-cell adhesion/ disengagement, transendothelial migration, and finally anchoring to the BM niche (Lapidot *et al.* 2005; Cancelas *et al.* 2006; Muguruma *et al.* 2006). However, the underlying physiological function of these events is not fully understood (Wright *et al.* 2001; Mayack *et al.* 2008).

Stromal cell-derived factor-1 (SDF-1, also called Chemokine (CXC motif) Ligand 12 or CXCR12) and its receptor CXCR4 (Dar *et al.* 2005; Lapidot *et al.* 2005; Neiva *et al.* 2005) as well as underlying signaling pathways, including the Rac family molecules, are proposed to regulate HSC mobilization and homing, but also play a role in cell survival and proliferation (Cancelas *et al.* 2005; Lapidot *et al.* 2005). HSCs express CXCR4, while SDF-1 is constitutively expressed by endothelial cells, osteoblasts, and other stromal cells and stored in the bone matrix (Peled *et al.* 1999; Kortesidis *et al.* 2005). Rapid downregulation of SD-1 by both translational and post-translational mechanisms is critical for optimal mobilization of HSCs from the BM towards circulation (Abkowitz *et al.* 2003; Kopp *et al.* 2005). Granulocyte-colony

stimulating factor (G-CSF) which is widely used clinically during stem cell-based transplantation procedures is shown to induce HSCs mobilization (Petit *et al.* 2002). The mechanism of G-CSF-induced mobilization of HSCs is primarily based on a decreasing SDF-1 in osteoblasts, while increasing SDF-1 in peripheral circulation after G-CSF treatment (Petit *et al.* 2002). Furthermore, G-CSF could regulate SDF-1 expression in BM at the transcriptional level (Semerad *et al.* 2005).

Expression of SDF-1 by endothelial cells also induces HSCs to undergo transendothelial migration mediated by E and P-selectins (Katayama *et al.* 2003). Similarly, during stem cell homing, high levels of SDF-1 on the surface of osteoblasts attract HSCs expressing CXCR4 to return home to the osteoblast niche (Kiel *et al.* 2005; Kopp *et al.* 2005). Additionally, formation of the adherens complex by N-cadherin and β-catenin proteins may play an important role for anchoring HSCs to the osteoblastic niche (Zhang *et al.* 2003; Muguruma *et al.* 2006). Recently, the Ca^{2+}-sensing receptor was found to facilitate the maintenance of HSCs in the osteoblastic niche. Adams *et al*. (Adams *et al.* 2006) have studied homing and mobilization of HSCs in Ca^{2+}-sensing receptor knockout mice. They found that deficiency of the Ca^{2+}-sensing receptor leads to the release of HSCs into the bloodstream. Interestingly, although HSC homing to the BM in these animals was not disrupted, the cells were unable to remain retained in the osteoblastic niche (Adams *et al.* 2006).

1.4.3. Tie2 receptor in malignancy

In cancer, elevated expression of Tie2 was originally observed in the endothelium of the neovasculature of different solid tumors. Peters and colleagues (Peters *et al.* 1998) were the first group to show that Tie2 was expressed in the

vascular endothelium of both normal breast tissue and breast tumors. However, the proportion of Tie2 positive microvessels was higher in tumors. Furthermore, this group showed that Tie2 expression appeared to be more intense in vascular hot spots at the leading edge of the invasive tumors (Peters *et al.* 1998). Higher expression of Tie2 was found in the vasculature of several human tumors including prostate cancer (Caine *et al.* 2003), hepatocellular carcinoma (Tanaka *et al.* 2002), non-small cell lung cancer (Takahama *et al.* 1999), hemangioma (Yu *et al.* 2001), Kaposi's sarcoma (Brown *et al.* 2000), astrocytoma (Zadeh *et al.* 2004) melanoma (Siemeister *et al.* 1999), retinal and choroidal neovascularization (Hangai *et al.* 2001).

Increased Tie2 receptor expression in solid tumors is positively correlated with increased malignancy suggesting that elevated Tie2 expresion leads to pathologic angiogenesis. Based on this hypothesis, two groups used a soluble form of the extracellular domain of murine Tie2 (ExTEK) to block Tie2 action and showed that ExTEK can inhibit tumor angiogenesis and growth *in vivo* (Lin *et al.* 1997; Zadeh *et al.* 2004). Furthermore, an adenoviral vector containing cDNA for the soluble Tie2 receptor (AdExTek) was able to significantly inhibit the growth of a murine mammary carcinoma (4T1) and a murine melanoma (Lin *et al.* 1998).

In addition to the expression of Tie2 in the vascular structures of tumors, several studies have shown that Tie2 is also expressed in the tumor cells of several neoplasms (Muller *et al.* 2002; Shirakawa *et al.* 2002; Wang *et al.* 2005; Schliemann *et al.* 2006), however, the role of Tie2 expression in the extravascular regions of tumors is not known. Wang *et al.* (Wang *et al.* 2005) examined the expression of Tie2 and its ligands in gastric tumor samples isolated from patients and in gastric cancer cell lines by PCR (Polymerase Chain Reaction), IHC and western blotting, and showed that

expression of Tie2 and its ligands Ang1 and Ang2 was elevated. They concluded that Tie2 and its ligands might be involved in the initiation and progression of gastric cancer.

Tie2 and its ligands were also found to be overexpressed in both acute and chronic myeloid leukemia (AML and CML) cell lines and patient samples (Muller *et al.* 2002; Schliemann *et al.* 2006). Similar results have been observed in some erythroblastic and megakaryoblastic cell lines (Kukk *et al.* 1997). Loges and colleagues (Loges *et al.* 2005) studied the prognostic relevance of the Tie2/Ang signaling system using qRT-PCR reaction in a group of 90 patients younger than 61 years with AML and showed that high Ang2 mRNA expression in peripheral myeloblast cells represents an independent prognostic factor for overall survival in AML patients. This finding suggests a role for Tie2 in stem cell proliferation or differentiation and pathogenesis of hematologic neoplasia.

Shirakawa *et al*. (Shirakawa *et al.* 2002) compared Tie2 expression in inflammatory breast cancer, which is characterized by rapid tumor progression and poor prognosis, with Tie2 expression in non-inflammatory breast cancer specimens. In the inflammatory breast cancer, they found that Tie2 was not only expressed at higher levels in the endothelial cells and tumor infiltrating monocytes, but also expressed in the inflammatory cancer cells. They also demonstrated that treatment of inflammatory breast cancer xenografts in the mammary pad of female BALB/c nude mice with soluble Tie2 (Ad-Tie2) resulted in reduced tumor growth and suppression of lung metastasis (Shirakawa *et al.* 2002). These observations support a role for Tie2/Ang signaling in inflammatory breast cancer.

Conclusion:

Tie2 is a receptor tyrosine kinase which is highly expressed by HSCs, endothelial progenitor cells and the vascular endothelium. In this section, we have summarized the different roles of the Tie2 receptor in angiogenesis, maintenance of hematopoiesis, and malignany. We have also discussed the important signaling pathways in angiogenesis and mobilization/homing of HSCs as well as known and putative functions of the Tie2 receptor in the regulation of angiogenesis, HSCs self-renewal, mobilization, and homing.

1.5. Biology of the Lungs

1.5.1. Lung airway and alveolar epithelium

The lungs are one of the most complex organs in the body and are composed of over 40 different cell types. Their primary function is the exchange of oxygen and carbon dioxide between the external environment and the pulmonary circulation (Bloom *et al.* 1975). Each lung is divided into five lobes: three in the right lung and two in the left lung. The trachea first divides into the left and right primary bronchi which supply each lung. Each primary bronchi gives rise to the secondary bronchi, which supply the lobes of the lung before dividing again to form the tertiary or segmented bronchi which supply the segments of each lobe (Bloom *et al.* 1975). The bronchi branch many times into smaller and smaller airways known as bronchioles that have a diameter less than 1 mm. The trachea and bronchi have cartilage support and submucosal glands, however, bronchioles have neither cartilage support nor submucosal glands (Bloom *et al.* 1975).

The respiratory epithelium in the bronchioles is composed of ciliated columnar cells with a few Goblet cells that secrete a mucous that functions to trap inhaled particles (Bloom *et al.* 1975). In the terminal and respiratory bronchioles, Goblet cells are entirely replaced by Clara cells, which are columnar non-mucous and non-ciliated secretory epithelial cells (Bloom *et al.* 1975) and were first described by Max Clara in 1937 (Clara 1937). Clara cells line the pulmonary airways and are localized mainly in the proximal or central portion of the pulmonary acinus at the junction between the conducting airways and the alveolar space (Bloom *et al.* 1975; Evans *et al.* 1978). The primary function of Clara cells is to protect the bronchiolar epithelium by secreting a

variety of different surfactant proteins including SP-A, SP-B, SP-D (Walker *et al.* 1986; Wong *et al.* 1996) and a 10 kDa protein known as Clara Cell Secretory protein (CCSp or CC10) (Bedetti *et al.* 1987). It has been shown that Clara cells detoxify harmful substances inhaled into the respiratory system via the cytochrome P450 enzymes found in their smooth ER (Boyd 1977). Furthermore, experimental studies on animal models suggest that Clara cells can function as stem cells to repair damaged bronchial epithelium (Evans *et al.* 1978; Plopper *et al.* 1992).

Each bronchiole terminates in grape-like sac clusters known as alveoli that are surrounded by a network of thin-walled capillaries. These capillaries are separated from the alveoli by only 0.2 μm as both structures have extremely thin walls (Bloom *et al.* 1975). The alveolar ducts and the alveoli are lined with a simple squamous epithelium composed of type I and type II alveolar cells (pneumocytes). The majority of the alveolar surface area (about 90%), is covered by squamous type I alveolar cells which form a thin barrier through which gas exchange occurs (Bloom *et al.* 1975). Type I alveolar cells are extremely thin cells and as such are very susceptible to injury. Type II alveolar cells are cuboidal in shape, with short microvilli along their apical surface and comprise about 15% of the cells in the distal lung (Bloom *et al.* 1975). These actively dividing cells are able to differentiate into both type I and type II alveolar cells (Evans *et al.* 1975). Therefore, it is postulated that type II alveolar cells may serve as a progenitor cell for alveolar type I cells, particularly during re-epithelialization of the alveolus after lung injury (Mason 2006). Type II cells synthesize and secrete surfactant proteins including SP-A, SP-B, SP-C and SP-D (Mason 2006). As mentioned above, SP-A, SP-B and SP-D are also synthesized by

Clara cells (Walker *et al.* 1986; Wong *et al.* 1996) however SP-C is the only surfactant protein which is exclusively synthesized by alveolar type II cells (Mason *et al.* 2000).

Surfactant proteins are a complex mixture of lipids and proteins (lipoprotein complex) that work to reduce the surface tension of the alveolar surface, allowing the alveoli to expand during inspiration, and preventing their collapse during expiration (Pattle 1955). Other important functions of alveolar type II cells are: (i) transporting sodium from the alveolar fluid into the interstitium so as to minimize alveolar fluid and thereby to maximize gas exchange and (ii) regulation of the inflammatory response by secreting a variety of growth factors and cytokines (Fehrenbach 2001; Mason 2006).

1.5.2. Epithelial injury and inflammation in the lung

An average person with moderate activity breathes approximately 11,000 liters of air containing potentially harmful gases and particles everyday (Wright 2003), which results in constant exposure to harmful agents. In addition to harmful gases such as ozone, small particles less than 3 to 5 microns in diameter can penetrate into the alveolar sacs and larger particles will form deposits on the epithelial layer of the upper airways (Adamson *et al.* 1999; Wright 2003). Defense of the respiratory system in the upper airway involves ciliated columnar cells that line the airway and a layer of mucus secreted by Goblet cells that also line the upper airways (Kyd *et al.* 2001). Rhythmic beating of cilia transports mucus and particles/pathogens trapped in the mucus through the larger airways into the pharynx where it is swallowed. In the lower airways however, due to the requirements of gas exchange, alveoli are not protected by mucus. Instead, the host defense in alveolar sacs relies principally on cellular (phagocytes)

immune responses. The junction between the terminal conducting airways and the alveolar sac is an important anatomic landmark because host defenses change dramatically at this level from largely mechanical clearance of offending agents to humoral and cellular/phagocytic responses on the alveolar surface (Bouthillier *et al.* 1998; Imrich *et al.* 2007).

The resident mononuclear phagocytes in the lung are alveolar macrophages, the tissue equivalent of monocytes in the blood. The pulmonary alveolar macrophage is a large cell (15-50 μm), with a large number of organelles and inclusions containing a vast repertoire of enzymes such as peroxidase, lysosome, and acid-hydrolases which are used to destroy microorganisms (Klebanoff *et al.* 1984). The role of alveolar macrophages in destroying microorganisms as well as in removal of dust and other inhaled particles during inflammation and injury in the alveoli has been well established (Imrich *et al.* 2007).

In response to serious threats, circulatory white blood cells, specifically neutrophils, can be recruited to the lung to help ingest and kill foreign particles. Guided by chemotactic factors, circulatory monocytes will then migrate to the site of inflammation and subsequently differentiate into macrophages. Activated alveolar macrophages and other inflammatory cells are the main source of growth factors and cytokines which profoundly affect endothelial, epithelial and mesenchymal cells in the local microenvironment of the lungs (Khalil *et al.* 1993; Perkins *et al.* 1993; Imrich *et al.* 2007). There are a variety of growth factors such as FGF family members, HGF (Hepatocyte Growth Factor), and EGF family members secreted by fibroblasts and inflammatory cells that can stimulate type II cell proliferation (Morimoto *et al.* 2001; Ware 2002). Although alveolar epithelial cells are vital for the maintenance of the

pulmonary air/blood barrier, they are also known to play a major role in the regulation of immune responses in the lung (Sato *et al.* 2002). After epithelial injury, the alveolar epithelial cells can greatly enhance the lung defenses through increasing secretion of a variety of cytokines (Stadnyk 1994; Sato *et al.* 2002; Manzer *et al.* 2008) and surfactant proteins such as SP-A and SP-D (McIntosh *et al.* 1996).

SP-A and SP-D play important roles in the innate immunity of the lung including phagocytosis, cytokine production and chemotaxis (Wright 2004). Using a rat model of pulmonary infection, Restrepo *et al*. (Restrepo *et al.* 1999) showed that SP-D stimulated the uptake of a pulmonary pathogen, *Pseudomonas aeruginosa* by alveolar macrophages. Furthermore, inflammatory cytokines, such as interleukin 1 (IL-1), interleukin 6 (IL-6), interleukin 8 (IL-8) and tumor-necrosis factor (TNF) have been shown to be produced and secreted by inflammatory cells. These cytokines also regulate inflammatory reactions either directly or indirectly through the induction of the synthesis of cellular adhesion molecules or other cytokines by other cell types such as alveolar type II cells. For example, Dentener *et al*. (Dentener *et al.* 2000) described a human alveolar epithelial cell line producing LPS-binding protein, a protein known to play a central role in the defense from bacterial endotoxins, in response to IL-1ß and TNF-α.

In addition to small particles and bacteria, the toxicity of some gases such as ozone on the lung epithelial cells has been well documented (Vincent *et al.* 1997; Bouthillier *et al.* 1998; Adamson *et al.* 1999). Vincent and colleagues (Vincent *et al.* 1997) showed that 4 hours of exposure to 0.8 ppm ozone followed by 32 hours of exposure to clean air induced epithelial cell damage. The health effects of ozone on human lungs has also been investigated by different groups (Broeckaert *et al.* 1999;

Frampton *et al.* 1999; Avissar *et al.* 2000). Broeckaert *et al*. (Broeckaert *et al.* 1999) showed that exposure of exercising participants to an average of 0.07 ppm ozone over 2 hours increased airway permeability due to epithelial injury.

1.5.3. Tissue renewal in the lung

The alveolar epithelium is the largest epithelial surface of the body exposed to the external environment with an average surface area greater than 70 square meters (Bloom *et al.* 1975). Alveolar epithelium is mainly composed of AT1 cells which are extremely thin cells and are very susceptible to injury during inhalation. Rapid repair of the denuded alveolar surface after injury is key to survival (Theise *et al.* 2002). This unique feature of lung epithelial cells suggests that at least one progenitor cell per alveolar sac is required to accomplish rapid coverage and ensure the maintenance of lung tissues (Driscoll *et al.* 2000). Thus, a large number of cells must function as a "ready reserve" to repair damaged alveolar surface area. Previous studies suggest that Clara cells and AT2 cells function as progenitor cells of alveolar epithelial cells (Evans *et al.* 1975; Evans *et al.* 1978). Brody, *et al*. (Brody *et al.* 1987) isolated Clara cells from rabbits and implanted them into nude mice to investigate the role of Clara cells in the repair of the bronchial epithelium. These isolated Clara cells, led to the seeding and development of a cuboidal epithelium in the denuded trachea, suggesting that Clara cells may function as progenitor cells for the respiratory epithelium in injured lungs. Furthermore, Driscoll and colleagues (Driscoll *et al.* 2000) demonstrated up regulation of telomerase, a stem/progenitor cell marker after acute oxygen injury in alveolar epithelial cells in rodents (mice and rats). This suggests that alveolar epithelial cells either contain a subpopulation of stem/progenitor cells, or that the majority of alveolar

epithelial cells can undergo reactivation into a progenitor-like state in response to injury. These putative progenitor cells are shown to be relatively more proliferative and resistant to injury-induced apoptosis and that they must be evenly distributed over the alveolar surface (Driscoll *et al.* 2000; Reddy *et al.* 2004). Stem cells are undifferentiated cells that have two unique properties: first, they have the ability to renew themselves almost indefinitely through cell division and second, they can differentiate into multiple cell lineages (Slack 2000). Indeed, tissue-specific stem cells or somatic stem cells are capable of maintaining and regenerating terminally differentiated cells within their own specific tissue (Slack 2000).

Putative endogenous lung epithelial progenitor cells have been identified and proposed to play a role as progenitor cells in the process of lung repair (Reynolds *et al.* 2000; Engelhardt 2001; Giangreco *et al.* 2002; Reddy *et al.* 2004; Kim *et al.* 2005). In fact, current evidence supports the existence of multiple stem cell niches in the lung tissue (Otto 2002). These cells have been located within the adult lung in the basal layer of the upper airways, within or near pulmonary neuroendocrine cells (Reynolds *et al.* 2000; Engelhardt 2001; Reddy *et al.* 2004) as well as at the bronchoalveolar junction (Giangreco *et al.* 2002; Kim *et al.* 2005). Bronchoalveolar stem cells (BASC) discovered by Kim and colleagues (Kim *et al.* 2005) reside at the bronchoalveolar junction and express stem cell antigens (Sca-1, c-kit,) and both alveolar type II (SP-C) and airway epithelial cell markers (CC10). These cells have been shown to be resistant to naphthalene-induced epithelial injury, proliferate after injury *in vivo,* and are also multipotent in clonal assays *in vitro*. BASCs may also be putative sites of tumorgenesis as increased number of BASCs has been observed in the early stages of tumorgenic

lesions in the *Lox-K-ras* transgenic mouse model of lung adenocarcinoma (Kim *et al.* 2005).

1.5.4. Contribution of bone marrow-derived cells (BMDCs) to lung epithelial repair

As mentioned before, the lung is a complex organ with a limited regenerative capacity and that the process of tissue renewal relies mainly on the activation of resident somatic stem cells residing in the damaged tissue (Slack 2000; Engelhardt 2001; Otto 2002). However, evidence is now emerging that progenitor cells derived from the BM are also able to reach their target tissue through the blood stream (Wright *et al.* 2001), and cross the lineage barrier to contribute to postnatal tissue renewal by supporting local stem cells of various solid organs, a process which is termed "developmental plasticity". These phenomena occur normally, but at a low frequency *in vivo* (Wagers *et al.* 2002) and required tissue damage for BM stem cell recruitment and selective survival advantage for propagation (Lagasse *et al.* 2000). The biological mechanisms underlying stem cell plasticity are still debated, and the exact mechanisms are not entirely understood.

Although, several investigators failed to reproduce these original findings (Balsam *et al.* 2004; Murry *et al.* 2004; Nygren *et al.* 2004), other studies demonstrated that BMDCs possess an unexpected degree of plasticity, and serve as precursors for differentiated cells of multiple organs such as the heart (Orlic *et al.* 2001), liver (Petersen *et al.* 1999; Theise *et al.* 2000; Jang *et al.* 2004) and brain (Mezey *et al.* 2003). Contribution of BMDCs to the repair of lung epithelium is summarized in Table 2.

Table 2: Summary of publications examining contribution of BMDCs to the repair of lung epithelium.

Tissue	Model	Tissue of Origin	Method of Detection	Study
Lung	m	HSC enrichment	Y chromosome FISH, RT-PCR	(Krause *et al.* 2001)
Lung	m	*lacZ* expresser BM	X-gal staining, IHC	(Kotton *et al.* 2001)
Lung	m	HSC	EGFP	(Wagers *et al.* 2002)
Lung	m	Whole BM	Y chromosome FISH, RT-PCR	(Theise *et al.* 2002)
Lung	m	MSC	Y chromosome FISH	(Ortiz *et al.* 2003)
Lung	m	EGFP labeled BM	Flow cytometry	(Abe *et al.* 2003)
Lung	h	Sex-mismatched donor BM	Y chromosome FISH, PCR	(Kleeberger *et al.* 2003)
Lung	h	Sex-mismatched donor BM	X and Y chromosome FISH, IHC	(Suratt *et al.* 2003)
Lung	m	GFP labeled fetal liver	IHC for $CD45^-$, GFP^+ cells	(Ishizawa *et al.* 2004)
Lung	m	GFP labeled BM	Flow cytometry, IHC, RT-PCR	(Hashimoto *et al.* 2004)
Lung	m	EGFP labeled BM	Flow cytometry	(Yamada *et al.* 2004)
Lung	h	Sex-mismatched donor HSC	Y chromosome FISH, IHC	(Mattsson *et al.* 2004)
Lung	m	HSC enrichment	Flow cytometry	(Dooner *et al.* 2004)
Lung	m	GFP labeled MSC	IF for GFP and IHC	(Rojas *et al.* 2005)
Lung	h	EPCs	IF and IHC	(Yamada *et al.* 2005)

Table 2: Continued

Lung	h	GFP labeled MSC	IF, Flow cytometry	(Wang *et al.* 2005)
Lung	m	Sex-mismatched GFP labeled donor BM	Y chromosome FISH, RT-PCR, Flow cytometry	(Loi *et al.* 2006)
Lung	m	Sex-mismatched donor BM	Y chromosome FISH, IHC	(MacPherson *et al.* 2006)
Lung	m	GFP labeled MSC	Flow cytometry	(Gupta *et al.* 2007)
Lung	m	EGFP labeled MSC	Flow cytometry	(Xu *et al.* 2007)
Lung	m	GFP labeled donor BM	Flow cytometry, IF, RT-PCR,	(Wong *et al.* 2007)
Lung	r	Sex-mismatched GFP labeled donor BM	Y chromosome FISH, GFP^+ cells and IHC	(Spees *et al.* 2008)
Lung	r	DAPI-labeled MSC	IF and IHC	(Zhao *et al.* 2008)
Lung	m	Sex-mismatched GFP labeled donor BM	Y chromosome FISH, IF and IHC	(Rejman *et al.* 2009)

Definition of abbreviations: m: Mice, h: Human, r: Rat, EGFP, Enhanced green fluorescent protein, MSC, Mesenchymal stem cells, EPCs: Endothelial progenitor cells, FISH: Fluorescence in situ hybridization, IF: Immunofluorescence staining, IHC: Immunohistochemistry staining

The bone marrow (BM) is a soft tissue inside the core of most bones that contains heterogeneous populations of stem cells mainly HSCs and mesenchymal stem cells. As discussed before (section 1.4.2), both the osteoblastic and vascular niches play important roles in regulating BMDC mobilization, the process by which BMDCs leave the BM and enter the circulatory system to reach their target tissue (Wright *et al.* 2001). It is proposed that local tissue injury is "sensed" by BM stem cells which induces BMDC mobilization towards the site of injury (Figure 2). BM stem cells are recruited to the site of injury and differentiate through promoting structural and functional repair (Yamada *et al.* 2004; Kajstura *et al.* 2005; Rojas *et al.* 2005; MacPherson *et al.* 2006).

Using a bleomycin-induced lung injury model, Kotton, *et al.* (Kotton *et al.* 2001) assessed the capacity of BM cells to serve as precursors of lung alveolar cells. Following injection of LacZ-labeled BM cells in wild-type recipient mice, engraftment of BM stem cells in recipient lung parenchyma as cells with the morphological and molecular phenotype of alveolar type I epithelium, but not type II was shown (Kotton *et al.* 2001). However, Theise, *et al* (Theise *et al.* 2002) reported engraftment of BM stem cells into both alveolar type I and II cells. In this study, Theise and colleagues injected whole BM cells from age-matched male donors into a cohort of lethally irradiated female mice. Using the fluorescent *in situ* hybridization (FISH) assay, they detected Y-chromosome positive type I and type II pneumocytes as early as 5 days post-transplantation (Theise *et al.* 2002). Additionally, using fluorescence-activated cell sorting (FACS), they demonstrated that transplantation of male derived $CD34^{+}$ lin^{-} BM cells into female mice shows a similar pattern of pulmonary engraftment (Theise *et al.* 2002). Rojas, Xu *et al.* (Rojas *et al.* 2005) also provided evidence that transfer of

BMDCs could protect the lung epithelium against bleomycin-induced lung injury. They suggest that recruitment of BMDCs to the site of injury is partly mediated by cytokines that are secreted by injured lung tissue, but not by normal lung tissue. Overall, these studies support the hypothesis that BMDCs are able to cross the lineage barrier and contribute to postnatal lung tissue renewal.

Conclusion:

Lungs are exposed to a high rate of epithelial cell injury, chronic inflammation and a constant state of tissue renewal, which develops as a consequence of continued exposure to environmental insults. In this section, in addition to summarizing the physiology of the lung, recent knowledge related to epithelial injury and the process of tissue renewal in the lung has been discussed. The plasticity of HSCs, and the importance of BMDCs as a back up system in tissue renewal of different organs particularly lung epithelial repair have also discussed.

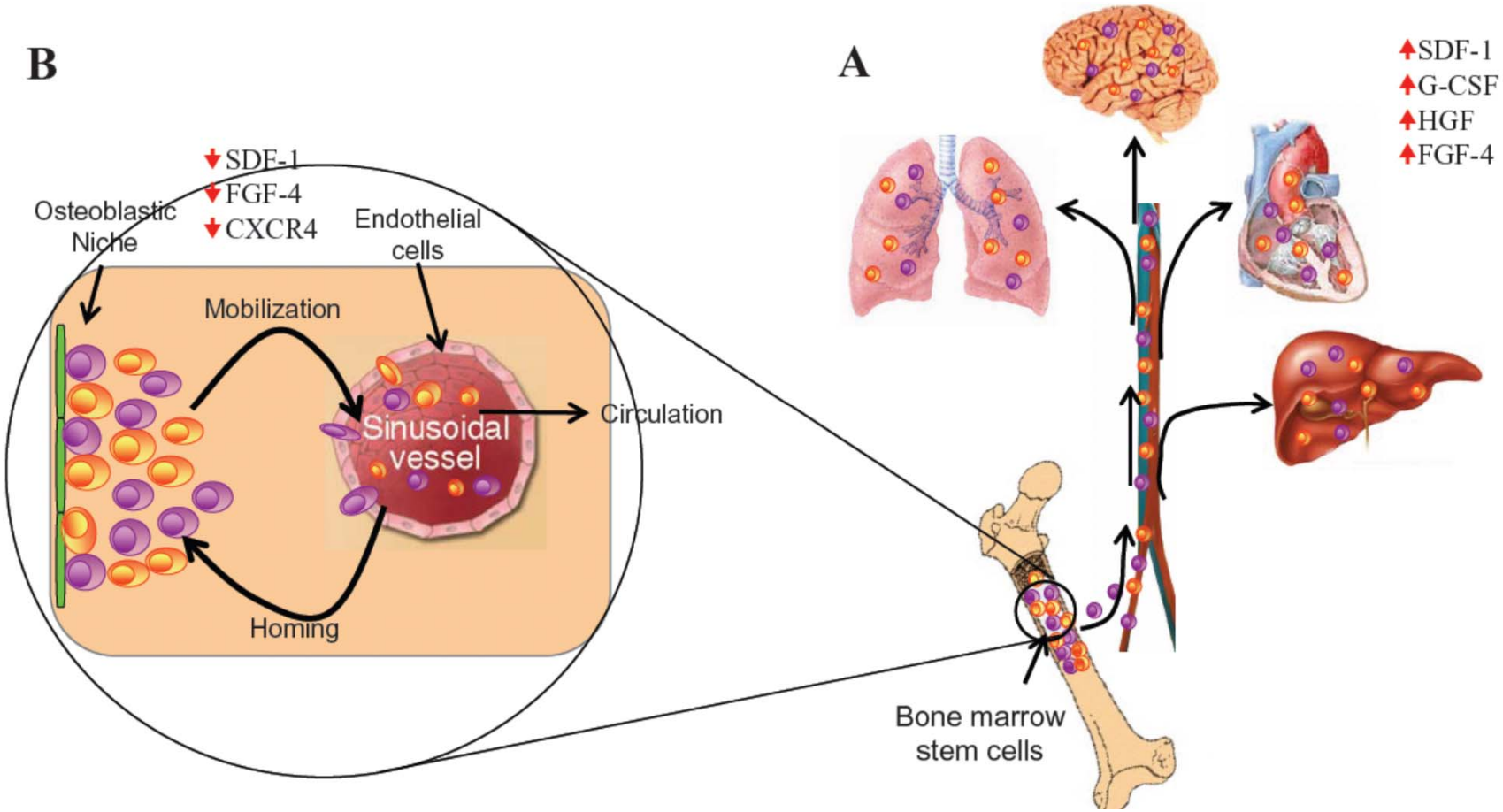

Figure 2. Overview of the mobilization HSCs in the repair of solid-organ tissue. (A) In chronic tissue injury, mediators such as SDF-1, G-CSF, HGF, FGF-4 are released into the peripheral blood, acting as signals to recruit HSCs to the site to injury. (B) HSCs leave their niche in the bone marrow in response to decreases in both SDF-1 and CXCR4 expression, begin to mobilize and are released into the circulation towards the site of the injured tissue. Once HSCs reach the target tissue, their fate may change according to the new microenvironment that they encounter. Source of images with modification: The liver: www.stanford.edu, The lung: www.topnews.in, The brain: www.ipmc.cnrs.fr, The Heart: www.nlm.nih.gov, The bone: www.schneiderchildrenshospital.org

1.6. Epithelial cell damage, inflammation and carcinogenesis

The association of inflammatory cells such as lymphoctyes and macrophages with tumor cells was reported nearly a century and a half ago (Virchow 1863). Based on this observation, a primary role for inflammatory cells in neoplastic development was hypothesized. Epidemiologic observations demonstrated that individuals with respiratory diseases caused by chronic inflammation are at a higher risk for subsequent development of lung cancer (Cohen *et al.* 1977). It is believed that tissues that normally undergo rapid renewal might also be expected to experience increased cancer incidence, as the high turnover rate might require a large number of activated stem cells (Danese 2008; Engels 2008; Farinati *et al.* 2008; Lee *et al.* 2009). In fact, organs such as the skin, the lungs, and the gastrointestinal tract, which are continuously exposed to environmental insults, and consequently are in a constant state of renewal, are the primary sites for a large proportion of human cancers (Danese 2008; Farinati *et al.* 2008; Lee *et al.* 2009). Along with advances in cancer biology, much has been learned in terms of the molecular mechanisms that govern the association between inflammation and development of many types of neoplasia. These include skin (Perez-Moreno *et al.* 2008; Zheng *et al.* 2008), lung (Engels 2008; Lee *et al.* 2009), colon (Maggio-Price *et al.* 2006; Danese 2008), gastric (Farinati *et al.* 2008; Tu *et al.* 2008) and mammary cancers (Cole 2009), and supports the idea that there is a functional association between inflammation and tumorigenicity.

Chronic inflammation in the lung, which develops as a consequence of continued exposure to environmental insults, leads to repetitive tissue damage and a constant state of renewal. The presence of highly reactive nitrogen and oxygen species

released from inflammatory cells interacts with DNA in proliferating epithelium and increases the rate of mitotic error through genomic alterations such as point mutations, deletions, or rearrangements (Walser *et al.* 2008). Indeed, *p53* mutations are a common occurrence not only in tumors, but also in chronic inflammatory diseases such as rheumatoid arthritis and inflammatory bowel disease (Wistuba *et al.* 1997; Coussens *et al.* 2002).

It is hypothesized that genetic changes in the airway epithelium of smokers may predict or identify individuals at increased risk for lung cancer (Lee *et al.* 2009). Chronic airway inflammation also contributes to alterations in the bronchial epithelium and lung microenvironment, providing a situation that leads to pulmonary carcinogenesis. For instance, inflammation-inducible cyclooxygenase-2 (COX-2) is upregulated in non-small cell lung cancer (Dohadwala *et al.* 2006; Krysan *et al.* 2008) and is suggested to play an important role in carcinogenesis through inhibition of host immunity. Elevated expression of COX-2 in lung adenocarcinoma was also proposed to be associated with its invasion and metastasis (Achiwa *et al.* 1999). Associations between inflammation and lung cancer also indicate an increased risk for lung cancer in COPD (Chronic obstructive pulmonary disease) and asthma patients (Krysan *et al.* 2008). Interestingly, the protective effect of aspirin or other non-steroidal anti-inflammatory drugs on many neoplasias (Cuzick *et al.* 2009) including lung cancer has also been reported (Schreinemachers *et al.* 1994; Malkinson 2004; Malkinson 2005; Van Dyke *et al.* 2008).

Epithelial-mesenchymal transition (EMT) was initially described as a process essential in embryonic development, composed of a shift from an epithelial phenotype to a highly motile fibroblastoid or mesenchymal phenotype (Huber *et al.* 2005). In

addition to embryonic development, EMT has been implicated in chronic inflammation and cancer development (Gotzmann *et al.* 2004). More recently a role for EMT in a variety of malignancies, including lung cancer has been described (Dasari *et al.* 2006; Soltermann *et al.* 2008). Different pathways including Transforming Growth Factor-β (TGF-β), PI3K/Akt, ROS, receptor tyrosine kinase/Ras signaling, and *Wnt* pathways have been shown to be involved in EMT during tumor development (Gotzmann *et al.* 2004; Huber *et al.* 2005; Radisky *et al.* 2005). Furthermore, the association between inflammation and EMT progression in the development of lung cancer has been described (Dohadwala *et al.* 2006; Krysan *et al.* 2008; Hotz *et al.* 2009; Wu *et al.* 2009). For instance, IL-1β and PGE2, inflammatory mediators in the lung, were shown to decrease E-cadherin expression and promote EMT in non-small cell lung cancer (Dohadwala *et al.* 2006; Krysan *et al.* 2008). Recently, Hayashida *et al.* (Hayashida *et al.* 2006) showed that overexpression of CRT can induce EMT through the downregulation of E-cadherin expression at both the protein and transcript levels. Overexpression of CRT in Madin-Darby Canine Kidney Epithelial (MDCK) cells was shown to alter intracellular Ca^{2+} homeostasis leading to the up-regulation of Slug (a repressor of the E-cadherin promoter) and suppression of the E-cadherin transcription (Hayashida *et al.* 2006). Whether CRT can affect EMT through its other functions requires further investigation.

Although EMT has been widely implicated in the metastatic process of epithelial malignancy, recent work of Mani and colleagues (Mani *et al.* 2008) demonstrated a direct link between EMT and gain of epithelial stem cell properties. Their work suggests that inflammation in the lung may also impact stem cell properties via EMT-dependent events in the early stages of carcinogenesis of lung cancer, thus

implicating the inflammatory pulmonary environment in both lung cancer initiation and progression.

Conclusion:

The correlation between chronic inflammation, epithelial injury and cancer has been long known. The association between inflammation and cancer is further discussed in this section. We also discussed the role of different signaling pathways involved in inflammation, EMT, and cancer, and the possible role of CRT in the induction of EMT via downregulation of E-cadherin expression. Since there is a potential role for BMDCs in lung epithelial repair during chronic epithelial injury, BMDCs can be considered as an alternative source of malignant transformation associated with inflammation and injury in the lung.

1.7. Lung cancer

Lung cancer is the leading cause of cancer-related death in both developed and developing countries (Lam *et al.* 2004; Alberg *et al.* 2005; Canadian Cancer Statistics 2009; Jemal *et al.* 2009; Jung *et al.* 2009). Although the rate of lung cancer deaths for males is decreasing in the developed countries, the rate of lung cancer in women has increased in the last few decades, which is attributed to the increased percentage of female smokers (Ginsberg 2005; Walser *et al.* 2008). It has been reported that more women die of lung cancer than any other cancer, including breast cancer, ovarian cancer and uterine cancers combined (Lam *et al.* 2004). Although tobacco smoking is the main risk factor for lung cancer, accounting for about 90% of the cases in men and 70% of the cases in women (Wynder *et al.* 1950; Alberg *et al.* 2005; Ginsberg 2005), a number of etiological factors including exposure to air pollution, occupational exposure to asbestos, arsenic and other carcinogens, exposure to environmental tobacco smoke, cooking oil vapour and radon have been identified to also influence lung cancer incidence (Alberg *et al.* 2005; Ginsberg 2005).

Despite advances in cancer research and technology, the average 5-year survival rate for lung cancer patients is still only approximately 14% , indicating that there has been virtually no improvement in the survival rate as compared to other cancers such as breast or prostate cancer (Comis 2003). This is mainly due to: 1) the development of metastases when the primary lung tumors are still small and are not detected, 2) early detection of lung cancer is hindered and difficult to achieve due to a lack of clinical diagnostic markers (Mountain *et al.* 2003) leading to diagnosis at an advanced stage in the majority of patients when the prognosis is poor.

Despite the fact that most lung cancers are the result of tobacco smoking, lung cancer is also a significant health problem in those with no history of smoking (Subramanian *et al.* 2007; Sun *et al.* 2007). It is estimated that, approximately 25% of lung cancer cases worldwide are not related to tobacco use, accounting for over 300,000 deaths each year (Huber 2007; Sun *et al.* 2007). Universally, lung cancer in non-smokers comprises an estimated 15% of cases in men and 53% in women (Parkin *et al.* 2005). However, there are major geographical differences in the incidence of lung cancer in non-smokers, particularly in Asia, where 60 to 80% of women with lung cancer are non-smokers (Huber 2007; Sun *et al.* 2007). There are significant differences in the lung cancers arising in non-smokers as compared to smokers in terms of epidemiological, clinical and molecular characteristics, suggesting that they are two different forms of lung cancer (Huber 2007; Sun *et al.* 2007).

Lung cancer is categorized into two major histological groups based on the size and appearance of the malignant cells under the light microscope: 1) Small Cell Lung Cancers (SCLC), which represent about 20% of lung cancers and 2) Non-Small-Cell Lung Cancers (NSCLC) which represent the remaining 80% of lung cancers (Travis *et al.* 1995; Travis 2002). NSCLC is further divided into squamous cell carcinoma, adenocarcinoma (including bronchiolo-alveolar carcinoma), large cell carcinoma and mixed types. This classification, although based on simple patho/morphological criteria, has very important implications for clinical management and prognosis of the disease. A brief description of types of lung cancer is provided below.

1.7.1. Small cell lung cancer

SCLC, also called "oat cell carcinoma", is the less common form of lung cancer and is distinct from NSCLC based on clinical and biological characteristics. This type of lung cancer tends to arise in peribronchial locations which infiltrate the bronchial submucosa, grows rapidly, and forms a large mass (Zakowski 2003). The "oat" cell contains dense neurosecretory granules, producing a variety of peptide hormones, which frequently leads to a wide range of associated endocrine/paraneoplastic syndromes. SCLC metastasizes early in the course of the disease, usually spreading to mediastinal lymph nodes, liver, bones, adrenal glands, and the brain (Zakowski 2003; Kalemkerian *et al.* 2008). SCLC is initially sensitive to chemotherapy and radiation, but carries a poor prognosis and often presents as metastatic form of the tumor. Due to its sensitivity to chemotherapy and radiation, surgery doesn't play a role in its management except in rare situations. SCLC is strongly associated with smoking (Barbone *et al.* 1997; Rosti *et al.* 2006; Hann *et al.* 2008; Kalemkerian 2008; Owonikoko *et al.* 2008).

The most common molecular abnormality identified in SCLC is amplification of the *myc* family of oncogenes *MYC*, *MYCN*, and *MYCL* (Little *et al.* 1983; Nau *et al.* 1985). C-*myc*, a member of the *myc* family, is found more frequently in relapsed forms of tumors, therefore its expression in SCLC indicates a poor prognosis (Little *et al.* 1983).

1.7.2. Non-small cell lung cancer (NSCLC)

NSCLC is a common name for a group of lung cancers with heterogeneous histology. The three main types of NSCLC are a) squamous cell carcinoma b) large cell carcinoma and c) adenocarcinoma. These are grouped together because their diagnosis, staging, prognosis, and treatment are similar (Travis 2002).

1.7.2.1. Squamous cell carcinoma

Squamous cell carcinoma (SCC), accounting for 20% to 25% of lung cancer, commonly arises in the larger lobar and segmental bronchi of the central part of the lung, but grows very slowly (Collins *et al.* 2007). Therefore, the pre-cancerous phase of SCC may last several years during which abnormal, but not cancerous cells are found in the sputum and chest X-rays with no evidence of tumor growth (Patz 2000; Collins *et al.* 2007). SCC has a very strong association with smoking, frequently found in males (Muscat *et al.* 1995) and unlike adenocarcinomas, generally metastasizes late in the disease course (Patz 2000).

SCC was the most frequent histologic type of lung tumor prior to the 1990s (el-Torky *et al.* 1990). However, more recent studies have reported a shift in the relative frequency of lung cancer types such that adenocarcinoma now is more frequent than SCC, particularly in women (Vincent *et al.* 1977; Tanaka *et al.* 1988; el-Torky *et al.* 1990; Migaldi *et al.* 1996). A review of the histopathologic data for lung carcinomas of almost 5000 patients entered into a tumor registry between 1964 and 1985 in the United States shows that adenocarcinoma is the most common lung tumor in women, accounting for approximately 40% of the cases (el-Torky *et al.* 1990). Interestingly, SCC has remained the major histologic tumor type in men, but its incidence has

decreased from 50 to 37%, while the incidence of adenocarcinoma has increased from 13 to 27% (el-Torky *et al.* 1990).

1.7.2.2. Large cell carcinoma (LCC)

LCC is a poorly differentiated, fast-growing form of lung cancer that shows no evidence of differentiation to either a squamous or a glandular phenotype (adenocarcinoma). LCC occurs less frequently than other lung cancers and accounts for only 10% of total lung cancers (Travis *et al.* 1995). Histological features of malignant cells are large nuclei, abundant cytoplasm and usually well defined cell borders (Travis *et al.* 1995; Travis 2002). LCCs generally behave like adenocarcinomas in terms of presenting at the periphery of the lung as large masses, but spread more aggressively (Travis *et al.* 1995; Travis 2002). Another feature of LCCs is that they are strongly associated with smoking and metastasize very early (Travis 2002). Large cell neuro-endocrine carcinoma is a major subtype of LCC and is believed to be derived from neuroendocrine cells (Fernandez *et al.* 2006). It is proposed that large cell neuro-endocrine carcinoma of the lung is a poorly differentiated, high-grade neuroendocrine tumor that is morphologically and biologically classified in between atypical carcinoid and SCLC (Fernandez *et al.* 2006).

1.7.2.3. Adenocarcinoma

Adenocarcinomas are the most common subtype of NSCLC, accounting for 40% of all lung cancers (Alberg *et al.* 2005). According to epidemiological studies, adenocarcinoma has exceeded SCC as the most common type of lung carcinoma

during the past decade, and its early metastasis has become increasingly common (Vincent *et al.* 1977; Tanaka *et al.* 1988; el-Torky *et al.* 1990; Migaldi *et al.* 1996; Alberg *et al.* 2005; Collins *et al.* 2007). Adenocarcinomas usually appear as histologically heterogeneous peripheral masses (frequently starts near the gas-exchanging surface of the lung) and metastasize during the early stages of tumor growth (Travis *et al.* 1995; Travis 2002; Collins *et al.* 2007). Clara cells and alveolar type II cells, two major cell types present at bronchiole/alveolar junction (Raz *et al.* 2006) are proposed to be the most common sites of transformation in lung adenocarcinoma. Adenocarcinomas have been reported to frequently occur in patients with underlying lung disease (Travis *et al.* 1995). Despite the fact that most cases of lung adenocarcinoma are linked to tobacco smoking, adenocarcinoma is also the most common form of lung cancer amongst non-smokers (particularly female non-smokers), young people, and women of all ages (Muscat *et al.* 1995; Subramanian *et al.* 2007; Sun *et al.* 2007). Bronchioalveolar carcinoma, a subtype of adenocarcinoma, is more common amongst female non-smokers and may have different responses to current treatments (Raz *et al.* 2006; Song *et al.* 2007). Although there are inconsistencies between IHC and electron microscopy (EM) studies, most studies indicate that non-mucinous bronchioalveolar carcinoma consists of Clara cells or alveolar type II cells (Raz *et al.* 2006; Song *et al.* 2007).

1.7.3. Stages of NSCLC cancer

After diagnosis of NSCLC, staging of lung cancer through a combination of methods is needed to determine how far the disease has spread. Understanding the

stages of NSCLC is crucial in terms of therapeutic and prognostic decisions (Mountain 1997; Pfister *et al.* 2004).

Occult stage: Also called *the hidden stage* in which malignant cells are found in the sputum, but a solid tumor cannot be detected in the lung by imaging or bronchoscopy (Mountain 1997; Clifton F. Mountain 2000).

Stage 0: At this stage, abnormal cells can only be found in a local area and in a few epithelial layers of cells which may become malignant and spread into adjacent normal tissue. Another term for this type of lung cancer is *carcinoma in situ* (Mountain 1997; Clifton F. Mountain 2000; Pisters *et al.* 2007).

Stage I: Patients with stage I NSCLC are considered to have "local" disease. In this stage a small size tumor or growth (3 cm or smaller) is formed in the lung, but has not spread to the surrounding normal tissue or lymph nodes or any other distant organ. The average 5-year survival rate at this stage is 47% (Mountain 1997; Clifton F. Mountain 2000; Pisters *et al.* 2007).

Stage II: This stage of NSCLC is still considered local disease, with an increased likelihood that the cancer has spread to the nearby lymph nodes, but not to any distant sites. The average 5-year survival rate at this stage is decreased to yet 26%. Stage II is subdivided into stages IIA and IIB (Mountain 1997; Clifton F. Mountain 2000; Pisters *et al.* 2007). In stage IIA, the tumor is 3 cm or smaller and has invaded nearby chest structures. At this stage, one or more lymph nodes on the same side of the chest are involved, but there is no spread to distant sites.

Stage IIB is assigned in two situations: **1)** the tumor is larger than 3 cm with invasion to nearby tissue and spread to one or more lymph nodes on the same side of the chest, **2)** the tumor has not spread to the lymph nodes, but has either spread to the

chest wall, the diaphragm, the pleura, or pericardium. The tumor may also have spread to the main bronchus of the lung and is 2 cm or more from the carina (where the trachea joins the bronchi) (Mountain 1997; Clifton F. Mountain 2000; Pisters *et al.* 2007).

Stage III: Stage III is also subdivided into stages IIIA (surgical) and IIIB (non-surgical) (Mountain 1997; Clifton F. Mountain 2000; Pisters *et al.* 2007). In stage IIIA, the tumor can vary in size, and has invaded lymph nodes on the same side of the chest. The tumor may have also spread to the chest wall, diaphragm, pleura, main bronchus or the membrane around the heart, however it has not spread to the trachea. In stage IIIB, the tumor can vary in size and has spread to the lymph nodes on the opposing side of the chest. The tumor may also spread to chest wall, diaphragm, trachea, sternum, esophagus, heart. The tumor may be found in more than one location on the same lobe of the lung, and in the pleural fluid. The average 5-year survival rate at this stage is only 8% (Mountain 1997; Clifton F. Mountain 2000; Pisters *et al.* 2007).

Stage IV: Stage IV lung cancer is the most advanced stage in which the cancer has spread to the lymph nodes as well as other lobes of the lungs or to other parts of the body such as the brain, liver, adrenal glands, kidneys, or bone. The average 5-year survival rate at this stage is very low (2%). Unfortunately, lung cancer is often diagnosed at this late stage when the tumor has already spread to other parts of the body (Mountain 1997; Clifton F. Mountain 2000; Socinski *et al.* 2003; Pisters *et al.* 2007).

1.7.4. Molecular biology of NSCLC

Normal cell growth and proliferation is tightly regulated by the balance of growth-promoting and growth-inhibiting factors. This allows differentiated cells to grow in a well controlled and regulated manner, in order to maintain the normal integrity and functioning of the organ. One of the hallmarks of malignant tumors is uncontrolled cell proliferation. Like other neoplasia, lung cancer also occurs as a result of multiple molecular alterations including activation and overexpression of oncogenes, deletion and reduced expression of tumor suppressor genes, and various types of cytogenetic events (Wistuba *et al.* 1997; Wistuba *et al.* 2000). Oncogenes, growth factors, and their receptors, play a central role during lung tumorigenesis. EGF and its receptor (EGFR) have been identified as being key elements in the process of cell growth and proliferation.

EGFR is a 170 kDa membrane protein consisting of an extracellular EGF-binding domain, a short transmembrane region, and an intra-cellular domain with ligand-activated tyrosine kinase activity (Chen *et al.* 1989). EGFR has two common ligands: EGF and transforming growth factor-alpha (TGF-α) (Chen *et al.* 1989). Binding of TGF-α to EGFR results in the activation of the tyrosine kinase domain, followed by phosphorylation, and an increase in cytosolic Ca^{2+} within target cells. This results in increased DNA synthesis and proliferation as well as differentiation of the affected cell (Chen *et al.* 1989). Increased activity of the EGFR has been implicated in a variety of solid tumors including NSCLC, (Rusch *et al.* 1997) and its expression is a poor prognostic indicator in NSCLC patients (Ohsaki *et al.* 2000). Reissmann *et al*. (Reissmann *et al.* 1999) studied the expression of the *cyclin D1* and *EGFR* genes by

Northern blot and IHC analysis in a group of 298 NSCLC specimens, and observed that *EGFR* gene was overexpressed in 13% of the cohort.

EGFR has been shown to be overexpressed in many solid tumors including lung and breast cancer (Biscardi *et al.* 2000; El Hiani *et al.* 2009). This has led to the development of therapies targeting EGFR including anti-EGFR antibodies to block the growth of human tumor cells and chemotherapeutic agents which block the tyrosine kinase activity of these receptors (erlotinib or gefitinib). Unfortunately, all patients who initially respond to EGFR inhibitor therapy will eventually develop a resistance to the drugs (Pao *et al.* 2005), which is due to a second mutation in the EGFR (Pao *et al.* 2005).

The *RAS* family of oncogenes (*H-ras*, *K-ras*, and *N-ras*) encode a GTP-binding protein named RAS that generates a growth-promoting signal (Malumbres *et al.* 2003). The genes and their encoded proteins play a vital role in several signal transduction pathways in normal cells and have been shown to be deregulated in many neoplasias (Malumbres *et al.* 2003). A mutation in oncogenic *RAS*, results in a loss of stability of hydrolyzed GTP, resulting in a constitutively active RAS-GTP growth-promoting activity (Malumbres *et al.* 2003). Oncogenic *K-ras* is the most frequently activated *RAS* gene in lung cancer and is usually caused by a point mutation (Slebos *et al.* 1992). *K-ras* mutations have been detected in approximately 20-30% of lung adenocarcinomas, 15-20% of all NSCLCs, but are rarely observed in SCLCs (Richardson *et al.* 1993; Salgia *et al.* 1998). The majority of the point mutations occur in *K-ras* codons 6, 12 or 13 (Richardson *et al.* 1993; Salgia *et al.* 1998). Several studies (Slebos *et al.* 1990; Mitsudomi *et al.* 1991) have reported a correlation between the presence of *K-ras* mutations and poor prognosis of NSCLC patients. Lipid

modification of RAS (farnesylation) has been shown to be regulated by the enzyme farnesyltransferase and is essential for RAS activity (Omer *et al.* 1997). As such, several farnesyltransferase inhibitors are currently being investigated in clinical trials to control tumor growth (Omer *et al.* 1997; Kim *et al.* 2006).

Several tumor suppressor genes including *p53*, *p16* and *RB* have been shown to be involved in lung cancer (Richardson *et al.* 1993; Salgia *et al.* 1998). The tumor suppressor gene *p53* is located at chromosome region 17p13.1 and encodes a 53 kDa nuclear protein (Vogelstein *et al.* 1992). p53 is responsible for maintaining genomic integrity in the face of DNA damage from gamma or UV irradiation, blocking cell cycle progression in late G_1 phase, and triggering apoptosis (Sidransky *et al.* 1996). Mutations in the *p53* gene are one of the most common genetic changes associated with cancer, and lead to the loss of its tumor suppressor function and ability to induce apoptosis (Sidransky *et al.* 1996; Stuppia *et al.* 1997). Mutation of the *p53* gene is reported in 40–60% of all NSCLCs, with a higher incidence in SCCs as compared to adenocarcinomas (Nishio *et al.* 1996). *p53* point mutations have been reported in lung tumors which correlate with benzo(a)pyrene-induced damage caused by cigarette smoking, and are mostly due to a GC to TA transversion resulting in missense mutations (Greenblatt *et al.* 1994). The prognostic value of p53 expression or mutations is controversial, since p53 mutations have been linked to positive cisplatin-based chemotherapy or radiotherapy response in patients with NSCLC (Kandioler-Eckersberger *et al.* 1999; Matsuzoe *et al.* 1999).

$p16^{Ink4A}$ is another targeted tumor suppressor protein belonging to the family of cell cycle regulators known as *cyclin-dependent kinase inhibitors* (CDKI). $p16^{Ink4A}$ regulates retinoblastoma (RB) function by binding to cyclin-dependent protein kinase

4 (CDK4) and CDK6. This binding blocks the activity of CDK4 and promotes cell cycle progression through G_0/G_1 phase (Marx 1994; Sherr 1996). Therefore, *p16*^{Ink4A} inactivation is another means for tumors to disrupt the p16^{Ink4a}-cyclin D1-CDK4-RB cell cycle control pathway (Marx 1994). Inactivation of the *p16*^{Ink4A} gene by hypermethylation and homozygous deletion has been detected in most NSCLCs (You *et al.* 1998). Detection of a specific alteration in oncogenes or tumor suppressor genes in pre-neoplastic or pre-invasive lesions suggests that these abnormalities may be useful as biomarkers for lung cancer. The ultimate goal of using these biomarkers would be to identify individuals at high risk for developing lung cancer, diagnose lung cancer during its early stages, and monitor the efficiency of lung cancer therapies.

1.8. Mouse models of human lung cancer

In recent years, several mouse models for human NSCLC and SCLC have been characterized. Mouse models for lung cancer include strains that are susceptible to spontaneous and chemically-induced lung tumors as well as several transgenic mouse strains that express known viral and cellular oncogenes (Rehm *et al.* 1991; Meuwissen *et al.* 2001; Wang *et al.* 2006) (Shimkin *et al.* 1975). The primary goal for developing mouse models of human lung cancer is to gain insight into the biology of the disease. This is accomplished by dissecting the molecular pathways involved in initiation and progression of lung cancer. The susceptibility and occurrence of spontaneous lung tumors varies largely between inbred-mouse strains (Shimkin 1955; Manenti *et al.* 2003). Spontaneous lung cancer develops in approximately 3% of wild-type mice, and has a higher incidence in inbred strains (Shimkin 1955). Among them, A/J and SWR mice are the most sensitive strains, while other strains like O20 and BALB/c are moderately sensitive. CBA and C3H are relatively resistant strains, while C57BL/6 and DBA are almost completely resistant to spontaneous lung tumors (Shimkin 1955). CD-1 is the outbred-mouse line commonly used in toxicology and carcinogenicity bioassays with a 21.8% mean incidence of spontaneous lung tumors (Manenti *et al.* 2003) which is lower than the lifetime incidence of spontaneous lung tumors in A/J mice or SWR/J mice but similar to that of BALB/c mice. The prevalence of lung tumors in the A/J strain is about 100% by 18-24 months of age, which is shown to have a strong correlation with a polymorphism in the second intron of oncogene *K-ras* (You *et al.* 1992).

Although not all of these mouse lung tumors are identical to human lung cancer, spontaneous lung adenocarcinomas in mice are quite similar to human adenocarcinomas in morphology, histopathology, and molecular characteristics (Jackson *et al.* 2001; Meuwissen *et al.* 2005; Wang *et al.* 2006). Mouse models for lung adenocarcinoma can thus serve as a valuable tool not only for understanding the molecular mechanisms that control the development of this disease, but also for the development and validation of new tumor intervention strategies as well as for the identification of markers for early diagnosis.

The first mouse models of human lung cancers were developed using chemical carcinogens (Croninger *et al.* 1958). These potentially carcinogenic agents are polycyclic aromatic hydrocarbons and nitrosamines derived from tobacco and ethyl carbamate (Goldman *et al.* 2001). Induction of lung tumors with chemical carcinogens is a very reproducible approach particularly for pulmonary adenoma and adenocarcinomas (Shimkin *et al.* 1975). Strains such as A/J and SWR mice that have a high frequency of spontaneous lung tumors are also very responsive to chemical induction of lung tumors (Shimkin *et al.* 1975). In addition to pulmonary adenocarcinoma, mouse models for pulmonary SCC have also been developed by intratracheal intubation of methyl carbamate (MC) (Nettesheim *et al.* 1971) or prolonged topical application of N-nitrosomethyl-bis-chloroethylurea (NMBCU) or N-nitroso-trischloroethylurea (NTCU) (Rehm *et al.* 1991).

Advances in transgenic technology to generate conventional transgenic animals has extensively improved the ability to study the role of specific genes in the process of transformation and tumor progression *in vivo* (Whitsett *et al.* 2001). The first generation of transgenic mouse models for lung cancer constitutively expressed cell

cycle regulatory genes in the pulmonary epithelium (Dutt *et al.* 2006). Two promoters have been extensively used to direct the transgene to cells in the mouse lung are: the *SP-C* promoter, which targets gene expression primarily to the alveolar type II cells (Glasser *et al.* 1991) and the *Clara Cell secretory protein (CCSP)* promoter, which targets the transgene expression to the non-ciliated secretory cells of the airways (Stripp *et al.* 1992; Ray *et al.* 1995). These two promoters have been used to deliver many regulatory proteins specifically to the lung cells to study their role in lung development, physiology, and oncogenic transformation (Whitsett *et al.* 2001). Studying expression of surfactant protein gene and protein using *in situ* hybridization and IHC suggest that alveolar type II cells are the predominant cell type in murine pulmonary adenomas (Mason *et al.* 2000).

The first targeted oncogene for induction of tumors in the lung was the simian virus large T antigen (T Ag). Both the *SP-C* (Wikenheiser *et al.* 1992; Wikenheiser *et al.* 1997) and *CCSP* (DeMayo *et al.* 1991; Magdaleno *et al.* 1997) promoters were used to direct the expression of the T Ag to the target cells in the lung. Expression of T Ag in these models leads to a rapid transformation of the pulmonary epithelium and results in an adenocarcinoma that becomes visible within the first few months of life. Lung-specific expression of different targeted proteins, such as c-myc (Geick *et al.* 2001), and the human achaete schuete gene (Linnoila *et al.* 2000) or deletion of tumor suppressor genes such as dominant-negative *p53* (Tchou-Wong *et al.* 2002), generate pulmonary oncogenic transformation in mice leading to different types of lung cancer. However, in mouse models of lung adenocarcinoma (similar to human), *K-ras* mutations are one of the most common genetic alterations and are frequently associated with alterations in the p53 pathway (Jackson *et al.* 2001; Wang *et al.* 2006).

Although the *SP-C* and *CCSP* promoters are valuable tools in the establishment of mouse models for lung cancer, these two promoters activate gene expression early in development, which limits the use of this type of mouse models in studying lung cancer initiation and progression. Gene transcription under the control of the *SP-C* promoter starts at embryonic day 10 (Wert *et al.* 1993) and the *CCSP* promoter is active at around embryonic day 17 (Ray *et al.* 1996). Expression of genes that disrupt the process of lung development will result in an embryonic lethal phenotype, which limits investigation of lung cancer progression. Moreover, in a conventional transgenic approach, transcription of the transgene is permanent, meaning that once transcription of the transgene is initiated, it is irreversible. Thus, to overcome the limitations of using conventional transgenic approaches in studying lung cancer, investigators have generated conditional transgenic mouse models.

The most effective regulatory systems for conditional transgenic mice are the ligand-inducible binary transgenic systems (Lewandoski 2001). They consist of at least two transgene constructs; a regulator transgene and a target transgene. The regulator transgene encodes a transcription factor whose transcriptional activity is controlled by the administration of an exogenous compound (for example tetracycline in the tetracycline-responsive binary system). The regulator is placed under the control of a tissue-specific promoter to facilitate expression of the transcription factor in the tissue of interest. Cre/LoxP-mediated modification technology (Gu *et al.* 1993) including excision, inversion, insertion and many other approaches are being widely used to generate transgenic mice to study tumor development in the lung using conditional alleles of tumor suppressor genes as well as oncogenes.

Jackson and colleagues (Jackson *et al.* 2001) developed a mouse model of lung adenocarcinoma by employing a method based on the Cre-loxP recombination system to conditionally activate an allele of oncogenic *K-ras* in the lung. They infected the lung with a recombinant adenovirus expressing Cre-recombinase, to induce oncogenic K-ras expression in the lungs of transgenic mice. Four weeks post-infection, the mice showed an onset of adenomatous alveolar hyperplasia, which further developed into adenocarcinomas at 9-12 weeks post-infection. Adenovirus administration enabled investigators to precisely map the initiation of tumorigenesis, and characterize the stages of tumor progression in these mice. Of particular interest, lung cancer in this mouse model did not metastasize to other organs, possibly due to rapid local tumor progression resulting in a shortened life span. The same mouse model generated by another group also showed a similar phenotype (Meuwissen *et al.* 2001).

Conditional transgenic mouse models will further clarify the specific molecular mechanisms occurring during the process of initiation and progression of lung cancer by allowing for the cell-specific-regulated ablation or expression of genes in the lung. Another advantage of conditional lung tumor models is that they can serve as useful models to discover new and potentially clinically relevant biomarkers for lung cancer that are indicative of the early stages of the disease (Dutt *et al.* 2006; Wakamatsu *et al.* 2007).

1.9. Rationale

The current model for lung cancer development suggests that tumors develop as part of a multi-step transformation of a normal cell into a malignant cell through elevated oncogene function in combination with the loss of tumor suppressor genes (Sato *et al.* 2007; Wakamatsu *et al.* 2007; Diaz-Meco *et al.* 2008). Chronic cigarette smoking results in lung inflammation and epithelial damage that activates a chronic wound repair program (Walser *et al.* 2008). Several groups have reported genetic damage in the early stages (pre-neoplastic lesions) of tumor development in lung epithelial cells of current or former smokers (Wistuba *et al.* 1997; Spira *et al.* 2004; Reynolds *et al.* 2006; Spira *et al.* 2007). This highlights a role for epithelial cell damage, tissue renewal and inflammation in the initiation and progression of lung cancer via different pathways, such as up-regulation of oncogenes, downregulation of tumor suppressors and EMT (Wistuba *et al.* 1997; Spira *et al.* 2004; Walser *et al.* 2008).

Recent studies have also demonstrated the ability of BMDCs to respond to epithelial damage and contribute to epithelial repair in the lung (Kotton *et al.* 2001; Ishizawa *et al.* 2004; Yamada *et al.* 2004). BM stem cells have been shown to possess an unexpected degree of plasticity and often reside in other tissues including the lungs and contribute to the process of epithelial repair (Petersen *et al.* 1999; Kotton *et al.* 2001; Ishizawa *et al.* 2004; Yamada *et al.* 2004). The traditional view of neoplasia and tumorgenesis indicates that tumors generally originate from the transformation of their tissue-specific stem cells. However, BMDCs which are frequently recruited to sites of inflammation and tissue injury, may also undergo malignant transformation and

represent a potential source of neoplasia (Houghton *et al.* 2004; Liu *et al.* 2006; Avital *et al.* 2007; Janin *et al.* 2009; Worthley *et al.* 2009).

Using the *Helicobacter*-infected mouse model of gastric cancer, Houghton and colleagues (Houghton *et al.* 2004) demonstrated that gastric cancers originated from BMDCs. This provides a direct link not only between chronic inflammation and carcinogenesis, but also initiation of gastric cancer from BMDCs. In support of this finding, several studies have shown a rare occurrence of tumors originated from the donor BM cells in patients with a history of BM transplantation (Avital *et al.* 2007; Janin *et al.* 2009; Worthley *et al.* 2009). This suggests that the same disease processes which has been observed in the mouse may also occur in humans.

A transgenic mouse model overexpressing CRT under the control of the *Tie2* promoter (referred as *Tie2-CRT* mice) was previously generated in our laboratory. These mice show a high incidence of tumor development in the lungs. Several proteomic studies showed changes in CRT expression in different human cancers, (Zhu *et al.* 1999; Brunagel *et al.* 2003; Kageyama *et al.* 2004; Toquet *et al.* 2007; Vougas *et al.* 2008; Alur *et al.* 2009) however, no data are available concerning the role of CRT in lung cancer development. The *Tie2* promoter is active in endothelial cells, endothelial progenitor cells and HSCs (Iwama *et al.* 1993; Sato *et al.* 1993; Arai *et al.* 2004). The unexpected observation of reproducible lung tumor formation in the *Tie2-CRT* mice suggested a possible role of vascular integrity and HSCs (besides alveolar and Clara cells) in the lung tumorigenecity. Therefore, in the current study we further characterized this transgenic mouse model and examined the possible role that HSC might play in the lung cancer development in *Tie2-CRT* mice.

1.10. Hypothesis

Overexpression of CRT in endothelial cells and HSCs results in an increased inflammatory response in the *Tie2-CRT* mice that facilitates mobilization and recruitment of HSCs to the lungs. Ultimately, this higher rate of inflammation in the lungs leads to the malignant transformation of the recruited HSCs and the formation of lung adenocarcinoma.

To test this hypothesis, we examined the following aims:

1. To characterize the lung tumors developed in *Tie2-CRT* mice by studying:
   1.1. Histogenesis of lung tumors developed in *Tie2-CRT* mice.
   1.2. *In vivo* and *in vitro* progression of lung tumors observed in *Tie2-CRT* mice.
   1.3. Properties of lung tumor cells isolated from *Tie2-CRT* mice.

2. To investigate whether the mobilization of HSCs is altered in *Tie2-CRT* mice by:
   2.1. Examining changes in HSC number in the BM and circulating blood of *Tie2-CRT* mice as compared to their *wt* littermates.
   2.2. Test the ability of HSCs to grow under anchorage independent conditions.

3. To measure changes in endogenous CRT expression in human and mouse lung adenocarcinomas.

CHAPTER II: MATERIALS AND METHODS

2.1. Reagents and chemicals

Dulbecco's Modified Eagle Medium (DMEM), RPMI 1640, OPTI-MEM® I (Reduced Serum Medium), Fetal Bovine Serum (FBS), Agarose (DNA grade), granulocyte macrophage colony stimulating factor (GM-CSF), IL-3 and Low Melting Point Agarose (L.M.P Agarose) were all purchased from Invitrogen (Burlington, ON). Western Blotting Luminol Reagent was purchased from Santa Cruz Biotechnology (Santa Cruz, CA). Nitrocellulose membrane, pre-stained broad-range and low-range protein standard markers and DC Protein Assay kit were obtained from Bio-Rad Laboratories (Mississauga, ON). Primers used for PCR were all ordered from Sigma Genosys (Sigma-Aldrich, Oakville, ON). All other chemicals used were of the highest analytical grade and were purchased from Sigma (Sigma-Aldrich, Oakville, ON), Fisher (Fisher Scientific, Ottawa, ON) or VWR (VWR International, Mississauga, ON).

2.2. Antibodies

Antibodies used for immunohistochemistry (IHC), immunofluorescence (IF) and western blotting were: SP-C, CC10, CRT, Mac-3, CD117 (c-kit), Tie2, CD133, CD31, vWF, Sca-1, CD34, HA, E-Cadherin, VEGFR-3, PTEN, p53, P-Akt (Ser473), α-Fetoprotein and α-actin. The majority of antibodies used were commercially available with the exception of anti-CRT which was a gift from Dr. Marek Michalak (University of Alberta) and anti-VEGFR-3 which was a gift from Dr. Daniel Dumont (University of Toronto). Further details for each individual antibody are outlined in

Table 3. Secondary antibodies were purchased from Jackson ImmunoResearch Laboratories (West Grove, PA, USA) and detailed specifications for each antibody used are highlighted in Table 4.

Table 3: List of primary antibodies and dilution factors used in this study

Antibody	Species	Application	Dilution	Catalog #	Source
CC10	Rabbit	IHC	1/1000	sc-25555	Santa Cruz Biotechnology
CD117 (c-kit)	Rabbit	IHC	1/50	sc-168	Santa Cruz Biotechnology
CD133	Rabbit	IHC, IF	1/200	ab19898	Abcam
CD31 (PECAM)	Rat	IHC, IF	1/250	550274	BD Biosciences
CD34	Rat	IHC	1/100	119301	Biolegend
CRT	Goat	IHC WB	1/200 1/400	N/A	Dr. Marek Michalak U of Alberta
E-Cadherin	Rabbit	IHC	1/50	4065	Cell Signaling
HA Tag	Rabbit	IHC WB	1/3000 1/10000	600-401-384	Rockland
HA Tag	Rabbit	WB	1/200	026k4801	Sigma-Aldrich
Ki67	Mouse	IHC	1/200	550609	BD Biosciences
Mac-3	Rat	IHC	1/100	sc-19991	Santa Cruz Biotechnology
P53	Mouse	IHC WB	1/50 1/200	sc-6243	Santa Cruz Biotechnology
P-Akt (Ser473)	Rabbit	WB	1/1000	9271S	Cell Signaling
PTEN	Rabbit	IHC WB	1/100 1/200	138G6	Cell Signaling
Sca-1	Rat	IHC	1/200	108101	R&D System
SP-C	Rabbit	IHC	1/800	sc-13979	Santa Cruz Biotechnology
Tie2	Rabbit	IHC	1/200	sc-324	Santa Cruz Biotechnology
VEGFR-3	Rat	IHC	1/200	N/A	Dr. Dan Dumont, U of Toronto
vWF	Rabbit	IHC	1/800	A0082	Dako
α-actin	Rabbit	WB	1/1000	A2066	Sigma-Aldrich
α-Fetoprotein	Mouse	IHC	1/100	MAB1368	R&D System

Table 4: List of secondary antibodies and dilution factors used in this study

Antibody	Species	Application	Dilution	Catalog #	Source
Biotin-SP-conjugated	Donkey anti-mouse	IHC	1/400	715-067-003	Jackson Immunoresearch
Biotin-SP-conjugated	Donkey anti-goat	IHC	1/400	705-065-003	Jackson Immunoresearch
Biotin-SP-conjugated	Goat anti-rabbit	IHC	1/400	111-065-045	Jackson Immunoresearch
Biotin-SP-conjugated	Goat anti-rat	IHC	1/400	112-065-008	Jackson Immunoresearch
Cy2-conjugated	Goat anti-Rabbit	Flow cytometry	1/70	111-225-144	Jackson Immunoresearch
Fab fragment	Goat anti-mouse IgG	IHC	1/10	115-007-003	Jackson Immunoresearch
FITC-conjugated	Donkey anti-mouse	IF	1/70	715-095-150	Jackson Immunoresearch
FITC-conjugated	Goat anti-rabbit	IF	1/70	111-095-008	Jackson Immunoresearch
FITC-conjugated	Goat anti-rat	IF	1/70	112-095-008	Jackson Immunoresearch
HRP-Conjugated	Goat Anti-Rabbit	WB	1/10000	111-035-003	Jackson Immunoresearch
HRP-Conjugated	Goat Anti-Rat	WB	1/5000	Sc-2006	Santa Cruz Biotechnology
HRP-Conjugated	Rabbit Anti-Goat	WB	1/10000	305-035-003	Jackson Immunoresearch
R-Phycoerythrin-conjugated	Donkey anti-rat	Flow cytometry	1/100	712-116-153	Jackson Immunoresearch
Texas Red-conjugated	Goat anti-rabbit	IF	1/70	111-075-003	Jackson Immunoresearch
Texas Red-conjugated	Mouse anti-rat	IF	1/70	212-075-082	Jackson Immunoresearch

2.3. Generation of *Tie2-CRT* transgenic mice

To express exogenous CRT specifically in endothelial cells and HSCs, the CRT gene was placed under the control of the endothelial cell specific *Tie2* promoter (Dumont *et al.* 1992; Sato *et al.* 1993). As shown in Figure 3, the transgene cassette consisted of the *Tie2* promoter, the *Tie2* enhancer and the full-length CRT cDNA. To distinguish between endogenous CRT and exogenous CRT, a hemagglutinin tag (HA) was added to the carboxyl-terminus of the CRT cDNA upstream of the KDEL ER retention signal. The cassette was inserted in the *Hind III/Not I* sites of the pSPTg.T2FpAXK plasmid (a generous gift from Dr. T.N. Sato, University of Texas, Southwestern Medical Center). The plasmid was then digested with *Sal I* and the 691 kb fragment containing the *Tie2* promoter, *Tie2* enhancer, CRT-HA cDNA and SV40 polyadenylation site (Fig. 3) was gel purified. Transgenic mice were generated by microinjecting the transgene into fertilized CD-1 oocytes using standard techniques at the Genetic Model Centre of the University of Manitoba. Eight founder *Tie2-CRT* mice were identified which were bred at the R.O Burrell laboratory at St. Boniface Research Centre to establish colonies. Animals were housed according to the Animal Care and Use Committee (CCAC) guidelines and regulations and were monitored over several generations to determine their phenotype.

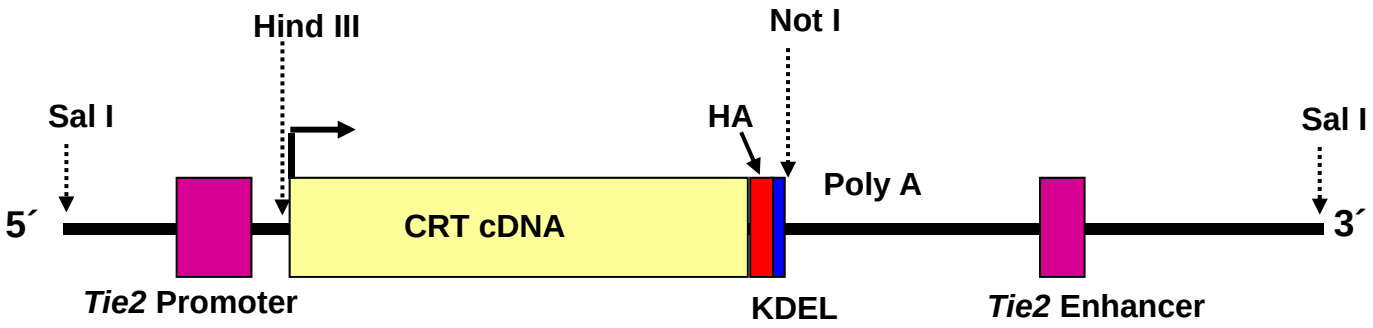

Fig. 3. Schematic diagram showing the transgene used to generate *Tie2-CRT* mice.
The transgene cassette consists of the full length CRT cDNA including the NH_2-terminal signal sequence and the COOH-terminal followed by the HA epitope tag and a KDEL ER retrieval signal. The CRT-HA cDNA was cloned into the Hind III/Not I sites of the pSPTg.T2FpAXK plasmid. The transgene was under the control of the *Tie2* promoter and also contained a polyA signal as well the *Tie2* Enhancer. The construct was linearized by digestion with SalI, gel purified, and microinjected into fertilized CD1 oocytes. The fertilized oocytes were then transferred into the oviduct of pseudopregnant CD1 mice. I would like to acknowledge Dr. Nasrin Mesaeli for designing and generating the transgene cassette used in generation of *Tie2-CRT* mice, Melanie Durston and Michael Wiwchar for establishing the mice colonies, genotyping and initial histo-pathological analysis of the mice.

2.4. Genotyping of transgenic mice

2.4.1. Isolation of genomic DNA

Genomic DNA was isolated from the tails of 4 week founder mice and subjected to PCR analysis to identify mice bearing the transgene. Briefly, a 2-5 mm tail segment was cut and homogenized in a buffer containing 10 mM Tris, pH 8.0, 0.1 M EDTA (Ethylene Diamine Tetraacetic Acid), 0.5% SDS (Sodium Dodecyl Sulfate) and 0.3 mg/ml proteinase K. Tissue lysate was incubated at 37°C for 1 hour followed by incubation at 50°C overnight. The samples were then cooled on ice for 5 minutes and 100µl of 4M NaCl was added to the mixture and incubated on ice for 10 minutes to precipitate any remaining proteins in the sample. The tubes were then centrifuged at 14,000 rpm for 10 minutes at room temperature. The supernatants were extracted with phenol/chloroform/isoamyl alcohol (25:24:1, v/v), and the samples were centrifuged at 14,000 rpm for 2 minutes at room temperature. Following a second extraction with chlorofom/isoamyl alcohol, to remove any residual phenol, the supernatant was collected, transferred into a new tube, and genomic DNA was precipitated by adding isopropanol and mixing. The tubes were then centrifuged at 14,000 rpm for 20 minutes at room temperature. The DNA pellet was washed with 70% ethanol and air dried on the benchtop. The genomic DNA was resuspended in 50-100µl of Tris/EDTA buffer (0.1M Tris, 1mM EDTA pH 8.0) and incubated at 65°C for 10 minutes. The concentration of DNA was then calculated using a GeneQuant *pro* RNA/DNA spectrophotometer (Fisher Scientific, Ottawa, ON).

2.4.2. PCR analysis

0.5-1µg of genomic DNA isolated from mice tails was used for PCR analysis. The 5′ primer (Tie2-5′) used for PCR corresponded to a sequence in the mouse *Tie2* promoter region, 5′-GGGAAGTCGCAAAGTTGTGAGTT-3′, and the 3′ primer (CR3′) corresponded to the 5' end of the CRT cDNA coding sequence, 5′-ATCTTCACCTCATACGTGTTGTCCGGCC-3′. The PCR reaction contained 10mM dNTP mix, 10µM of each primer, 50mM $MgCl_2$, 1X *Taq* Buffer and 0.5µl *Taq* DNA polymerase (Invitrogen, Burlington, ON) in a total volume of 50µl. The optimum annealing temperature was determined as being 60°C. The DNA was amplified by a single denaturing cycle for 15 minutes at 94°C followed by 35 amplification cycles as follows: 94°C for 30 sec; 60°C for 1 minute and 72°C for 45 sec. PCR products were separated on a 1% agarose gel and visualized by ethidium bromide staining. Images were obtained using the Bio-Rad Gel-Doc system and Quantity One program. A 650 bp fragment was amplified from the transgene and was only detected in samples from transgenic mice (Fig. 4).

2.4.3. Western blot analysis

Western blot analysis was carried out on proteins isolated from mouse tail samples using a rabbit anti-HA antibody from Rockland (Gilbertsville, PA, USA) to detect expression of exogenous CRT. Further details of the western blot analyses carried out in this study are explained in section 2.10.

2.4.4. Histological analysis

Expression of ectopic CRT was evaluated in different tissues including the lungs, aorta, BM and white blood cells by immunohistochemistry (IHC) and immunofluorescent (IF) staining as described in section 2.7. A rabbit anti-HA antibody from Rockland (Gilbertsville, PA, USA) was used to detect CRT-HA.

2.5. Tissue preparation

2.5.1. Soft tissue

For necropsy, animals were euthanized following an overdose of pentobarbital (CEVA SANTE ANIMALE, La Ballastière, Montreal, QC) (60 mg/kg i.p). Body weight was measured and recorded. Following euthanasia, blood was collected directly via cardiac puncture with a 1 ml syringe and blood smears were prepared. A portion of the whole blood was collected in EDTA coated tubes from BD Biosciences (Mississauga, ON) and used for a complete blood count (CBC). Plasma was collected by centrifugation of whole blood at 1,500 rpm for 10 minutes and stored at -80°C for future studies. The blood cell profiles were examined by the Clinical Pathology Laboratory of the Province of Manitoba Veterinary Services Branch using an Abbott Cell Dyn 3500. Blood glucose was measured immediately after euthanasia using the OneTouch UltraSmart Blood Glucose Monitoring System from Lifescan.

Tissue samples were collected during necropsy and fixed either in 4% formalin in phosphate buffered saline (1X PBS) or Zinc buffer. Tissues were then frozen in optimal cutting temperature (OCT) compound or embedded in paraffin using an automated tissue processor and histology suite located at the Institute of

Cardiovascular Sciences, St. Boniface Hospital Research Centre. Visible tumors were detected at the time of necropsy by examining the lungs using a Nikon stereo-microscope. Digital images of tissue samples were collected using a Nikon CoolPix 900 digital camera. Paraffin embedded tissue sections were further processed for histological and IHC examination as outlined below.

2.5.2. Bone decalcification and sectioning

Femurs and tibiae were collected from mice and were fixed in 4% formalin overnight. Bones were then washed in 1X PBS for a minimum of 30 minutes and were decalcified using a decalcification solution containing 4% hydrochloric acid (Fisher Scientific, Ottawa, ON) and 4% formic acid (Sigma-Aldrich, Oakville, ON). Bones were then removed from the decalcification solution and again washed in 1X PBS for 30 minutes. They were then subjected to an increasing sucrose gradient, 1 ml of 10%, 15%, and 20% sucrose in 1X PBS, for 2-3 minutes each. Next, bones were incubated in a solution of 1:1 optimal cutting temperature (OCT) (Fisher Scientific, Ottawa, ON) and 20% sucrose overnight at 4°C. Bones were then placed in OCT, frozen and kept at -80°C for later use. 4 micron bone sections were obtained using a cryostat and sections were post-fixed in cold acetone (-20°C) for 5-10 minutes. Sections were then processed for IHC as described below.

2.5.3. Isolation of bone marrow cells from femurs and tibia

Femur and tibiae (from both male and female mice) were harvested and the end of the bone was cut with a razor blade or scalpel to expose the marrow. BM cells were flushed out of the bone shaft using a 1 ml syringe equipped with a 26-gauge

needle filled with cold FACS buffer (5% FBS in 1X PBS). The syringe needle was moved up and down inside the bone to flush out any residual marrow. The red blood cells in BM were depleted using ammonium chloride lysis buffer (1.5 M NH_4Cl, 100 nM $KHCO_3$, 10 nM Na_4EDTA) for 15 minutes at room temperature (Current Protocols in Cytometry 1997). BM cells were then washed with cold FACS buffer and centrifuged at 400 x g for 15 minutes at 4°C. This step was repeated for a second time, the FACS buffer was discarded, and BM cells were collected (Current Protocols in Cytometry 1997). Isolated BM cells were then used for flow cytometry analysis or magnetic bead cell sorting.

For maintaining BM cells in culture, the procedure was repeated with replacing FACS buffer by RPMI media supplemented with 10% FBS and Penicillin/Streptomycin (Pen/Strep). Isolated BM cells were then used for soft agar cultures as described below.

2.5.4. Isolation of White Blood Cells using Ficoll-Hypaque solution

Whole blood (approximately 700-1000 µl) was collected from each mouse by cardiac puncture, placed in EDTA coated tubes from BD Biosciences (Mississauga, ON) and inverted gently to mix. The samples were centrifuged at 400 x g for 15 minutes at 4°C. 2 ml of Ficoll-Hypaque solution containing sodium diatrizoate (Sigma-Aldrich, Oakville, ON) and Ficoll Type 400 (Sigma-Aldrich, Oakville, ON) was added to the blood cells and inverted gently to mix. The samples were then centrifuged at 400 x g for 20 minutes at 18° to 25°C. The top layer of white blood cells (Buffy coat) was collected and transferred into a 2 ml tube. White blood cells were then washed twice

with ice cold 1X PBS and centrifuged at 400 x g for 15 minutes at 4°C. The supernatant was then discarded and white blood cells were collected.

2.6. Histological staining

Tissues were collected from both *Tie2-CRT* and *wt* animals (male and female) and used for histological and immunohistological examination. Tissues were fixed in 4% formalin for at least 72 hours and embedded in paraffin using a tissue processor (Thermo Shandon Excelsior Advanced Automatic Tissue Processor, Fisher Scientific, Ottawa, ON) and embedding machine (Shandon Histocentre 2 Embedding Center, Fisher Scientific, Ottawa, ON). Tissue sections (4μm) were prepared from representative paraffin blocks using a Shandon Finesse E Microtome Sectioner (Fisher Scientific, Ottawa, ON) and mounted on Superfrost Plus slides (Fisher Scientific, Ottawa, ON). The slides were dried overnight at 50°C in a slide dryer (Fisher Scientific, Ottawa, ON), cooled to room temperature and stored in a slide box at room temperature until use. For staining, slides were de-paraffinized in xylene for 10 minutes followed by rehydration by sequential incubation in 100, 95, 85, 75 and 50% ethanol for 3 minutes each. Slides were then washed with distilled water for 5 minutes and used for either Hematoxylin and Eosin (H&E) or IHC staining as described bellow.

2.6.1. H&E staining

For H&E staining a standard protocol of Harris Hematoxylin was used (Prophet *et al.* 1994). Briefly, after de-paraffinization and rehydration (as described above),

sections were washed in distilled water and stained in Harris hematoxylin solution for 8 minutes. Sections were then washed with running tap water for 5 minutes and differentiated in 1% acid alcohol (1% hydrochloric acid in 70% ethanol) for 30 seconds followed by another wash in running tap water for 1 minute. The intensity of hematoxylin staining was adjusted using a bluing solution (0.2% lithium carbonate in distilled water) for 30-60 seconds. Sections were then washed in running tap water for 5 minutes and dehydrated in 95% alcohol for a few seconds followed by counterstaining in eosin-phloxine solution for 30-60 seconds. Next, sections were washed and dehydrated through 95% alcohol and two changes of absolute alcohol for 5 minutes each and then cleared in xylene for 15 minutes. Slides were then mounted with Permount (Fisher Scientific, Ottawa, ON) and images were obtained using a Zeiss Axioskop2 microscope equipped with an AxioCam (Carl Zeiss Canada Ltd., Toronto). Images were analyzed with the Axiovision 4.6 program (Carl Zeiss Canada Ltd., Toronto).

2.6.2. Mucicarmine Staining

To examine the expression of mucin by lung cells, we used the previously described mucicarmine staining technique (Prophet *et al.* 1994). Briefly, sections were first de-paraffinized, rehydrated, and stained in Mayer's hematoxylin (Vector Inc, Burlington, ON) for 10 minutes. After a 5 minute wash in running tap water, sections were stained with mucicarmine solution at room temperature for 1 hour. Sections were then washed in distilled water for 5 minutes followed by staining with Metanil yellow for 30-60 seconds. Finally, sections were dehydrated with 95% alcohol and two changes of absolute alcohol for 5 minutes each and cleared in xylene for 15 minutes.

Slides were mounted with Permount (Fisher Scientific, Ottawa, ON) and images were collected as described above.

2.6.3. Oil Red O staining

Oil Red O (ORO) staining is commonly used to identify exogenous or endogenous lipid deposits in frozen sections of fresh or formalin-fixed tissue. For ORO staining, we used an established standard method (Prophet *et al.* 1994). Briefly, slides of frozen sections were air dried for 30-60 minutes at room temperature and then fixed in 4% formalin for 5-10 minutes. Slides were then washed in distilled water for 5 minutes and placed in 85% propylene glycol (in distilled water) for 10-15 minutes followed by staining with ORO (0.5% Oil Red O in propylene glycol) for 2-6 hours at room temperature. Slides were then washed in 85% propylene glycol for 5 minutes followed by a wash in distilled water for 5 minutes. Sections were then counter stained with Mayer's hematoxylin for 30 seconds and washed with distilled water for 5 minutes. Slides were mounted with aqueous mounting media and images were taken using a Zeiss Axioskop2 microscope.

2.6.4. Giemsa staining

Blood smears were prepared immediately from fresh whole blood obtained by cardiac puncture at the time of necropsy. Briefly, one drop of the blood was placed on a glass slide. A clean spreader slide was used to pick up the blood droplet behind the spreader and make the blood smear. The blood smear was then dried for 30 minutes at room temperature and used for Giemsa and MPO staining. For Giemsa staining, blood smears were fixed for 30 seconds by immersing in absolute methanol followed by

staining with freshly prepared 5% Giemsa stain solution from Sigma (Sigma-Aldrich, Oakville, ON) for 20-30 minutes. The blood smears were then washed using tap water and left to dry at room temperature.

2.6.5. Myeloperoxidase (MPO) staining

MPO is a peroxidase enzyme abundantly present in neutrophil granulocytes and in the lysosomes of monocytes of the myeloid cell lineage (Klebanoff 1999). To evaluate the presence of MPO in the white blood cells of *Tie2-CRT* and *wt* mice, blood smears were stained for MPO using a standard method (Haematology. 1993). Briefly, the blood smears were fixed for 30 seconds using a fixative (pH=6.6) containing Na_2HPO_4 (0.2 g anhydrous), KH_2PO_4 (1.0 g anhydrous), distilled water (300 ml), 37% formalin (250 ml) and acetone (450 ml). The blood smear was then stained in MPO reagent containing 10 mg AEC substrate (3-amino-9-ethylcarbazole), 6 ml DMSO (dimethyl sulfoxide), 50 ml acetone buffer and 0.005 ml of 30% H_2O_2 for 8 minutes at room temperature followed by a quick wash with distilled water. The blood smear was then counterstained with Mayer's hematoxylin for 30 seconds and rinsed with distilled water. The blood smear was air-dried and mounted with Permount (Fisher Scientific, Ottawa, ON).

2.7. Immunostaining

2.7.1. Immunohistochemistry (IHC) staining

Paraffin embedded mouse tissue was used for IHC. Paraffin sections of 4μm thickness were prepared using a Shandon Finesse E Microtome Sectioner (Fisher Scientific, Ottawa, ON). Sections were mounted on Superfrost Plus slides (Fisher Scientific, Ottawa, ON) and, dried overnight at 50°C in a slide dryer (Fisher Scientific, Ottawa, ON). For immunostaining, slides were first de-paraffinized in xylene and hydrated in graded ethanol to distilled water, followed by washings with a solution of 1X PBS (pH 7.4). Heat-induced Epitope Retrieval (HIER) was performed by placing the slides in a pre-warmed steamer (60-90°C) with citrate buffer (0.1 M citric acid, 0.1 M sodium citrate, pH 6.0) in a Coplin Jar for 30 minutes. The slides were then removed, and allowed to cool to room temperature for 20 minutes while they were remained in citrate buffer. They were then washed three times for 5 minutes in 1X PBS. Blocking solution (1.5 ml maleic acid, 0.5 ml FBS, 50 μl Tween 10%, 0.5 ml of stock blocking (Roche, Mississauga, ON) in 2.5 ml 1X PBS) was added to each slide and the slides were incubated in a humidified chamber for 30 minutes at room temperature to decrease background staining. The slides were then washed three times for 5 minutes in 1X PBS and incubated with 3% H_2O_2 (in 1X PBS) for 10 minutes at room temperature. The slides were then incubated with the Avidin and Biotin blocking Kit (Vector Inc, Burlington, ON) for 15 minutes followed by three washes with 1X PBS for 5 minutes.

Primary antibodies were then diluted (as listed in Table 3) in blocking solution and incubated with tissue sections at 4°C overnight in a humidified chamber. The next

day, the slides were washed three times for 5 minutes with 1X PBS. When using mouse primary antibodies on mouse tissues, sections were first incubated with unconjugated AffiniPure Fab Fragment goat anti-mouse IgG (Jackson ImmunoResearch Labs) for 1 hour to block endogenous mouse IgG. Next, biotinylated secondary antibody was diluted in blocking solution (as listed in Table 4) and incubated on the sections for 1 hour at room temperature. The slides were then washed again three times for 5 minutes in 1X PBS and ABC solution (Vector Inc, Burlington, ON) was added to the slides and incubated for 30 minutes at room temperature. After washing, DAB substrate (3,3-diaminodbenzidine) was added to the sections and incubated for 2-5 minutes. The reaction was stopped by the addition of distilled water for 5 minutes. Nuclei were counter stained with Mayer's hematoxylin for 3 minutes followed by 30 seconds in basic water (0.2% lithium carbonate in distilled water). The slides were then washed and dehydrated as described above and mounted with Permount (Thermo Fisher Scientific, Ottawa, ON). As a negative control, sections were processed as above but addition of primary antibody was omitted.

2.7.2. Immunofluorescence (IF) staining

2.7.2.1. IF staining of cells

Lung tumor cells isolated from *Tie2-CRT* mice as well as human lung tumor cells lines (A549 and H460) were grown on glass coverslips overnight in DMEM supplemented with 10% FBS and 10% Pen/Strep (100 units/ml). Coverslips were washed with cold 1X PBS and cells were fixed in 4% formaldehyde for 15 minutes at room temperature. Cells were then washed with 1X PBS three times to remove fixative, and blocked with blocking buffer (1X PBS containing 0.1% saponin and 2%

milk powder) for 30 minutes at room temperature. Cells were then incubated at 4°C overnight with primary antibodies diluted in blocking buffer (Table 3). After the incubation with primary antibody, coverslips were washed three times with 1X PBS containing 0.1% saponin, and incubated with either Fluorescein Isothiocyanate (FITC)-conjugated or Texas Red conjugated secondary antibody (Table 4, 1/70 dilution) for 1 hour in the dark at room temperature.

For co-immunostaining experiments, after the incubation with the first primary and secondary antibody, coverslips were washed three times with 1X PBS containing 0.1% saponin and the second primary antibody of interest (diluted in blocking buffer Table 3) was added to the cells and incubated at 4°C overnight in the dark. Next day, coverslips were washed three times with 1X PBS containing 0.1% saponin, and incubated with the second fluorescent labeled secondary antibody (Table 4, 1/70 dilution) for 1 hour in the dark at room temperature. Coverslips were then mounted on slides using ProLong Gold mounting media with DAPI (Invitrogen, Burlington, ON) for nuclear staining.

2.7.2.2. IF staining of tissues

Paraffin embedded mouse lung tissue was used for IF staining. Tissue sections (4μm thick) were prepared from paraffin blocks. Following de-paraffinization and rehydration (as described above), sections were washed in distilled water and used for IF staining. For antigen retrieval, the slides were incubated in preheated citrate buffer (0.1 M citrate acid, 0.1 M sodium citrate, pH 6.0) and placed in a steamer at 90-100°C for 30 minutes. The slides were then removed, cooled to room temperature and washed three times for 5 minutes with 1X PBS. Blocking solution (1.5 ml maleic acid, 0.5 ml

FBS, 50 µl Tween 10%, 0.5 ml of stock blocking buffer (Roche, Mississauga, ON) in 2.5 ml 1X PBS) was added to each slide and incubated in a humidified chamber for 30 minutes at room temperature. Primary antibodies (Table 3) were diluted in blocking solution and incubated with the tissue sections at 4°C overnight in a humidified chamber followed by subsequent washes with 1X PBS the following day. A fluorescent secondary antibody (Table 4) was diluted in blocking solution and incubated with the sections for 1 hour at room temperature in the dark. The slides were then washed three times with 1X PBS for 5 minutes. This step was repeated for co-staining. Slides were then mounted with an anti-fade mounting reagent containing DAPI (Invitrogen, Burlington, ON) and covered with a coverslip.

2.8. Microscopy and imaging

Slides were viewed using a Zeiss Axioskop2 microscope equipped with an AxioCam cooled digital camera. Digital images were captured and analyzed with Axiovision 4.6 software from Carl Zeiss. (Carl Zeiss Canada Ltd., Toronto).

2.9. Cell Culture

2.9.1. Establishment of a lung adenocarcinoma cell line from *Tie2-CRT* mice

To study the progression of the lung tumors observed in *Tie-CRT* mice *in vitro*, we established a lung adenocarcinoma primary cell line isolated from the tumors found in these mice. Fresh lung tumor tissues were excised from the lungs of *Tie2-CRT* mice and placed in sterile 1X PBS containing 10% Pen/Strep. The tumor was dissected away

from the surrounding normal lung tissue and then minced into small pieces under aseptic conditions. The minced tissue was incubated in 0.2 mg/ml collagenase type IV (Roche, Mississauga, ON) in 1X PBS at 37°C for 30 minutes with continuous rotation. 1X PBS containing 10% Pen/Strep was added to the cell suspension and then centrifuged at 1,000 x g for 15 minutes at 4°C. The supernatant was discarded, then 5 ml of DMEM containing 20% FBS and 10% Pen/Strep was added to the pellet and cells were further dissociated by trituration using a wide bore sterile pipette. The cell suspension was then plated in tissue culture plates and incubated in an incubator. Cells were then sub-cultured every two days for a period of 5 weeks to establish a lung tumor cell line. Once the cell line was established, several aliquots were frozen and stored in liquid nitrogen.

2.9.2. A549 (Human lung adenocarcinoma cell line)

To compare the data obtained from the cell lines of *Tie2-CRT* mice with human lung adenocarcinoma, we used an established human lung adenocarcinoma cell line (A549 cell line). The A549 cell line was purchased from the American Type Culture Collection (ATCC, VA, USA). Cells were grown in DMEM supplemented with 10% FBS, 10% Pen/Strep 100 units/ml. The media was changed every 48 hours and cells were sub-cultured when they reached 90% confluence.

2.10. Western Blot analysis

The expression of different proteins of interest in tumor cells and tissue isolated from experimental animals was evaluated using western blot analysis. Samples were lysed using ice cold new RIPA buffer (250 mM NaCl, 20mM Tris, 1 mM EDTA, 1 mM EGTA, 1 mM Na_3VO_4, 30 mM NaF, 10mM $Na_4P_2O_7$, 0.5% sodium deoxycholate, 1% Nonidet P-40, 1% Triton X-100, 0.5µM PMSF and a protease inhibitor cocktail) and centrifuged at 7,000 rpm for 10 minutes at 4°C. The protein concentration of each sample was analyzed using a DC protein assay kit from BioRad (BioRad, Mississauga, ON) according to the manufacturer's protocol. A total of 30µg of protein for each sample was separated on SDS-polyacrylamide gels (SDS-PAGE) (percentage varied from 7.5-15% depending on the size of the protein being examined). Low-range or broad range pre-stained protein ladder (Bio Rad, Mississauga, ON) was used to determine the molecular mass of the proteins. The proteins were then transferred to nitrocellulose membrane using a semidry transfer system. The details of solutions used for western blot analysis as well as the protocol used for preparing different concentrations of SDS-PAGE are outlined in Table 5 and Table 6.

Table 5. List of solutions, their composition and preparation for SDS-PAGE Western blot analysis.

Steps	Solution	Composition	Preparation
Casting gels	4 X Separating Gel Buffer	1.5 M Tris, 0.4% SDS, pH=8.8	54.52g Tris Base and 1.2g SDS Adjust pH to 8.8 and bring to a final volume of 300ml with ddH_2O. Store at RT
	4 X Stacking Gel Buffer	0.5 M Tris, 0.4% SDS, pH=6.8	12.14g Tris Base and 0.8g SDS Adjust pH to 6.8 and bring to a final volume of 200ml with ddH_2O. Store at RT
Electrophoresis	5 X SDS-PAGE Running Buffer	125 mM Tris, 960 mM Glycine, 0.5 % SDS, pH~8.3	15.1g Tris Base, 72g Glycine, 5 g SDS Make up to 1L with ddH_2O and store at RT or 4°C. For 1 X Running buffer: Dilute 1:5 with ddH2O
Transfer	1 X Transfer Buffer	25 mM Tris, 19.2 M Glycine 20% Methanol, pH~8.3	6.0g Tris Base, 28.8g Glycine, 400ml Methanol Make up to 2L with ddH_2O, Store at 4°C and use cold.
Washing	10 X PBS	137mM NaCl, 2.7mM KCl, 10mM Na_2HPO_4, 1.76 mM KH_2PO_4, pH=7.4	14.4 g Na_2HPO_4, 2.4 g KH_2PO_4, 2 g KCl, 80 g NaCl Make up to 1L with ddH_2O and store at RT.
	1 X PBST	13.7mM NaCl, 0.27mM KCl, 0.1mM Na_2HPO_4, 0.176 mM KH_2PO_4, 0.1% Tween 20, pH~7.4	200ml 10 X PBS, 200 µ1 Tween 20 Make up to 2L with ddH_2O and store at RT.
Blocking antibodies	5% milk in PBS		5% Non-fat skim milk powder in PBS
Diluting antibodies	1% milk in PBS		1% Non-fat skim milk powder in PBS

SDS = sodium dodecyl sµlfate, **ddH_2O** = double-distilled water, **RT** = room temperature, **PBS** = phosphate buffered saline, **PBST** = PBS Tween 20

Table 6: Protocol used for preparing different concentrations of SDS-PAGE gels.

Separating Gel

	7.5%		**10%**		**12.5%**		**15%**		**17.5%**	
	20ml	40ml	20ml	40ml	20ml	40ml	20ml	40ml	10ml	40ml
ddH_2O	9.65	19.3	8	16	6.8	12.6	4.85	9.8	1.67	6.66
4X Separating Gel Buffer	5	10	5	10	5	10	5	10	2.5	10
Acryl amide	5	10	6.7	13.4	8.35	16.7	10	20	5.84	23.34
TEMED	5µl	15µl	15µl	15µl	15µl	20µl	15µl	20µl	15µl	20µl
10% APS	75µl	150µl	150µl	150µl	150µl	200µl	150µl	200µl	150µl	200µl

3% Stacking Gel

	5ml	**10ml**	**20ml**
DDH2O	2.9	5.9	11.8
4X Stacking Gel Buffer	1.25	2.5	5
Acryl amide	0.95	1.9	3.8
TEMED	10	20	20
10% APS	100µl	200µl	200µl

APS = ammonium persulphate
Separating and Stacking Gel Buffers: see Table 4

Procedure for running gels:
75 V in Stacking Gel for 20-30 min
125 V in Separating Gel until it goes to bottom of gel

To prevent non-specific antibody binding, nitrocellulose membranes were incubated in 1X PBS containing 5% non-fat skim milk powder for 30 minutes at room temperature prior to antibody detection. The membrane was then incubated with primary antibody diluted in 1% non-fat skim milk powder in 1X PBS or 1% bovine serum albumin in 1X PBS as recommended by the manufacturer. Subsequently, the primary antibody was removed and the membrane was washed twice for 15 minutes in 1X PBS containing 0.1% Tween and once in 1X PBS for 15 minutes. The membrane was then incubated with HRP (Horseradish Peroxidase)-conjugated secondary antibody (Table 4) corresponding to the primary antibody used. The secondary antibody was also diluted in 1% non-fat skim milk powder in 1X PBS and was added to the nitrocellulose membrane and incubated for 1 hour at room temperature with constant mixing. The wash steps were repeated as above. The membrane was then incubated in with ECL (Enhanced Chemiluminescence) (Santa Cruz Biotechnology, Inc. Santa Cruz, CA) for 5 minutes and images were captured using a Fluor-S Max Imager (BioRad). The relative density of protein bands corresponding to each specific protein was captured and quantified using Bio-Rad QuantityOne software. To evaluate equal loading, each nitrocellulose membrane was stripped and re-probed with an antibody to cytoskeletal α-actin (1/1000, Sigma-Aldrich). Data were presented as the ratio of the specific protein band density to that of the α-actin protein.

2.11. Soft agar colony assay

2.11.1. Tumor cells

To examine the anchorage-independent growth of tumor cells, cells were cultured in a soft agar colony forming assay for 2-3 weeks. Briefly, 1% Low Melting Point Agarose (Invitrogen, Burlington, ON) was prepared in distilled water and autoclaved. For base agar, 2X DMEM/F12 with 20% FBS was warmed to 40°C in a water bath for at least 30 minutes after which it was added to an equal volume of warmed 1% agarose. 1.5 ml of the 0.5% Agar contianing 1X DMEM/F12 and 10% FBS solution was then layered into the wells of a 6-well culture plate and permitted to solidify at room temperature under aseptic conditions.

For the top agar, 0.7% Low Melting Agarose was mixed with 2X DMEM/F12 containing 20% FBS resulting in a final concentration of 0.35% Agar containing 1X DMEM/F12 and 10% FBS. This solution was kept at 40 ºC in a water bath. Cells were then counted using a hemocytometer, and 5,000 cells were suspended in 1.5 ml of 0.35% agarose in DMEM/F12 + 10% FBS. The cell suspension was then layered onto the base agar in 6-well plates. The plate was then incubated at 37°C in a humidified incubator in an atmosphere of 5% CO_2 and 95% air. After two weeks, the plates were stained with 0.5ml of 0.005% Crystal Violet for >1 hour and then the number of colonies in each plate was counted using a stereo-microscope.

2.11.2. Bone marrow cells

To evaluate the proliferative capacity of BM cells of both *Tie2-CRT* and *wt* mice, isolated BM cells from these mice (section 2.5.3) were cultured for 14 days in

soft agar culture media as previously described (Horowitz *et al.* 2002). Soft agar used for BM cells was same as one used for tumor cells except the DMEM/F12 was replaced with RPMI media. Briefly, base agar was prepared as explained above using RPMI medium to give 0.5% Agar containing 1x RPMI and 10% FBS and 10ng/ml IL-3 (Interleukin 3) (Invitrogen Burlington, ON) and 10ng/ml GM-CSF (Invitrogen Burlington, ON). Top agar was also prepared as explained above using RPMI medium to give 0.35% Agar containing 1x RPMI and 10% FBS, with the addition of IL-3 and GM-CSF. A volume of 1.5 ml base agar (0.5% Agar contaiing 1 RPMI and 10% FBS) was added to each well of a 6-well culture plate and set aside to solidify at room temperature. Cells were then counted using a hemocytometer, and $5x10^4$ cells were suspended in 1.5 ml of 0.35% agarose in RPMI containing 10% FBS supplemented with IL-3 and GM-CSF. The plate was then incubated at 37°C in a humidified incubator in an atmosphere of 5% CO_2 and 95% air. After two weeks, the plates were stained with 0.5ml of 0.005% Crystal Violet for >1 hour and the number of colonies in each plate was counted using a stereo-microscope.

2.12. Non-adherent sphere assay

To evaluate the ability of lung tumor cells isolated from *Tie2-CRT* to form colonies in serum-free non-adherent culture conditions, we performed a non-adherent sphere assay, which is a well established method that has already been used by several investigators (Ponti *et al.* 2005; Ricci-Vitiani *et al.* 2007; Eramo *et al.* 2008; Visvader *et al.* 2008; Tirino *et al.* 2009). The sphere assay has been shown to be an excellent technique to isolate stem cells and progenitor cells on the basis of their ability for self-

renewal and the expression of different surface markers (Tirino *et al.* 2009). Thus, in this study, a non-adherent culture condition was used to form spheres with stem cell-like characteristics. Briefly, lung adenocarcinoma cells derived from *Tie2-CRT* mice were plated at low density (60 000 cells per well) in six-well plates in DMEM/F12 with 10% Pen/Strep but without FBS. Cells were incubated at 37°C with 5% CO_2 for a period of 4 weeks to grow and form spheres that could be visualized using an inverted phase-contrast microscope.

2.13. Magnetic bead cell sorting

To isolate CD133 positive cells from the BM, we used a magnetic bead cell sorting kit (Miltenyi Biotec Inc. CA, USA). BM cells expressing CD133 were positively selected according to the manufacturer's protocol. Briefly, BM cells were isolated from the long bones of *Tie2-CRT* and *wt* mice (male and female) as described in section 2.5.3. A total of 10^9 nucleated BM cells, as estimated using a hemocytometer, were incubated on ice with a rabbit anti-CD133 antibody for 30 minutes. Next, cells were incubated for 15 minutes with magnetic microbeads that were conjugated to goat anti-rabbit antibodies on ice.

Samples were then placed in a magnetic field for 5 minutes and the unlabelled cells in the supernatant were transferred to a new tube. Samples were removed from the magnetic field and the CD133 labeled BM cells were collected. Cells were then resuspended in 500 µL buffer and the magnetic field separation was repeated to enrich for CD133 positive cells. To confirm the degree of cell purification, aliquots of CD133 positive and CD133 negative sorted cells were stained with a CD133 antibody using

the IF staining protocol described in section 2.7.2. The number of CD133 positive cells isolated from 10^9 BM cells of *Tie2-CRT* mice and *wt* controls were determined using a hemocytometer and the values were then graphed for comparison.

2.14. Flow Cytometry analysis

HSCs are normally formed and stored in the BM of adults until they are fully matured and then released into the blood circulation (Calvi 2003; Zhang *et al.* 2003). The presence of circulating HSCs in the blood circulation during normal homeostasis suggests a turnover in BM niches (Calvi 2003; Zhang *et al.* 2003). Therefore, to investigate whether the mobilization of HSCs was altered in *Tie2-CRT* mice, the total number of HSCs in the circulating blood and BM was examined using flow cytometry (MoFlo XDP cell sorter, Beckman Coulter, Flow cytometry Laboratory, University of Manitoba). Briefly, BM and blood samples were collected from both transgenic and *wt* littermates as described in section 2.5. RBCs were removed from the samples by incubation in ammonium chloride lysis buffer (1.5M NH_4Cl, 100nM $KHCO_3$, 10nM Na_4EDTA) for 15 minutes at room temperature (Current Protocols in Cytometry 1997). 10 ml of lysis buffer was used for every 1 ml of blood sample.

For immunostaining, cells were washed 2-3 times with FACS buffer (5% FBS in 1X PBS) and incubated with blocking buffer (1X PBS containing 0.1% saponin and 2% milk powder) for 30 minutes on ice. After 2-3 washes with FACS buffer, cells were re-suspended in 50µl of FACS buffer. Cells were then incubated with primary antibodies of interest (Table 3) and diluted in blocking buffer for 1 hour on ice. For co-immunostaining, primary antibodies raised in different species were mixed and

incubated with cells simultaneously. We co-stained c-kit (rabbit anti-mouse) with CD34 (rat anti-mouse) or c-kit (rabbit anti-mouse) with Sca-1 (rat anti-mouse). Cells were then washed 2-3 times with FACS buffer and the pellets from the final wash were suspended in 50µl of FACS buffer containing a mixture of secondary antibodies (for the two species) conjugated with fluorochromes. Cy2-conjugated goat anti-rabbit (1/70 dilution) and R-phycoerythrin-conjugated donkey anti-rat (1/100 dilution) were used for co-staining of the cells. Samples were mixed gently and incubated for 30 minutes on ice in the dark. Cells were then washed 2-3 times with FACS buffer and suspended in 200-300µl FACS buffer containing 1% PFA and then analyzed with a flow cytometer (MoFlo XDP cell sorter). In order eliminate non-specific signals during the flow cytometer experiments, we applied dual color compensation using unstained cells, green-only cells (Cy2 alone), red-only cells (R-phycoerythrin) and cells that had been labeled only with primary antibodies.

2.15. Tissue microarray and semi-quantitative scoring (H-scores)

To evaluate CRT expression in human lung adenocarcinoma, we carried out IHC staining for CRT on human tissue microarray (TMA) slides using a goat anti-CRT antibody. Briefly, a lung adenocarcinoma (grade I-III, 33 cases) TMA slide was obtained from US Biomax Inc. Each slide contained 96 cores of specimens (diameter 1 mm, 5 µm thickness each) from a malignant tumor, adjacent tissue and normal tissue.

The dilution factor of the CRT antibody was first optimized for IHC staining using normal lung tissue. TMA slides were then deparaffinized in xylene and rehydrated through a serial dilution of alcohol followed by washings with a solution of

1X PBS (pH 7.4). Sections were then submitted to heat-induced antigen retrieval in citrate buffer followed by incubation in blocking solution as described in section 2.7. For immunostaining, CRT primary antibody was diluted in blocking solution, added to the TMA slides, and incubated at 4°C overnight in a humidified chamber followed by subsequent washes with 1X PBS the following day. A biotinylated anti-goat secondary antibody was prepared in blocking solution and added to the slides and incubated for 1 hour at room temperature. The slides were then washed with 1X PBS and incubated with ABC solution (Vector Inc, Burlington, ON) for 30 minutes at room temperature. Staining of the antigen was then visualized using DAB substrate (3,3-diaminodbenzidine) and the sections were then counterstained with Mayer's hematoxylin (Vector Inc, Burlington, ON). The slides were washed, dehydrated, mounted with Permount (Thermo Fisher Scientific, Ottawa, ON), and used for microscopic examination and study comparison. To validate of the specificity of the CRT antibody in these IHC assays, CRT antibody was pre-incubated with 50 fold excess of CRT recombinant protein (a generous gift from Dr. Marek Michalak-Department of Biochemistry, University of Alberta) for 4 hours at 4ºC. The blocked antibody was then added to the TMA slide and the slides were then processed for IHC. Negative controls were obtained by processing the TMA slides in the same manner, but by omitting the primary antibody.

For evaluation of immunohistochemical staining, semi-quantitative scoring (H-scores) was used to assess positive staining for CRT protein expression in TMAs according to the method described previously by Skliris *et al.* (Skliris *et al.* 2008). The H-score was calculated by a semi-quantitative assessment of both staining intensity (scale 0–3) and the percentage of positive cells (0–100%), which, when multiplied,

generated a score ranging from 0 to 300. The intensity score was made on the basis of the average intensity of staining where 0 = negative, 1 = weak, 2 = intermediate and 3 = strong. Statistical analysis was carried out on the H-score data obtained. Scoring of the sections was performed by two blinded independent individuals.

2.16. Statistics

Statistical analysis of the data was carried out by using the two-tailed Student's *t*-test to determine significant differences at a p value ≤ 0.05. The data were plotted as the mean ± SE of individual experimental values.

CHAPTER III: RESULTS

3.1. Characterization of the *Tie2-CRT* mouse model

3.1.1. Detection of transgene expression

We have generated a transgenic mouse model overexpressing CRT under the control of the *Tie2* promoter. In total, eight transgenic founders were generated and used to establish colonies. To identify the transgenic mice in each litter, we used PCR of genomic DNA and specific primers Tie2-5′ and CR3′. Fig. 4A shows a representative PCR of genomic DNA isolated from *wt* and *Tie2-CRT* mice. As shown, amplification of *Tie2-CRT* genomic DNA produced the expected 650 bp fragment, while no signal was detected in the *wt* control. In order to demonstrate specific expression of the transgene CRT-HA in transgenic mice lines we carried out western blot assay and immunostaining with a rabbit anti-HA antibody on different tissues obtained from *Tie2-CRT* mice. Fig. 4B shows a representative western blot with the anti-HA antibody of the lung and white blood cells isolated from *Tie2-CRT* and *wt* littermates. A 62 kDa protein band was detected only in lung, white blood cells Fig. 4B, mouse tail (data not shown) and arteries (data not shown) of *Tie2-CRT* mice illustrating activity of *Tie2* promoter in the lung and white blood cells.

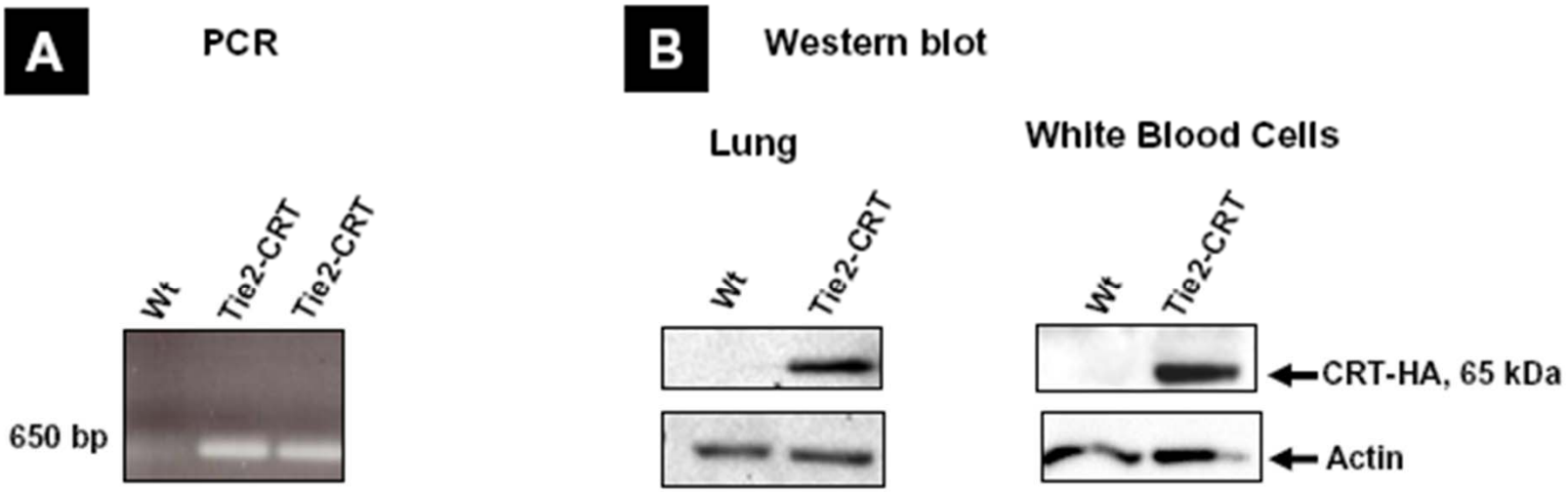

Fig. 4. Detection of transgene expression with PCR and Western Blot analyzing

Transgenic mice were identified by PCR analysis of genomic DNA isolated from tail biopsies as described in "Materials and Methods". (A) shows a representative PCR of genomic DNA of *Tie2-CRT* mice and *wt* littermates (n=10). A 650 bp amplicon was detected in samples from transgenic mice only. (B) A representative Western blot analysis with anti-HA antibody in the lung and white blood cells isolated from *Tie2-CRT* and *wt* littermates to examine the expression of the transgene in these tissues (n=10). Whole cell lysate from lung tissue and white blood cells were used for Western blot analysis using an anti-HA antibody and anti-actin as a loading control. A single protein band at 65 kDa was detected in protein samples isolated from *Tie2-CRT* mice only.

Fig. 5 shows IHC analysis of transgene (CRT-HA) expression in the EC of descending aorta of *Tie2-CRT* mice as compared to their *wt* littermates. CRT-HA was highly expressed only in the EC of vascular wall of *Tie2-CRT* mice (Fig. 5 black arrows). HA positive cells (black arrows) were also detected in the sections prepared from the femurs of *Tie2-CRT* mice. In addition to BM sinusoid endothelial cells (Fig 6, red arrows), other BM cells also highly expressed CRT-HA (Fig 6, black arrows).

To detect the expression of ectopic CRT (CRT-HA) in HSCs and endothelial progenitor cells in the BM, we performed IF staining using antibodies against CD34 and CD31 which are HSCs and endothelial progenitor cell markers respectively (Yin *et al.* 1997; Kisanuki *et al.* 2001). Fig. 7A shows co-expression of CD34 (green) and HA (red) in polymorphonuclear (PMN) progenitor cells derived from the myeloid lineage of hematopoietic cells (white arrows). Fig. 7B (white arrows) illustrates co-expression of CD31 (green) and HA (red) in endothelial progenitor cells of the BM cells isolated from *Tie2-CRT* mice. Together, these data confirmed the expression of the transgene (CRT-HA), in the target tissues of *Tie2-CRT* mice.

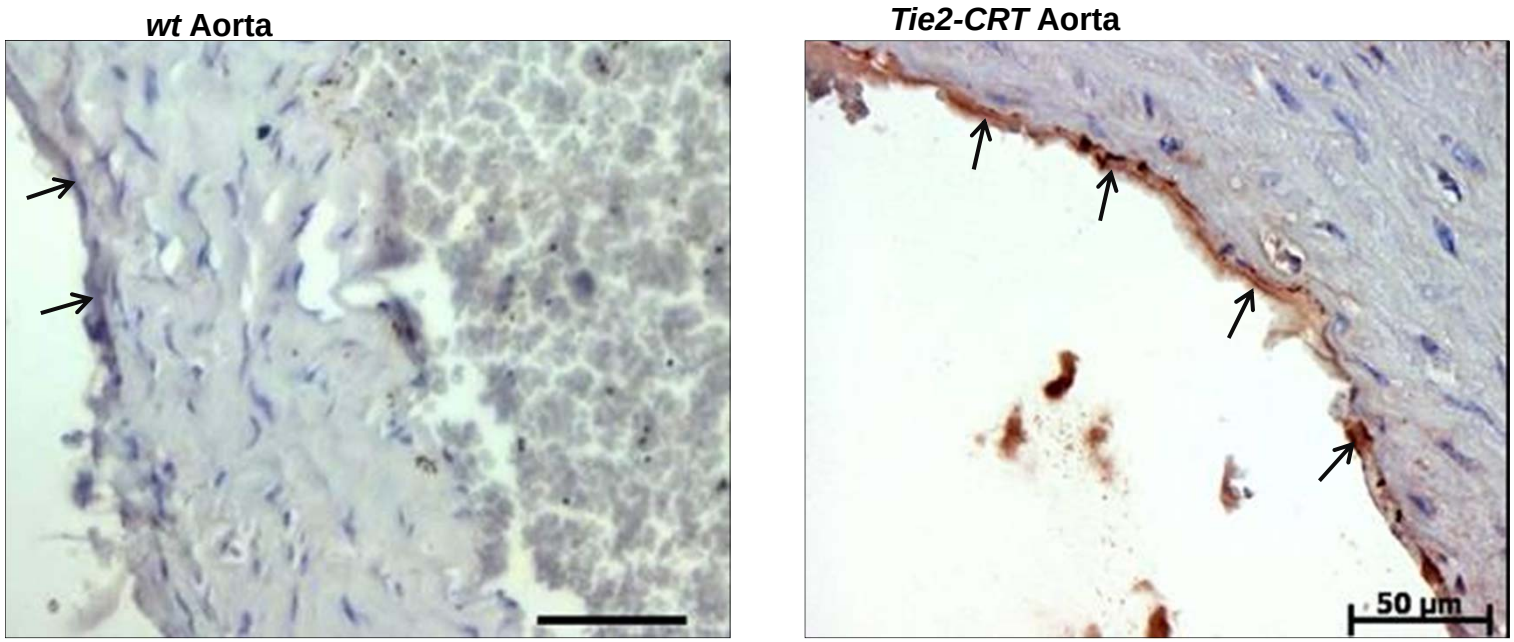

Fig. 5. Immunohistochemical staining with HA antibody to examine CRT-HA transgene expression.
Representative IHC analysis of CRT-HA expression in endothelial cell layer of the aorta in *Tie2-CRT* transgenic mice as compared to a non- transgenic littermate (n=4). CRT-HA positive endothelial cells (black arrows) were detected by immunohistochemistry of sections prepared from the descending aorta of *Tie2-CRT* mice using an anti-HA antibody. Scale bars, 50 µm.

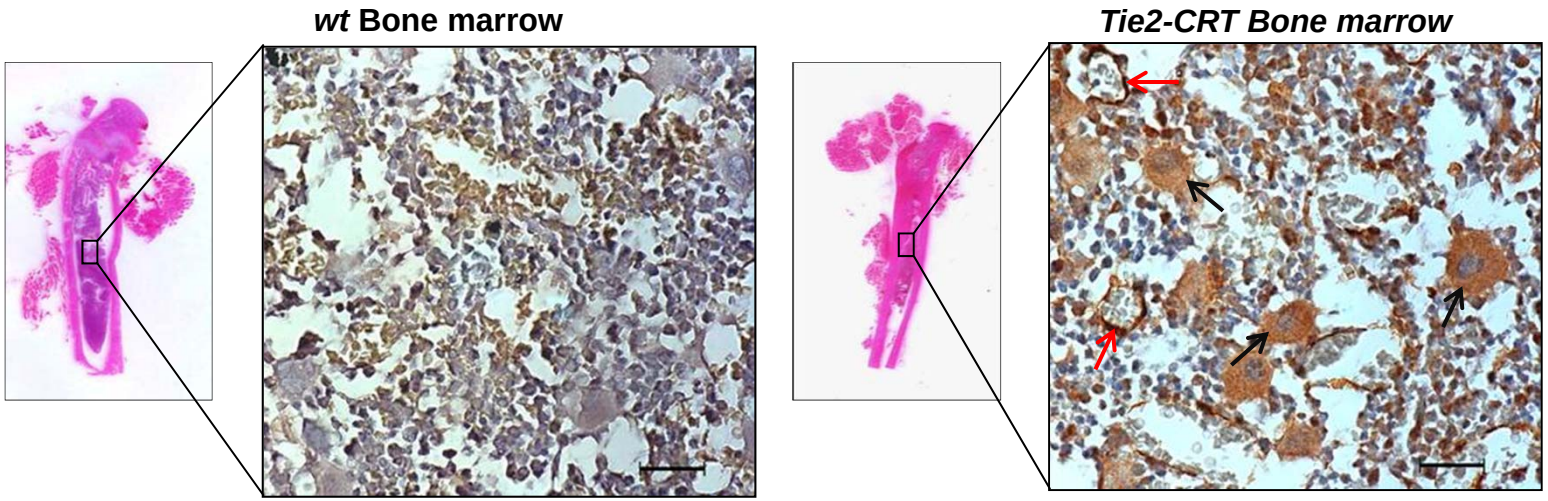

Fig. 6. Detection of CRT-HA expression in bone marrow cells of *Tie2-CRT* mice using immunohistochemistry (IHC) staining with HA antibody.

Representative IHC analysis of CRT-HA expression in bone marrow cells in *Tie2-CRT* transgenic mice as compared to a non-transgenic littermate (n=4). CRT-HA positive cells (black arrows) were detected by IHC in sections prepared from the femurs of *Tie2-CRT* mice using an anti-HA antibody followed by the avidin-biotin horseradish peroxidase and DAB (brown color) and counterstained with Mayer's hematoxylin as described in "Materials and Methods". The endothelial cell layer of microcapillaries in the bone marrow are also expressed CRT-HA (red arrows). Scale bars, 50 μm

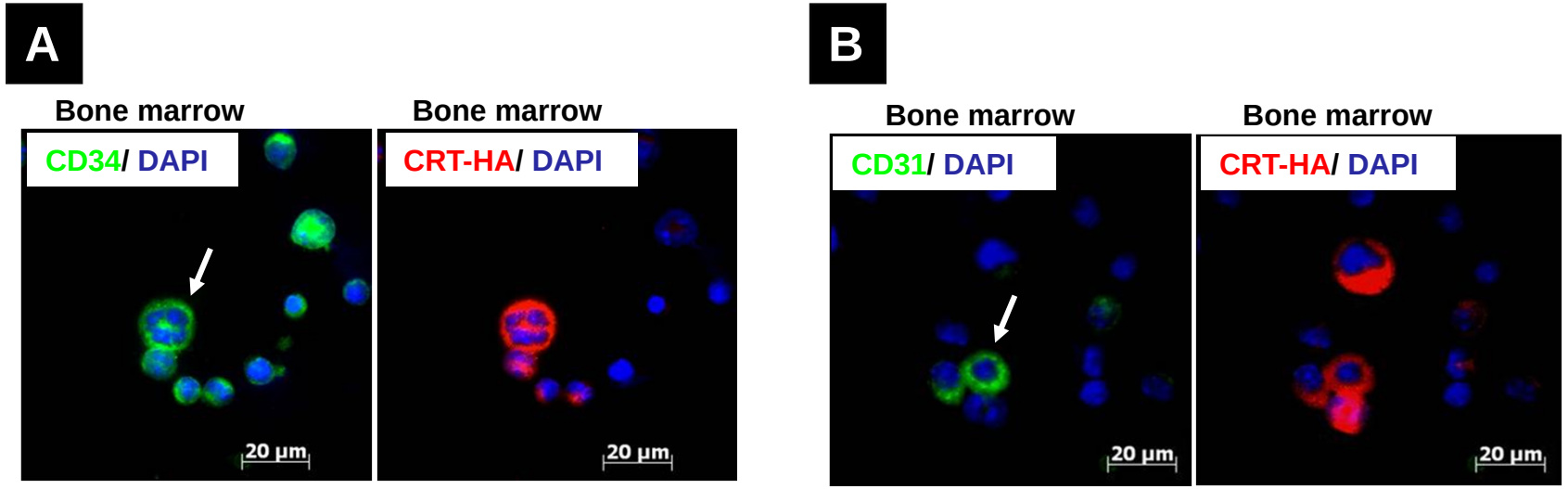

Fig. 7. Detection of CRT-HA expression in cells isolated from bone marrow of *Tie2-CRT* mice using immunoflorescence (IF).

(A) Representative IF images showing co-expression of CD34 antigen (green) and CRT-HA (red) in polymorphonuclear (PMN) progenitor cells (white arrows) which belong to the myeloid lineage (n=6). (B) Representative IF images showing co-expression of CD31 antigen (green) and CRT-HA (red) in endothelial progenitor cells in bone marrow (n=6). Nuclei of the cells were counterstained with DAPI (blue). Scale bars indicate 20 µm.

3.1.2. General characteristics of *Tie2-CRT* mice

Body weight and blood glucose of both *wt* and *Tie2-CRT* mice were measured at the time of necropsy as described in "Materials and Methods". Fig. 8A and B show that there was no significant changes in either body weight or blood glucose concentration in *Tie2-CRT* mice as compared to their *wt* littermates. Blood cell profiles of *wt* and *Tie2-CRT* mice were also examined using an automated cell counter and there were no significant changes in the number of WBC (Fig. 9A) or RBC (Fig. 9B) in *Tie2-CRT* mice as compared to *wt* control animals. Similarly, there were no significant changes in blood hemoglobin concentration (Fig. 9C) in *Tie2-CRT* mice (15 mg/dl) as compared to *wt* controls (13.9 mg/dl).

Fig. 10 shows light microscopic images of representative blood smears obtained from *wt* and *Tie2-CRT* mice stained with Giemsa (Fig. 10A and 7B, n=30) and MPO (Fig. 10C and 7D, n=8) as described in "Materials and Methods". As seen in this figure, the morphology of both WBCs and RBCs appears normal in *Tie2-CRT* mice (Fig. 10B) compared to *wt* littermate controls (Fig. 10A). However, WBCs isolated from *Tie2-CRT* mice failed to express MPO (compare Fig. 10C with 10D).

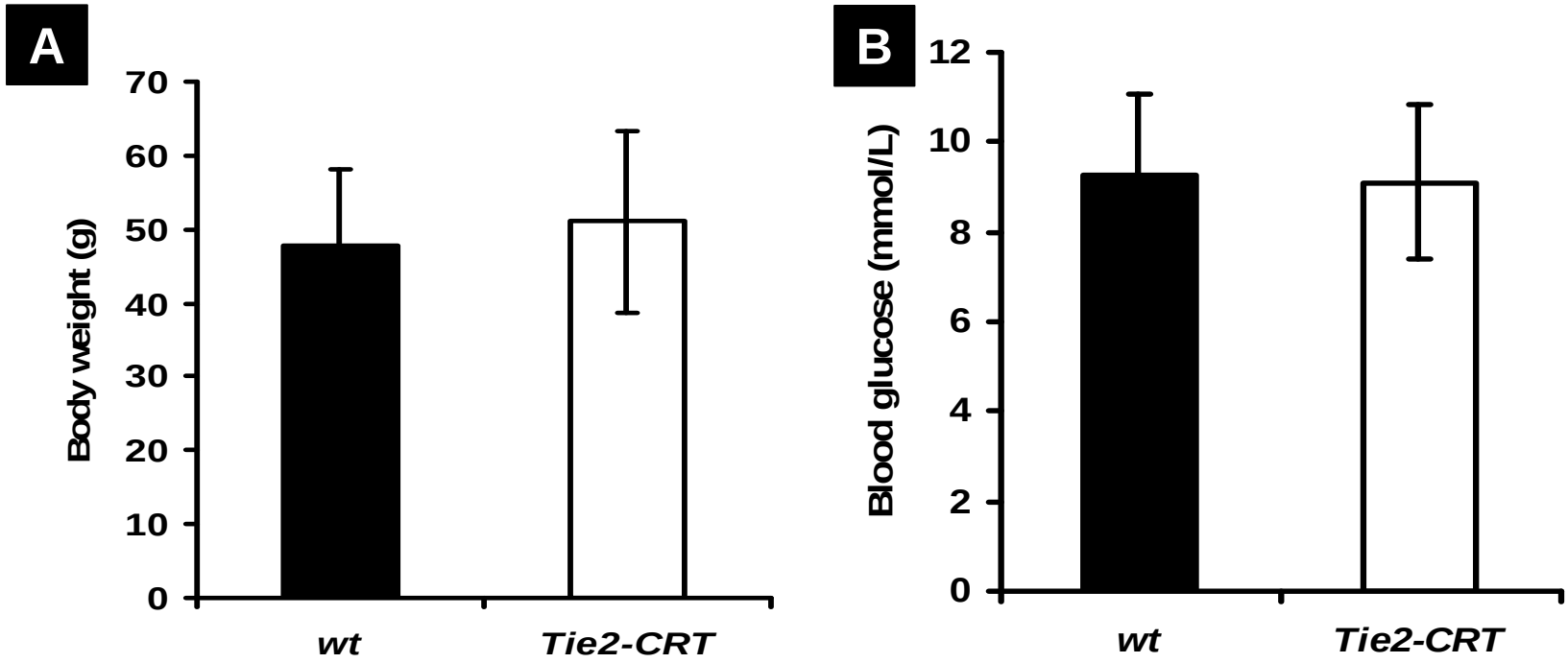

Fig. 8. General characteristics of *Tie2-CRT* mice compared to non-transgenic littermates.
Body weight and blood glucose concentration were measured following euthanasia as described in "Materials and Methods". Bar graphs in A and B show no significant change in the body weight or blood glucose concentration of *Tie2-CRT* transgenic mice as compared to *wt* littermates. Bar graphs are mean ± SE of n=40 mice in each group.

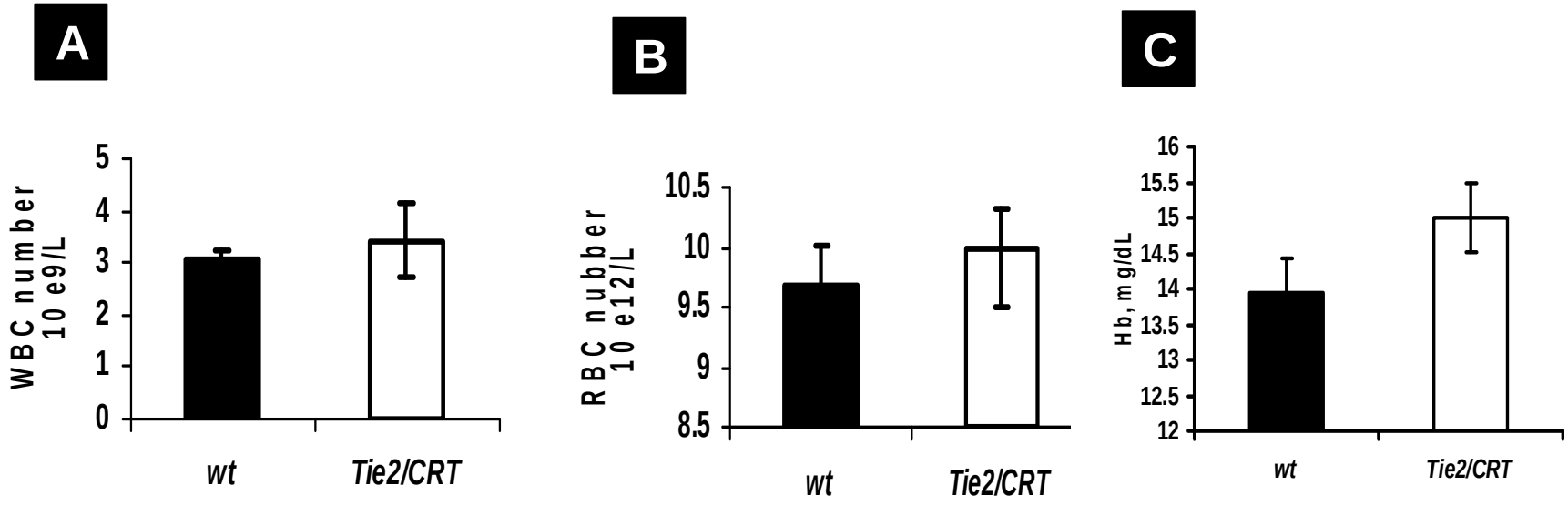

Fig. 9. Blood cell profiles of *Tie2-CRT* mice compared to *wt*.

The blood cell profiles of both *Tie2-CRT* mice and *wt* controls were examined using an automated cell counter. (A) The number of white blood cells (WBC) in *Tie2-CRT* mice did not differ from *wt* controls. (B) There was no significant difference in the number of red blood cells (RBC) in *Tie2-CRT* mice as compared to *wt* controls. (C) Similarly, there were no significant changes in blood hemoglobin (Hb) concentration in *Tie2-CRT* mice (15 mg/dl) as compared to their *wt* controls (13.9 mg/dl). Bar graphs are mean ± SE of n=6 samples in each group.

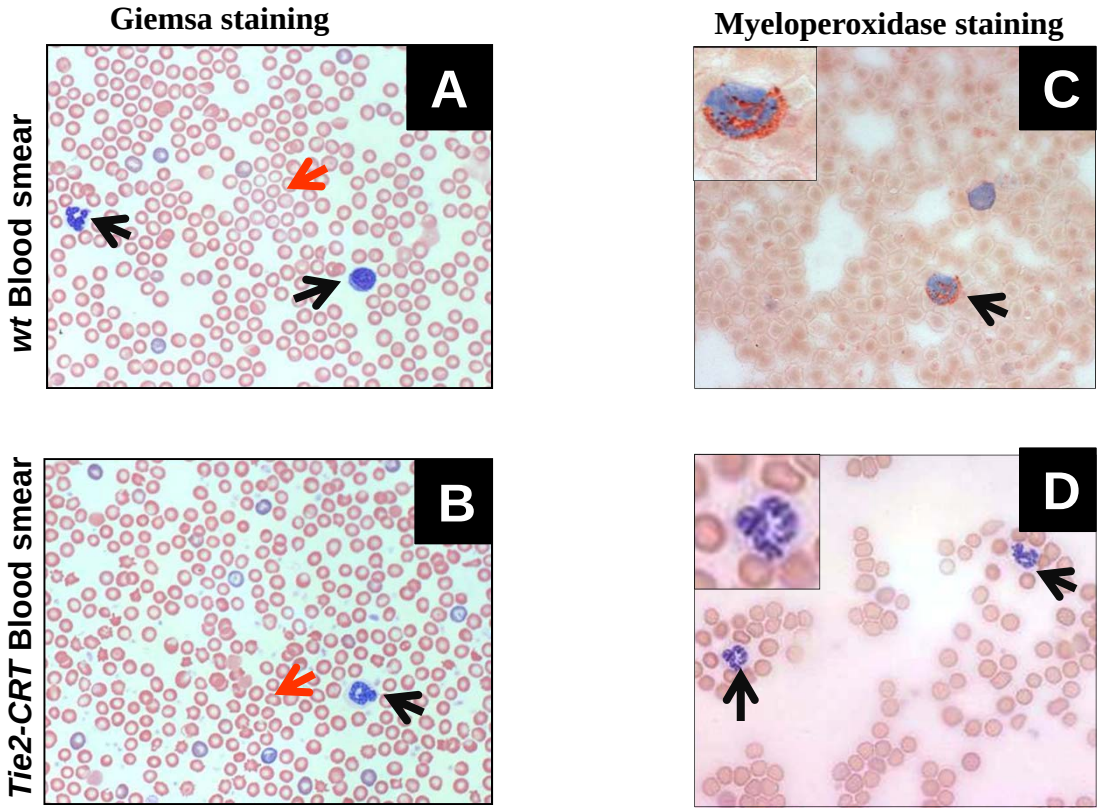

Fig. 10. Morphological analysis of blood cells from *Tie2-CRT* mice.
Representative (>10 mice per group) light microscopy images of blood smears obtained from *wt* (A) and *Tie2-CRT* (B) mice stained with Giemsa as described in "Materials and Methods". Morphology of both WBCs (black arrows) and RBCs (red arrow) is normal in *Tie2-CRT* mice as compared to their *wt* littermates. C and D show light microscopic images of representative blood smears obtained from *wt* and *Tie2-CRT* transgenic mice stained for myeloperoxidase (n=7). C, inset, shows a *wt* neutrophil stained positive for myeloperoxidase in contrast to neutrophils of *Tie2-CRT* mice which were negative for myeloperoxidase (D, inset).

3.1.3. Increased incidence of lung cancer in *Tie2-CRT* mice

Necropsies of *Tie2-CRT* transgenic mice demonstrated localized hemorrhagic lesions in different tissues, including the uterus (Fig. 11A), ovaries (Fig. 11B), liver (Fig. 11C) and lungs (Fig. 11C). As the *Tie2-CRT* mice aged, they suffered from labored breathing, suggesting a lung defect. Indeed, at the time of necropsy the presence of solid tumors were observed on the pleural surface of the lung and was confirmed by examining the lobes of the lungs under a stereo–microscope (Fig. 12).

Fig. 12A-D illustrates the morphology of lungs of *Tie2-CRT* mice at different stages of lung tumor. Lungs isolated from young *Tie2-CRT* mice showed signs of congestion and reddish discoloration on their periphery (Fig. 12A black arrows) suggesting possible onset of an inflammatory response. Histology of the lung at this stage also confirmed congestion accompanied with accumulation of inflammatory cells in the lung (Fig. 14B and C). With age, animals developed visible tumors at the periphery of the lung that had a soft, smooth surface with a white to tan appearance (Fig. 12C, black arrow). At later more advanced stages, the tumor spreads and invades all of the lobes of the lungs (Fig. 12D).

Fig. 13A shows the incidence of lung tumors in *Tie2-CRT* mice as compared to *wt* littermates at different ages. As illustrated in the bar graph, (Fig. 13A) 50% of *Tie2-CRT* animals less than 12 months of age developed lung tumors as compared to just 14% of *wt* mice. This incidence increased to 65.7% in 12 to 18 month old *Tie2-CRT* mice, whereas the incidence of lung tumor in *wt* littermates was only 20%. In mice older than 18 months, 93% of *Tie2-CRT* mice had fully developed lung tumors while only 23% of *wt* mice had fully developed lung tumors. Further studies showed that

tumor formation in *Tie2-CRT* mice occurs in both sexes with similar frequency (Fig. 13B).

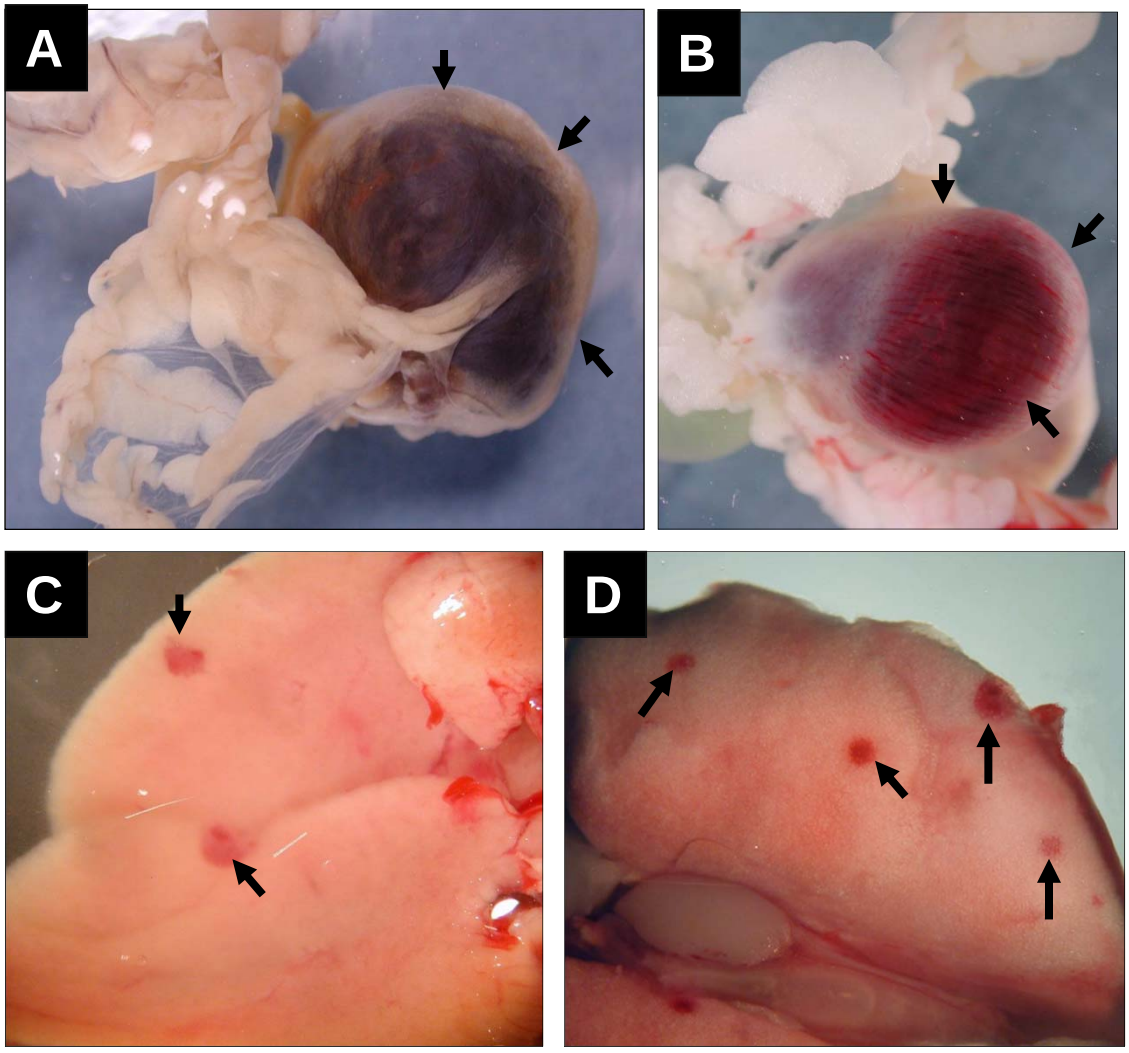

Fig. 11. Localized hemorrhagic lesions in *Tie2-CRT* mice.
Tie2-CRT mice show signs of hemorrhage in different organs: (A) shows a hemorrhagic uterus (black arrows), (B) the ovaries (black arrows) and (C and D) point hemorrhages were observed in the liver and the lungs respectively (black arrows).

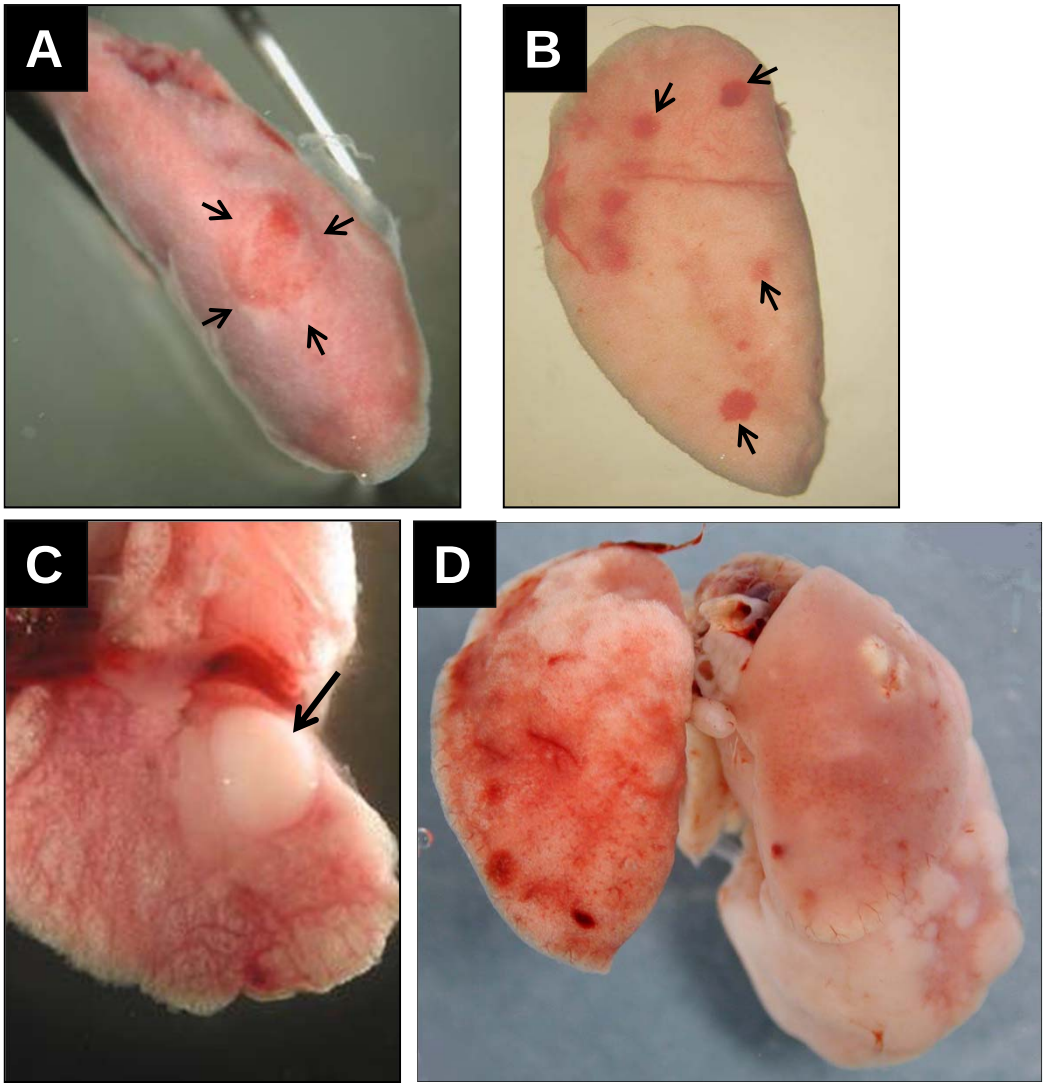

Fig. 12. Lung phenotype of the*Tie2-CRT* mice.
A-D show the gross morphology of the lungs of *Tie2-CRT* mice at different stages of lung tumor development. A and B show lungs at the early stages of tumor formation. At this stage, there are discolorations and focal hemorrhagic regions in different lobes of the lung (black arrows). As the lesions progress with age, they acquire a more spherical shape with a smooth surface and a white to tan color (C). These tumors usually appear peripherally. This lesion (black arrow) represents the fully developed adenocarcinoma. At later stages, the lesion spreads to invade all of the lobes of the lung (D).

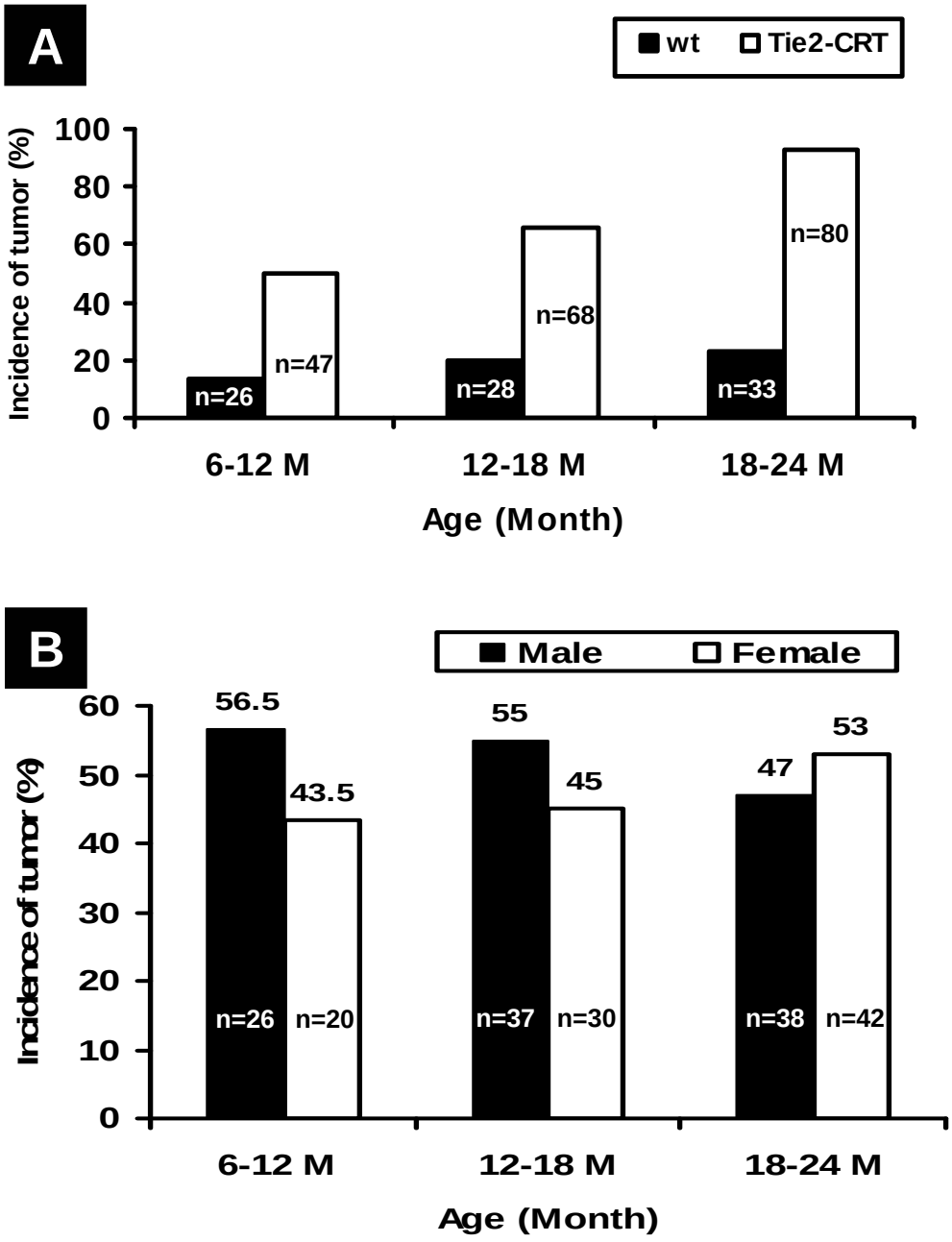

Fig. 13. Incidence of lung tumors in *Tie2-CRT* transgenic mice as compared to *wt* littermates.

(A) Bar graph shows a significantly higher incidence of lung tumors in *Tie2-CRT* mice as compared to *wt* littermates at all ages examined. As *Tie2-CRT* mice aged, there were a increase in tumors observed from 50% to 93%, white bars. However, the incidence of lung tumors in *wt* mice only showed a slight increase as the mice aged (black bars). n, indicates the number of mice examined in each group. (B) The incidence of tumor formation in *Tie2-CRT* mice is similar in both sexes. Numbers on the bar graph show the percentages of lung tumors and "n" indicates the number of mice in each group.

3.1.4. Histological characterization of lung tumors in *Tie2-CRT* mice

Histological analysis revealed that the tumors in *Tie2-CRT* mice spontaneously arise in the alveolar region of the lung and continue to grow over time to form a dense cellular peripheral tumor (Fig. 14). Fig. 14A and B show representative H&E staining of lung sections isolated from a young *wt* (A) and a young *Tie2-CRT* (B) mouse. As shown in the Fig. 14B, lung tissue isolated from *Tie2-CRT* mice has undergone changes in the alveolar architecture as a result of an increase in cell number in the respiratory epithelium, congestion and chronic inflammation as compared to *wt* lung tissue (Fig. 14A). The next stage of the tumor development is formation of atypical adenomatous hyperplasia (AAH) in the peripheral airway. AAH refers to a lesion in the lung of the genetically modified mice that precedes the adenoma stage (Jackson *et al.* 2001).

At the AAH stage, pre-malignant cells in various states of dysplasia are seen in the regions where the lung architecture is disrupted and has an abnormal appearance (Fig. 14C). Fig. 14C is a photomicrograph of H&E staining of a lung section demonstrating focal epithelial hyperplasia seen in the alveoli of *Tie2-CRT* mice. This lesion consists of relatively uniform atypical cuboidal cells with different size of nuclei (Fig. 14C). Black arrows in Fig. 14C demonstrate RBC accumulation in the lung which is indicative of increased congestion. The regions of epithelial hyperplasia will progress to neoplasia with uniform populations of hypertrophic cuboidal cells forming glandular structures followed by adenoma and the presence of small peripheral nodules in the lung (Fig. 14D). These nodules eventually form peripheral tumors with glandular/papillary structures (Fig. 14E). Fig. 14E shows a fully developed lung

adenocarcinoma seen in *Tie2-CRT* mice at low magnification. Fig. 14F is shown at a higher magnification to highlight the glandular pattern of tumor cells.

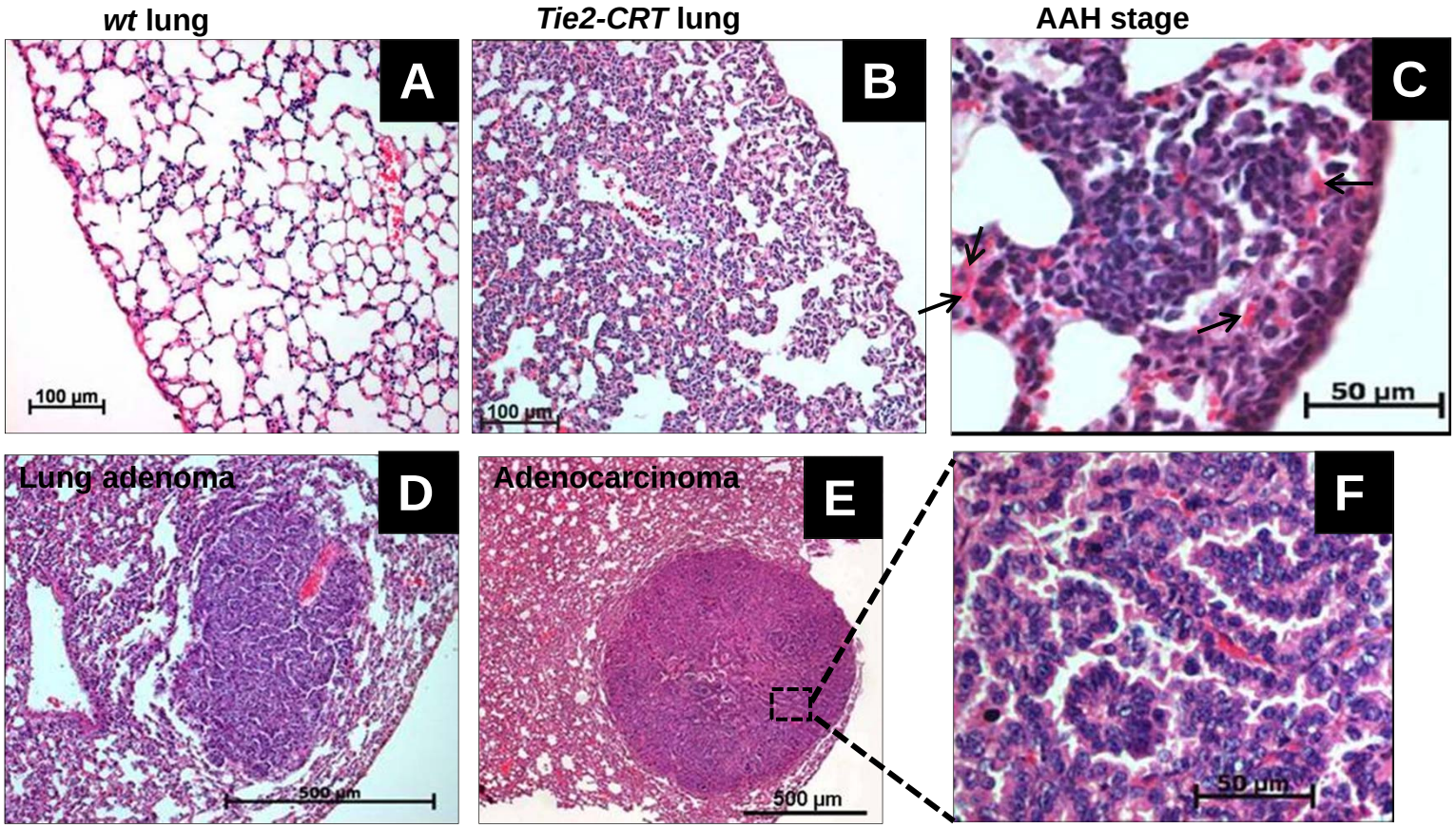
wt lung
Tie2-CRT lung
AAH stage
A
B
C
100 µm
100 µm
50 µm
Lung adenoma
Adenocarcinoma
D
E
F
500 µm
500 µm
50 µm

Fig. 14. Stages of lung tumors observed in *Tie2-CRT* mice.
Four μm paraffin sections of lung from *wt* and *Tie2-CRT* mice were processed for H&E staining to analyze the type and stages of lung tumors. Photomicrographs showing representative (>10 mice in each group) H&E staining of lung sections isolated from *wt* (A) and young (3-6 month) *Tie2-CRT* mice (B) demonstrating changes in the alveolar architecture in *Tie2-CRT* mice. These changes include respiratory epithelium hyperplasia in *Tie2-CRT* as compared to *wt* lung. As the *Tie2-CRT* ages, lung morphology changes to form focal epithelial hyperplasia in the alveoli of *Tie2-CRT* mice (C) which consists of relatively uniform atypical cuboidal to columnar cells and red blood cells (black arrows) accumulated in the lung, a further indication of increased congestion. Epithelial hyperplasia will then progress into sites of neoplasia, forming glandular structures in the lung known as adenoma (D). Finally, the adenoma proceeds to form fully developed adenocarcinoma (E, low magnification). At higher magnification (F) the lung tumors of *Tie2-CRT* mice are of a glandular pattern with their own established vasculature and irregular shaped cells. Scale bars are included in each image.

3.1.5. Immunohistochemical characterization of lung cancer in *Tie2-CRT* mice

To study the histogenesis of the lung tumors seen in *Tie2-CRT* mice, we examined the expression of the alveolar type II marker SP-C and the bronchiolar cell marker CC10 in these tumors. These are two common markers used to characterize cells in lung tumors in order to determine the cell of origin of the tumor (Mason *et al.* 2000; Kim *et al.* 2005). As illustrated in Fig. 15, the tumor cells of *Tie2-CRT* mice were positive for SP-C expression (Fig. 15C) and negative for CC10 expression (Fig. 1DB). However, lung tumors observed in *wt* mice are either SP-C negative (Fig. 15C) or SP-C positive adenocarcinoma (Fig. 15C). Another marker which is used to characterize cells in lung tumors is mucin. The mucicarmine method was used to examine mucin production by lung tumor cells in *Tie2-CRT* mice as described in "Materials and Methods". As illustrated in Fig. 15D, the tumor cells of *Tie2-CRT* mice do not express mucin. These data illustrate that the tumors in *Tie2-CRT* mice are composed of alveolar type II cells, but not Clara cells.

Similar to human lung adenocarcinoma, the gross morphology of the lung adenocarcinoma observed in *Tie2-CRT* mice showed a white-tan appearance. Therefore, to examine whether this was a consequence of lipid deposition, ORO staining was performed on lung tumor sections. Fig. 15F is a representative ORO staining of a lung tumor section showing red coloration for lipid deposits in lung tumor cells (Fig. 15F, inset). These lipid deposits could be surfactant-rich lipoproteinaceous material including SP-C secreted by the tumor cells.

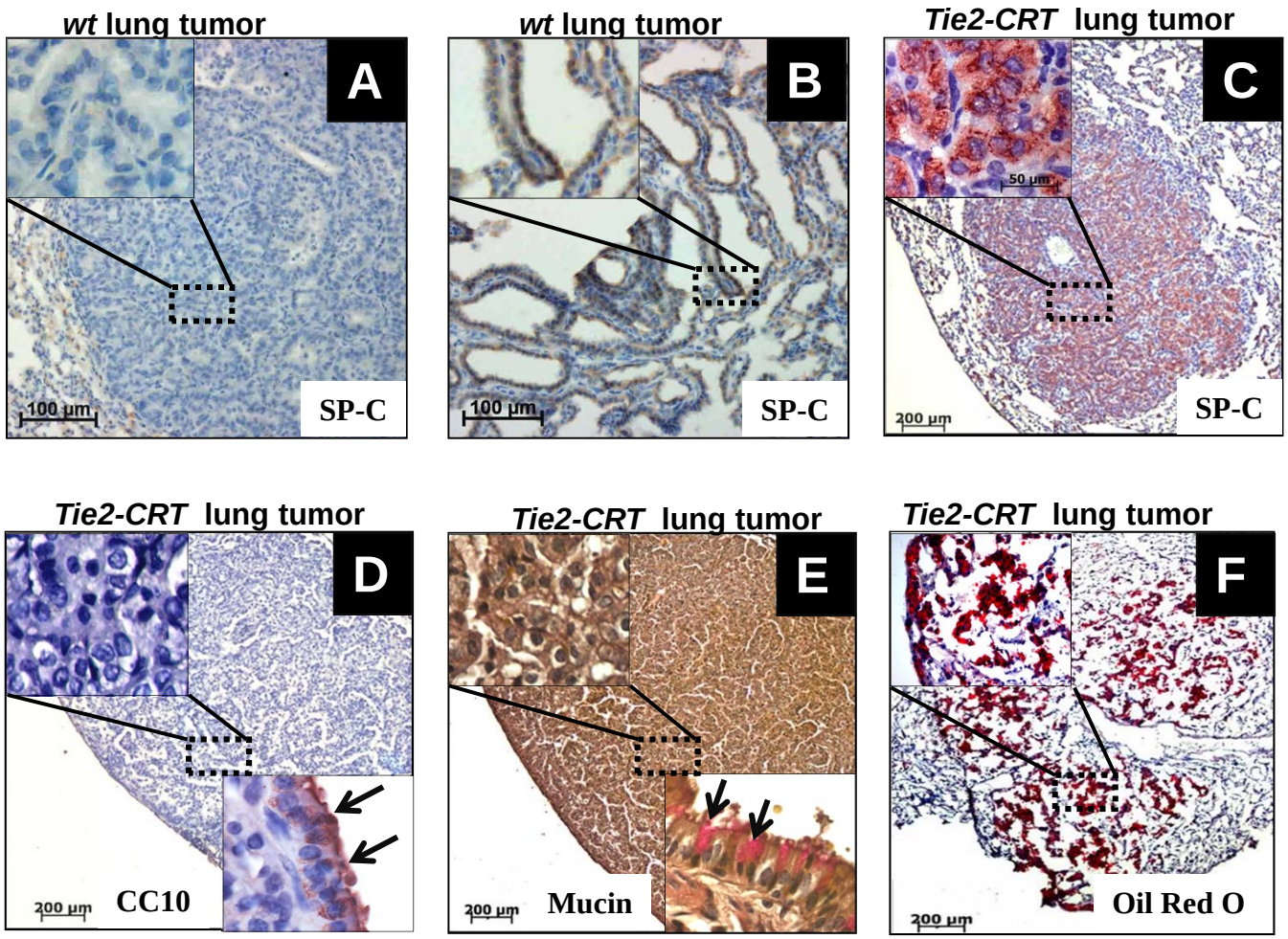
wt lung tumor
A
100 µm
SP-C
wt lung tumor
B
100 µm
SP-C
Tie2-CRT lung tumor
C
50 µm
200 µm
SP-C
Tie2-CRT lung tumor
D
200 µm
CC10
Tie2-CRT lung tumor
E
200 µm
Mucin
Tie2-CRT lung tumor
F
200 µm
Oil Red O

Fig. 15. IHC characterization of lung tumors in *Tie2-CRT* mice.
IHC staining for (A, B, and C) SP-C, an alveolar type II marker shows that the lung adenocarcinoma of *Tie2-CRT* mice are SP-C ^{pos} (C) while lung tumors observed in *wt* mice are either SP-C ^{neg} (A) or SP-C ^{pos} (B). As seen in the picture, immuno histochemical properties of tumor cells of the *Tie2-CRT* mice lung adenocarcinoma (C) are different as compared to lung adenocarcinoma seen in *wt* mice (n=2, B and C). Furthermore, IHC staining for CC10, a bronchial marker shows that the lung adenocarcinoma of *Tie2-CRT* mice are CC10 ^{neg} (D). Insets in (A, B and C) show a higher magnification of tumor section stained for SP-C protein (B and C brown color) or absence of SP-C in tumor cells (A). Insets in (D) show the absence of CC10 in tumor cells with higher magnification (top inset) and the presence of CC10 (brown color) in Clara cells of a bronchiole from the same section as the positive control (lower inset, blue arrows). (E) shows mucin staining of tumor cells in the lung tissue using the mucicarmine technique, which indicates mucin-negative tumor cells in advanced lung tumors from *Tie2-CRT* mice. Insets in (E) showing lack of mucin secretion by tumor cells at higher magnification (top inset) and some mucin positive cells (pink color) in the bronchiole cells from the same section as a positive control (lower inset, blue arrows). Tumor sections also stained positive for lipid deposits using oil-red-O staining (F), indicating large amounts of surfactant-rich lipoproteinaceous material secreted by tumor cells. Scale bar, 200 μm.

We also examined changes in cell proliferation in the lung of *wt* and *Tie2-CRT* mice *in vivo* by examining the expression of Ki-67, a nuclear protein that is strictly associated with cell proliferation (Minami *et al.* 2002). Fig. 16A and C show only a few cells staining positive for Ki67 in the lungs of a *wt* mouse illustrating a small but ongoing cell proliferation in the normal lung tissue. As compared to the *wt* lung, the *Tie2-CRT* lungs contained a higher number of cells staining for Ki-67. As seen in Fig. 16B and D, Ki-67 staining was observed in both the tumor region (B, black arrows) and the area adjacent to the tumor (B, red arrows) but a decrease level as compared to the tumor section. This indicates a high rate of proliferation in the lung tumor (Fig. 16D) as compared to the adjacent tissue (Fig. 16B).

3.1.6. Evaluation of lung inflammation in *Tie2-CRT* mice

As mentioned above, upon necropsy, we often observed that lungs isolated from *Tie2-CRT* mice, showed signs of congestion and reddish discoloration on the periphery of the lungs. To examine the possible inflammation in the lungs of *Tie2-CRT* mice we examined the presence of inflammatory cells by IHC. An anti-Mac-3 antibody, a known marker for macrophages (Noorman *et al.* 1997), was used for IHC analysis. As shown in Fig. 17, prior to detectable tumor formation in the lungs of *Tie2-CRT* mice there was a high level of Mac-3 staining indicative of increased numbers of macrophages infiltrating the lungs of these mice (Fig. 17B, black arrows) as compared to *wt* littermates (Fig. 17A, black arrows).

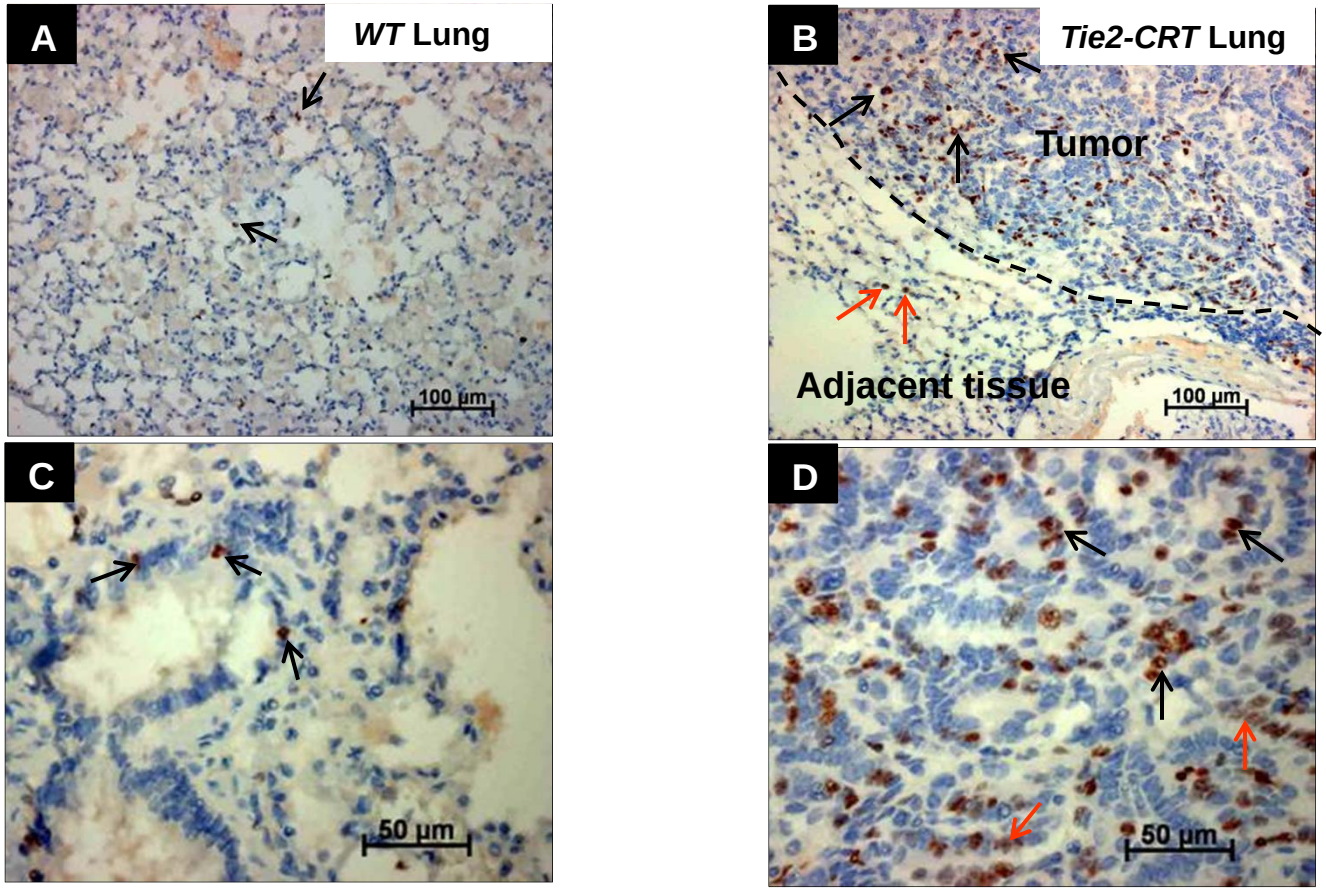

Fig. 16. Ki-67 expression in the lung sections of *wt* and *Tie2-CRT* mice.

IHC using a Ki-67 antibody, a nuclear protein that is strictly associated with cell proliferation was carried out as described in "Materials and Methods" (n=4). Few cells in *wt* lungs stained positive with an anti-Ki-67 antibody (A and C, black arrows) whereas a higher number of Ki-67 positive cells were seen in *Tie2-CRT* lung both in the tumor region (B and D black arrows) and in the normal tissue adjacent to the tumor (B, red arrows). Scale bars are as included in each image.

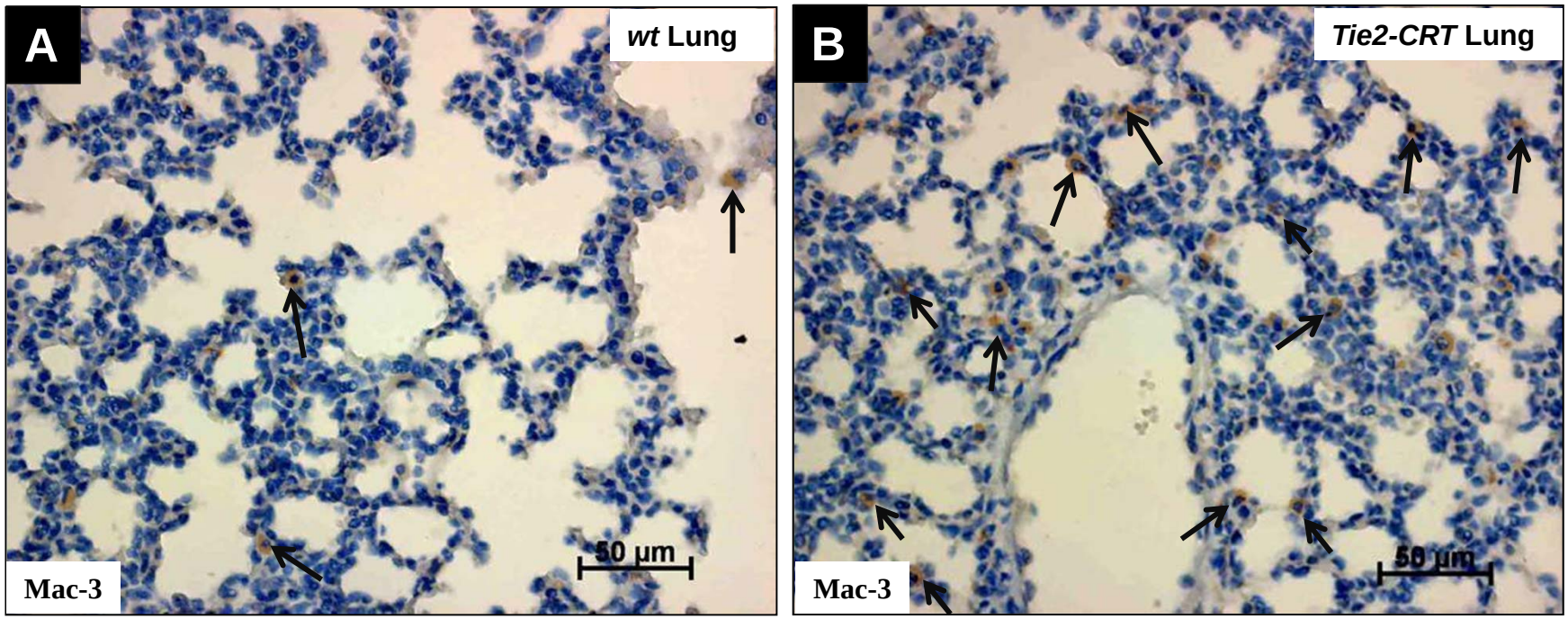

Fig. 17. Evidence of inflammation in the lung of *Tie2-CRT* mice.
Presence of inflammatory cells in the lung of *Tie2-CRT* mice was confirmed by IHC using a Mac 3 antibody, a known marker for macrophages. Representative images of lung sections of young *wt* (A) and *Tie2-CRT* (B) mice (n=3) stained with anti-Mac 3 antibody and DAB demonstrating an increased number of macrophages present in the lung of *Tie2-CRT* mice (B, black arrows) as compared to *wt* littermates (A, black arrows).

3.1.7. Development of liver tumors in *Tie2-CRT* mice

In addition to our observation of lung tumors in *Tie2-CRT* mice, we frequently observed tumors in the liver, which sometimes were accompanied by lung tumors. The incidence of primary liver tumors in mice has previously been reported (Andervont 1950; Andervont *et al.* 1962) and ranges from 15-55% in C3H and 20-29% in CBA mice, and typically arises only in mice over 12 months of age (Andervont 1950). We sought to determine whether the liver tumors observed in *Tie2-CRT* mice were due to lung metastases or were a consequence of CRT overexpression, we partially characterized these liver tumors. Figure 18 shows representative sections of the liver tumors seen in *Tie2-CRT* mice with different appearances including adenoma (Fig. 18A, black arrows), hemorrhagic (Fig. 18B, black arrows) and a mixed tumor (Fig. 18C and D, black arrows).

We also examined the incidence of liver tumors in the *Tie2-CRT* mice. The bar graph in Fig. 19 shows the frequency of liver tumors (of all types) observed in *Tie2-CRT* mice as compared to *wt* littermates at different ages. As shown in Fig. 19, in *wt* mice younger than 12 months, no tumors were observed, but 2% of *Tie2-CRT* mice developed liver tumors. This incidence increased to 25% in 12 to 18 month old *Tie2-CRT* mice, while the frequency of liver tumors in *wt* littermates only increased to 7%. The incidence of liver tumors in mice older than 18 months of age increases to 34% in *Tie2-CRT* mice and 25% in *wt* control mice. Overall, the frequency of liver tumors in *Tie2-CRT* mice (Fig. 19) was lower than that of the lung tumors (Fig. 13).

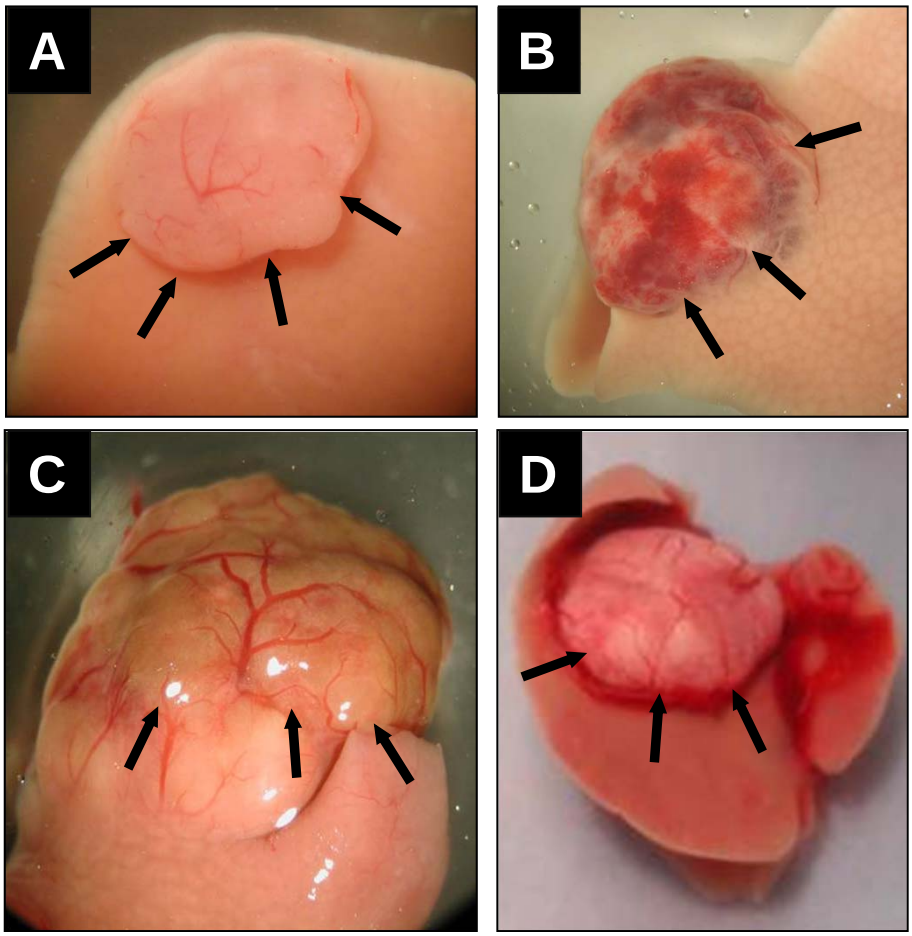

Fig. 18. Morphology of liver tumors observed in *Tie2-CRT* mice.
A-D Images of liver tumors observed in *Tie2-CRT* mice. In contrast to the lung tumors observed in *Tie2-CRT* mice, three different types of tumors in the liver were seen including adenocarcinoma (A), hemorrhagic (B) and mixed tumors (C and D).

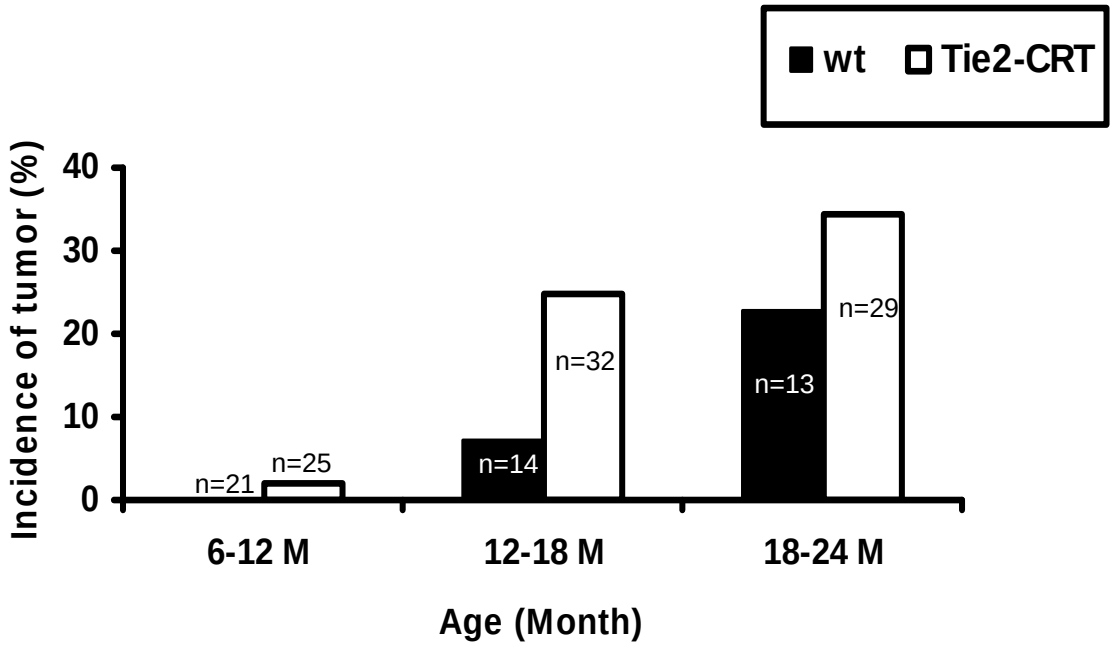

Fig. 19. Incidence of liver tumors in *Tie2-CRT* transgenic mice.
The bar graph shows the frequency of liver tumors observed in *Tie2-CRT* mice as compared to their *wt* littermates at different ages. The incidence of liver tumors appeared to increase with age in both the *wt* and *Tie2-CRT.* In *wt* mice, no liver tumors were detected when the mice were less than 12 months old, but this number increased to 25% in mice over 18 months of age (black bars). The incidence of liver tumors in *Tie2-CRT* mice increased from 3% in less than 12 month old mice to 34% in mice over 18 months of age. n= number of mice examined in each group.

Fig. 20 shows H&E staining of sections from a liver tumor from *wt* (Fig. 20A) and *Tie2-CRT* mice (Fig. 20B, C, D). As seen in this figure, liver tumors of *Tie2-CRT* mice had diverse histological characteristics including hemorrhagic (Fig. 20B), adenocarcinoma (Fig. 20C) and mixed (Fig. 20D) structure. To further study the histogenesis of the liver tumors observed in *Tie2-CRT* mice, we performed IHC using antibodies against α-fetoprotein (AFP), a specific marker for fetal hepatocytes and a biomarker of hepatocellular carcinoma, and SP-C (alveolar type II cell marker). As illustrated in Fig. 21, some of the cells in the tumor region stained positive for AFP (Fig. 21A, black arrows). Furthermore, only a subset of liver tumors in *Tie2-CRT* mice contained SP-C positive cells (Fig. 21B, C). Fig. 21D shows IHC on a section of a liver tumor labeled with an antibody against HA. Expression of CRT-HA in the endothelial cell layer of vessels (Fig.21D, black arrows) and capillaries in the tumor area (Fig. 21C, red arrows) was observed. However, the tumor cells themselves did not express CRT-HA, which indicates that the tumor cells in the liver are not derived from either endothelial cells or HSCs. These results illustrate that only a subset of liver tumors in *Tie-2 CRT* mice could be linked to lung cancer, as evident by SP-C expression in these tumors. Further studies are needed to fully characterize the origin of liver tumors in these mice and study the correlation of liver tumors to lung tumors in the *Tie2-CRT* mice.

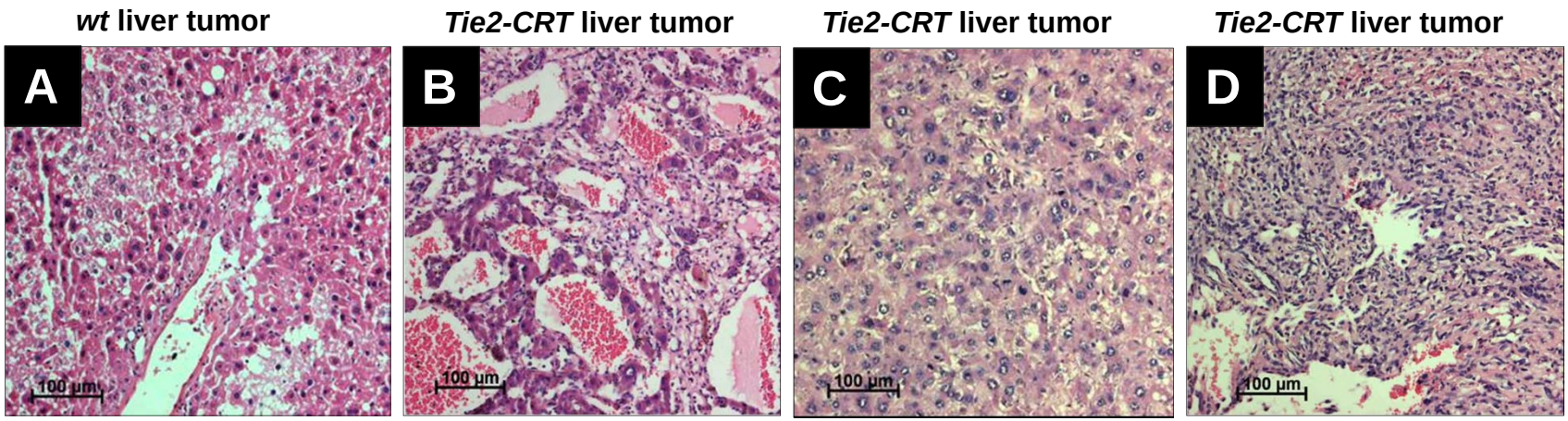

Fig. 20. Liver tumors of *Tie2-CRT* mice show diverse histological characteristics.
A-C represent H&E staining of sections (n=11) from different tumors in the liver of *wt* (A) and *Tie2-CRT* mice (B-D). Tumors in the liver of *Tie2-CRT* mice (B-D) show diverse histological characteristics as compared to *wt* liver tumors (A). Histological characteristics of the tumors in *Tie2-CRT* mice include hemorrhagic (B), glandular (C) and mixed (D) structure. Scale bars indicate 100 µm.

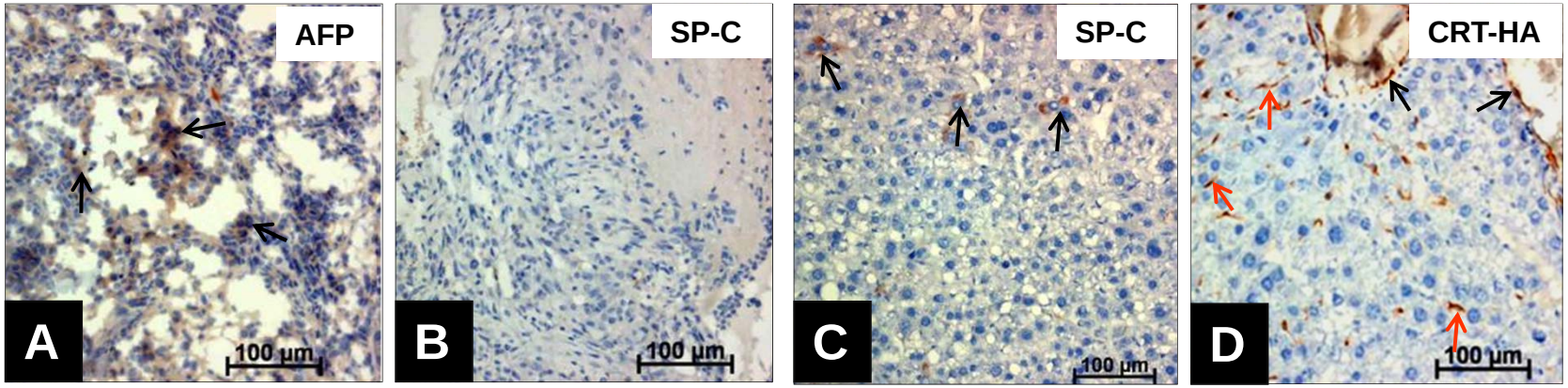

Fig. 21. Immunohistochemical characterization of liver tumors developed in *Tie2-CRT* mice.
IHC on sections from tumors in the liver was carried out using anti- alpha-fetoprotein (AFP) (A), anti-SP-C (B, C) and anti HA (D) antibodies to determine the phenotype of the liver tumors (n=5 for each antibody). Some of the liver tumor cells stained positive for AFP (A, black arrows) whereas the staining of liver tumors with SP-C was diverse. Some liver tumors did not stain with an anti-SP-C antibody (B) while others contained cells which expressed SP-C (C, black arrows). (D) shows IHC on a liver tumor section using an antibody against HA demonstrating expression of CRT-HA by the endothelial cell layer of vessels (D, black arrows) and capillaries in the tumor area (D, red arrows). However, the tumor cells themselves did not express CRT-HA. Scale bars indicate 100 µm.

3.1.8. Characterization of tumor cells in lung cancer of *Tie2-CRT* mice

In these transgenic mice, ectopic CRT expression is driven by the *Tie2* promoter. We therefore examined expression of both endothelial cell and HSC markers in the lung tumor cells in an effort to elucidate the origin of these tumor cells. As shown in Fig. 22A, expression of CD31 (endothelial cell marker) was restricted to the lining of the vessels and capillaries in both *wt* (Fig. 22D, black arrow) and *Tie2-CRT* mice (Fig. 22A, black arrow), and absent in the tumor cells of fully developed adenocarcinoma (Fig. 22A, blue arrows). Conversely, there was heterogeneous expression of CD34 (Fig. 22B, black arrows) and CRT-HA (Fig. 22C, black arrows) in the tumor region.

Fig. 23 shows representative images of H&E stained tumor sections (Fig. 23A) as well as IHC staining using anti-SP-C (Fig. 23B) and anti-CC10 antibodies (Fig. 23C). As demonstrated in Fig. 23, at least three different cell types can be identified. These cells have been classified into three groups. Group A are neoplastic, cuboidal cells, with moderate to large nuclei that form a glandular structure in the tumor area (Fig. 23A, black arrow). These epithelial cells stained positive for SP-C (Fig. 23B, black arrow), but are negative for CC10 (Fig. 23C, black arrow). Group B are non-glandular, neoplastic polygonal cells, with ill-defined cell borders, and a strongly eosinophilic cytoplasm as seen with H&E staining (Fig. 23A, blue arrow). This group of tumor cells stained negative for both SP-C (Fig. 23B, blue arrow) and CC10 (Fig. 23C, blue arrow). Group C are stromal cells with a spindle shape and oval nuclei (Fig. 23A, red arrow). This group of cells also lacks expression of SP-C (Fig. 23B, red arrow) and CC10 (Fig. 23C, red arrow).

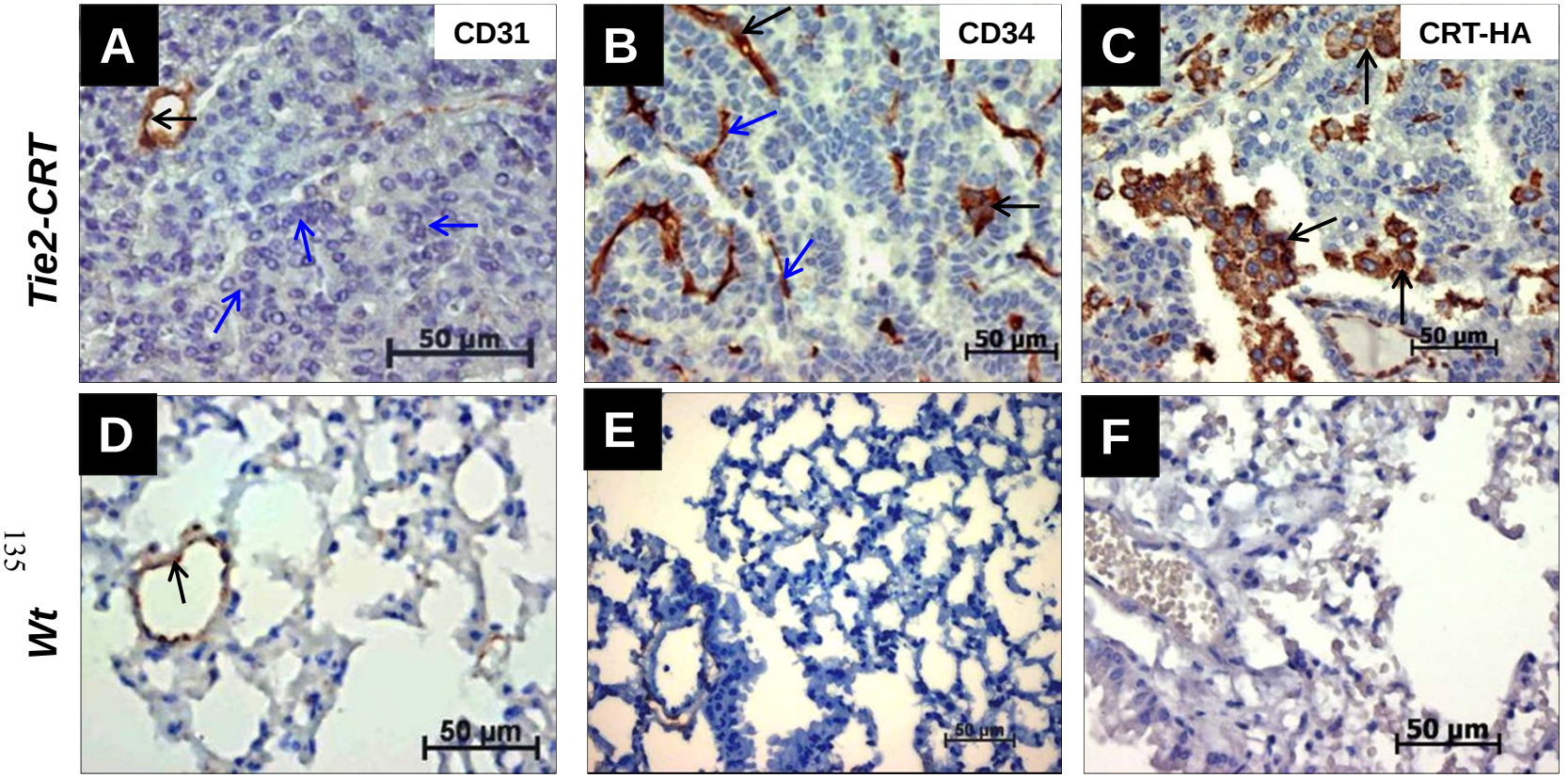

Fig. 22. Expression of CRT-HA, CD34 and CD31 in lung tumors of *Tie2-CRT* mice.
Representative IHC staining (n=4 for each antibody) with CD31, CD34 and HA of the sections of lung tumors from *Tie2-CRT* mice (A, B, C) and *wt* controls (D, E and F). Endothelial cells (black arrows in A and D) lining the capillaries were CD31 positive, whereas tumor cells were not (blue arrows in A). A population of non-epithelial cells from lung adenocarcinomas isolated from *Tie2-CRT* mice stained positive with an anti-CD34 antibody (B, blue arrows). (C) shows expression of CRT-HA by tumor cells (black arrows) as compared to *wt* littermate lungs (F). Scale bars for all photomicrographs represent 50 µm.

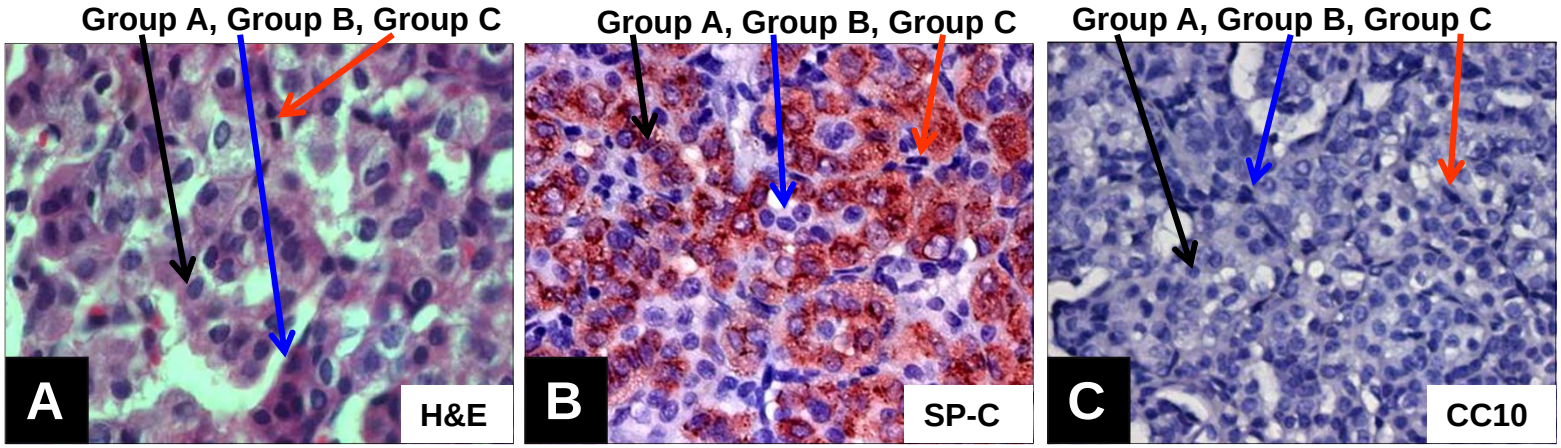

Fig. 23. Heterogeneous population of tumor cells in lung cancer of *Tie2-CRT* mice.

(A-C) Photomicrographs showing H&E and IHC on sections from lung tumor using anti-SP-C and CC10 antibodies demonstrating three different groups of cells in fully developed tumors. Group A: neoplastic cuboidal cells with a moderate to large amount of nuclei which stained positive for SP-C, but negative for CC10 (black arrows). Group B: neoplastic polygonal cells with ill-defined cell borders and a large amount of strongly eosinophilic cytoplasm in H&E staining (blue arrows). This group of tumor cells stained negative for both SP-C and CC10. Group C: stromal cells with a spindle to polygonal shape and an oval nucleus. This group of cells do not express either SP-C or CC10 (red arrows).

To further characterize the cellular composition of the lung tumors from *Tie2-CRT* mice, we carried out IHC on sequential lung sections of these mice (Fig. 24A-F). Fig. 24 is a representative image of CRT-HA staining (Fig. 24A, B and C) and corresponding adjacent sections stained for CD34 (Fig. 24D), SP-C (Fig. 24E) and VEGFR-3 (Fig. 24F) respectively. As shown in Fig. 24E, neoplastic epithelial cells which were positive for SP-C (Fig. 24E, black arrows) did not express CRT-HA (Fig. 24B, black arrows). Furthermore, a subset of tumor cells expressing CRT-HA (Fig. 24C, black arrow) were positive for CD34 (Fig. 24D) or VEGFR-3 (Fig. 24F. black arrow). These data illustrate that a subset of cells expressing CRT-HA contribute to the neovascularization of the lung adenocarcinoma of *Tie2-CRT* mice.

Fig. 25 shows representative staining with E-cadherin, a marker of epithelial cells (Fig. 25A), and vWF (von Willebrand factor), a marker of endothelial cells (Fig. 25B). As seen in this figure, the neoplastic cuboidal cells (group A) express E-cadherin (Fig. 25A, black arrow), but do not express vWF (Fig. 25B, black arrow) suggesting that these cells are epithelial cells. Subsets of group B tumor cells were negative for both E-cadherin (Fig. 25A, blue arrow) and vWF (Fig. 25B, blue arrow). In contrast, group C cells stained positive for vWF (Fig. 25B, red arrow), but not for E-cadherin (Fig. 25A, red arrow) suggesting that these are endothelial cells. Altogether, these observations indicate a diverse protein expression signature for tumor cells which confirms their heterogeneity.

Since the *Tie2* promoter is also active in HSCs, we carried out IF with specific antibodies to HSC markers. Co-immunofluorescence staining of tumor sections using anti-HA, anti-Sca-1, anti-CD34, and anti-c-kit antibodies showed co-expression of HA (Fig. 26A, red) with Sca-1 (Fig. 26A, green) and CD34 (Fig. 26B, green). Fig. 26C

also shows co-expression of CD34 (Fig. 26C, red) and c-kit (Fig. 26C, green) in lung tumor sections. Immunohistochemical characteristics of the three different cell types seen in the tumors are summarized in Table 7. As shown in Table 7, group B tumor cells express both exogenous CRT (CRT-HA) and HSC markers suggesting that HSCs may contribute to the formation of these lung tumors in the *Tie2-CRT* mice.

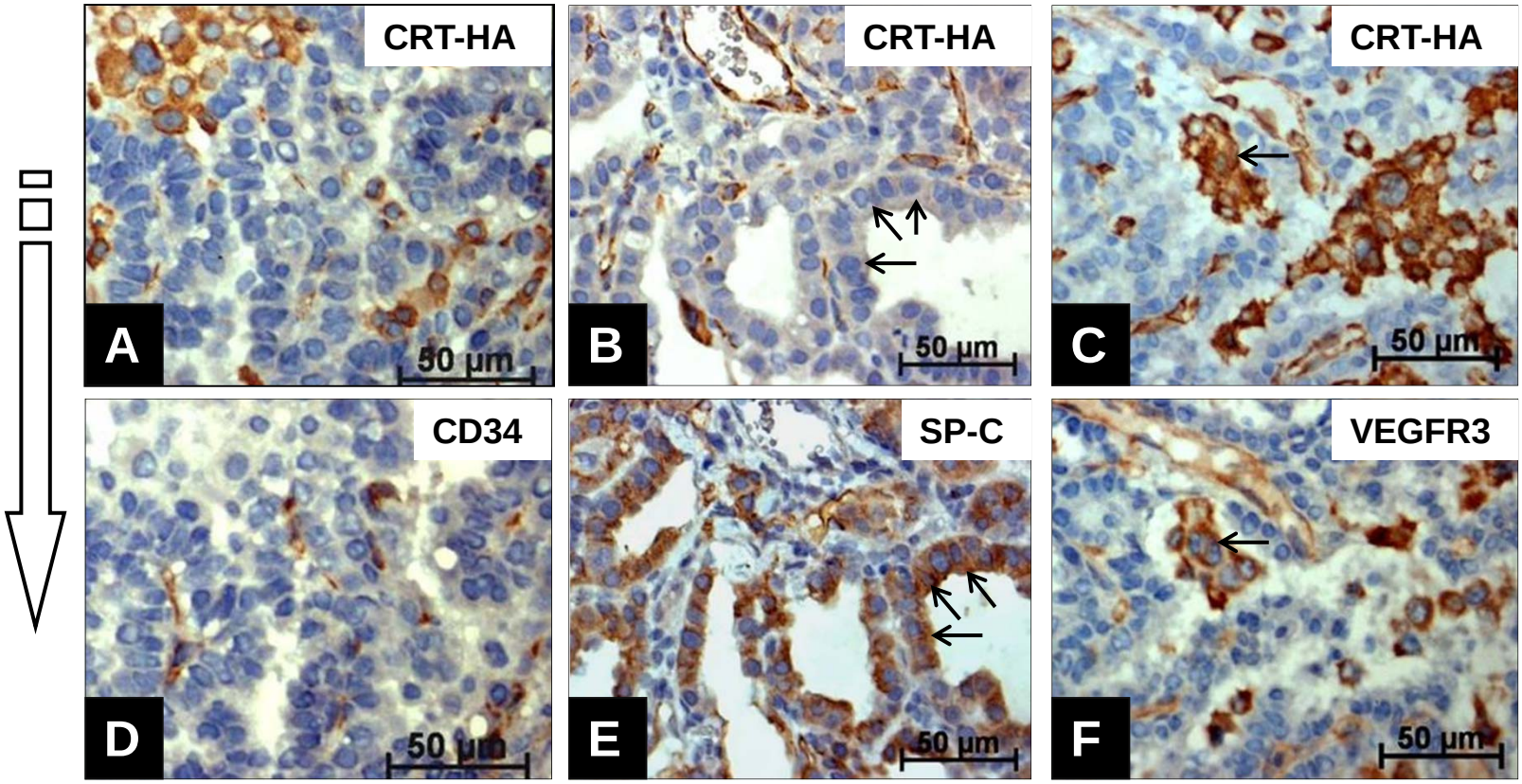

Fig. 24. Characterization of lung tumor cells in *Tie2-CRT* mice.
Representative IHC staining on sequential tumor sections (n=4 for each antibody) using an HA antibody to label CRT-HA (A, B and C) and corresponding adjacent sections were stained using CD34 (D), SP-C (E) and VEGFR-3 (F) antibodies respectively. Neoplastic epithelial cells, which are positive for SP-C (E, black arrows), did not express CRT-HA (B, black arrows). However, a group of cells in the tumor region co-stained with CD34 and CRT-HA (D and A) as well as VEGFR-3 and CRT-HA (C and F). Scale bars for all photomicrographs indicate 50 µm.

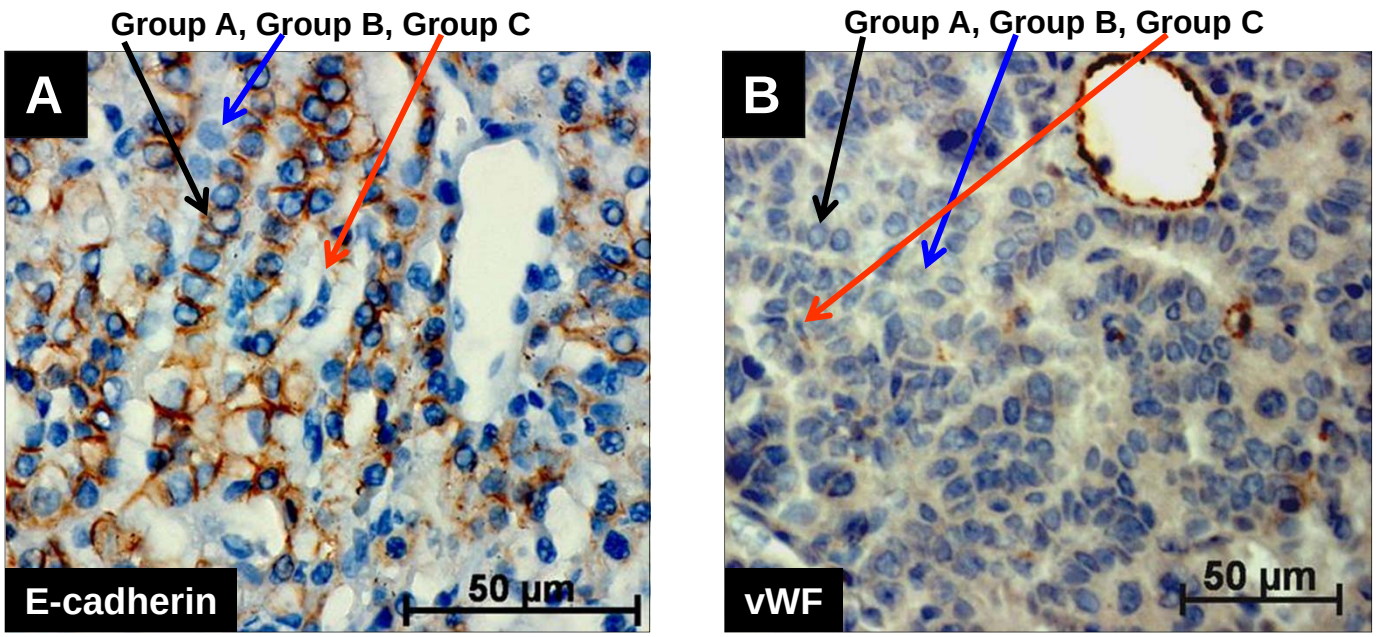

Fig. 25. E-cadherin and vWF expression patterns in *Tie2-CRT* lung tumors.
(A) IHC staining of lung tumor sections using an anti-E-cadherin antibody (n=4). As seen, group A tumor cells (epithelial structure) are stained positive for E-cadherin (A, black arrow) while group B (A, blue arrow) and C (A, red arrow) tumor cells do not express E-cadherin. (B) A representative image of tumor sections stained for vWF (n=6). Neoplastic epithelial cells belonging to group A stained negative for vWF (B, black arrow). Group B tumor cells were also negative for vWF (B, blue arrow), however, group C cells stained positive for vWF (B, red arrow). Scale bars indicate 50 µm.

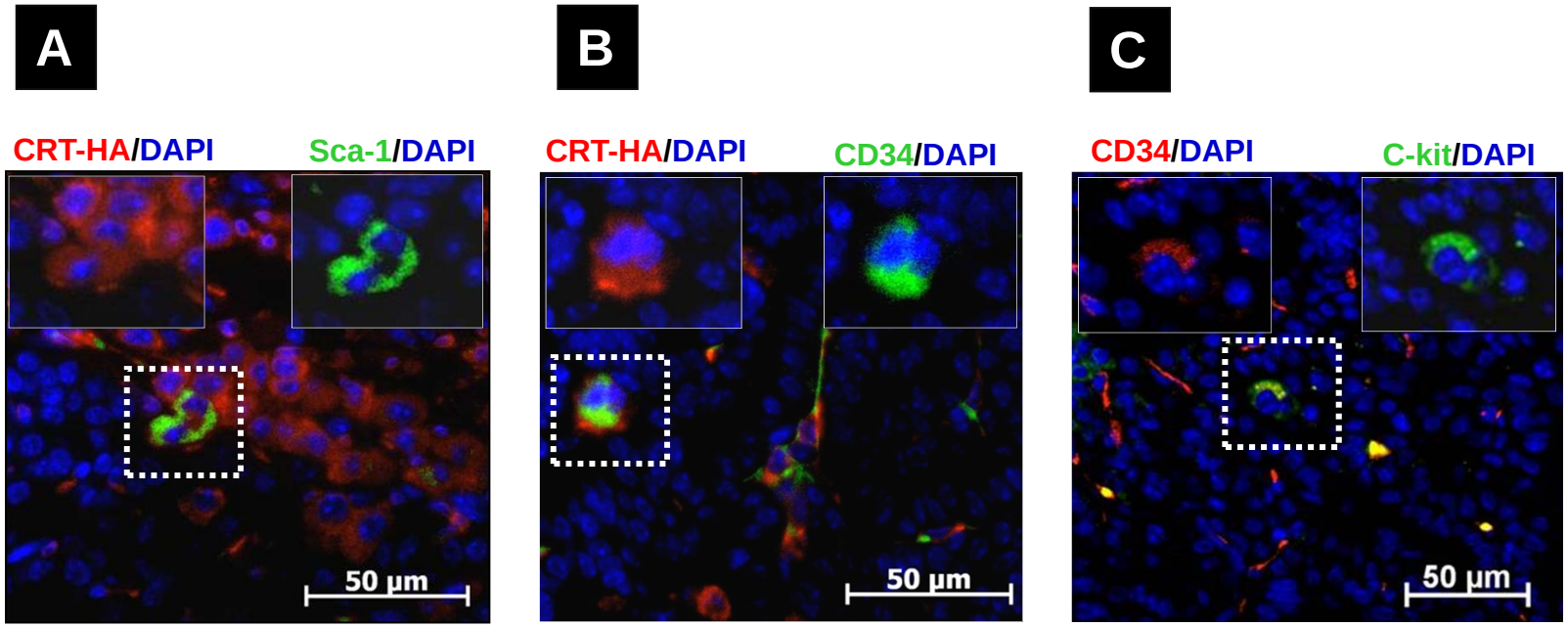

Fig. 26. Co-expression of stem cell markers and HA-CRT in the lung of *Tie2-CRT* mice.
Representative immunofluorescence images of lung sections (from n=3) containing tumors co-stained with (A) anti-HA (red) and either anti Sca-1 (green) or (B) anti CD34 (green). (C) Cells were alternatively co-stained with anti-CD34 (red) and anti-c-kit (green) as described in "Materials and Methods". A portion of cells in the tumor region co-stained with CRT-HA and the above mentioned stem cell markers (A,B). The nuclear stain DAPI (blue) was used as a counter stain. Scale bars indicate 50 µm.

Table 7: Immunohistochemichal characteristics of the different cell types observed in lung adenocarcinomas from *Tie2-CRT* mice.

Cell Type / Marker	Group A	Group B	Group C
SP-C	Positive	Negative	Negative
CC10	Negative	Negative	Negative
E-Cadherin	Positive	Negative	Negative
CRT-HA	Negative	Positive	Positive
CD31	Negative	Negative	Positive
vWF	Negative	Negative	Positive
CD34	Negative	Positive	Positive
c-kit	Negative	Positive	Negative
Sca-1	Negative	Positive	Negative
VEGFR-3	Negative	Positive	Positive

3.1.9. Evaluation of lung cancer progression in *Tie2-CRT* mice

To evaluate tumor development, we carried out IHC analysis of lung tumors at different stages of tumor progression (AAH, adenoma and fully developed adenocarcinoma, n=3 in each group). During the early stages of tumor formation (AAH), the hyperplastic cells formed a glandular structure with heterogeneous expression of SP-C (Fig. 27B) and few cells expressing CRT-HA (Fig. 27F). Interestingly, the cells expressing SP-C do not express CRT-HA. At this stage many of the cells in the tumor area express c-kit and CD133 (Fig. 28B and F). Furthermore, cells in the tumor area also express Sca-1 and CD34 (Fig. 29B and F), although to a lesser extent.

At the adenoma stage, IHC staining revealed heterogeneous expression of SP-C in the tumor. Cells with a glandular structure (Group A tumor cells) express SP-C (Fig. 27C, black arrows), whereas non-glandular tumor cells did not express SP-C (Fig. 27C, blue arrows). Additionally, the non-glandular cells in the tumor region highly expressed CRT-HA (group B and C cells) (Fig. 27G, black arrows). Furthermore, expression of c-kit (Fig. 28C), CD133 (Fig. 28G), and Sca-1 (Fig. 29C) was significantly decreased in the adenoma stage. However, CD34 expression was maintained (Fig. 29G). Overall, the expression of HSC markers and CRT-HA was restricted to SP-C negative cells.

In the fully developed adenocarcinoma, when most neoplastic cells with a glandular structure expressed SP-C (Fig. 27D), we observed only a very few cells expressing c-kit (Fig. 28D), CD133 (Fig. 28H) and Sca-1 (Fig. 29D). At this stage, CRT-HA expression was observed in clusters of non-glandular tumor cells and vascular regions (Fig. 27H, black arrows), which did not express SP-C (Fig. 27D,

black arrow). These observations suggest a differentiation dependent protein expression by tumor cells, in which at the initial stages of tumor formation, cells in the tumor express HSC markers (including CD133, Sca-1, c-Kit) and exogenous CRT, but as the tumor progresses into adenocarcinoma, the epithelial tumor cells with glandular structure lose the expression of HSC markers, while non-glandular tumor cells express exogenous CRT.

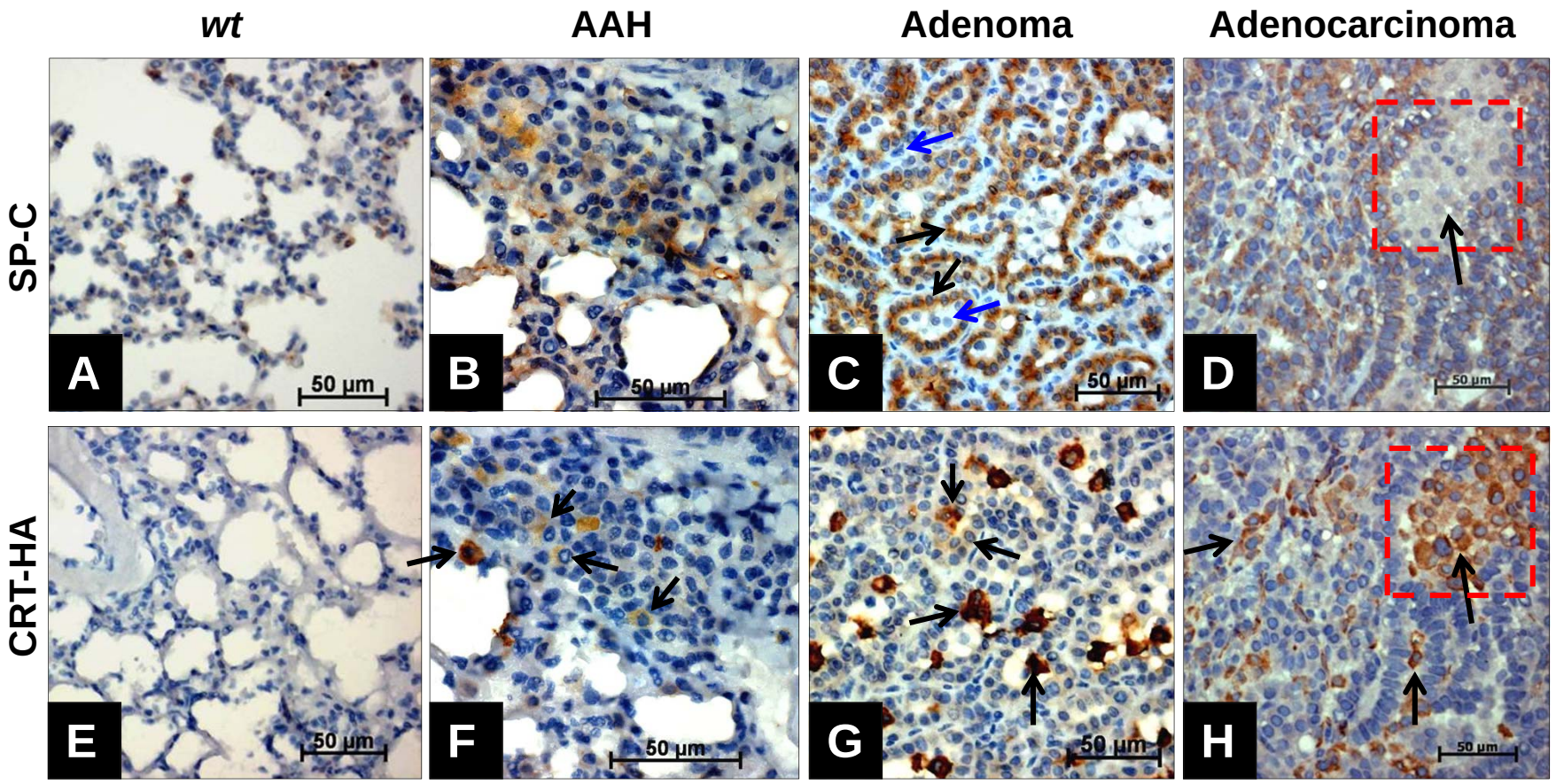

Fig. 27. Evaluation of SP-C and CRT-HA expression at different stages of lung tumor of *Tie2-CRT* mice.
To evaluate SP-C and CRT-HA expression during tumor development, sequential tumor sections at different stages were processed for IHC with antibodies to SP-C (A-D) and HA (E-H). As shown in (B-D) and (F-H), the expression of CRT-HA did not co-localize with SP-C. B-D show that as the tumor progresses from AAH to fully developed adenocarcinoma, the number of epithelial tumor cells expressing SP-C increases while CRT-HA expression is restricted to the irregular shaped cells dispersed between the epithelial tumor cells (F-H, black arrows). n=3, Scale bars indicate 50 µm.

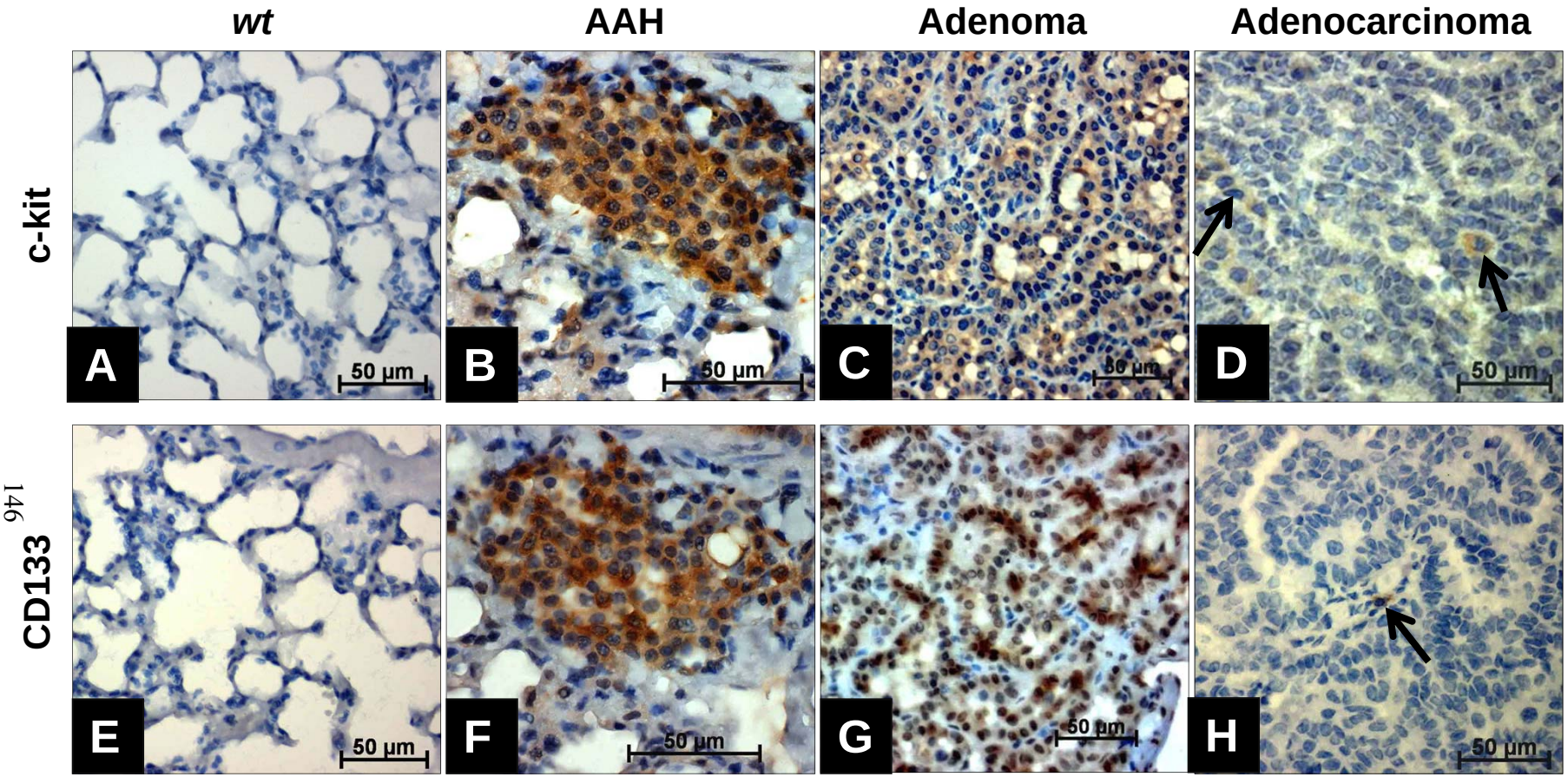

Fig. 28. Evaluation of c-kit and CD133 expression at different stages of lung cancer in *Tie2-CRT* mice.
Representative photomicrographs of the lung sections of *wt* (A,E) and *Tie2-CRT* mice (B-D and F-H) stained with c-kit and CD133. No significant staining with anti-c-kit (A) and CD133 (E) antibodies were observed in *wt* lung sections. During the early stages of tumor development most of the cells in the AAH stained positive for both c-kit (B) and CD133 (F). At the adenoma stage, the staining intensity with both c-kit (C) and CD133 (G) in the tumor cells was reduced as compared to AAH. In the adenocarcinoma stage only a few cells still stained positive for c-kit (D, arrow) and CD133 (H, arrow). n= 3, Scale bars indicate 50 µm.

wt
AAH
Adenoma
Adenocarcinoma
Sca-1
CD34
A
B
C
D
E
F
G
H
50 µm

Fig. 29. Evaluation of Sca-1 and CD34 expression at different stages of lung tumor of *Tie2-CRT* mice.
Representative photomicrographs of the lung sections of *wt* (A,E) and *Tie2-CRT* mice (B-D and F-H) stained with Sca-1and CD34. In the *wt* lung sections no staining with anti-Sca-1antibody was observed (A), while only endothelial cells of capillaries stained positive for CD34 (E). At the early stages of tumor development, a significant number of the cells of the AAH stained positive for both Sca-1(B) and CD34 (F). In adenomas, the staining intensity with Sca-1(C) and CD34 (G) was largely in the neo-vasculature as compared to AAH. In the adenocarcinoma stage, only a few cells still stained positive for Sca-1(D, arrow). Similar to the adenoma stage, microcapillaries of the adenocarcinoma stained positively with CD34 (H, black arrows) while a few irregular shaped cells located between the epithelial cells expressed CD34 (H, blue arrows). n= 3, Scale bars indicate 50 μm.

3.1.10. *In vitro* tumorigenicity assay of *Tie2-CRT* adenocarcinoma ells

Next we asked whether cells develop from tumors of lung of *Tie2-CRT* mice have *in vitro* tumorigenic potential. Anchorage-independent growth of tumor cells is one of the hallmarks of transformation, and correlates strongly with tumorigenicity and invasiveness in many types of tumors (Pavelic *et al.* 1980; Dodson *et al.* 1981). The ability of cells to grow and form colonies in a semi-solid medium (soft agar) is a routine test used to determine if cells are capable of anchorage independent growth. Therefore, to examine the tumorigenicity of tumor cells *in vitro*, we assessed the ability of isolated cells from *Tie2-CRT* lung adenocarcinoma to form colonies in soft agar. We first established a continuous lung adenocarcinoma cell line derived from the lung tumors of *Tie2-CRT* mice as described in "Materials and Methods". Fig. 30A shows a representative image of a monolayer of lung adenocarcinoma cells derived from a lung tumor harvested from a *Tie2-CRT* mouse. These cells were then cultured in soft agar for 3 weeks to allow them to grow and form colonies in the soft agar media (Fig. 30B). Fig. 30C shows a representative plate with 3 week old colonies stained with crystal violet. The colonies were counted using a stereo-microscope and this revealed that a small population of the seeded cells (2.82% of total seeded cells) were able to form colonies in this assay (142.5±27.3 colonies in each plate, n=6). Fig. 30D is a representative H&E staining of a tumor sphere section showing its histological features as a group of intact tumor cells grown in a spheroid shape.

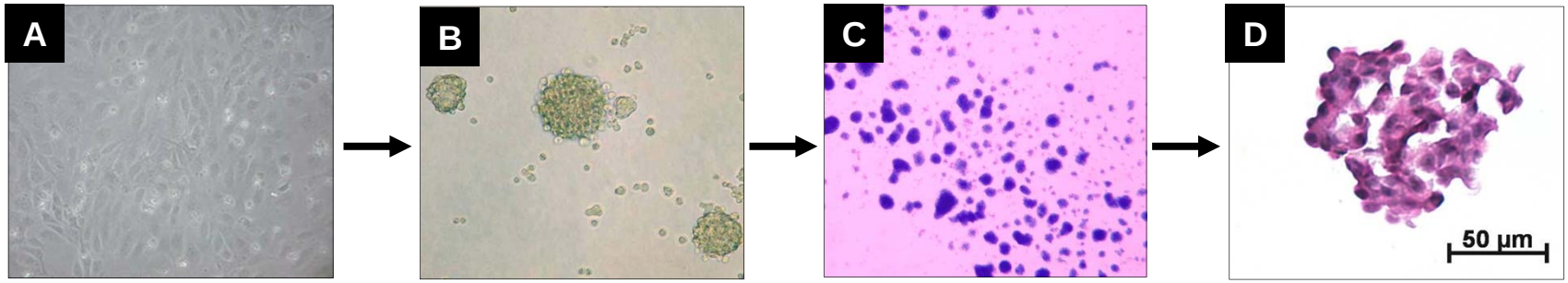

Fig. 30. *In vitro* tumorigenicity assay of mouse lung adenocarcinoma cells isolated from *Tie2-CRT* mice (Soft agar colony formation assay)

To examine the tumorigenic potential of the adenocarcinoma cell line established from *Tie2-CRT* mice *in vitro*, we assessed the anchorage-independent growth of these cells in soft agar as described in "Materials and Methods". (A) 5 10^3 cells of adenocarcinoma cells of *Tie2-CRT* mice were embedded in 0.5% agar and allowed to grow for 3 weeks. Tumor cells were able to grow and form colonies in soft agar media (B). Plates were then stained with crystal violet and examined for the presence of colonies under a dissecting microscope (C). (D) A representative H&E staining of one tumor sphere cryosection illustrating the cellular structure of these tumor spheres . Scale bars indicate 50 µm.

3.1.11. *In vitro* evaluation of tumor sphere differentiation

To examine the differentiation potential of tumor spheres, they were grown in a medium containing 10% serum. Fig. 31 shows the differentiation potential of one tumor sphere (Fig. 31A) when seeded in a tissue culture plate with medium containing 10% FBS. The tumor sphere attached to the plate and gradually migrated to form a monolayer of adherent cells (Fig. 31B and C). Tumor cells located at the edge of the tumor sphere had a flattened appearance and morphologically distinct from the cells located in the middle of the sphere.

IF staining of tumor spheres after 3 days of growth in a regular culture plate with media containing FBS was carried out to examine the expression of Sca-1, CD133 and Tie2 in these cells. Fig. 32 shows a representative image of co-staining for CD133 (Fig. 32A red) and Sca-1 (Fig. 32B green) on one tumor sphere after 3 days of growth in media containing 10% FBS, demonstrating the expression of CD133 and Sca-1 by cells only within the sphere of tumor cells. However on the edge where the cells form a monolayer, there is no expression of these markers (Fig. 32A and B).

Tie-2 expression in tumor spheres was also examined using a Tie-2 specific antibody (Fig. 32C). Fig. 32C shows expression of Tie-2 (Fig. 32C, red) by cells in the middle of the tumor sphere and loss of Tie-2 expression in the cells located on the periphery of the sphere growth after 3 days in culture (Fig. 32C). These observations suggest that cells in the periphery of tumor sphere undergo at least partial differentiation as they acquire a more adherent phenotype.

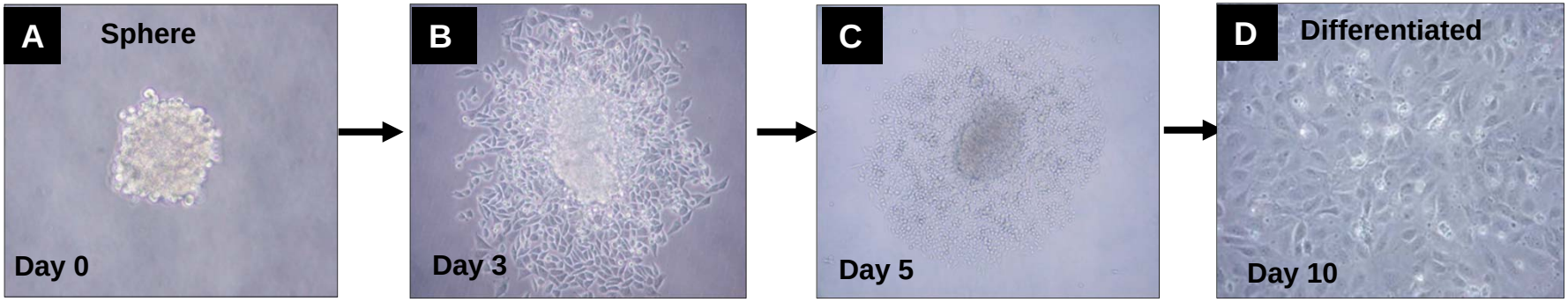

Fig. 31. *In vitro* evaluation of tumor sphere differentiation.
A-C show a representative (n=6) examination of the differentiation potential of tumor spheres (from soft agar) by plating colonies in tissue culture plate and allowing them to adhere and grow in a media containing 10% serum. As shown in B, tumor spheres placed in a plate containing media with 10% FBS attached to the plate and gradually differentiated into a monolayer of adherent cells (B and C). As the cells from the colony migrate out, they undergo morphological changes, however, the cells in the centre still maintain a spheroid morphology. After approximately 2 weeks all of the cells had spread to form a monolayer (D).

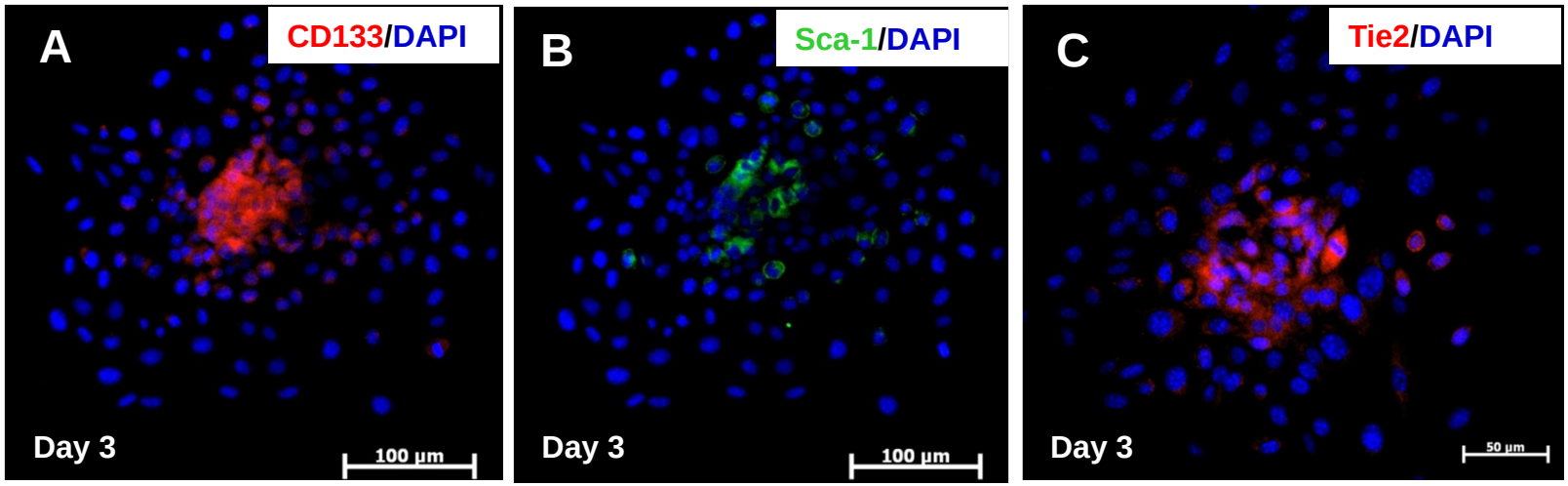

Fig. 32. IF examination of *in vitro* tumor sphere differentiation.
Growth of one tumor sphere placed in media containing 10% serum is examined by IF staining using stem cell markers. Tumor spheres were able to adhere to the plate and gradually differentiate into a monolayer of adherent cells. Tumor cells located at the edge of tumor sphere growth represent more differentiated cell type as compared to the cells located in the middle of tumor. After differentiation, tumor cells on the edge lose their ability to express CD133 (A) and Sca-1 (B) while cells in the middle of colony that remain undifferentiated, stained positive for CD133 (A) and Sca-1 (B). (C) shows expression of Tie-2 by cells in the middle (undifferentiated) region of tumor sphere and loss of Tie-2 expression in the differentiated cells located in the periphery of the tumor sphere. n=3, CD133 (Texas red, red), Sca-1 (FITC, green) and nuclei blue (DAPI), scale bars indicate 100 µm.

3.1.12. Immunohistochemical characterization of undifferentiated (tumor spheres) and differentiated tumor cells.

To further characterize undifferentiated tumor cells (tumor spheres) and differentiated tumor cells (adherent monolayer), we evaluated expression of HSC markers in two different forms of tumor cells using IF methods. Fig. 33 is a representative IF staining of tumor spheres (Fig. 33, A-F) and differentiated tumor cells (Fig. 33, G-L) using different markers as illustrated in Table 8. As shown in Fig. 33, the undifferentiated form of tumor cells (tumor spheres) express CRT-HA (Fig. 33F) and different stem cell markers including CD133 (Fig. 33C), Sca-1(Fig. 33D), c-kit (Fig. 33E), but do not express SP-C, CC10 or E-cadherin (Fig. 33A, B and C). In contrast, when tumor spheres are cultured in monolayers (differentiated tumor cells), they express SP-C and E-cadherin, but lose stem cell marker expression (Fig. 33G-H). Collectively, these data show that at the initial stages of neoplastic transformation, tumor cells display a non-epithelial phenotype and express HSC proteins. However, after growth in a monolayer, they differentiate into epithelial cells as evident by expression of epithelial markers and lose the HSC antigens. The immunohistochemical characteristics of tumor spheres and differentiated form of lung tumor cells are summarized in Table 8.

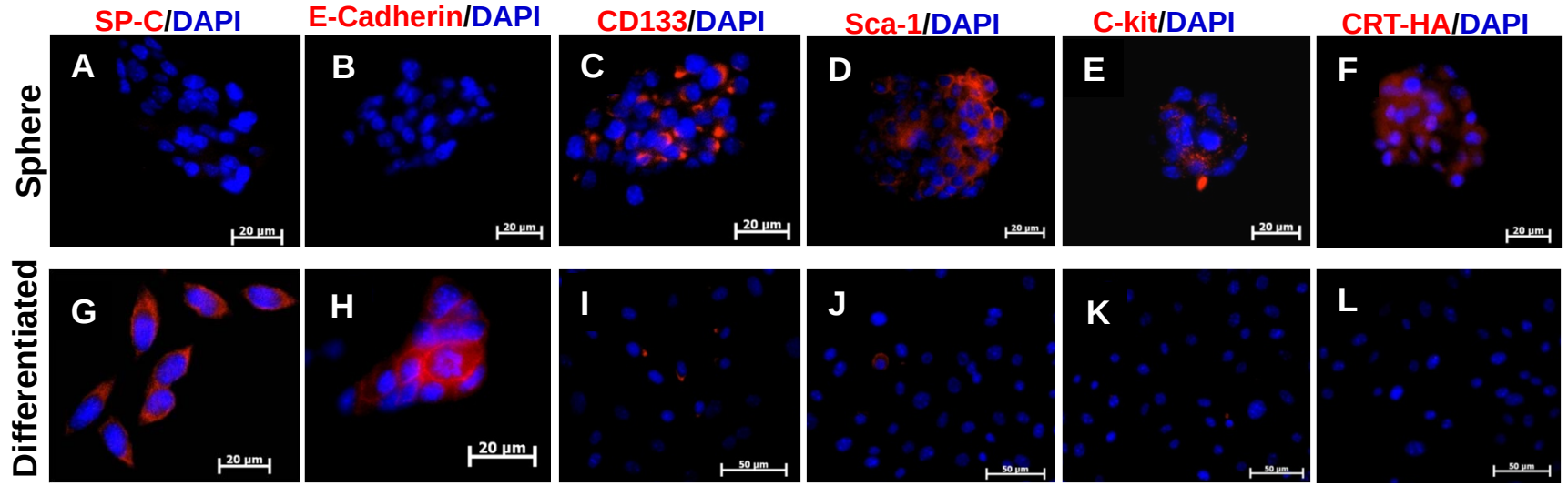

Fig. 33. Characterization of tumor spheres (undifferentiated form) and adherent (differentiated) tumor cells.

Tumor spheres grown in soft agar were isolated and fixed in 4% paraformaldehyde and embedded in OCT. Five µm cryosections were prepared and used for IF staining using different antibodies as listed in A-F. A-F, IF staining of tumor spheres (un-differentiated) and G-L are IF staining images of differentiated tumor cells. As shown, tumor spheres did not express SP-C (A) and E-cadherin (B, marker of epithelial cells), while they stained positive for CD133 (C), Sca-1 (D), c-kit (E), and CRT-HA (F). Differentiated tumor cells express SP-C (G) and E-cadherin (H) while they stained negative for CD133 (I), Sca-1 (J), c-kit (K), and CRT-HA (L). n=3, Scale bars indicate as shown in each image.

Table 8. Immunohistochemical characteristics of undifferentiated (tumor spheres) and differentiated forms of lung tumor cells in *Tie2-CRT* mice.

Marker	Differentiated	Undifferentiated
SP-C	Positive	Negative
CC-10	Negative	Negative
E-Cadherin	Positive	Negative
CD133	Negative	Positive
CD34	Negative	Positive
CD31	Negative	Negative
Sca-1	Negative	Positive
c-kit	Negative	Positive
CRT-HA	Negative	Positive
Tie2	Negative	Positive

3.1.13. Non-adherent sphere assays using lung tumor cells isolated from *Tie2-CRT* mice.

To better understand the mechanisms of initiation and progression of the lung tumors observed in *Tie2-CRT* transgenic mice, lung tumor cells were isolated and a cell line was established from them as described in "Materials and Methods". Next, we asked whether these tumor cells have the capacity for self-renewal. To address this question, we examined the ability of isolated lung tumor cells to expand and generate undifferentiated sphere-like cellular masses in a proliferative serum–free medium (Ponti *et al.* 2005; Ricci-Vitiani *et al.* 2007; Eramo *et al.* 2008). After 4 weeks of culture in these conditions, lung tumor spheres were formed as a cluster of growing undifferentiated tumor cells (Fig. 34A and B). We examined the characteristics of these tumor spheres with IF staining using different stem cell markers. Similar to tumor spheres generated in soft agar culture, the tumor spheres formed in this medium express different stem cell markers including CD34 (Fig. 34C), Sca-1(Fig. 34D), CD133 (Fig. 34E) and CRT-HA (Fig. 34F). These data show that cells isolated from *Tie2-CRT* lung tumors have the ability to expand and generate sphere-like cellular masses under non-adherent conditions, and that some of cells in these spheres have stem cell characteristics and also express CRT-HA.

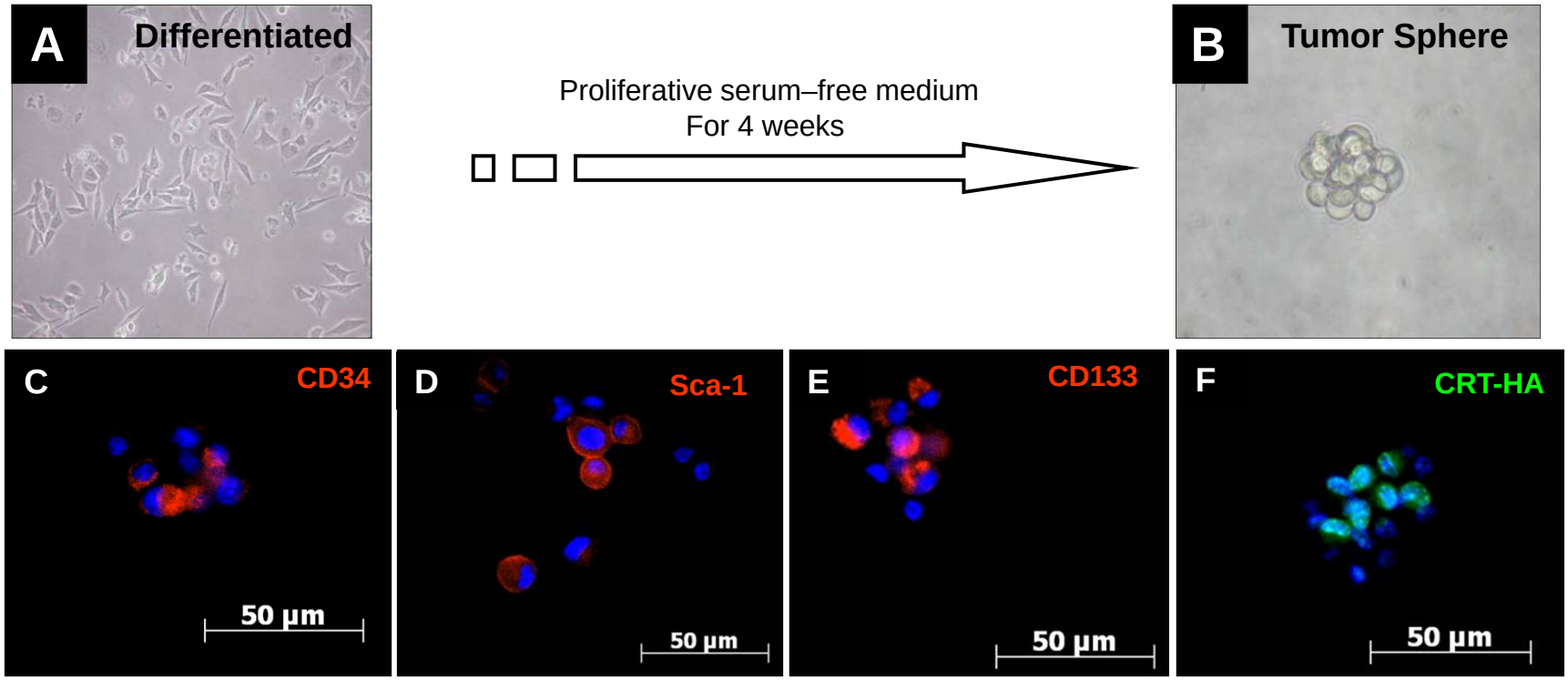

Fig. 34. Non-adherent culture conditions for tumor sphere production

To examine the ability of lung tumor cells isolated from *Tie2-CRT* to form colonies in serum-free non-adherent culture conditions, we performed a non-adherent sphere assay. Lung tumor cells grown on the plate (A) were cultured in a proliferative serum–free medium. After 4 weeks of culture, undifferentiated sphere-like cellular masses (B) formed as a cluster of growing undifferentiated tumor cells. C-F show the immunophenotypic characterization of these tumor spheres. As shown, tumor spheres express different stem cell markers including CD34 (C), Sca-1 (D), CD133 (E) as well as CRT-HA (F). n=3, Scale bars indicate 50 µm.

3.1.14. Characterization of differentiated and undifferentiated human lung adenocarcinoma cells (A549).

To determine the similarities between our *Tie2-CRT* lung cancer model and human lung cancer, we repeated the soft agar assays using A549 human lung adenocarcinoma cell line. For comparison we also examined H460 human lung large cell carcinoma (LCC) cells. As illustrated in Fig. 35 and 36, both cell lines express SP-C (Fig. 35G and 36G) and CC10 (Fig. 35H and 36H). Furthermore, undifferentiated tumor spheres isolated from A549 cells (Fig. 35A) and H460 cells (Fig. 36A) express the stem cell markers CD133 (Fig. 35D and 36D) and c-kit (Fig. 35E and 36E). After differentiation, these cells lose the expression of CD133 (Fig. 35I and 36I) and c-kit (Fig. 35J and 36J) antigens, similar to *Tie2-CRT* mice cell line. In contrast to immunophenotypic characterization of undifferentiated tumor spheres isolated from *Tie2-CRT* mice, undifferentiated tumor spheres (undifferentiated cells) from human A549 cells and H460 cells stained positive for SP-C (Fig. 35B and 36B) and CC10 (Fig. 35C and 36C). These data support the previously published data that both A549 and H460 human cell lines have a bronchiole alveolar origin.

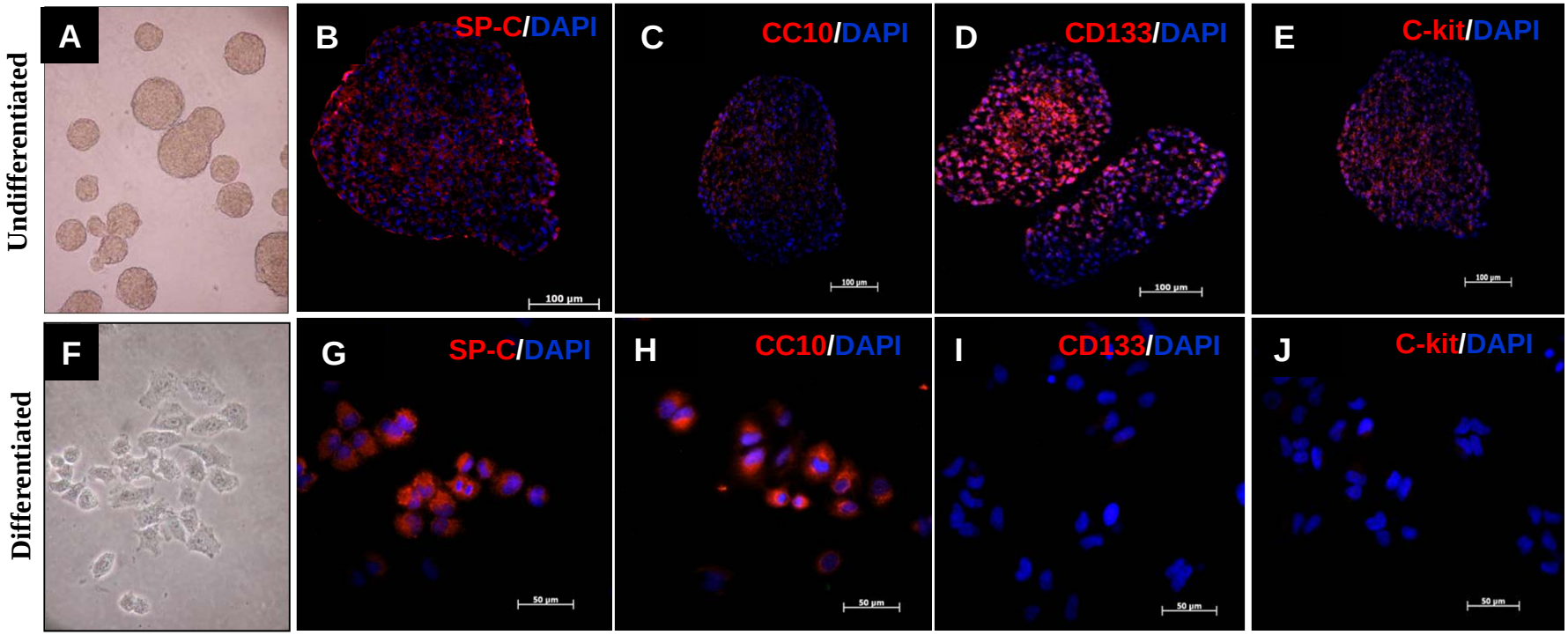

Fig. 35. Characterization of differentiated and undifferentiated human lung adenocarcinoma cell line (A549).

Tumor spheres were prepared in soft agar and fixed in 4% paraformaldehyde and embedded in OCT. Five µm cryo sections were prepared and used for IF staining using different antibodies as listed in each IF image. Photomicrographs of undifferentiated tumor spheres from A549 cells (A) and differentiated tumor cells (F) showing morphology of these cells in the culture. IF staining of undifferentiated (tumor spheres) (B-E) and differentiated tumor cells (G-J) with SP-C, CC10, CD133 and c-kit. As shown, both differentiated cells and tumor spheres express SP-C (B and G respectively) and CC-10 (C and H respectively). Undifferentiated cells also stained positive for CD133 (I) and c-kit (J), while differentiated cells did not express either CD133 (D) or c-kit (E). n=3, Scale bars indicate 50 µm.

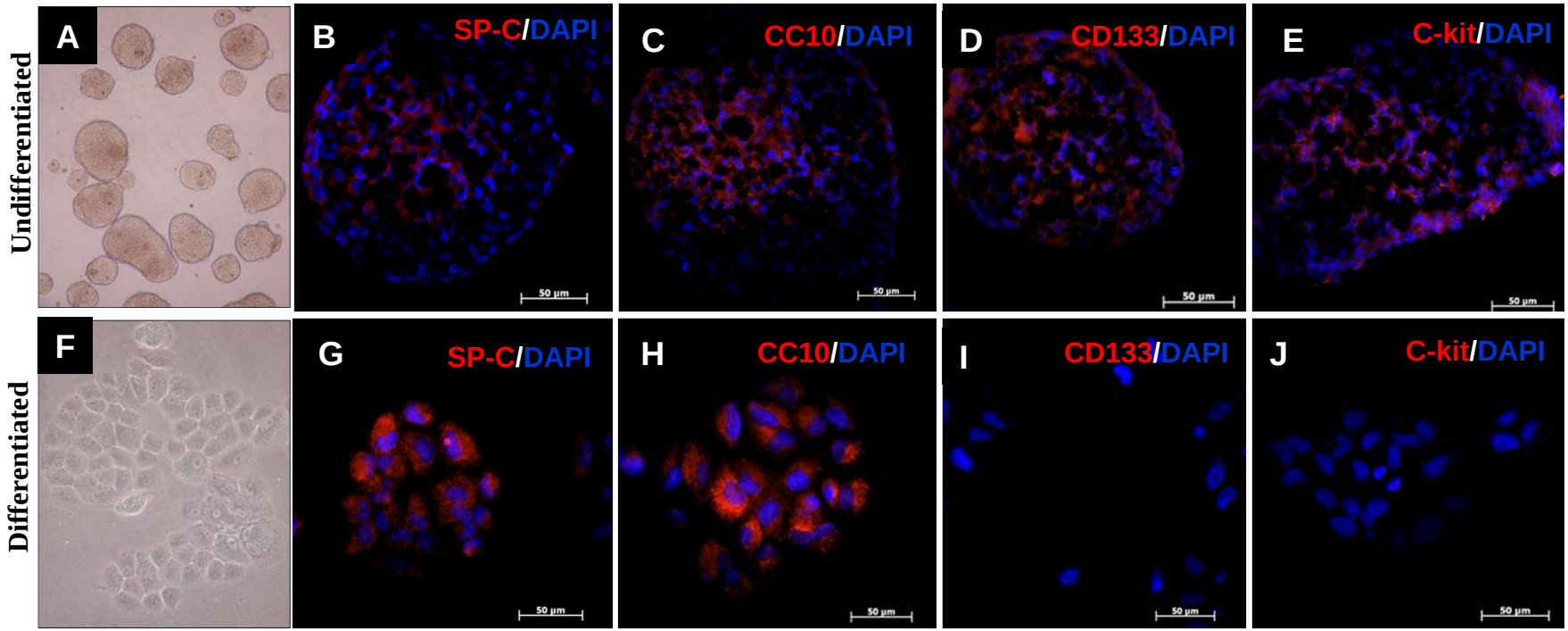

Fig. 36. Characterization of differentiated and undifferentiated human lung large cell carcinoma cell line (H460).

Tumor spheres were prepared in soft agar and fixed in 4% paraformaldehyde and embedded in OCT. Five µm cryo-sections were prepared and used for IF staining using different antibodies as listed in IF images. Photomicrograph of undifferentiated tumor spheres from H460 cells (A) and differentiated tumor cells (F) showing morphology of these cells in the culture. IF staining of undifferentiated (tumor spheres) (B-E) and differentiated tumor cells (G-J) with SP-C, CC10, CD133 and c-kit are shown. Both differentiated and tumor spheres express SP-C (B and G respectively) and CC-10 (C and H respectively). Undifferentiated cells stained positive for CD133 (I) and c-kit (J), while differentiated cells did not express CD133 (D) and c-Kit (E). n=3, Scale bars indicate 50 µm.

3.1.15. *In vitro* clonogenic assay of BM cells in soft agar media.

Our data showed that at the initial stages of lung tumor formation, the tumor cells express stem cell markers (Fig. 37) suggesting that BM cells may play a role as the cell of origin for lung tumors seen in *Tie2-CRT* mice. Therefore we examined the proliferative capacity of BM cells of *Tie2-CRT* mice as compared to *wt* control. The generation of hematopoietic colonies in a semi-solid medium (soft agar) is a common test used to evaluate the proliferative capacity of BM cells *in vitro* (Bradley *et al.* 1966; Broxmeyer 1984). As such, we isolated BM cells from both *Tie2-CRT* and *wt* mice and cultured them in soft agar (Horowitz *et al.* 2002) as described in "Materials and Methods".

Fig. 37A and C are photomicrographs of BM cells from *wt* (and *Tie2-CRT* mice, respectively, cultured in soft agar. After 2 weeks, colonies of BM cells from both *wt* (Fig. 37B) and *Tie2-CRT* mice (Fig. 37D) were generated in soft agar. Plates were stained with crystal violet and then the number of colonies in each plate was counted using a stereo-microscope. As shown in the bar graph (Fig. 37E), the number of colonies generated from the BM of *Tie2-CRT* mice was significantly higher than the number of colonies generated from the BM of *wt* mice ($p<0.05$, $n=3$). The higher colony-forming ability of the BM cells isolated from *Tie2-CRT* mice suggests that these cells are more proliferative and may have increased tumorigenicity *in vivo* as compared to those of their *wt* littermates.

Colonies were also isolated and used for IF staining for further characterization. Fig. 38, A-F show representative images of colonies stained for CRT-HA, CD133 and SP-C. As expected, colonies generated from *Tie2-CRT* mice expressed CRT-HA transgene (Fig. 38D) whereas colonies isolated from their *wt*

littermates did not express CRT-HA (Fig. 38A). Colonies generated from both *wt* and *Tie2-CRT* expressed CD133 (Fig. 38B and E), but not SP-C protein (Fig. 38C and F).

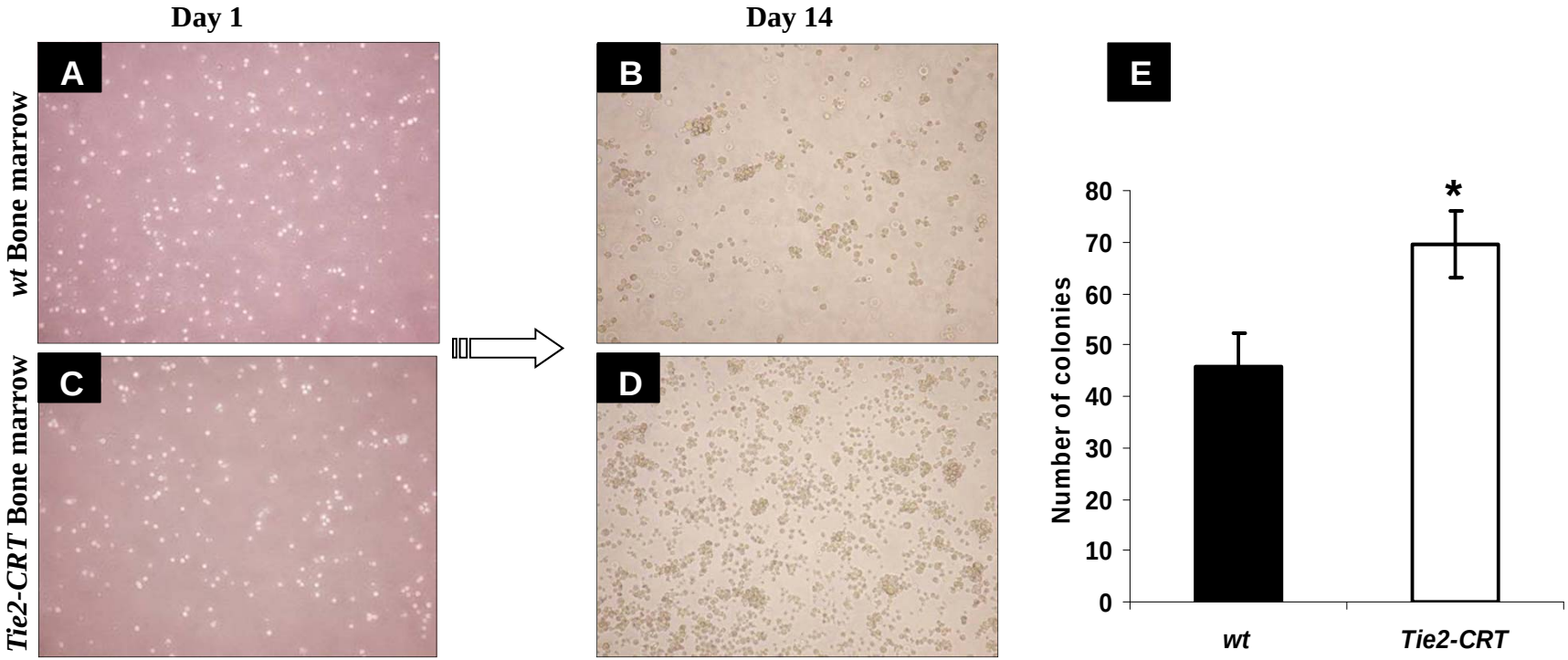

Fig. 37. *In vitro* clonogenic assay of bone marrow cells in soft agar culture.
Bone marrow cells were isolated from *wt* and *Tie2-CRT* mice as described in "Materials and Methods". $5x10^4$ bone marrow cells from *wt* (A) and *Tie2-CRT* (C) mice were cultured in soft agar supplemented with 10ng/ml GM-CSF and IL-3 and allowed to grow for 14 days. After 2 weeks, bone marrow cells from both *wt* (B) and *Tie2-CRT* (D) were able to grow and form colonies in soft agar. The two-tailed Student's t-test was used to determine significant differences between the two values. The bar graph (E) shows mean SE of number of colonies counted under microscope from three different mice in each group. *$p<0.05$, significantly different from *wt.*

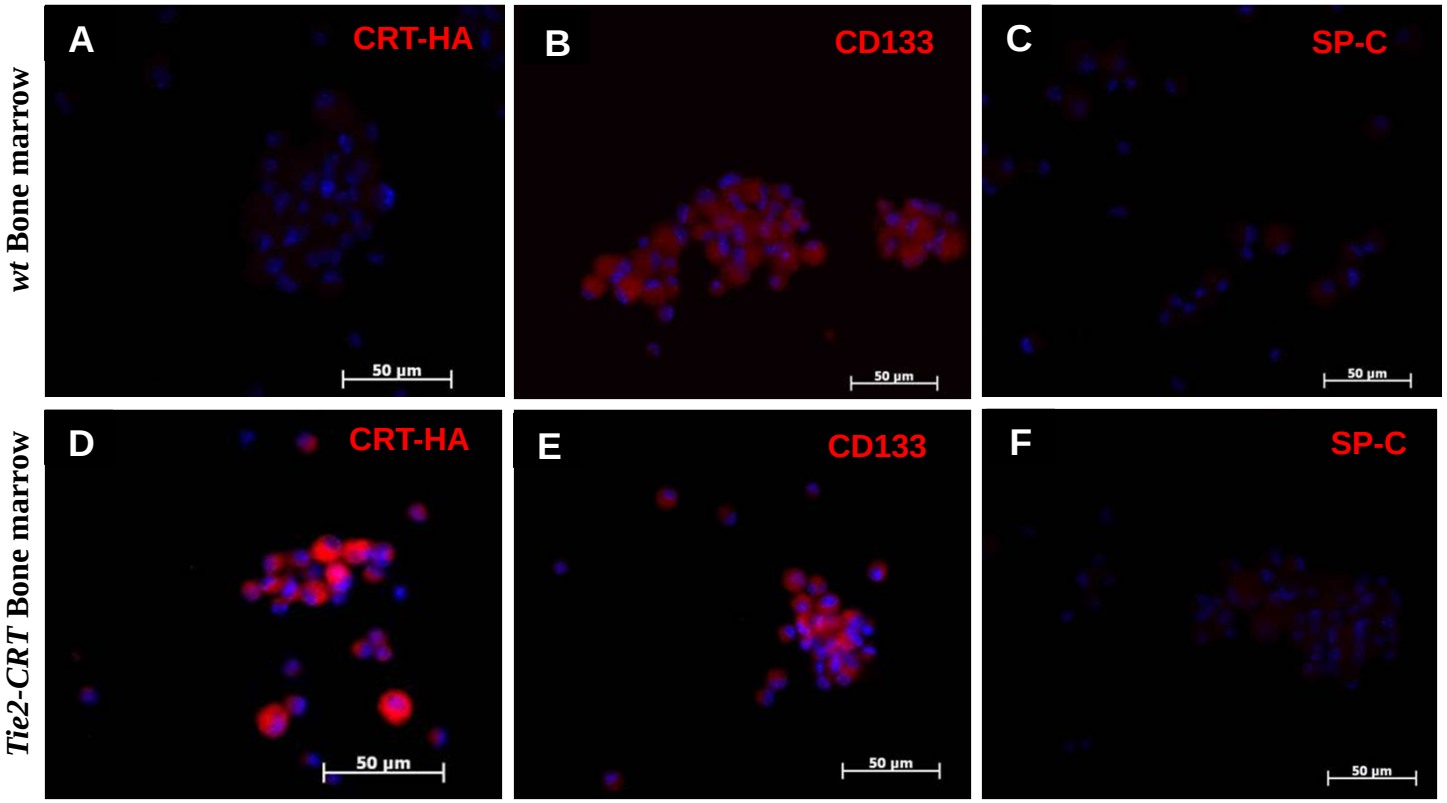

Fig. 38. IF examination of colonies generated from bone marrow cells of *wt* and *Tie2-CRT* mice in soft agar culture. (A-F) show representative colonies stained for CRT-HA, CD133 and SP-C (n=3 for each antibody). Colonies generated from *Tie2-CRT* mice expressed CRT-HA (F). Both *wt* and *Tie2-CRT* bone marrow colonies expressed CD133 (D and G) while neither expressed SP-C, a marker of alveolar type II cells. Scale bars indicate 50µm

3.2. HSC alterations in *Tie2-CRT* mice

It has long been known that adult BM cells serve as precursors for HSCs (Fliedner 1998). However, several studies have suggested that cell populations derived from the BM of adult rodents have the ability to cross lineage barriers, and serve as precursors for differentiated cells of different organs including lung (Kotton *et al.* 2001; Ishizawa *et al.* 2004; Yamada *et al.* 2004; Rojas *et al.* 2005). In the majority of these studies using animal models, recruitment of BM cells to the lung occurs in response to induced epithelial injury and inflammation. Lung inflammation can result in epithelial injury and release of inflammatory cytokines that will subsequently lead to the recruitment of BM cells to the lung (Yamada *et al.* 2004; Krause 2008).

As shown in Fig. 13 and 14, discoloration and inflammation were observed in the lung of young *Tie2-CRT* mice. Furthermore, double IF staining for CD34, c-kit and Sca-1 also revealed existence of cells which stained positive for stem cell markers in the lungs of *Tie2-CRT* but not *wt* mice (Fig. 26 A-C). An increase in the number of inflammatory cells and presence of HSCs in the lung of *Tie2-CRT* mice raises the question of whether the rate of mobilization of HSCs from BM and the number of HSCs in the circulation of *Tie2-CRT* mice is increased. Thus, to address these questions we examined changes in the number of HSCs in the BM and blood of *Tie2-CRT* mice using flow cytometry.

3.2.1. Analysis of HSC in the peripheral blood of *wt* and *Tie2-CRT* mice.

Blood samples were collected from both *Tie2-CRT* transgenic mice and *wt* littermates by cardiac puncture. Cells were stained with different markers of HSCs

including CD34, c-kit and Sca-1 and analyzed by flow cytometry as described in "Materials and Methods". Fig. 39 shows a representative result (n=7) obtained from flow cytometry experiments using blood cells. Bar graph (Fig. 40A) shows no significant changes in the number of Sca-1^+/c-kit^+ dual stained cells in the *Tie2-CRT* mice as compared to *wt* controls. However, the number of $CD34^+$/c-kit^+ dual stained HSCs in the blood of *Tie2-CRT* mice was significantly higher than in *wt* littermates (Fig. 40B). Fig. 40C demonstrates that the population of Sca-1^+/c-kit^+ cells was 1.61 fold higher in *Tie2-CRT* mice as compared to their *wt* littermates, while $CD34^+$/c-kit^+ cells were 2.09 fold higher ($p<0.05$, n=7) in *Tie2-CRT* mice as compared to *wt* mice. The increased number of HSCs in the circulation suggests an elevated rate of HSC mobilization in *Tie2-CRT* mice in contrast to *wt* mice, which could contribute to the observed increase in stem cells in the lung tissue of *Tie2-CRT* mice (Fig. 27).

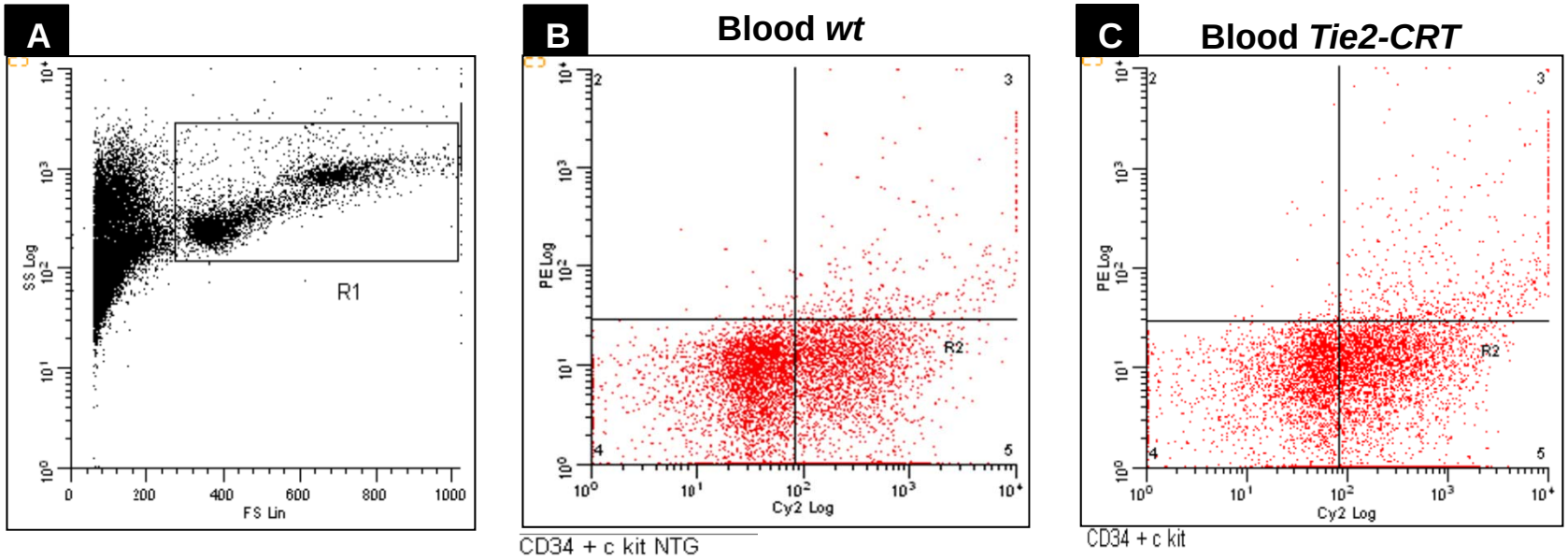

Fig. 39. Analysis of circulatory HSCs in *wt* and *Tie2-CRT* mice.
Circulatory white blood cells of both *wt* and *Tie2-CRT* mice were isolated and analyzed by flow cytometry. The window in (A) shows the population of leukocytes considered for evaluation (R1). B and C show representative sorting of blood cells isolated from *wt* (B) and *Tie2-CRT* (C) mice using CD34 and c-kit antibodies.

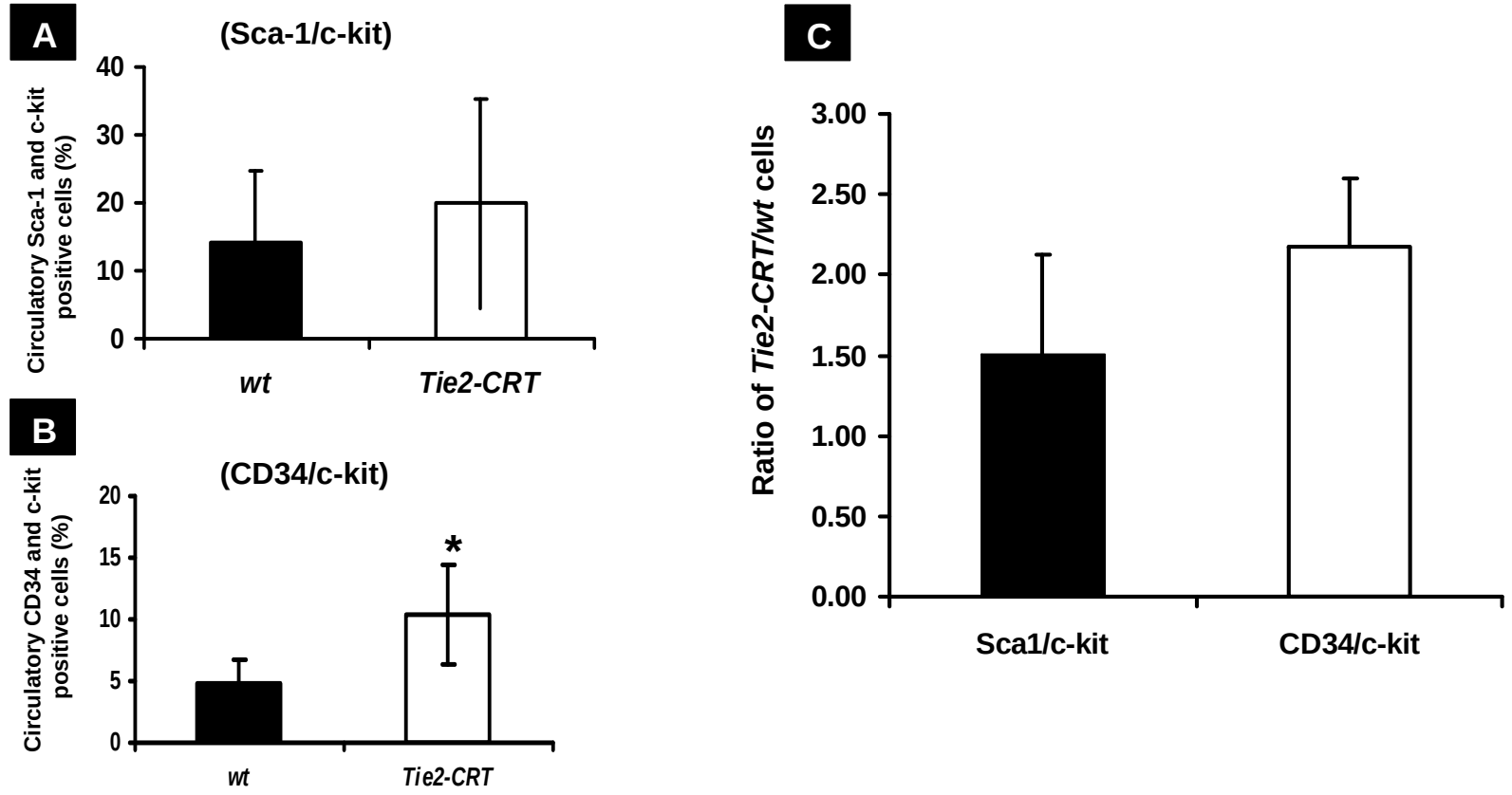

Fig. 40. Number of [Sca-1^{pos}c-kit^{pos}] and [CD34^{pos}c-kit^{pos}] HSCs in the circulation of *Tie2-CRT* as compared to *wt* mice.
Bar graphs show the percentage of [Sca-1^{pos}c-kit^{pos}](A) and [CD34^{pos}c-kit^{pos}] (B) HSCs in the circulation of *Tie2-CRT* mice as compared to their *wt* littermates. The number of [CD34^{pos}c-kit^{pos}] HSCs in the blood of *Tie2-CRT* mice is significantly higher than for *wt* littermates (B) while there were no significant changes in the number of [Sca-1^{pos}c-kit^{pos}]HSCs in the *Tie2-CRT* mice as compared to *wt* controls (A). Furthermore, [Sca-1^{posc}-kit^{pos}] and [CD34^{posc}-kit^{pos}]HSCs were higher in *Tie2-CRT* mice as compared to their *wt* littermates (C). Values are mean ± SE of blood samples isolated from 7 *Tie2-CRT* and *7* wt mice.
*$p<0.05$, significantly different from their *wt*.

3.2.2. Analysis of HSC in the BM of *Tie2-CRT* mice and their *wt* littermates

In addition to evaluating the HSC population in the peripheral blood, we examined the population of HSCs in the BM of *Tie2-CRT* mice and compared them to their *wt* littermates. BM cells were collected from both *Tie2-CRT* transgenic mice and *wt* littermates, and stained with different markers and analyzed using a flow cytometer. Fig. 41 shows a representative data obtained from flow cytometry experiments using BM cells. Bar graphs in Fig. 42 show no significant changes in the number of Sca-1^+/c-kit^+ (Fig. 42A) and $CD34^+$/c-kit^+ (Fig. 42B) doubly stained cells in the BM of *Tie2-CRT* mice as compared to *wt* controls. Over all, there was only a 1.38 fold increase in the number of Sca-1^+/c-kit^+ cells and a 1.33 fold increase in the number of $CD34^+$/c-kit^+ HSCs in BM of *Tie2-CRT* mice as compared to their *wt* controls. These increases were not statistically significant (Fig. 42C).

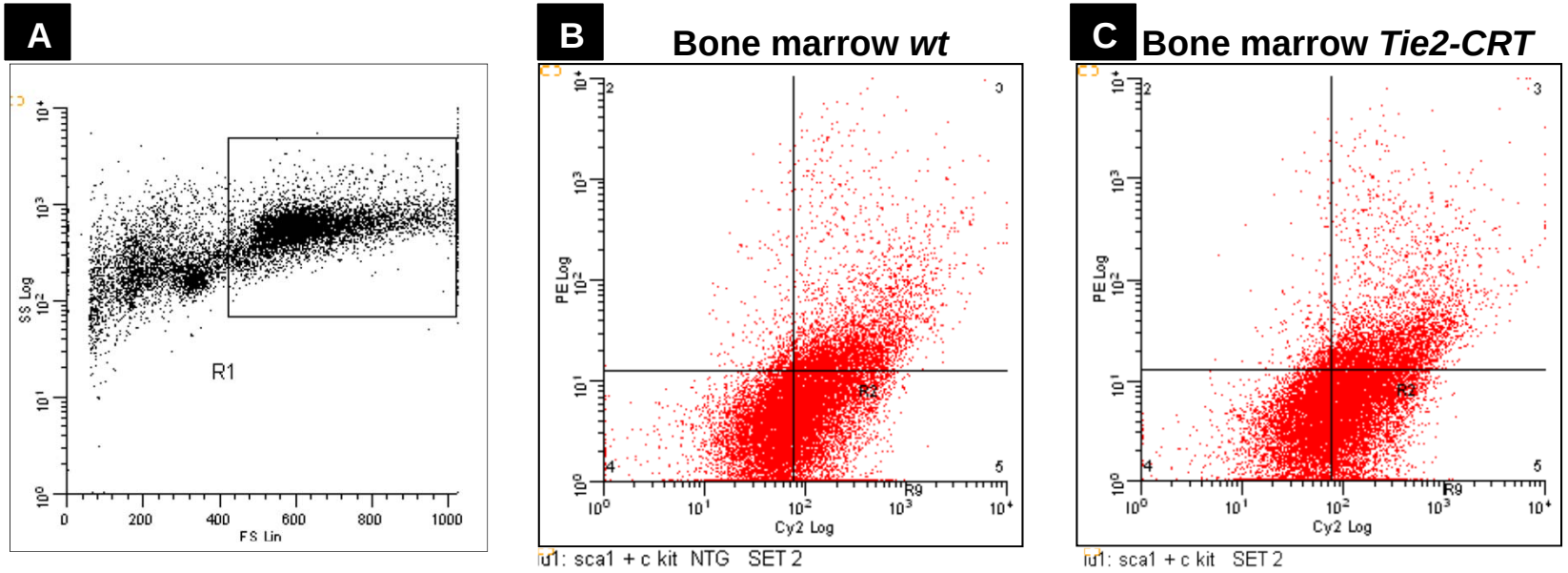

Fig. 41. Analysis of the HSC population in the bone marrow of *wt* and *Tie2-CRT* mice

Bone marrow cells of both *wt* and *Tie2-CRT* mice were isolated and analyzed using flow cytometry. The window in (A) shows the population of bone marrow cells (R1) considered for evaluation by flow cytometery. B and C show representative dot plots of sorted of bone marrow cells isolated from *wt* (B) and *Tie2-CRT* (C) mice using Sca-1 and c-kit antibodies.

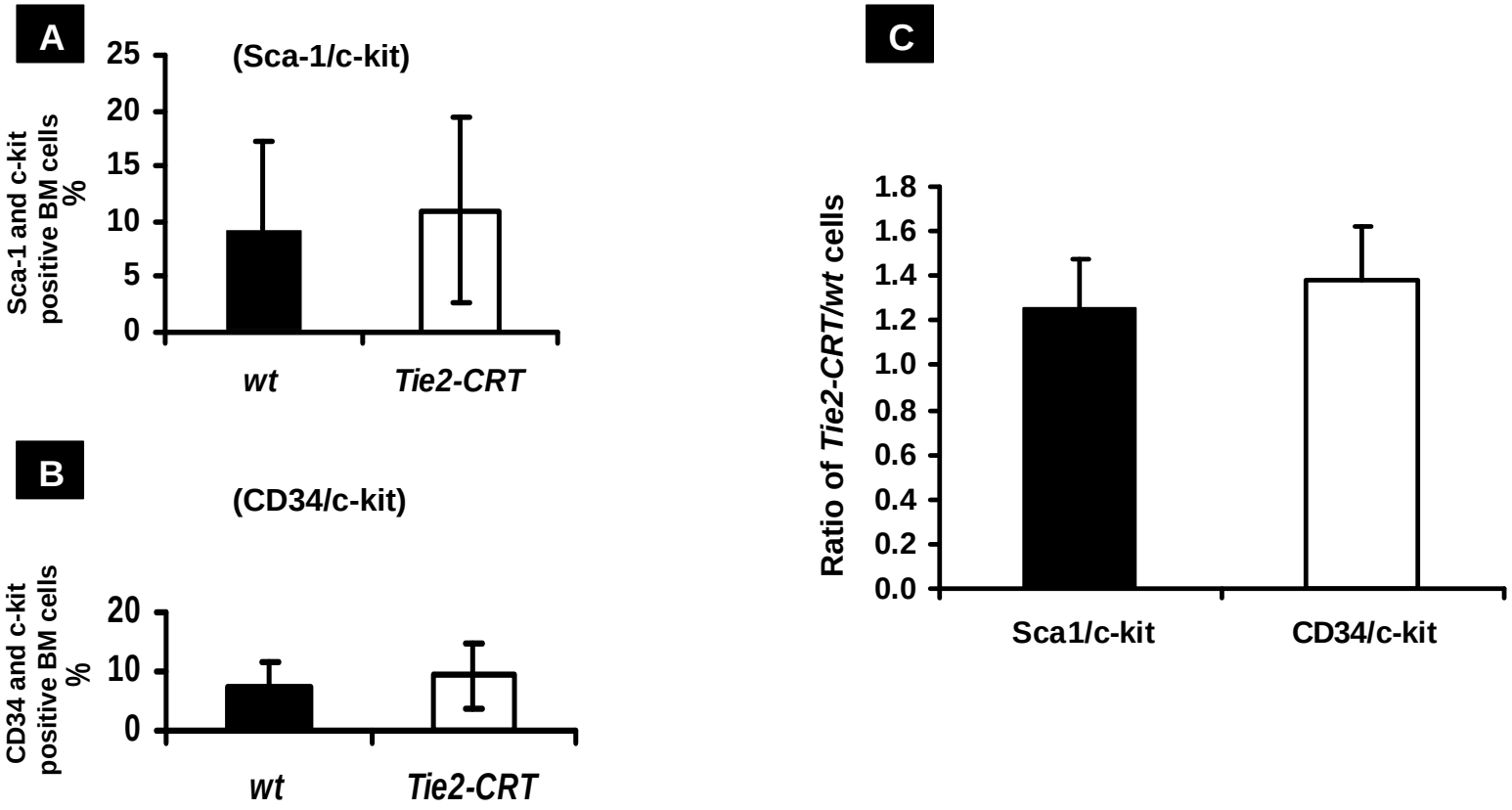

Fig. 42. Examining [Sca-1^{pos}c-kit^{pos}] and [CD34^{pos}c-kit^{pos}] HSCs in the bone marrow (BM) of *Tie2-CRT* as compared to *wt* mice.

Bar graphs show the number of [Sca-1^{pos}c-kit^{pos}](A) and [CD34^{pos}c-kit^{pos}] (B) HSCs in the bone marrow of *Tie2-CRT* mice as compared to their *wt* littermates. Values are mean ± SE of bone marrow samples isolated from 7 *Tie2-CRT* and *7* wt mice.

3.2.3. Evaluation of the bone marrow CD133 positive cells in *wt* and *Tie2-CRT* mice.

CD133 was originally described as a marker of normal HSCs (Yin *et al.* 1997) however, it has gained more prominence as a marker of cancer stem cells in solid tumors (Singh *et al.* 2003; Ponti *et al.* 2005; Ricci-Vitiani *et al.* 2007; Eramo *et al.* 2008; Chan *et al.* 2009). Increased numbers of CD133 positive cells in the BM of myelodysplastic syndrome patients has been reported (Auberger *et al.* 2005). Since CD133 positive cells are proposed as a putative tumor initiating stem cells, we examined the number of CD133 positive cells in the BM of *Tie2-CRT* mice and *wt* littermates. CD133 positive cells were isolated from the BM of *wt* and *Tie2-CRT* mice using a magnetic bead sorting kit as described in "Materials ad Methods". As seen in Fig. 43, the number of CD133 positive cells in the BM of *Tie2-CRT* mice is significantly greater than that of *wt* mice ($p<0.05$, $n=3$). A higher number of $CD133^{+}$ cells in the BM of *Tie2-CRT* mice not only suggests a higher rate of hematopoiesis in these transgenic animals as compared to *wt* control mice but also may indicate a possible increased tumorgenesis capacity of BM cells of *Tie2-CRT* mice.

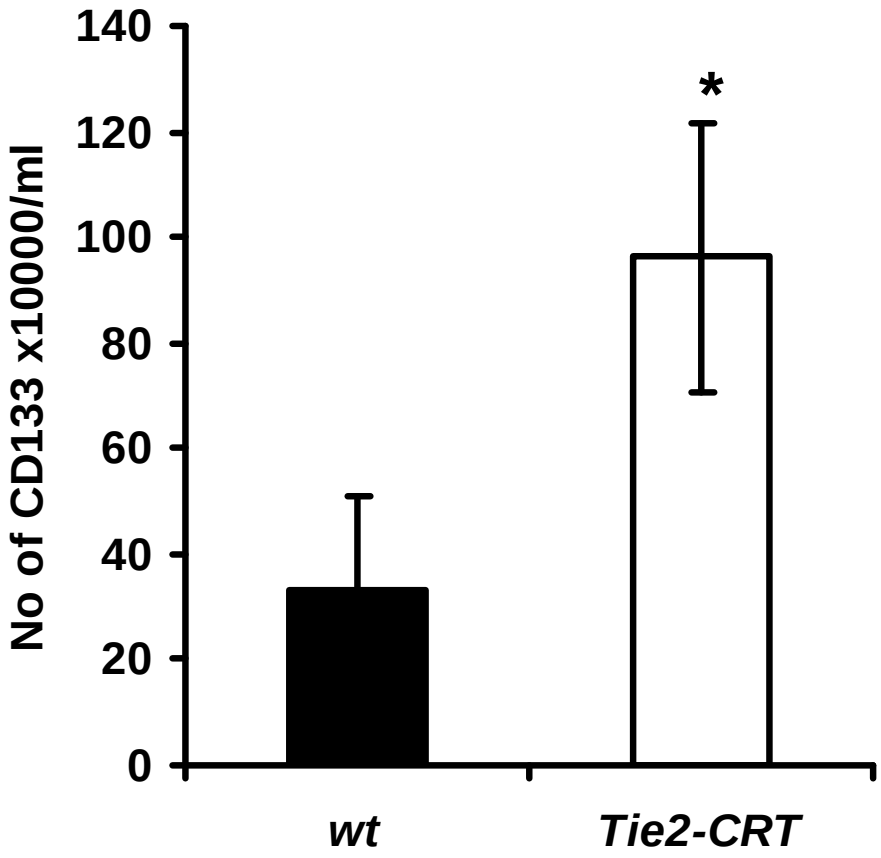

Fig. 43. Evaluation of CD133 positive bone marrow cells in *wt* and *Tie2-CRT* mice.

Cells were isolated from the bone marrow of *wt* and *Tie2-CRT* mice using CD133 magnetic beads. The bar graph is the mean ± SE of the number of cells isolated from 3 *wt* and 3 *Tie2-CRT* mice. *$p<0.05$, significantly different from the *wt* mice.

3.3. Expression of CRT in human and *Tie2-CRT* mice lung adenocarcinomas

In this study, we have shown a relationship between the expression of exogenous CRT and lung tumor development in *Tie2-CRT* transgenic mice. Furthermore, differential expression of CRT in various types of human tumors and cell lines has previously been reported (Kageyama *et al.* 2004; Jazii *et al.* 2006; Sarvaiya *et al.* 2006; Du *et al.* 2007; Toquet *et al.* 2007; Eric *et al.* 2009). However, there are no reports on CRT expression in human lung adenocarcinoma. Thus, we tested whether there is any alteration in the expression of endogenous CRT in human lung adenocarcinoma as well as in the lung tumors observed in *Tie2-CRT* mice.

3.3.1. Evaluation of endogenous CRT expression in *Tie2-CRT* lung adenocarcinoma

We evaluated the expression of endogenous CRT in the lung tumors observed in *Tie2-CRT* mice using IHC and western blot analysis. Following validation of the CRT antibody, we performed IHC on different sections of lung tumors and adjacent normal tissues. As seen in Fig. 44, IHC analysis with the CRT antibody shows expression of endogenous CRT in the epithelial cells of the lung tumor. In the normal adjacent lung tissue, endogenous CRT was expressed uniformly in the cells of the lung. To quantify the changes in the endogenous CRT expression we performed western blot analysis using a goat anti-CRT antibody. Visible tumors were isolated from the adjacent tissue and homogenized in RIPA buffer for western blot analysis. Fig. 45 shows a typical western blot of CRT expression in three different tumors and

corresponding adjacent lung tissues. There were no significant differences in the expression levels of endogenous CRT in the lung tumors observed in *Tie2-CRT* mice as compared to their normal lung tissues (Fig. 45). The results obtained from western blotting correlates with the expression of CRT observed with IHC in *Tie2-CRT* lung tumors and adjacent tissues.

3.3.2. Evaluation of endogenous CRT expression in the *Tie2-CRT* lung tumor derived cell line.

We next evaluated the expression of endogenous CRT in differentiated and undifferentiated cells of the *Tie2-CRT* lung tumor derived cell line. Soft agar colony forming assays were used to isolate the tumor spheres (undifferentiated cells) from the *Tie2-CRT* lung tumor cell line. Proteins were isolated from both tumor spheres and differentiated cells, and used for western blotting to evaluate any changes in the expression of CRT. Fig. 46 demonstrates that there was no significant difference in total CRT expression between undifferentiated tumor spheres and differentiated cells. Altogether, these data suggest that there is no association between the expression of endogenous CRT and the progression of lung tumors in *Tie2-CRT* mice.

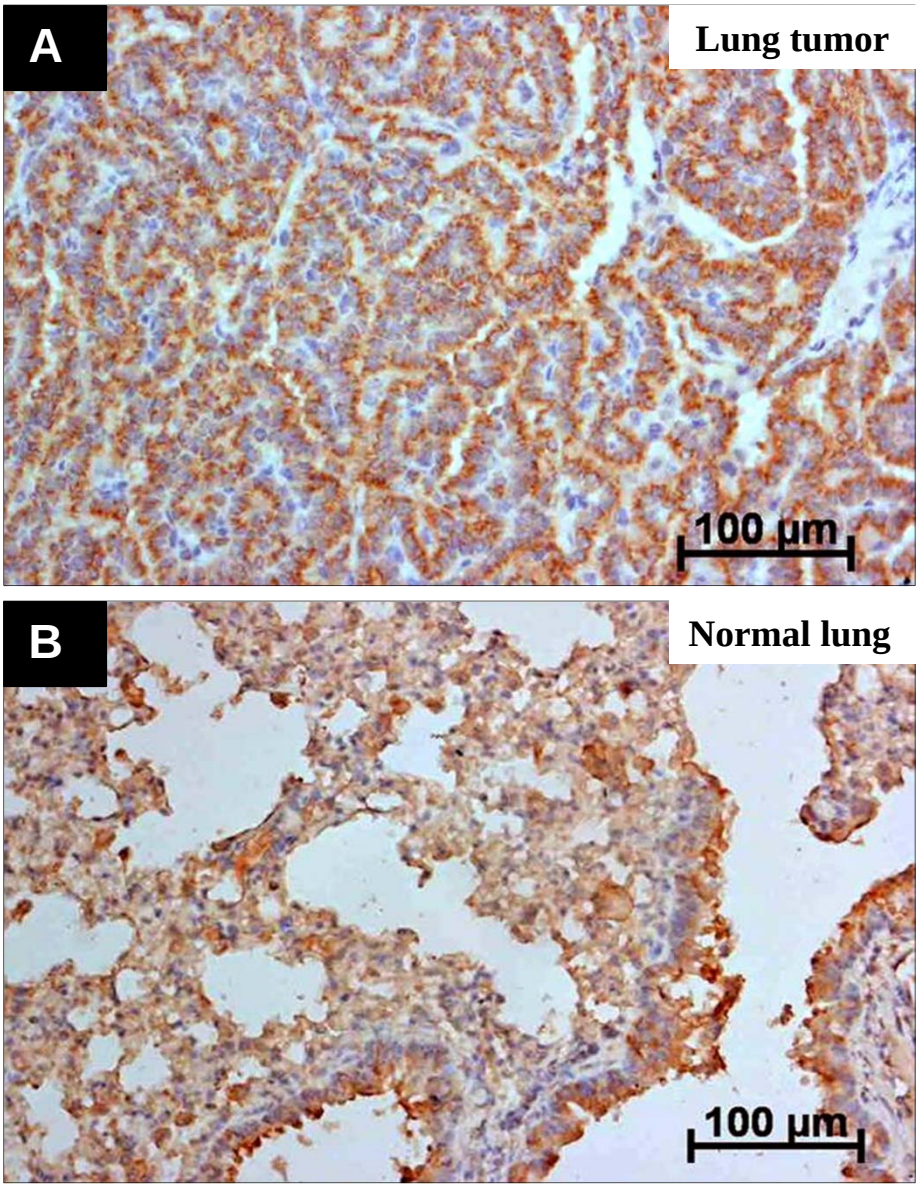

Fig. 44. Evaluation of endogenous CRT expression in *Tie2-CRT* lung adenocarcinoma.

Four µm paraffin sections of lung tumors of *Tie2-CRT* mice were processed for IHC with a goat anti-CRT antibody. (A) A representative (n=3) IHC image with CRT antibody showing endogenous CRT expression in the lung tumor and (B) adjacent normal tissue.

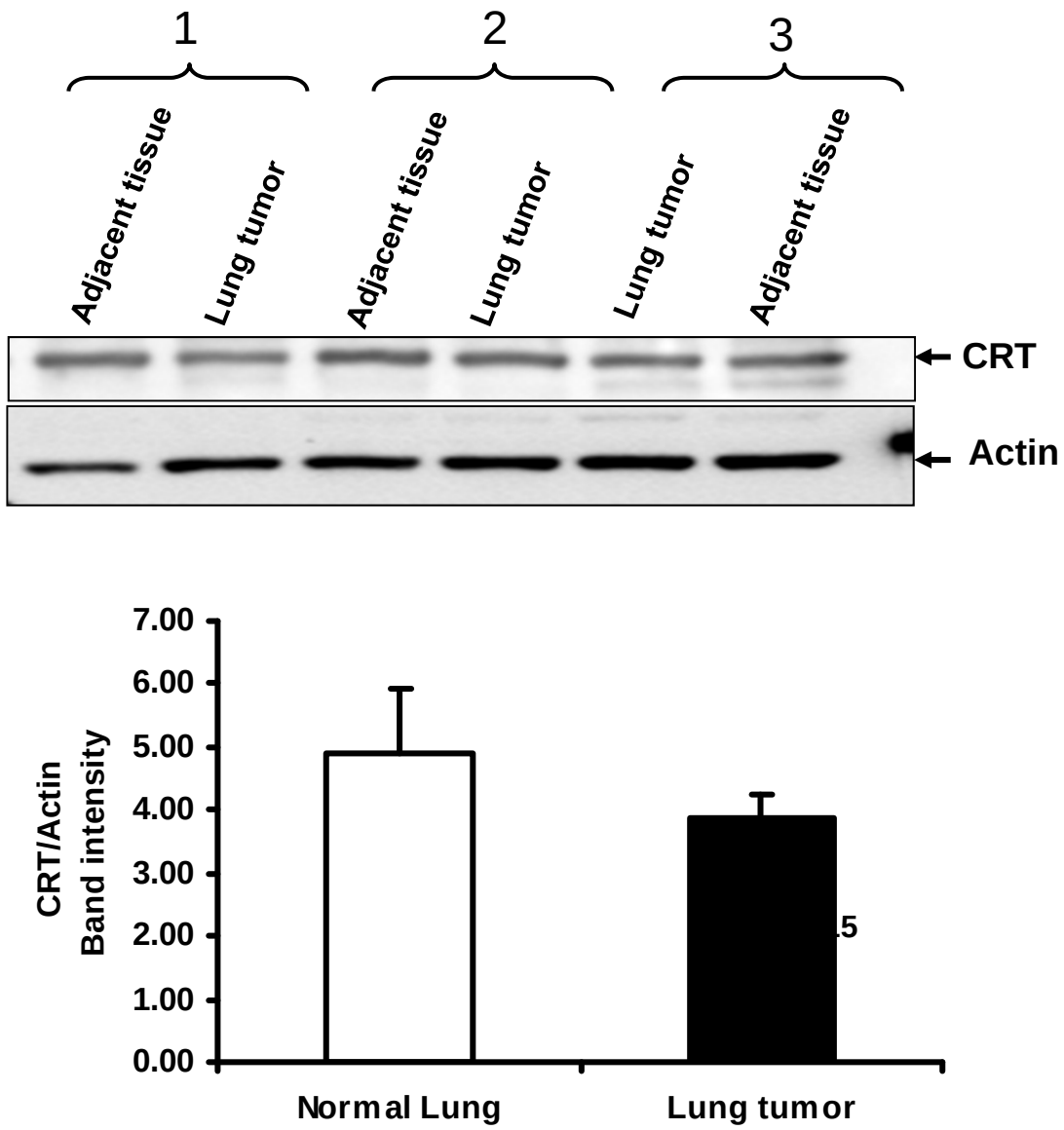

Fig. 45. Western blot analysis of CRT expression in *Tie2-CRT* lung adenocarcinoma.

Visible lung tumors were separated from the adjacent tissue. Tissues were then homogenized in RIPA buffer and solubilized proteins were resolved on a 10% SDS-PAGE gel. Western blotting was carried out using an anti-CRT antibody. The upper panel shows a representative western blot of CRT expression in three different tumors and their corresponding adjacent lung tissues. The bar graph shows the mean SE of CRT expression in 3 separate lung tumors and their corresponding adjacent tissues.

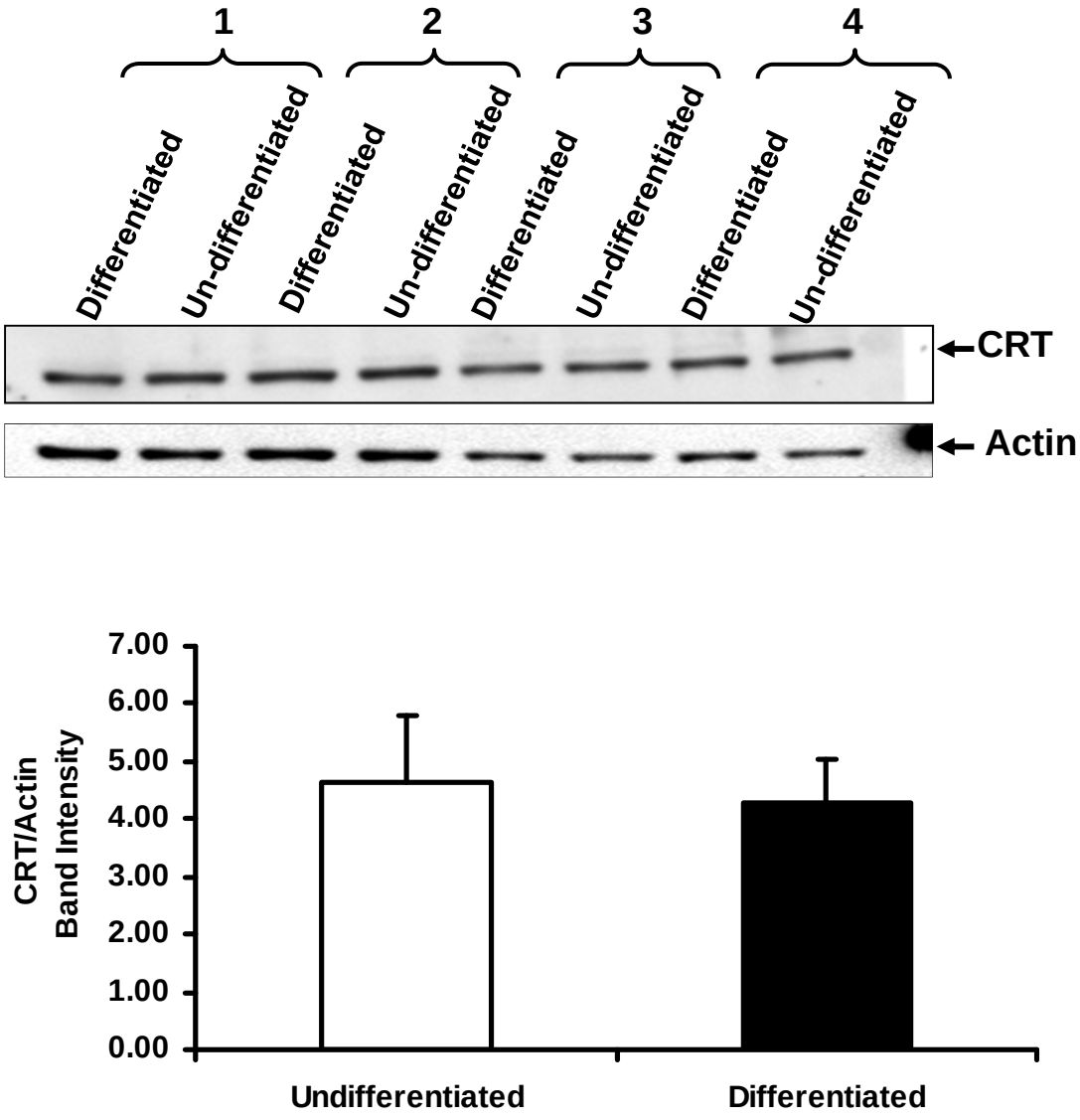

Fig. 46. Evaluation of CRT protein levels in the *Tie2-CRT* lung tumor derived cell line.

Western blot analysis showing the expression of endogenous CRT in differentiated (adherent) and undifferentiated (tumor sphere) *Tie2-CRT* lung tumor cells. Proteins were isolated from both tumor spheres and differentiated cells and used for western blotting. The upper panel shows a representative western blot using an anti-CRT antibody. The lower panel is a bar graph of the quantification of CRT from the above mentioned western blot. The band density of CRT was normalized to actin (loading control). Values represent the mean SE of 4 separate preparations.

3.3.3. Evaluation of CRT expression in the A549 human lung adenocarcinoma cell line

As highlighted earlier, several groups reported differential expression of CRT in various types of human tumors and cell lines. As such, we evaluated the expression of CRT in the differentiated and undifferentiated stages of the A549 human lung adenocarcinoma cell line. We used the soft agar colony forming assays to isolate tumor spheres (undifferentiated cells) from the A549 cell line. Proteins were isolated from both undifferentiated and differentiated A549 cells, and used for western blot analysis to measure changes in the expression of CRT. Fig. 47 shows a representative western blot for CRT expression in differentiated and undifferentiated A549 cell. As shown, undifferentiated tumor cells express significantly higher levels of CRT as compared to differentiated tumor cells suggesting that unlike the lung tumors of *Tie2-CRT* mice, there is an association between the expression of endogenous CRT and the progression of human lung adenocarcinoma.

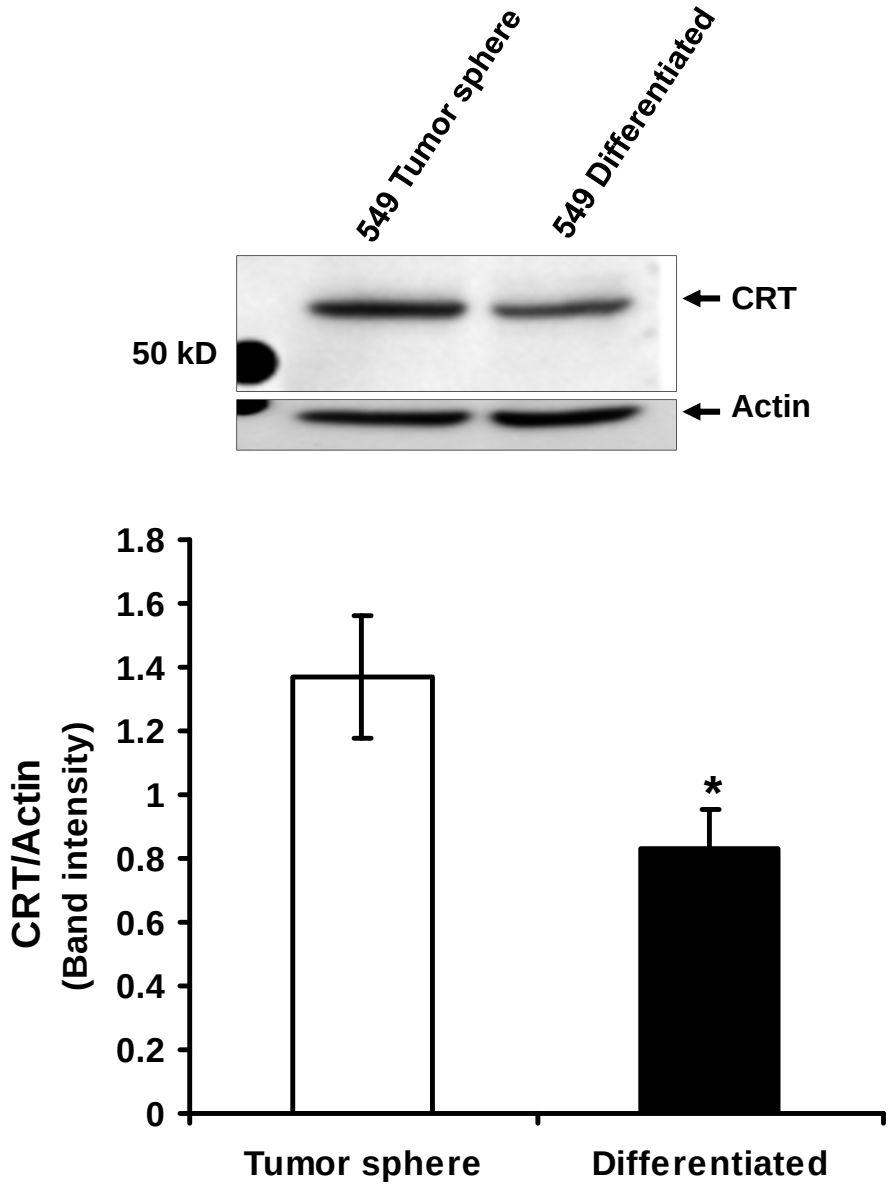

Fig. 47. CRT expression in tumor spheres and differentiated cells of the human lung adenocarcinoma cell line (A549).

A representative western blot showing the expression of CRT in tumor spheres and differentiated monolayers of the A549 cell line. Soft agar colony forming assays were used to generate and isolate the tumor spheres (undifferentiated cells) of the A549 cell line. The bar graph shows the mean SE of the ratio of CRT to actin band intensity from four different experiments. *$p<0.05$, significantly different from the tumor spheres.

3.3.4. Evaluation of CRT expression in human lung adenocarcinoma using tissue microarray (TMA).

To determine whether the changes in the expression of CRT in differentiated and undifferentiated human lung adenocarcinoma cell line represents changes in the human lung adenocarcinoma *in vivo* we carried out a semi-quantitative IHC on TMA sections (from US Biomax Inc.). The TMA slides contained 96 cores of lung adenocarcinoma specimens from malignant tumors (grade I-III, 33 cases), adjacent tissue and normal tissue as explained in "Materials and Methods". Fig. 48A and B show representative images of TMA cores from malignant tumor and adjacent normal tissues stained for CRT. IHC studies showed lower CRT expression in the tumor regions compared to the adjacent normal tissue (Fig. 48A and B). Semi-quantitative scoring (H-scores) was used to quantify CRT expression in human lung tissue. As shown in Fig. 48C there were a significant decrease in CRT expression in the tumor regions as compared to the adjacent normal tissue ($p<0.005$).

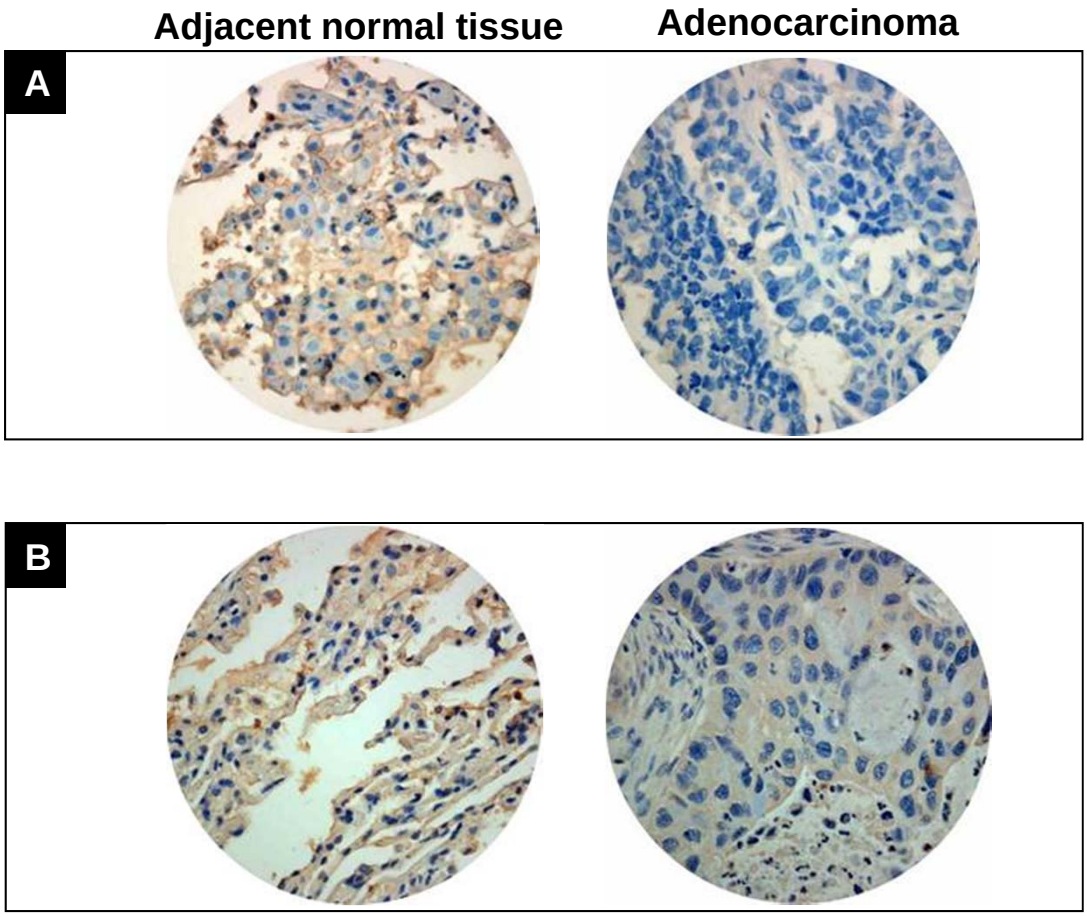
Adjacent normal tissue
Adenocarcinoma
A
B
C
300
250
200
150
100
50
0
H Score
*
Adjacent tissue
Tumor

Fig. 48. Evaluation of CRT expression in human lung adenocarcinomas using tissue microarray (TMA).

IHC with an anti-CRT antibody was carried out on two human TMA sections to examine the CRT protein expression in human lung adenocarcinomas. Two representative cores from the TMA of malignant tumors (A and B, right panel) and adjacent normal tissues (A and B, left panel) stained for CRT are shown. Expression of CRT was evaluated using H-Scoring as described in "Materials and Methods". (C) The bar graph shows the semi-quantitative (H Score) analysis of CRT expression in the human lung adenocarcinomas using TMA. Values are means ± SE of 30 separate TMA cores of adenocarcinoma and their adjacent normal tissues. *$p<0.05$, significantly different from adjacent normal tissue.

3.3.5. Expression of p53, PTEN and phospho-Akt in the lung tumors in *Tie2-CRT* mice.

There are several lines of evidence implicating different proteins including PTEN (Soria *et al.* 2002; Yanagi *et al.* 2007; Iwanaga *et al.* 2008), Akt (Diaz-Meco *et al.* 2008) and p53 (Nishio *et al.* 1996) in the development of lung cancer. Thus to determine whether these proteins (p53, PTEN and P-Akt) are altered during the development of lung tumors in *Tie2-CRT* mice, we used western blot analysis of lung tumors as compared to adjacent to normal tissues. Fig. 49 shows a western blot with an antibody specific for PTEN on tissue lysates from isolated lung tumors seen in *Tie2-CRT* mice and their adjacent normal tissue. There was no significant change in the level of PTEN protein expression in lung tumors as compared to adjacent normal tissue (Fig. 49). However, the expression of p53 tumor suppressor protein was significantly lower in the lung tumors (Fig. 50) as compared to adjacent normal tissue ($n=3$, $p<0.05$).

Since the lysis buffer used for preparation of these tissues was not supplemented with phosphatase inhibitors, we were not able to evaluate expression of phospho-Akt in these samples. To examine changes in phospho-Akt (S473) levels in lung tumors, we used undifferentiated (tumor spheres) and differentiated tumor cells of *Tie2-CRT* mice. Western blot analysis showed no significant change in the level of phospho-Akt protein expression in undifferentiated tumor spheres as compared to differentiated form (Fig. 51). These data suggest that there is no difference in the Akt activity in these cells.

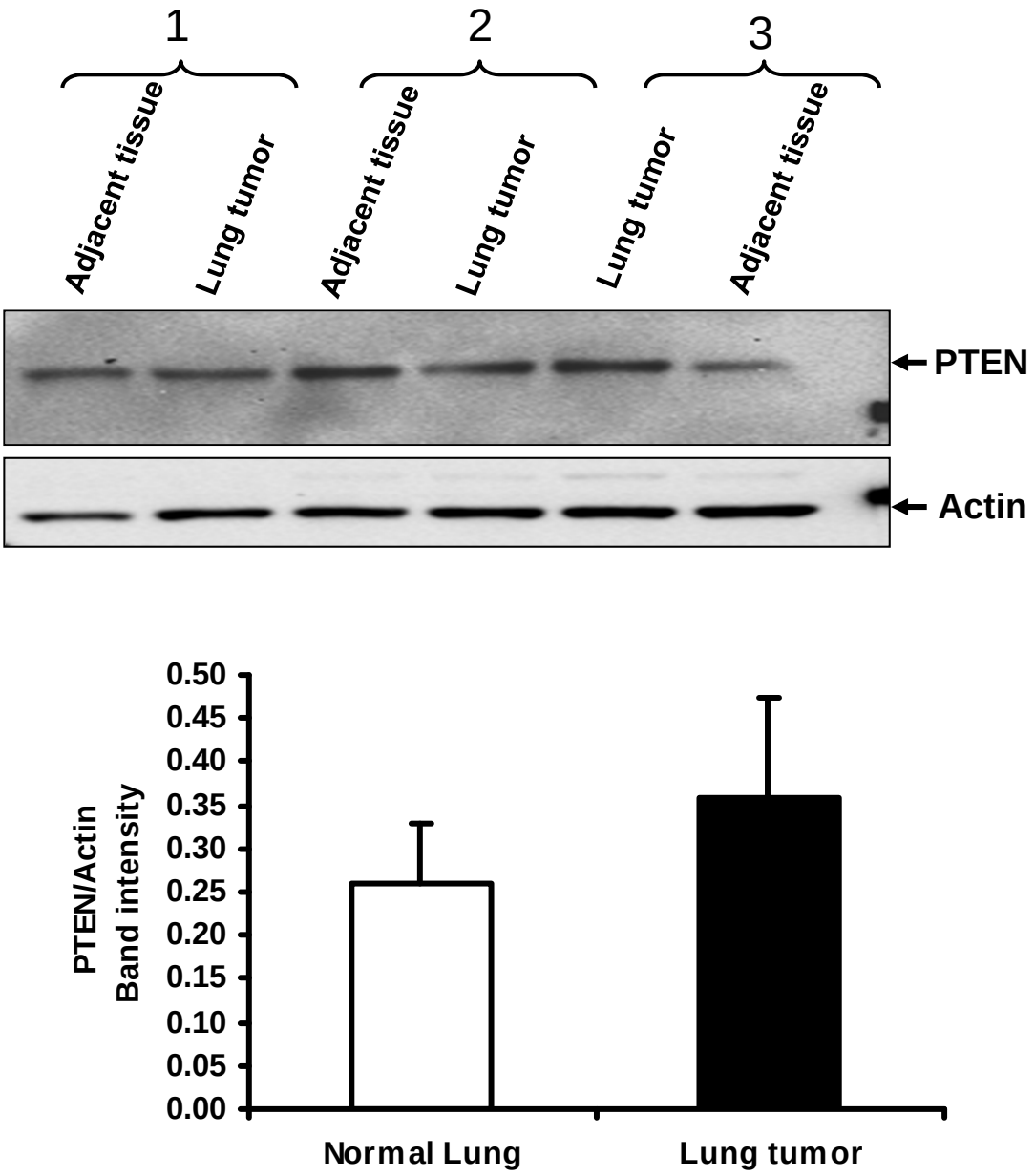

Fig. 49. PTEN protein level in *Tie2-CRT* mice lung tumor and adjacent normal tissue.

The upper panel shows a western blot with anti-PTEN antibody and actin (loading control) on tissue lysates isolated from lung tumors and the adjacent lung tissue of *Tie2-CRT* mice. The bar graph shows the mean SE of ratio of PTEN/actin band intensity from three separate mice.

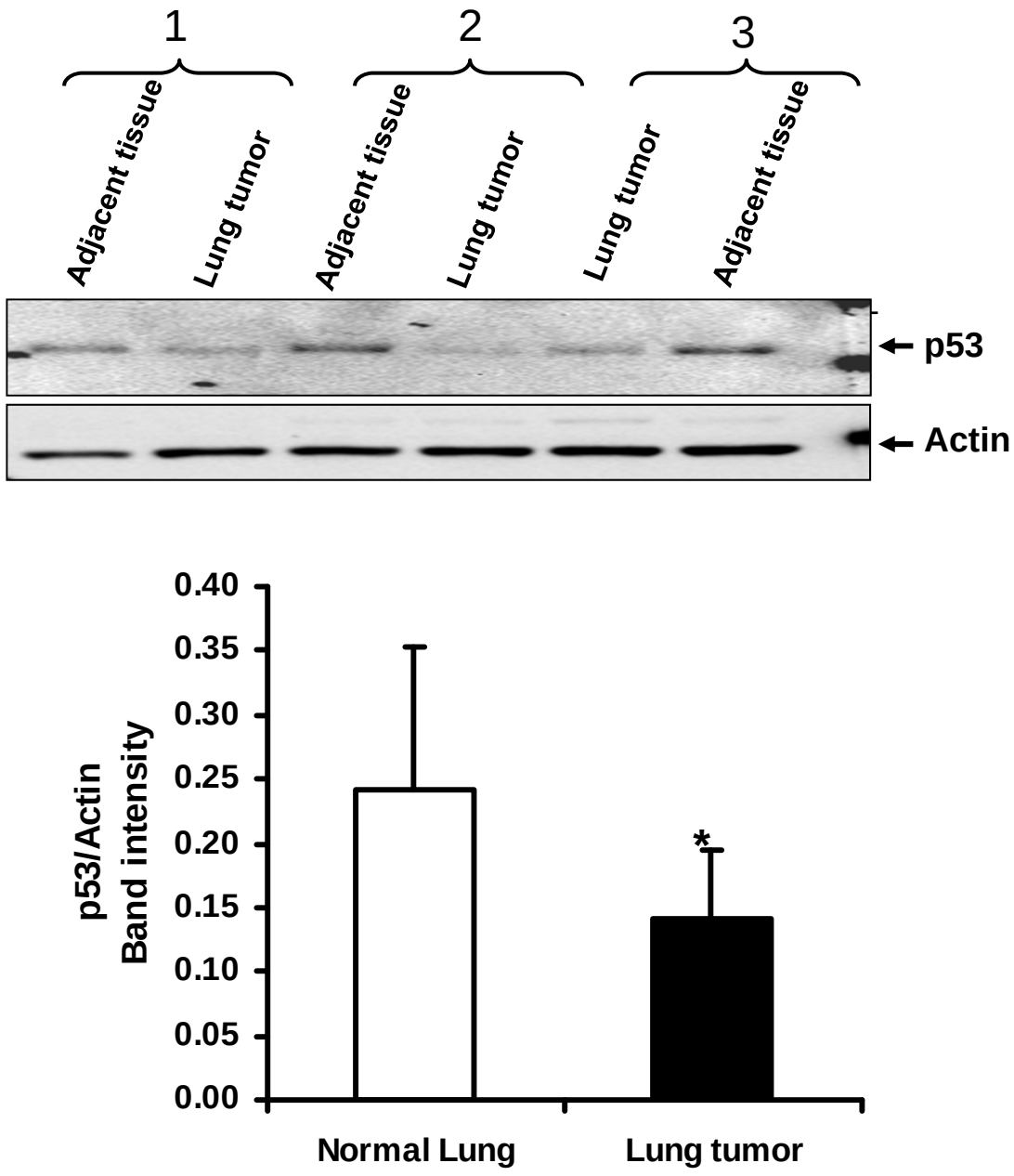

Fig. 50. p53 protein level in *Tie2-CRT* mice lung tumor and adjacent normal tissue.

The upper panel shows a western blot with anti-p53 antibody and actin (loading control) of tissue lysates isolated from lung tumors and adjacent lung tissue of *Tie2-CRT* mice. The bar graph shows the mean SE of ratio of p53/actin band intensity of three separate mouse tissue. *$p<0.05$, significant different from adjacent normal tissue.

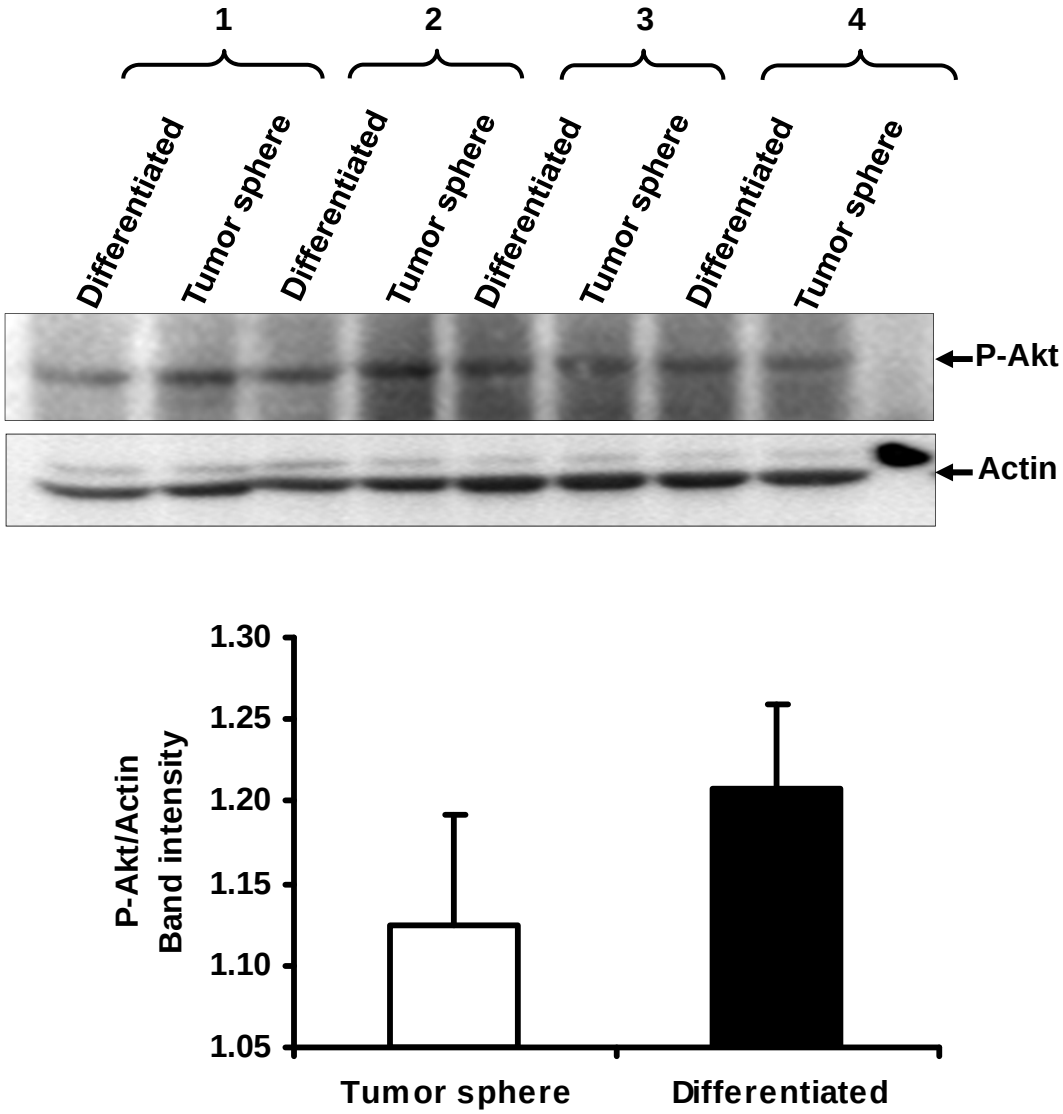

Fig. 51. Phospho-Akt level in tumor spheres and differentiated *Tie2-CRT* mice lung tumor cells.

A representative western blot showing the expression of CRT in tumor spheres and differentiated monolayers of the *Tie2-CRT* tumor derived cell line. Soft agar colony forming assays were used to generate and isolate the tumor spheres (undifferentiated cells) of *Tie2-CRT* mice tumor derived cell line. The upper panel is a representative western blot with anti-P-Akt (S473) antibody and actin (loading control) of proteins isolated from both tumor spheres and differentiated *Tie2-CRT* tumor cells. The bar graph shows the mean SE of ratio of P-Akt/actin band intensity of four different experiments.

CHAPTER IV: DISCUSSION

CRT is a multifunctional Ca^{2+}-buffering chaperone protein that is localized to the lumen of the ER. As such, it has diverse biological roles including ensuring proper folding of newly synthesized proteins and regulation of Ca^{2+} homeostasis (Milner *et al.* 1991; Gelebart *et al.* 2005). In addition to its critical role in cardiovascular development (Mesaeli *et al.* 1999), CRT has been reported to be important in many key biological processes such as angiogenesis (Pike *et al.* 1998), cell adhesion, migration (Opas *et al.* 1996; Coppolino *et al.* 1997; Hayashida *et al.* 2006) and apoptosis (Nakamura *et al.* 2000; Mesaeli *et al.* 2004). For instance, CRT overexpressing cells are more sensitive to drug-induced apoptosis (Nakamura *et al.* 2000; Kageyama *et al.* 2002), whereas cells lacking CRT are more resistant to drug or UV-induced apoptosis (Nakamura *et al.* 2000; Mesaeli *et al.* 2004). Overexpression of CRT has been shown to increase the expression of both vinculin and N-cadherin (Opas *et al.* 1996; Fadel *et al.* 1999) which results in increased cell spreading and adhesion, whereas down regulation of CRT results in the converse effect (Leung-Hagesteijn *et al.* 1994; Opas *et al.* 1996). Altered CRT expression has been illustrated in various types of tumors (Bini *et al.* 1997; Yu *et al.* 2000; Kageyama *et al.* 2004; Du *et al.* 2007; Toquet *et al.* 2007), however the mechanism and significance of this phenomenon is not yet known.

4.1. Characterization of lung tumor development in *Tie2-CRT* mice

Several studies have suggested a role for exogenous CRT in regulating angiogenesis and cell growth thus affecting tumor growth (Pike *et al.* 1998; Pike *et al.*

1999; Liu *et al.* 2005). For example, the recombinant N-terminal fragment of CRT, known as vasostatin, has been reported to inhibit angiogenesis and prevent endothelial cell proliferation (Pike *et al.* 1998). In contrast, overexpression of vasostatin in neuroendocrine tumor cells, enhances malignant behavior (Liu *et al.* 2005). Although these studies suggest a role for exogenous CRT in angiogenesis and tumor growth, no direct evidence for the role of endogenous CRT in angiogenesis and tumor progression is available. Therefore, to study the *in vivo* function of CRT in angiogenesis and vascular development, we generated a transgenic mouse model (*Tie2-CRT* mice) overexpressing CRT specifically in endothelial cells. This was achieved by using the *Tie2* promoter (Fig. 3), a commonly used promoter for generation of endothelial cell and HSC specific transgenic mouse models (Dumont *et al.* 1992; Sato *et al.* 1993; Kisanuki *et al.* 2001; Arai *et al.* 2004; Shaw *et al.* 2004) In the current study, PCR, western blot and immunohistochemical analysis confirmed expression of exogenous CRT in the lungs (Fig. 4B), white blood cells (Fig. 4B), aorta (Fig. 5) and bone marrow cells (Fig. 6 and 7).

The *Tie2-CRT* mice appeared to grow and develop normally as was evident by their general characteristics including body weight, blood glucose (Fig. 8) and blood cell profiles (Fig. 9). However, with increased age, they displayed signs of labored breathing and edema. Upon necropsy, we observed that *Tie2-CRT* mice have hemorrhagic lesions in various tissues including the lungs, ovaries, uterus, and liver (Fig. 11). The most striking phenotype of these mice was their increased incidence of lung cancer (Fig. 12) which developed at a higher rate than *wt* mice as the mice aged. Therefore, the purpose of this study was to first characterize the lung tumors observed in *Tie2-CRT* mice. According to their histology and IHC marker profiles, the tumors in

Tie2-CRT mice have been characterized as adenocarcinoma (Fig. 14 and 15). Lung adenocarcinoma is the most common subtype of lung cancer with an increasing incidence worldwide, (Alberg *et al.* 2005) however, the cell of origin of this tumor type remains to be identified. As such, the second aim of this study was to use *Tie2-CRT* mice as a model of lung cancer to investigate the mechanisms underlying the initiation and progression of lung adenocarcinoma.

During the early stages, lungs isolated from *Tie2-CRT* mice show signs of inflammation as evidenced by increased congestion and a reddish discoloration on the periphery of the lungs (Fig. 13A and B). This was further investigated by histology (Fig. 14B and C) and IHC (Fig. 17) indicating an ongoing inflammatory response in the lungs of *Tie2-CRT* mice. A correlation between chronic inflammation and lung cancer (risk and progression) has recently been shown in both individuals with lung cancer as well as in individuals at high risk of lung cancer (McKeown *et al.* 2004; Lu *et al.* 2006; Wistuba 2007; Engels 2008; Lee *et al.* 2009). For instance, higher levels of inflammatory markers, such as plasma C-reactive protein, has been shown to be associated with the progression of bronchial dysplasia in smokers (Sin *et al.* 2006)

Chronic airway inflammation can lead to lung cancer via different pathways. Highly reactive nitrogen and oxygen species (RNS and ROS) released from inflammatory cells interact with DNA in the proliferating epithelium which results in an increased rate of mitotic error through genomic alterations such as point mutations, deletions, or rearrangements (Walser *et al.* 2008). Inflammation also changes the lung microenvironment through inflammatory signaling, which subsequently leads to pulmonary carcinogenesis. For instance, prostaglandin E2 (PGE2) and IL-1β (and other inflammatory cytokines derived from stromal and immune cells) reduce E-

cadherin expression via a MAPK/Erk-dependent up-regulation of the transcriptional repressors: zinc-finger E-box binding homeobox 1 (ZEB-1) and Snail (Charuworn *et al.* 2006; Dohadwala *et al.* 2006; Krysan *et al.* 2008).

The ongoing inflammatory response in the lung of *Tie2-CRT* mice could be due to altered function of leukocytes upon overexpression of CRT. Indeed, our data in Fig. 10C and 10D illustrate lack of MPO (myeloperoxidase) expression in the leukocytes of *Tie2-CRT* as compared to the *wt* littermates. MPO is a lysosomal protein with peroxidase activity that is stored in the azurophilic granules found in granulocytes, and in the lysosomes of monocytes of the myeloid cell lineage (Klebanoff 1999). It is involved in many immune responses including tumor cell destruction (Weiss *et al.* 1982) and host defense (Klebanoff *et al.* 1984; Klebanoff 1999). Previous reports showed a role for CRT as a chaperone during the biosynthesis and maturation of MPO (Nauseef *et al.* 1995; Nauseef *et al.* 1998). However, the effect of overexpression of CRT on the folding and maturation of MPO remains unknown.

Folding of newly synthesized proteins in the ER is regulated by the luminal Ca^{2+} concentration (Lodish *et al.* 1990; Corbett *et al.* 2000). CRT, an ER chaperone protein, plays a crucial role in mediating the homeostasis of ER Ca^{2+} (Bastianutto *et al.* 1995; Mery *et al.* 1996). Alterations in the expression of CRT result in increased ER stress and changes in ER Ca^{2+} concentration which subsequently leads to impaired protein folding (Oyadomari *et al.* 2001; Mesaeli *et al.* 2004). Furthermore, overexpression of both calnexin and CRT has been shown to increase the initial folding steps in the biosynthesis of human thyroperoxidase (hTPO) (Fayadat *et al.* 2000). However, this increase did not result in an elevated amount of hTPO present at the cell surface thus affecting the level of hTPO in the cell (Fayadat *et al.* 2000).

Considering that both hTPO and MPO are heme containing peroxidases that are processed by CRT and calnexin chaperones in the ER, it can be postulated that overexpression of CRT might affect MPO maturation and subsequently MPO levels in a similar fashion to hTPO. Since the overexpression of CRT is driven by the *Tie2* promoter which is active in both endothelial cells and HSCs (bone marrow stem cells that also give rise to the blood leukocytes) (Iwama *et al.* 1993; Sato *et al.* 1993; Arai *et al.* 2004), it is not surprising that the biosynthesis of MPO in the leukocytes of these mice might be affected. The decreased MPO level may render these mice more susceptible to chronic inflammatory responses.

In the *Tie2-CRT* mouse model as lung tumors progress, the regions with discoloration on the periphery of the lungs develop into sites of neoplasia and atypical adenomatous hyperplasia (AAH) (Fig. 14C). AAH is a lesion in the lung that precedes the adenoma stage (Jackson *et al.* 2001). The AAH sites are comprised of a uniform population of hypertrophic cuboidal cells, which form glandular structures. As the number of cells increase in AAH, the lesion transforms into adenomas that are visible as peripheral nodules in the lung. These nodules eventually form small peripheral tumors with glandular/papillary structures (Fig. 14). Based on their histological appearance and immunophenotypic characteristics, the tumors in *Tie2-CRT* mice have been characterized as lung adenocarcinomas with a SP-C positive and CC10 negative phenotype (Fig. 15) suggesting the involvement of alveolar type II cells in the development of these tumors and not bronchial cells. Furthermore, IHC staining of the lung tumors observed in *wt* mice showed that these tumors are heterogenous with some being SP-C negative (Fig. 15C) while others were SP-C positive adenocarcinomas (Fig. 15C). These results suggest that the lung adenocarcinomas observed in *Tie2-CRT*

mice are derived from different origins as compared to those of their *wt* littermates. The absence of mucin secretion by lung tumor cells (Fig. 15E) also confirms that these tumors are not bronchiolar in origin. Mucins are a family of glycosylated proteins produced and secreted by a variety of epithelial cells including goblet cells in the bronchioles of the lungs (Voynow *et al.* 2004; Song *et al.* 2007).

Previous studies using *in situ* hybridization and IHC have shown that alveolar type II cells are the predominant cell type in most mouse models of pulmonary adenocarcinomas (Mason *et al.* 2000; Meuwissen *et al.* 2005; Wang *et al.* 2006). However, simultaneous detection of markers specific for both alveolar type II and Clara cells have also been reported (Sunday *et al.* 1999; Jackson *et al.* 2001), indicating that certain types of adenocarcinomas might be of multilineage pulmonary epithelial origin. Interestingly, in some cases, the overexpression of known oncogenes such as the simian virus 40 (SV-40) T antigen under the control of the human SP-C promoter has been reported to result in transgenic mice with adenocarcinomas expressing CC-10, but not SP-C (Wikenheiser *et al.* 1997). Kim *et al.* have suggested that stem cells at the bronchioalveolar duct junction could give rise to epithelial cells of both the alveolar and bronchial lineages (Kim *et al.* 2005). In *Tie2-CRT* mice, the expression of SP-C and the lack of expression of CC-10 and mucins by lung tumor cells indicate the involvement of alveolar type II cells in the formation of lung adenocarcinomas in these mice.

In addition to lung tumor development in *Tie2-CRT* mice, we observed a consistent development of tumors in the liver. Unlike the lung tumors, the liver tumors in these mice displayed a heterogeneous phenotype and histopathology (Fig. 18 and 20). Hepatocellular tumors are a very common age related tumor in mice (Andervont

1950; Andervont *et al.* 1962). The incidence of liver tumors in mice older than 12 months of age ranges between 15-55% in C3H, 20-29% in CBA, and 6.1-35.5% in CD-1 mice (Andervont 1950; Maita *et al.* 1988). The fatty liver Shionogi (FLS) mouse, a new inbred strain that develops spontaneous hepatic lipidosis, has a high incidence of hepatocellular carcinomas (40% of animals at 15-16 months of age) (Soga *et al*. 2003). Our data revealed that the incidence of liver tumors in *Tie2-CRT* mice appeared to increase with age from 3% in mice less than 12 months old to 34% in mice over 18 months of age (Fig. 19). Our data also illustrated that the incidence of liver tumors in the *wt* mice appeared at a lower frequency as compared to the incidence of lung tumors in *Tie2-CRT* (Fig. 13). The incidence of liver tumors in the *Tie2-CRT* increases from 50% in less than 12 month old mice to 93% in mice over 18 months of age (Fig. 19). The higher frequency of tumors in the lungs of *Tie2-CRT* mice as compared to the liver could be caused by the lung having a higher rate of tissue renewal and being more prone to chronic inflammation which renders them particularly susceptible to tumorigenesis (Malkinson 2004; Azad *et al.* 2008; Engels 2008; Walser *et al.* 2008).

Since the occurrence of liver tumors in *Tie2-CRT* mice was occasionally accompanied with lung tumors, we investigated whether the liver tumors observed in *Tie2-CRT* mice were derived from metastases of the of lung tumors or were a consequence of CRT overexpression. Studying the histogenesis of the liver tumors with IHC revealed the presence of cells within the tumors that stain positive for AFP (Fig. 21A), a specific marker for fetal hepatocytes and a biomarker of hepatocellular carcinoma, but do not stain for the SP-C protein (Fig. 21B). On the other hand, some of the liver tumors contained cells that stained positive for SP-C (Fig. 21C). These

observations suggest that some of the liver tumors might be derived from metastases from the lung tumors while others are likely primary liver tumors. Further studies are needed to characterize and identify the cell of origin of the liver tumors in the *Tie2-CRT* mice.

As is expected, the endothelial cell layer of vessels and capillaries in the tumor area express CRT-HA (Fig. 21D) because endothelial cells were the target cells for expression of the transgene (CRT-HA). However, liver tumor cells did not stain positive for CRT-HA (Fig. 21D). This is contrary to our observations in the lung tumors of *Tie2-CRT* mice in which lung tumor cells express CRT-HA (Fig. 22C). The lack of expression of CRT-HA by liver tumor cells suggested that the tumor cells in the liver are not derived from either endothelial cells or HSCs. Further studies are warranted to fully characterize the liver tumors of the *Tie2-CRT* mice and the mechanisms behind the progression and development of these tumors.

Histological examination of the lung adenocarcinoma in *Tie2-CRT* mice illustrated the lack of expression of CD31 (a marker of endothelial cells) by tumor cells (Fig. 22A), suggesting that tumor cells were not of endothelial origin, but may have arisen from different cell types or have undergone differentiation during tumor progression. Examination of a group of non-epithelial cells located in the lung adenocarcinoma region express CD34, a known marker of HSCs and neo-angiogenesis (Fig. 22B). However, IHC using the HA antibody revealed expression of CRT-HA by some of the tumor cells (Fig. 22C). Since we have shown that the CRT transgene is driven under the control of the *Tie2* promoter which is active in both endothelial cells and HSCs, this raises an important question: why are tumor cells expressing CRT-HA negative for CD34 and CD31? One possible explanation for this observation could be

the plasticity of HSCs (Wagers *et al.* 2002). In fact, reversible expression of CD34 by HSCs has been shown by different investigators (Bhatia *et al.* 1998; Dao *et al.* 2003). HSCs leave the BM as undifferentiated precursors expressing different markers including CD34. They enter the circulation, and home to the appropriate target tissue where they undergo further maturation and cross the lineage barrier to engraft into solid organs (Petersen *et al.* 1999; Theise *et al.* 2000; Orlic *et al.* 2001; Theise *et al.* 2002; Mezey *et al.* 2003; Jang *et al.* 2004). Once HSCs reach their target tissue, the requirement for continued expression of CD34 may therefore no longer be necessary.

Further histological examination of the adenocarcinoma in *Tie2-CRT* mice showed the presence of a heterogeneous population of cells composed of SP-C^{Pos}, $CC10^{Neg}$, E-$Cadherin^{Pos}$ epithelial cells (Fig. 23 and 25A) and cells which were positive for both HSCs markers (CD34, c-kit and Sca-1) and transgenic CRT, but negative for SP-C (Fig. 23B and 24E) and CC10 (Fig. 23C). Tumors are also highly vascularized as verified by the expression of CD34 (Fig. 22B) and vWF (Fig. 25B). Neovascularization is needed for the continuing growth of tumors (REFERENCE). The heterogeneous population of tumor cells in lung adenocarcinoma of *Tie2-CRT* mice has been classified into three groups based on their morphology and immunohistochemical characteristics as summarized in Table 7.

A heterogeneous population of tumor cells in both hematological and solid malignancies has previously been reported (Heppner 1984). Heterogeneous tumor cells have been suggested to arise from genetic and epigenetic differences in the cells during tumor evolution (Heppner 1984). A possible explanation for the heterogeneity of the tumor cell population is that the tumor is comprised of a bulk of neoplastic cells at different stages of differentiation which express different markers according to their

particular stage as well as vascular cells and fibroblasts. This postulate is in accordance with the cancer stem cell hypothesis (Hemmati *et al.* 2003; Jordan 2004). According to this model, heterogeneity arises from the existence of a group of cells within tumors known as tumor-initiating cells or cancer stem cells. These cells are a subset of the bulk tumor that can self-renew and differentiate into progenitor cells resulting in a heterogeneous population of tumor cells with differential protein expression (Hemmati *et al.* 2003; Jordan 2004).

Immunohistochemical studies on *Tie2-CRT* lung tumors have also demonstrated changes of tumor composition during the different stages of tumor progression including AAH, adenoma and fully developed adenocarcinoma (Fig. 27, 28 and 29). These data illustrate that during the initial stages of tumor formation, tumor cells expressed the transgene (CRT-HA) and HSC markers including CD133, Sca-1, and c-kit (Fig. 28 and 29). As the tumor progresses into an adenocarcinoma, the fully developed tumor cells lose the expression of HSC markers and become epithelial cells expressing SP-C (Fig. 27, 28 and 29).

Different respiratory stem cells residing in specialized niches, such as the bronchoalveolar duct junction, have been described and are hypothesized to be the putative cells of origin for lung adenocarcinoma (Kim *et al.* 2005). The particular stem cells described by Kim and colleagues (Kim *et al.* 2005) are known as bronchoalveolar stem cells (BASCs) and express both Clara cell-specific (CC10) and alveolar type II-specific (SP-C) proteins along with stem cell markers (Sca1 and CD34). In *Tie2-CRT* mice, ectopic CRT is driven by *Tie2* promoter which is active in endothelial cells, endothelial progenitor cells and HSCs, but a review of the current literature did not reveal activity of the *Tie2* promoter in BASCs. As such, the remaining question is

whether BASCs, HSCs and endothelial cells are involved in the progression of the lung tumors observed in *Tie2-CRT* mice. We predict that BASCs are not involved in the formation of these tumors due to the absence of CC10 staining in Tie2-CRT lung adenocarcinoma..

To better understand the development and progression of the lung tumors observed in *Tie-CRT* mice *in vitro*, a lung adenocarcinoma cell line from fully developed tumors isolated from these mice was established. Following the establishment of the lung tumor derived cell line, we first evaluated the tumorigenic capacity of these cells. Transplantation of tumor cells into immunocompromised mice represents a unique and favored method to assess tumorigenicity and meets the requirements for the evaluation of metastasis-related processes (Nagamachi *et al.* 1998). However, the non-adherent sphere assay is an alternative method that is increasingly being used by many investigators (Dodson *et al.* 1981). *In vitro* tumorigenicity assays with lung tumor cells using the soft agar assay, revealed that lung tumor cells isolated from *Tie2-CRT* mice possess anchorage-independent growth characteristics (Fig. 30) which demonstrate their potential tumorigenicity.

Our data illustrated that tumor spheres (prepared in soft agar assay) cultured in a media containing 10% FBS and on regular tissue culture plates, gradually differentiated into a monolayer of adherent cells (Fig. 31) highlighting the differentiation potential of tumor spheres. In fact, *in vitro* evaluation of tumor sphere differentiation demonstrated a differentiation dependent expression of HSC markers (CD133, Sca1 and Tie2) by tumor cells from *Tie2-CRT* mice (Fig. 32). These results showed that tumor spheres positive for CD133, Sca1 and Tie2 lost their ability to express these stem cell markers when the tumor spheres were allowed to adhere to the

culture plate and differentiate. After three days of culture, differentiation continued within the outer layer of cells surrounding the tumor spheres, as demonstrated by the lack of expression of CD133, Sca1 and Tie2 (Fig. 32). Overall, these data suggest that the monolayers of cells are comprised of various differentiated types of tumor sphere cells. This finding is in accordance with the differentiation potential of human lung cancers demonstrated by Eramo and colleagues (Eramo *et al.* 2008). They have shown the expression of CD133 by lung tumor spheres which was lost in sphere-derived adherent cells upon differentiation (Eramo *et al.* 2008).

Our data illustrated that tumor spheres (undifferentiated cells) derived from the lung tumors of *Tie2-CRT* mice express several different stem cell markers including CD133, Sca-1, and c-kit and exogenous CRT (Fig. 33C-F), but not SP-C and E-cadherin which are known markers of epithelial cells (Fig. 33A and 33B). Furthermore, sphere-derived adherent cells express SP-C and E-cadherin, but lose the expression of HSC markers and exogenous CRT (Fig. 33G-L). Overexpression of CRT was shown to downregulate E-cadherin expression (Hayashida *et al.* 2006) via enhanced binding of Slug to the E-box element in the E-cadherin promoter, a process which induces epithelial to mesenchymal transition (EMT). According to the EMT process, when tumor cells convert from the non-invasive to the invasive phenotype, they become anchorage-independent by switching from an epithelial to a more motile mesenchymal phenotype (Thiery *et al.* 2006; Prudkin *et al.* 2009). This process is also related to embryologic morphogenesis, fibrosis, and wound healing, but recently much attention has been given to EMT in the progression and metastasis of epithelial tumors (Thiery *et al.* 2006). The connection between EMT and tumor initiating cells or cancer stem cells has been investigated by different groups (Mani *et al.* 2008; Morel *et al.*

2008). They have demonstrated that the induction of EMT in differentiated breast cancer cells generate cancer stem cell-like cells with increased self-renewal ability and initiation of new tumors (Mani *et al.* 2008; Morel *et al.* 2008) suggesting that the cancer cells disseminated via EMT may also have properties of cancer stem cells.

The heterogeneity of the lung tumor cell population, the presence of cells with stem cell characteristics within the initial stages of the tumor, and the differentiation dependent expression of HSC markers by tumor spheres isolated from soft agar led us to further investigate the progression of lung tumors by performing non-adherent sphere assays using serum-free sphere cultures (Ponti *et al.* 2005; Ricci-Vitiani *et al.* 2007; Eramo *et al.* 2008). Putative tumor initiating cells have been identified on the basis of their ability for self-renewal and the expression of different surface markers. however due to limitation in our facilities we were not able to evaluate their tumorigenic capacity via serial passaging of tumor initiating cells in immunodeficient mice. Our immunohistochemical analysis revealed that the sphere-growing cells derived from the lung tumors of *Tie2-CRT* mice express different stem cell markers including CD34, Sca-1, and CD133 (Fig. 34). These findings are in agreement with a previous study (Eramo *et al.* 2008) in which long-term cultures of sphere-growing cells derived from human lung adenocarcinoma were shown to be highly enriched for CD133 expression, but negative for SP-C and CC10. These data suggest that the lung tumors observed in *Tie2-CRT* mice are non-epithelial in origin, and after differentiation they lose their stem cell phenotype and acquire an epithelial phenotype.

It has previously been shown that BM cells have the capacity to engraft into pulmonary epithelial cells (Theise *et al.* 2002; Yamada *et al.* 2004; Rojas *et al.* 2005; MacPherson *et al.* 2006). Thus it is reasonable to consider that tumor cells may arise

from HSCs since they are able to engraft into lung epithelial cells and following transformation and differentiation they may lose their stem cell markers. There are several possible mechanisms for engraftment of HSCs and the possible role for HSCs as the potential cells of origin of lung tumors in *Tie2-CRT* mice which are discussed further in the next section (section 4.2).

Using the soft agar assay, we generated lung tumor spheres from two human lung cancer cell lines, the A549 human lung adenocarcinoma cell line and the H460 human lung large cell carcinoma (LCC) cell line. Examining the immunohistochemical characteristics of the differentiated and undifferentiated stages of these two human lung cancer cell lines using IF staining revealed that both spheres and differentiated cells expressed SP-C and CC10, while expression of CD133 and c-kit antigens was lost upon differentiation (Fig. 35 and 36). This is in contrast to the lung tumor spheres of *Tie2-CRT* mice in which undifferentiated tumor spheres failed to express SP-C antigen (Fig. 33). One explanation for this observation is that the origin of both the A549 human lung adenocarcinoma and the H460 human lung LCC cell lines are from BASCs expressing SP-C and CC10 proteins and not HSCs (Eramo *et al.* 2008).

4.2. HSC alterations in *Tie2-CRT* mice

Expression of HSC markers by lung tumor spheres isolated from *Tie2-CRT* mice led us to consider HSCs as being prime candidates for the cells of origin of the lung tumors observed in these mice. As such, we first sought to determine if the proliferative capacity of BM cells from *Tie2-CRT* mice is defective. *In vitro* clonogenic assays of BM cells in soft agar media (Dicke *et al.* 1983; Horowitz *et al.*

2002) demonstrated a higher colony-forming ability of the BM cells isolated from *Tie2-CRT* mice as compared to *wt* controls (Fig. 37) suggesting that BM cells isolated from *Tie2-CRT* mice are more proliferative and potentially more tumorigenic. Future investigation of the tumorigenic capacity of BM cells from *Tie2-CRT* mice using transplantation of BM cells into immunocompromised mice may elucidate the mechanisms behind these findings.

IF examination of colonies generated from the bone marrow of *Tie2-CRT* mice using antibodies against CRT-HA, CD133 and SP-C confirmed that the colonies express exogenous CRT and CD133 and that these colonies are originally from the bone marrow, but not derived from alveolar type II cells (Fig. 38). A recent study by Du and colleagues has shown that decreased CRT expression in esophageal squamous carcinoma cells inhibits their colony formation in soft agar (Du *et al.* 2009). This observation was further confirmed by injection and growth of esophageal squamous carcinoma cells into immunocompromised mice (Du *et al.* 2009). In this study, overexpression of CRT in HSCs resulted in increased colony formation in soft agar (Fig. 37).

It is generally believed that BM cells serve as precursors for hematopoiesis (Becker *et al.* 1963; Zhang *et al.* 2003). However, there are a few critical studies that suggest that circulating cells derived from the bone marrow are able to home to sites of chronic injury to reconstitute non-hematopoietic tissues such as the lung (Kotton *et al.* 2001; Theise *et al.* 2002; Jang *et al.* 2004; Rojas *et al.* 2005). It is also possible that these cells (bone marrow derived cells) could be potential targets of mitotic error or mutation as cancer cells when recruited to the site of injury and may function as tumor initiating cells (Houghton *et al.* 2004). Our IHC studies demonstrated an increased

number of inflammatory cells and the presence of HSCs in the lung of *Tie2-CRT* mice at the initial stages of tumor formation (Fig. 14, 17, 28 and 29). This concentration of cells could induce the mobilization of HSCs to the blood circulation of *Tie2-CRT* mice. Analysis of the population of circulatory HSCs using flow cytometry revealed a significant increase in the number of $CD34^{+}$/c-kit^{+} HSCs (Fig. 40B) in the blood of *Tie2-CRT* mice as compared to their *wt* controls.

Previous studies have shown the mobilization of $CD34^{+}$ BM cells after coronary injury (Sata *et al.* 2002; Inoue *et al.* 2007). Increased circulatory levels of macrophage and neutrophil markers after coronary artery injury revealed that the mobilization of BMDCs is mainly due to an increased inflammatory response (Inoue *et al.* 2007). Growth factors and cytokines such as VEGF (Grunewald *et al.* 2006) G-CSF (Inoue *et al.* 2007) and SDF-1(Jin *et al.* 2006) have been strongly implicated as signals that mobilize BM derived stem cells into the peripheral circulation.

The ability of HSCs to mobilize and then return to their niche in the BM (homing) relies on several factors including specific molecular recognition, cell-cell adhesion/disengagement, trans-endothelial migration, and anchoring to the BM niche (Lapidot *et al.* 2005; Cancelas *et al.* 2006). The chemokine SDF-1 and its receptor CXCR4 are two well known proteins that play a crucial role in the regulation of HSC mobilization and homing (Dar *et al.* 2005; Neiva *et al.* 2005). SDF-1 is constitutively expressed by endothelial cells, osteoblasts, and other stromal cells, while HSCs express CXCR4 (Peled *et al.* 1999; Kortesidis *et al.* 2005). SDF-1 produced by endothelial cells induces HSCs to undergo trans-endothelial migration mediated by E- and P-selectins (Katayama *et al.* 2003). Activation of adhesion molecules such as VLA-4 (Very Late Antigen-4) and LFA-1(leukocyte function antigen-1) is also

required for mobilization and the subsequent migration in the BM towards the osteoblast surface (Kopp *et al.* 2005).

Adhesive contacts through N-cadherin or c-kit/ SCF (Stem cell factor) interactions may also hold HSCs anchored to the endosteal niche, promoting their quiescence (Driessen *et al.* 2003; Arai *et al.* 2004; Haylock *et al.* 2005). Thus, impaired adhesion to BM niches leads to aberrant niches and loss of quiescence which results in migration of BM cells into the peripheral blood. For example, HSCs of chronic myeloid leukemia (CML) patients have reduced expression of adhesion proteins including L-selectin, CD44 and N-cadherin (Bruns *et al.* 2009). In idiopathic myelofibrosis (IM), degradation of SDF-1 or cleavage of its receptor CXCR4 as a result of increased production of MMP-9 leads to the release of the HSCs into the peripheral blood (Xu *et al.* 2005).

As mentioned above, within the hematopoietic microenvironment in the BM, the microvascular endothelium not only acts as a gatekeeper to control the trafficking and homing of hematopoietic progenitors, but also provides cellular contacts and secretes cytokines and adhesion molecules that allow for the preservation of steady state hematopoiesis. Considering this information and that CRT plays a role in the synthesis of different adhesion molecules and MMPs (Opas *et al.* 1996; Fadel *et al.* 1999; Fadel *et al.* 2001; Wu *et al.* 2007) it is plausible to consider that overexpression of CRT in HSCs and the microvascular endothelium may alter the expression of adhesion molecules and consequently the rate of HSC mobilization.

Engraftment of BM cells into pulmonary epithelial cells has been shown previously (Theise *et al.* 2002; Yamada *et al.* 2004; Rojas *et al.* 2005; MacPherson *et al.* 2006). Our data (Fig. 40 and 42) have also demonstrated a higher rate of

mobilization of HSCs from *Tie2-CRT* mice as compared to *wt* mice and that they are potentially tumorigenic. Taken together, it is possible to consider that circulatory HSCs from *Tie2-CRT* mice in the lung epithelium serve as potential cells of origin for the lung tumors observed in *Tie2-CRT* mice.

There are several possible mechanisms for the engraftment of HSCs into pulmonary epithelial cells to play a role as the cell of origin for the lung adenocarcinoma in *Tie2-CRT* mice. One potential scenario is the fusion of a circulatory HSC with an alveolar epithelium to form a heterokaryon, a cell with multiple, genetically different nuclei, which converts the gene expression pattern of the original HSC to that of the alveolar epithelium. For instance, fusion of a macrophage, which would be BM derived, with an injured hepatocyte *in vivo* has been shown to result in reprogramming of the macrophage nucleus to express liver specific genes (Vassilopoulos *et al.* 2003). Herzog and colleagues have already demonstrated that fusion of BM derived epithelial cells occurs in the lungs of mice following BM transplantation (Herzog *et al.* 2007). Another possibility is that there are epithelial progenitor cells in the BM that can undergo engraftment as epithelial cells, but not as hematopoietic cells (Kucia *et al.* 2005; Kucia *et al.* 2005; Gomperts *et al.* 2006). A final possibility is that engraftment of HSCs occurs via multiple different mechanisms. Further investigation on the role of HSCs as cell of origin of lung adenocarcinoma from *Tie2-CRT* mice using sex mismatch transplantation of HSCs will elucidate the mechanisms behind these findings.

Our results show that there is a higher number of HSCs (Fig. 41) and $CD133^{+}$ cells (Fig. 43) in the BM of *Tie2-CRT* mice as compared to *wt* control mice, which is indicative of a higher rate of hematopoiesis in these transgenic animals. CD133 is a

transmembrane glycoprotein and a known marker of HSCs (Yin *et al.* 1997) as well as a marker of cancer stem cells in solid tumors (Singh *et al.* 2003; Ponti *et al.* 2005; Ricci-Vitiani *et al.* 2007; Eramo *et al.* 2008; Chan *et al.* 2009). The number of CD133 positive cells was shown to be increased in the BM of myelodysplastic syndrome patients (Auberger *et al.* 2005). It has also been postulated to be an adverse prognostic factor in acute leukemia (Wang *et al.* 2007) or during the progression of chronic gastritis into gastric cancer (Futagami *et al.* 2010). However, whether the increased number of CD133 positive cells in the BM is an indication of tumorgenesis is unclear and requires further investigation.

The increased rate of hematopoiesis in *Tie2-CRT* mice could be caused by ongoing chronic inflammation (Yamada *et al.* 2004; MacPherson *et al.* 2006) and the increased demand for leukocytes to participate in the immune response. As well, alteration of the expression of adhesion molecules and cytokines in the BM microvascular endothelium (Abkowitz *et al.* 2003; Katayama *et al.* 2003) due to the overexpression of CRT in HSCs and the microvascular endothelium results in increased hematopoiesis in these animals. Further investigation is required to identify the role of CRT in the alteration of hematopoiesis in *Tie2-CRT* mice.

4.3. Expression of CRT in human and *Tie2-CRT* mice lung adenocarcinoma

In the present study, we have seen that ectopic expression of exogenous CRT in *Tie2-CR*T transgenic mice results in lung tumors. Thus, it was important to investigate changes in the endogenous CRT expression in the lung tumors observed in *Tie2-CRT* mice, as well as in human lung adenocarcinoma. Our data show that the expression of CRT does not change significantly in *Tie2-CRT* lung adenocarcinoma tumor cells as compared to the adjacent tissue (Fig. 44 and 45). We also did not observe any significant changes in the expression of CRT in differentiated and undifferentiated stages of the *Tie2-CRT* lung tumor derived cell line (Fig. 46). These data suggest that there is an association between the expression of exogenous CRT, but not with endogenous CRT, and the development of lung tumors in *Tie2-CRT* mice. The role of exogenous CRT in the progression of various cancers has been investigated recently (Du *et al.* 2007; Alur *et al.* 2009; Chen *et al.* 2009). Chen and colleagues (Chen *et al.* 2009) showed that overexpression of CRT resulted in increased angiogenesis and facilitated proliferation and migration of gastric cancer cells. They also observed an association between CRT overexpression and increased microvessel density, increased tumor invasion, enhanced lymph node metastasis, and poorer survival in gastric cancer patients (Chen *et al.* 2009).

It has previously been shown that there is a correlation between the overexpression of CRT and poor prognosis for patients with esophageal squamous cell carcinoma (Du *et al.* 2007). This same group (Du *et al.* 2009) has recently shown that CRT plays a crucial role during tumorigenesis by enhancing cell motility and anoikis

resistance through cortactin (CTTN) in esophageal squamous cell carcinoma cells. Another group examined the effects of exogenous CRT expression in prostate cancer cells (Alur *et al.* 2009) using full length CRT and CRT mutants with different functional domains deleted. They showed that prostate cancer cells overexpressing exogenous CRT (particularly the P domain of CRT) produced fewer colonies in both a monolayer culture and soft agar suggesting an inhibitory effect for CRT on the growth and/or metastasis of prostate cancer cells (Alur *et al.* 2009). Collectively, these data show that the effect of exogenous CRT on tumor cells is cell type dependent. The precise mechanism underlying the role of exogenous CRT in the development of cancers awaits further investigation.

To date no data is available on changes in CRT expression in human lung adenocarcinoma, thus we examined changes in CRT level in human lung adenocarcinoma. We first examined the expression of CRT in differentiated (adherent tumor cells) and undifferentiated (tumor spheres) stages of the A549 human lung adenocarcinoma cell line. We observed a significant increase in the expression of CRT in the undifferentiated tumor cells as compared to the differentiated tumor cells (Fig. 47). This is in contrast to our previous results in which there was no significant difference in the expression of CRT in differentiated and undifferentiated stages of the *Tie2-CRT* lung tumor cell line (Fig. 46). Furthermore, evaluation of CRT protein expression in human lung adenocarcinoma using a lung adenocarcinoma tissue microarray also revealed a significant reduction in CRT expression in the tumor regions as compared to the adjacent lung tissue (Fig. 48) while the results from *Tie2-CRT* lung adenocarcinoma showed no significant differences in the expression of endogenous CRT in the tumor regions as compared to the adjacent normal tissue (Fig.

44 and 45). These data suggest that the mechanism of progression of *Tie2-CRT* lung adenocarcinoma is different from that of human lung adenocarcinoma.

Increased CRT expression in a number of cancers has been reported by different groups using 2-dimentional gel electrophoresis (Franzen *et al.* 1996; Bini *et al.* 1997; Du *et al.* 2007). However, our TMA studies demonstrated decreased CRT expression in the tumor region as compared to the adjacent tissues. This difference could be due to the different tumor types (none of the previous studies were from lung cancer), heterogeneity of the cells in the tumor, and the multiple signaling pathways affected by CRT during tumorigenesis. The results of TMA studies also suggest the potential application of CRT as a prognostic marker during the development of human lung adenocarcinoma.

It is still unclear whether differential expression of CRT in human lung adenocarcinoma is a consequence of tumor progression or if CRT alone (directly or indirectly) has a role in the initiation and progression of human lung adenocarcinoma. In normal prostate tissue, CRT is expressed at high levels and its expression is regulated by androgens in both the mouse and human prostate epithelial cells (Zhu *et al.* 1998). It has been shown that Ca^{2+} signaling pathways are among the most important pathways involved in tumorigenesis through activation of different signaling pathways including ERK (extracellular signal-regulated kinase) (Chuderland *et al.* 2008), Ca^{2+}-dependent transcription factors involved in cell cycle control such as cAMP response element binding (CREB) (Arnould *et al.* 2002) and nuclear factor of activated T-cells (NFAT) (Baksh *et al.* 2002; Neal *et al.* 2003). CRT is a major ER chaperone protein and regulator of Ca^{2+} homeostasis within the cell, and as such may have an important functional role during the progression of cancer.

We also examined the protein expression of known tumor suppressors such as p53, PTEN and phospho-Akt (proteins involved in growth factor mediated cell survival and cancer) in the lung tumors from *Tie2-CRT* mice. Although there were no changes in the level of PTEN (Fig. 49) and phospho-Akt (Fig. 51) in these tumors, expression of p53 protein (Fig. 50) was significantly decreased in the tumors as compared to the normal adjacent tissue. Alterations in the PTEN/Akt pathway are common events occurring in human malignancies, and are especially prevalent in breast cancer (Page *et al.* 2000; DeGraffenried *et al.* 2004; Panigrahi *et al.* 2004) whereas p53 mutations are more frequent in human and mouse lung cancer (Nishio *et al.* 1996; Wang *et al.* 2006).

p53 is a tumor suppressor protein which controls cell proliferation by arresting growth at cell cycle checkpoints (Harper *et al.* 1993; Sidransky *et al.* 1996) and triggering apoptotic cell death (Yonish-Rouach *et al.* 1991; Shaw *et al.* 1992). The *p53* gene is the most frequently mutated gene associated with cancer. *p53* mutations often lead to the loss of its tumor suppressor function and ability to induce apoptosis (Kastan *et al.* 1991; Sidransky *et al.* 1996; Stuppia *et al.* 1997). Furthermore, decreased expression of p53 has been reported in several cancers (Minami *et al.* 2002; Pizzi *et al.* 2002) while its overexpression is associated with induction of apoptosis (Orazi *et al.* 1996; Shao *et al.* 2000). Expression of CRT was shown to regulate p53 function, nuclear localization and subsequently cell behavior (Mesaeli *et al.* 2004; Liu *et al.* 2005). For example, overexpression of vasostatin (the N-terminal domain of CRT) in neuroendocrine tumor cells increased their malignant properties by downregulating tumor suppressor genes including *p53*, and *Rb* (Liu *et al.* 2005). More recently, CRT overexpression in mature cardiomyocytes was also shown to increase the activity of

pro-apoptotic factors such as, Bax (Bcl-2–associated X protein), p53 and caspase 8, promoting apoptosis via a Ca^{2+}-dependent pathway (Lim *et al.* 2008).

The association between inflammation and tumor progression is well established (Coussens *et al.* 2002) and many malignancies arise from sites of infection, chronic irritation and inflammation (Danese 2008; Engels 2008; Farinati *et al.* 2008; Lee *et al.* 2009). It is estimated that 15% of the worldwide cancer incidence can be attributed to chronic infections and inflammatory responses (Parkin *et al.* 2001). Proinflammatory cells and soluble mediators, such as cytokines and chemokines have the capacity to promote the propagation of cancer cells and their progression. TGF-β and Tumor Necrosis Factor-alpha (TNFα) are the two main pro-inflammatory cytokines in inflammatory pathways that increase tumorigenesis (Parsonnet 1997; Aggarwal *et al.* 2002). Nuclear factor kappa B (NF-κB) is a transcription factor that has been shown to play a central role in connecting inflammation and cancer (Naugler *et al.* 2008). In the lung, it has been shown that CRT in association with CD91 (also known as LDL receptor related protein) acts as pathogen associated molecular patterns (PAMPs) which can be recognized by the pulmonary collections, SP-A and SP-D (Gardai *et al.* 2003). This stimulates macrophage inflammatory responses which results in enhanced p38/MAPK activation and NFκB reporter activity suggesting a possible role for surface CRT in the pro-inflammatory action of surfactant proteins in the lungs (Gardai *et al.* 2003).

Pro-inflammatory cytokines have been shown to inhibit p53 activity (Hudson *et al.* 1999) which indicates a link between inflammation and tumorigenesis through p53 inactivation. The association between inflammation and EMT progression in the development of non-small cell lung cancer has been previously described (Dohadwala

et al. 2006; Krysan *et al.* 2008). This process is coordinated mainly though downregulation of E-cadherin expression via inflammatory mediators in the lung such as IL-1β and PGE2. This suggests that inflammation in the lung of *Tie2-CRT* mice may also impact stem cell properties via EMT-dependent events in the early stages of carcinogenesis in lung cancer. Inflammation can also promote EMT through other pathways such as NFκB (Wu *et al.* 2009). Furthermore, a link between EMT and cancer stem cells has been shown by different groups (Mani *et al.* 2008; Morel *et al.* 2008). Collectively, these findings may also suggest a transition of pulmonary epithelial cells in the lungs of *Tie2-CRT* mice to stem cell-like cells via EMT in the presence of inflammation in the lungs.

Another potential alternative mechanism for lung tumor initiation and progression in *Tie2-CRT* mice could be related to the increased permeability of blood vessels in these mice. It is known that inflammation leads to increased vascular permeability and promotes chemokine-mediated recruitment of immune cells such as monocytes, macrophages and other leukocytes (Wilhelm 1973; Klimenko *et al.* 1999) that can synthesize angiogenic cytokines and growth factors. Chen and colleagues have shown that overexpression of CRT increased expression and secretion of vascular endothelial growth factor (VEGF) (Chen *et al.* 2009), a growth factor that when in excess, often produces hyper-permeable leaky vessels (Proescholdt *et al.* 1999). Therefore, it is possible that overexpression of CRT in the microvascular endothelium in the lungs of *Tie2-CRT* mice or even the increased inflammation seen in the lungs resulted in increased permeability of blood vessels of the lungs which promotes leukocyte and HSC recruitment. Macrophages which are recruited by VEGF could also alter VEGF levels by producing the factor themselves and secreting

metalloproteinases that release extracellular matrix-bound VEGF (Bergers *et al.* 2000). Increased vascular permeability and secretion of VEGF was shown to accelerate the process of carcinogenesis (Mullin *et al.* 2000; Inoue *et al.* 2002).

The third possible mechanism for lung tumor progression in *Tie2-CRT* mice is the role of CRT in modulating tyrosine kinase pathways. It has long been known that tyrosine kinase signaling pathways are important in normal cellular physiology and that deregulation of these pathways contributes to the development of numerous types of human malignancies including lung cancer (Salgia *et al.* 1998; Biscardi *et al.* 2000). Like many other cancer cells, lung cancer cells also overexpress receptor tyrosine kinases (Salgia *et al.* 1998). Upon activation of receptor tyrosine kinases by growth factors, various biological functions are altered in the cells, including cell growth, migration/motility, and the activation of downstream signal-transduction events (Salgia *et al.* 1998; Biscardi *et al.* 2000). CRT, as an ER resident chaperone, could affect several tyrosine kinase signaling pathways involved in cell survival and apoptosis. Expression of CRT has been proposed to modulate apoptosis through different tyrosine kinase signaling pathways (Kageyama *et al.* 2002; Jalali *et al.* 2008). Previous work in our laboratory using CRT-deficient cells showed increased insulin receptor density and activity in the absence of CRT function (Jalali *et al.* 2008). CRT overexpression was also shown to increase the cell surface expression of the human insulin receptor (Ramos *et al.* 2007). These data together suggest a complex role for CRT in the modulation of tyrosine kinase signaling pathways which may have an effect during tumorigenesis and the regulation of tumor progression.

Based on the collective results obtained in this study, we can propose a model for the initiation and progression of the lung tumors observed in *Tie2-CRT* transgenic

mice involving HSCs and endothelial cells (Fig. 52). Our data demonstrate that increased inflammation and ongoing inflammatory responses are accompanied with the presence of HSCs in the lungs of *Tie2-CRT* mice. The mechanism behind this observation remains to be elucidated, but we postulate that overexpression of CRT in the microvascular endothelium in the lungs results in the production and release of inflammatory mediators by neighboring cells or increased permeability of blood vessels in the lungs which promotes HSC recruitment.

In the present study, we have shown that overexpression of CRT in HSCs and endothelial cells of *Tie2-CRT* mice may not only augmented the mobilization of HSCs towards the blood circulation, but could also result in an increased malignant behavior of HSCs which allows these cells to readily home to a target tissue, and initiate a tumor. At the same time, increased inflammation in the lungs makes this an organ that is a particularly susceptible target for the recruitment of HSCs and provides a suitable microenvironment for tumor initiation.

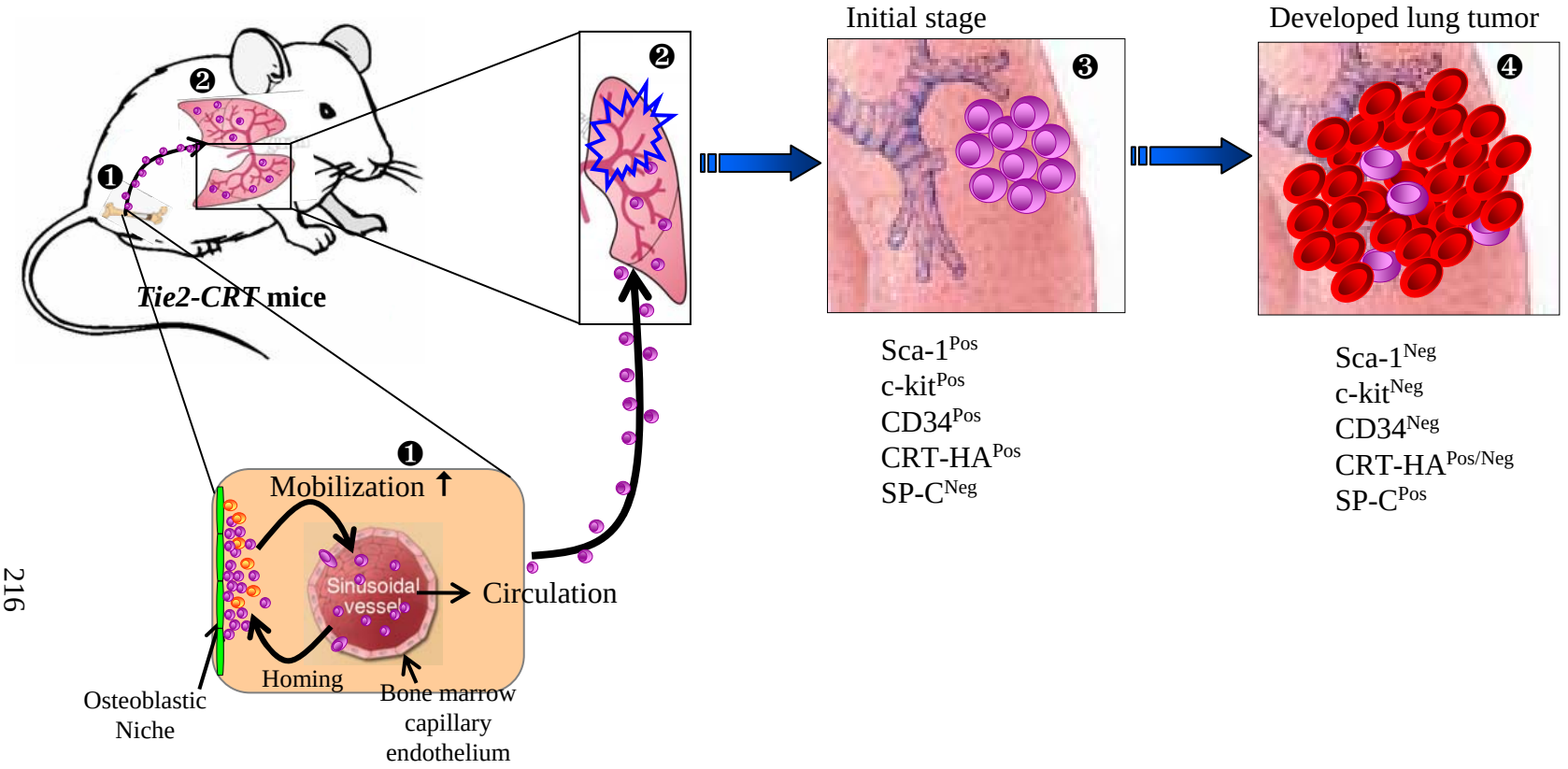

Figure 52. Summary of proposed model for development of lung tumors in *Tie2-CRT* mice. Overexpression of CRT in HSCs and the microvascular endothelium from the BM (1) and the lungs (2) in *Tie2-CRT* mice results in an increased rate of mobilization of HSCs and inflammation in the lungs. HSCs released into the blood circulation are recruited to the site of inflammation in the lungs. Inflammation in the lungs not only makes this organ a susceptible target tissue for the recruitment of HSCs, but also provides a suitable microenvironment for the initiation of tumors. At the initial stages (3), tumor cells are non-epithelial cells (SP-C^{Neg}) expressing HSC markers (Sca-1^{Pos}, c-kit^{Pos}, CD34^{Pos}) and transgenic CRT (CRT-HA^{Pos}), while after further development and progression they differentiate and lose their stem cell phenotype, acquiring an epithelial phenotype.

4.4. SUMMARY

I. *Tie2* driven overexpression of CRT is associated with the development of lung tumors in mice.

II. Lung tumors observed in *Tie2-CRT* mice were adenocarcinomas with a SP-C ^{Pos} and CC10 ^{Neg} phenotype.

III. Lung tumors in *Tie2-CRT* mice are composed of a heterogeneous population of cells.

IV. Cells derived from *Tie2-CRT* mice lung tumors are capable of anchorage independent growth, and the tumor spheres express HSC markers (CD133, c-kit, Sca-1, CD34), CRT-HA and Tie2.

V. Tumor spheres grown in a monolayer lose their HSC markers and express SP-C and epithelial markers.

VI. Undifferentiated cells of A549 and H460 human lung tumor cell lines are positive for SP-C, CC10 and HSC antigens suggesting a possible involvement of BASCs in these human lung tumors.

VII. There is an elevated rate of HSC mobilization in *Tie2-CRT* mice.

VIII. CRT expression is elevated in undifferentiated tumor spheres of the A549 human cell line as compared to differentiated cells.

IX. Reduced CRT expression is observed in the tumor region of the human lung adenocarcinoma as compared to the normal adjacent tissue.

X. p53 expression is reduced in the lung tumors of *Tie2-CRT* mice as compared to normal adjacent tissue.

4.5. FUTURE DIRECTIONS

In the present study, the *Tie2* promoter was used to overexpress CRT in endothelial cells (Sato *et al.* 1993). However, subsequent studies by other investigators showed that the *Tie2* promoter is also active in HSCs (Arai *et al.* 2004; Shaw *et al.* 2004). Therefore, one of the limitations of our study which hinders our ability to conclude the importance of vascular integrity in lung adenocarcinoma development is the lack of vessel wall-specific targeting for overexpression of CRT. To overcome this limitation, generation of transgenic mice using a more specific promoter for endothelial cells, such as VE-cadherin (Gory *et al.* 1999), would be interesting and could provide clearer results.

Another limitation of this study relates to use of CD-1 mice for the generation of *Tie2-CRT* mice. CD-1 mice are the outbred-mouse line commonly used in a broad range of genetic studies. However, the prevalence of spontaneous lung and liver tumors in CD-1 mice is about 21.8 and 6.1-35.5% respectively (Maita *et al.* 1988; Manenti *et al.* 2003) which is relatively high as compared to other mice strains. Therefore, it would be valuable to use a mouse strain that is resistant to the lung and liver tumors such as CBA or C3H mice (Andervont 1950; Shimkin 1955; Mezey *et al.* 2003) for studying the role of CRT in the development of lung and liver tumors.

In this study we have shown that the overexpression of CRT under the control of the *Tie2* promoter resulted in lung adenocarcinoma which correlates with increased inflammation in the lungs of *Tie2-CRT* mice. The molecular mechanisms involved in this process are not yet understood, but it is clear that increased inflammation in the lungs is a hallmark of the initiation and progression of lung tumors in these animals.

Further studies are needed to provide insight into the role of inflammation in the development of lung tumors by determining the contribution of inflammation, accumulation of inflammatory cells, and inflammatory responses to the tumorigenic process.

This study also provides evidence that the lung tumors which develop in *Tie2-CRT* mice originate from HSCs. We have shown through isolation and immunophenotypic characterization of lung tumor cells from *Tie2-CRT* mice (anchorage independent growth and non-adherent culture condition assays) that these cells are positive for HSCs antigens as well as CRT-HA. It is important to elucidate the exact role played by HSCs as the cells of origin for generating these lung tumors. Sex-mismatches BM transplantation from a donor to a recipient is a common technique used to study the participation of BM cells in the generation of non-hematopoietic tissues and tumors (Hudson *et al.* 1999). Thus, sex-mismatched BM transplantation will provide valuable information regarding the role of HSCs during the formation and progression of lung tumors in *Tie2-CRT* mice.

Our flow cytometry data indicates an increased rate of HSC mobilization in *Tie2-CRT* mice when compared to *wt* mice. This may be due to the increased inflammatory signals from the lung or the alteration of adhesion molecules involved in the migration and mobilization of HSCs. Therefore, to understand the mechanisms by which HSC mobilization in *Tie2-CRT* mice is increased, it will be necessary to investigate the role of CRT overexpression in the alteration of adhesion molecule expression of adhesion molecules as well as changes in inflammatory mediators which may lead to the increased mobilization of HSCs.

In the present study we have observed decreased protein expression of p53 in the lung tumors of *Tie2-CRT* mice as compared to normal adjacent tissue. This implicates p53 as being a potential key regulatory protein during the development of these lung tumors. A link between inflammation and tumorigenesis through p53 inactivation (Mesaeli *et al.* 2004; Liu *et al.* 2005) and also a role for CRT in the regulation of p53 function, nuclear localization and malignant cell behavior has previously been reported . Further investigation of p53 function and expression in CRT overexpressing HSCs isolated from *Tie2-CRT* mice is needed to provide insight into the regulatory role of CRT overexpression on p53 function.

CHAPTER V: REFERENCES:

Abkowitz, J. L., A. E. Robinson, et al. (2003). "Mobilization of hematopoietic stem cells during homeostasis and after cytokine exposure." Blood **102**(4): 1249-53.

Achiwa, H., Y. Yatabe, et al. (1999). "Prognostic significance of elevated cyclooxygenase 2 expression in primary, resected lung adenocarcinomas." Clin Cancer Res **5**(5): 1001-5.

Adams, G. B., K. T. Chabner, et al. (2006). "Stem cell engraftment at the endosteal niche is specified by the calcium-sensing receptor." Nature **439**(7076): 599-603.

Adamson, I. Y., R. Vincent, et al. (1999). "Cell injury and interstitial inflammation in rat lung after inhalation of ozone and urban particulates." Am J Respir Cell Mol Biol **20**(5): 1067-72.

Afshar, N., B. E. Black, et al. (2005). "Retrotranslocation of the chaperone calreticulin from the endoplasmic reticulum lumen to the cytosol." Mol Cell Biol **25**(20): 8844-53.

Aggarwal, B. B., S. Shishodia, et al. (2002). "The role of TNF and its family members in inflammation and cancer: lessons from gene deletion." Curr Drug Targets Inflamm Allergy **1**(4): 327-41.

Alberg, A. J., M. V. Brock, et al. (2005). "Epidemiology of lung cancer: looking to the future." J Clin Oncol **23**(14): 3175-85.

Alur, M., M. M. Nguyen, et al. (2009). "Suppressive roles of calreticulin in prostate cancer growth and metastasis." Am J Pathol **175**(2): 882-90.

Andervont, H. B. (1950). "Studies on the occurrence of spontaneous hepatomas in mice of strains C3H and CBA." J Natl Cancer Inst **11**(3): 581-92.

Andervont, H. B. and T. B. Dunn (1962). "Occurrence of tumors in wild house mice." J Natl Cancer Inst **28**: 1153-63.

Andrin, C., E. F. Corbett, et al. (2000). "Expression and purification of mammalian calreticulin in Pichia pastoris." Protein Expr Purif **20**(2): 207-15.

Arai, F., A. Hirao, et al. (2004). "Tie2/angiopoietin-1 signaling regulates hematopoietic stem cell quiescence in the bone marrow niche." Cell **118**: 149-161.

Arnould, T., S. Vankoningsloo, et al. (2002). "CREB activation induced by mitochondrial dysfunction is a new signaling pathway that impairs cell proliferation." Embo J **21**(1-2): 53-63.

Auberger, J., M. Dlaska, et al. (2005). "Increased CD133 expression in bone marrow of myelodysplastic syndromes." Leuk Res **29**(9): 995-1001.

Avissar, N. E., C. K. Reed, et al. (2000). "Ozone, but not nitrogen dioxide, exposure decreases glutathione peroxidases in epithelial lining fluid of human lung." Am J Respir Crit Care Med **162**(4 Pt 1): 1342-7.

Avital, I., A. L. Moreira, et al. (2007). "Donor-derived human bone marrow cells contribute to solid organ cancers developing after bone marrow transplantation." Stem Cells **25**(11): 2903-9.

Azad, N., Y. Rojanasakul, et al. (2008). "Inflammation and lung cancer: roles of reactive oxygen/nitrogen species." J Toxicol Environ Health B Crit Rev **11**(1): 1-15.

Baksh, S. and M. Michalak (1991). "Expression of calreticulin in Escherichia coli and identification of its Ca2+ binding domains." J Biol Chem **266**(32): 21458-65.
Baksh, S., C. Spamer, et al. (1995). "Identification of the Zn2+ binding region in calreticulin." FEBS Lett **376**(1-2): 53-7.
Baksh, S., H. R. Widlund, et al. (2002). "NFATc2-mediated repression of cyclin-dependent kinase 4 expression." Mol Cell **10**(5): 1071-81.
Balsam, L. B., A. J. Wagers, et al. (2004). "Haematopoietic stem cells adopt mature haematopoietic fates in ischaemic myocardium." Nature **428**(6983): 668-73.
Barbone, F., M. Bovenzi, et al. (1997). "Cigarette smoking and histologic type of lung cancer in men." Chest **112**(6): 1474-9.
Bass, J., G. Chiu, et al. (1998). "Folding of insulin receptor monomers is facilitated by the molecular chaperones calnexin and calreticulin and impaired by rapid dimerization." J Cell Biol **141**(3): 637-46.
Bastianutto, C., E. Clementi, et al. (1995). "Overexpression of calreticulin increases the Ca2+ capacity of rapidly exchanging Ca2+ stores and reveals aspects of their lumenal microenvironment and function." J Cell Biol **130**(4): 847-55.
Beals, C. R., N. A. Clipstone, et al. (1997). "Nuclear localization of NF-ATc by a calcineurin-dependent, cyclosporin-sensitive intramolecular interaction." Genes Dev **11**(7): 824-34.
Becker, A. J., C. E. Mc, et al. (1963). "Cytological demonstration of the clonal nature of spleen colonies derived from transplanted mouse marrow cells." Nature **197**: 452-4.
Bedetti, C. D., G. Singh, et al. (1987). " Ultrastructural localization of rat Clara cell 10 kd secretory protein by the immunogold technique using polyclonal and monoclonal antibodies." J. Histochem. Cytochem. **35**: 789-794.
Bergers, G., R. Brekken, et al. (2000). "Matrix metalloproteinase-9 triggers the angiogenic switch during carcinogenesis." Nat Cell Biol **2**(10): 737-44.
Berridge, M. J. (2002). "The endoplasmic reticulum: a multifunctional signaling organelle." Cell Calcium **32**(5-6): 235-49.
Bhatia, M., D. Bonnet, et al. (1998). "A newly discovered class of human hematopoietic cells with SCID-repopulating activity." Nat Med **4**(9): 1038-45.
Bini, L., B. Magi, et al. (1997). "Protein expression profiles in human breast ductal carcinoma and histologically normal tissue." Electrophoresis **18**(15): 2832-41.
Biscardi, J. S., R. C. Ishizawar, et al. (2000). "Tyrosine kinase signalling in breast cancer: epidermal growth factor receptor and c-Src interactions in breast cancer." Breast Cancer Res **2**(3): 203-10.
Bloom, W. F. and D. W. Fawcett (1975). Respiratory systems. Textbook of Histology, Philadelphia: Saunders: pp. 743–65.
Bouthillier, L., R. Vincent, et al. (1998). "Acute effects of inhaled urban particles and ozone: lung morphology, macrophage activity, and plasma endothelin-1." Am J Pathol **153**(6): 1873-84.
Boyd, M. R. (1977). "Evidence for the Clara cell as a site of cytochrome P450-dependent mixed-function oxidase activity in lung." Nature **269**(5630): 713-5.
Bradley, T. R. and D. Metcalf (1966). "The growth of mouse bone marrow cells in vitro." Aust J Exp Biol Med Sci **44**(3): 287-99.
Breton, J., M. C. Gage, et al. (2008). "Proteomic screening of a cell line model of esophageal carcinogenesis identifies cathepsin D and aldo-keto reductase 1C2

and 1B10 dysregulation in Barrett's esophagus and esophageal adenocarcinoma." J Proteome Res **7**(5): 1953-62.
Brody, A. R., G. E. Hook, et al. (1987). "The differentiation capacity of Clara cells isolated from the lungs of rabbits." Lab Invest **57**(2): 219-29.
Broeckaert, F., K. Arsalane, et al. (1999). "Lung epithelial damage at low concentrations of ambient ozone." Lancet **353**(9156): 900-1.
Brown, L. F., B. J. Dezube, et al. (2000). "Expression of Tie1, Tie2, and angiopoietins 1, 2, and 4 in Kaposi's sarcoma and cutaneous angiosarcoma." Am J Pathol **156**(6): 2179-83.
Brown, S., I. Heinisch, et al. (2002). "Apoptosis disables CD31-mediated cell detachment from phagocytes promoting binding and engulfment." **418**(6894): 200-203.
Broxmeyer, H. E. (1984). "Colony assays of hematopoietic progenitor cells and correlations to clinical situations." Crit Rev Oncol Hematol **1**(3): 227-57.
Brunagel, G., U. Shah, et al. (2003). "Identification of calreticulin as a nuclear matrix protein associated with human colon cancer." J Cell Biochem **89**(2): 238-43.
Bruns, I., A. Czibere, et al. (2009). "The hematopoietic stem cell in chronic phase CML is characterized by a transcriptional profile resembling normal myeloid progenitor cells and reflecting loss of quiescence." Leukemia **23**(5): 892-9.
Cahalan, M. D. and R. S. Lewis (1990). "Functional roles of ion channels in lymphocytes." Semin Immunol **2**(2): 107-17.
Caine, G. J., A. D. Blann, et al. (2003). "Plasma angiopoietin-1, angiopoietin-2 and Tie-2 in breast and prostate cancer: a comparison with VEGF and Flt-1." Eur J Clin Invest **33**(10): 883-90.
Calvi, L. M., et al. (2003). "Osteoblastic cells regulate the haematopoietic stem cell niche." Nature **425**: 841–846.
Canadian Cancer Statistics (2009).
Cancelas, J. A., A. W. Lee, et al. (2005). "Rac GTPases differentially integrate signals regulating hematopoietic stem cell localization." Nat Med **11**(8): 886-91.
Cancelas, J. A. and D. A. Williams (2006). "Stem cell mobilization by beta2-agonists." Nat Med **12**(3): 278-9.
Chai, W. R., Y. Chen, et al. (2008). "Mechanism of nuclear factor of activated T-cells mediated FasL expression in corticosterone -treated mouse Leydig tumor cells." BMC Cell Biol **9**: 31.
Chan, K. S., I. Espinosa, et al. (2009). "Identification, molecular characterization, clinical prognosis, and therapeutic targeting of human bladder tumor-initiating cells." Proc Natl Acad Sci U S A.
Charuworn, B., M. Dohadwala, et al. (2006). "Inflammation-mediated promotion of EMT in NSCLC: IL-1b mediates a MEK/Erk- and JNK/SAPK-dependent downregulation of E-cadherin." Proc Am Thorac Soc **D96.**
Chen, C. N., C. C. Chang, et al. (2009). "Identification of calreticulin as a prognosis marker and angiogenic regulator in human gastric cancer." Ann Surg Oncol **16**(2): 524-33.
Chen, C.-N., T.-E. Su, et al. (2007). "Calreticulin regulates cell proliferation and migration in gastric cancer cell line AGS." FASEB J. **21**(6): A1318-b-.

Chen, W. S., C. S. Lazar, et al. (1989). "Functional independence of the epidermal growth factor receptor from a domain required for ligand-induced internalization and calcium regulation." Cell **59**(1): 33-43.
Cheng, T., N. Rodrigues, et al. (2000). "Hematopoietic stem cell quiescence maintained by p21cip1/waf1." Science **287**(5459): 1804-8.
Chuderland, D. and R. Seger (2008). "Calcium regulates ERK signaling by modulating its protein-protein interactions." Commun Integr Biol **1**(1): 4-5.
Chung, J., A. G. Gao, et al. (1997). "Thrombspondin acts via integrin-associated protein to activate the platelet integrin alphaIIbbeta3." J Biol Chem **272**(23): 14740-6.
Clara, M. (1937). "Zur Histobiologie des Bronchialepithels." Z. mikrosk.-anat. Forsch. **4**: 321-347.
Clifton F. Mountain (2000). "The international system for staging lung cancer." Seminars in Surgical Oncology **18**(2): 106-115.
Cohen, B. H., E. L. Diamond, et al. (1977). "A common familial component in lung cancer and chronic obstructive pulmonary disease." Lancet **2**(8037): 523-6.
Cole, A. R., H. Ji, et al. (2000). "Proteomic analysis of colonic crypts from normal, multiple intestinal neoplasia and p53-null mice: a comparison with colonic polyps." Electrophoresis **21**(9): 1772-81.
Cole, S. W. (2009). "Chronic Inflammation and Breast Cancer Recurrence." J Clin Oncol.
Collins, L. G., C. Haines, et al. (2007). "Lung cancer: diagnosis and management." Am Fam Physician **75**(1): 56-63.
Comis, R. L. (2003). "A brief history of the research and treatment of lung cancer from 1970 to 2003." Int J Clin Oncol **8**(4): 230-3.
Coppolino, M. G., M. J. Woodside, et al. (1997). "Calreticulin is essential for integrin-mediated calcium signalling and cell adhesion." Nature **386**(6627): 843-7.
Corbett, E. F., K. M. Michalak, et al. (2000). "The conformation of calreticulin is influenced by the endoplasmic reticulum luminal environment." J Biol Chem **275**(35): 27177-85.
Coussens, L. M. and Z. Werb (2002). "Inflammation and cancer." Nature **420**(6917): 860-7.
Crabtree, G. R. (2001). "Calcium, calcineurin, and the control of transcription." J Biol Chem **276**(4): 2313-6.
Croninger, A. B., E. A. Graham, et al. (1958). "Experimental production of carcinoma with tobacco products. V. Carcinoma induction in mice with cigar, pipe, and all-tobacco cigarette tar." Cancer Res **18**(11): 1263-71.
Current Protocols in Cytometry (1997). John Wiley & Sons, Inc. New York **Appendix A.2A.1**.
Cuzick, J., F. Otto, et al. (2009). "Aspirin and non-steroidal anti-inflammatory drugs for cancer prevention: an international consensus statement." Lancet Oncol **10**(5): 501-7.
D'Andrea, L. D., G. Iaccarino, et al. (2005). "Targeting angiogenesis: structural characterization and biological properties of a de novo engineered VEGF mimicking peptide." Proc Natl Acad Sci U S A **102**(40): 14215-20.
Danese, S. (2008). "Inflammatory bowel disease and inflammation-associated colon cancer: partners in crime." Curr Drug Targets **9**(5): 360.

Dao, M. A., J. Arevalo, et al. (2003). "Reversibility of CD34 expression on human hematopoietic stem cells that retain the capacity for secondary reconstitution." Blood **101**(1): 112-8.
Dar, A., P. Goichberg, et al. (2005). "Chemokine receptor CXCR4-dependent internalization and resecretion of functional chemokine SDF-1 by bone marrow endothelial and stromal cells." Nat Immunol **6**(10): 1038-46.
Dasari, V., M. Gallup, et al. (2006). "Epithelial-mesenchymal transition in lung cancer: is tobacco the "smoking gun"?" Am J Respir Cell Mol Biol **35**(1): 3-9.
Davis, S., T. H. Aldrich, et al. (1996). "Isolation of angiopoietin-1, a ligand for the TIE2 receptor, by secretion-trap expression cloning." Cell **87**(7): 1161-9.
DeGraffenried, L. A., L. Fulcher, et al. (2004). "Reduced PTEN expression in breast cancer cells confers susceptibility to inhibitors of the PI3 kinase/Akt pathway." Ann Oncol **15**(10): 1510-6.
Delom, F. and E. Chevet (2006). "In vitro mapping of calnexin interaction with ribosomes." Biochem Biophys Res Commun **341**(1): 39-44.
DeMayo, F. J., M. J. Finegold, et al. (1991). "Expression of SV40 T antigen under control of rabbit uteroglobin promoter in transgenic mice." Am J Physiol **261**(2 Pt 1): L70-6.
Dentener, M. A., A. C. Vreugdenhil, et al. (2000). "Production of the acute-phase protein lipopolysaccharide-binding protein by respiratory type II epithelial cells: implications for local defense to bacterial endotoxins." Am J Respir Cell Mol Biol **23**(2): 146-53.
Diaz-Meco, M. T. and J. Moscat (2008). "Akt regulation and lung cancer: a novel role and mechanism of action for the tumor suppressor Par-4." Cell Cycle **7**(18): 2817-20.
Dicke, K. A., S. E. Tindle, et al. (1983). "Leukemic cell colony formation in soft agar by bone marrow cells and peripheral blood cells from untreated acute leukemia patients." Exp Hematol **11**(4): 341-50.
Dodson, M. G., J. Slota, et al. (1981). "Distinction of the phenotypes of in vitro anchorage-independent soft-agar growth and in vivo tumorigenicity in the nude mouse." Cancer Res **41**(4): 1441-6.
Dohadwala, M., S. C. Yang, et al. (2006). "Cyclooxygenase-2-dependent regulation of E-cadherin: prostaglandin E(2) induces transcriptional repressors ZEB1 and snail in non-small cell lung cancer." Cancer Res **66**(10): 5338-45.
Driessen, R. L., H. M. Johnston, et al. (2003). "Membrane-bound stem cell factor is a key regulator in the initial lodgment of stem cells within the endosteal marrow region." Exp Hematol **31**(12): 1284-91.
Driscoll, B., S. Buckley, et al. (2000). "Telomerase in alveolar epithelial development and repair." Am J Physiol Lung Cell Mol Physiol **279**(6): L1191-8.
Du, X. L., H. Hu, et al. (2007). "Proteomic profiling of proteins dysregulted in Chinese esophageal squamous cell carcinoma." J Mol Med **85**(8): 863-75.
Du, X. L., H. Yang, et al. (2009). "Calreticulin promotes cell motility and enhances resistance to anoikis through STAT3-CTTN-Akt pathway in esophageal squamous cell carcinoma." Oncogene.
Dumont, D. J., G. Gradwohl, et al. (1994). "Dominant-negative and targeted null mutations in the endothelial receptor tyrosine kinase, tek, reveal a critical role in vasculogenesis of the embryo." Genes Dev **8**(16): 1897-909.

Dumont, D. J., T. P. Yamaguchi, et al. (1992). "tek, a novel tyrosine kinase gene located on mouse chromosome 4, is expressed in endothelial cells and their presumptive precursors." Oncogene **7**(8): 1471-80.
Dutt, A. and K. K. Wong (2006). "Mouse models of lung cancer." Clin Cancer Res **12**(14 Pt 2): 4396s-4402s.
Egeblad, M. and Z. Werb (2002). "New functions for the matrix metalloproteinases in cancer progression." Nat Rev Cancer **2**(3): 161-74.
El Hiani, Y., V. Lehen'kyi, et al. (2009). "Activation of the calcium-sensing receptor by high calcium induced breast cancer cell proliferation and TRPC1 cation channel over-expression potentially through EGFR pathways." Arch Biochem Biophys **486**(1): 58-63.
Ellgaard, L., R. Riek, et al. (2001). "NMR structure of the calreticulin P-domain." Proc Natl Acad Sci U S A **98**(6): 3133-8.
Elton, C. M., P. A. Smethurst, et al. (2002). "Physical and functional interaction between cell-surface calreticulin and the collagen receptors integrin alpha2beta1 and glycoprotein VI in human platelets." Thromb Haemost **88**(4): 648-54.
el-Torky, M., F. el-Zeky, et al. (1990). "Significant changes in the distribution of histologic types of lung cancer. A review of 4928 cases." Cancer **65**(10): 2361-7.
Engelhardt, J. F. (2001). "Stem cell niches in the mouse airway." Am J Respir Cell Mol Biol **24**(6): 649-52.
Engels, E. A. (2008). "Inflammation in the development of lung cancer: epidemiological evidence." Expert Rev Anticancer Ther **8**(4): 605-15.
Eramo, A., F. Lotti, et al. (2008). "Identification and expansion of the tumorigenic lung cancer stem cell population." Cell Death Differ **15**(3): 504-14.
Eric, A., Z. Juranic, et al. (2009). "Effects of humoral immunity and calreticulin overexpression on postoperative course in breast cancer." Pathol Oncol Res **15**(1): 89-90.
Evans, M. J., L. J. Cabral, et al. (1975). "Transformation of alveolar type 2 cells to type 1 cells following exposure to NO2." Exp. Mol. Pathol. **50**: 22:142–.
Evans, M. J., L. J. Cabral-Anderson, et al. (1978). "Role of the Clara cell in renewal of the bronchiolar epithelium." Lab Invest **38**(6): 648-53.
Fadel, M. P., E. Dziak, et al. (1999). "Calreticulin affects focal contact-dependent but not close contact-dependent cell-substratum adhesion." J Biol Chem **274**(21): 15085-94.
Fadel, M. P., M. Szewczenko-Pawlikowski, et al. (2001). "Calreticulin affects beta-catenin-associated pathways." J Biol Chem **276**(29): 27083-9.
Farinati, F., R. Cardin, et al. (2008). "Helicobacter pylori, inflammation, oxidative damage and gastric cancer: a morphological, biological and molecular pathway." Eur J Cancer Prev **17**(3): 195-200.
Fayadat, L., S. Siffroi-Fernandez, et al. (2000). "Calnexin and calreticulin binding to human thyroperoxidase is required for its first folding step(s) but is not sufficient to promote efficient cell surface expression." Endocrinology **141**(3): 959-66.
Fehrenbach, H. (2001). "Alveolar epithelial type II cell: defender of the alveolus revisited." Respir Res **2**(1): 33-46.

Fernandez, F. G. and R. J. Battafarano (2006). "Large-cell neuroendocrine carcinoma of the lung." Cancer Control **13**(4): 270-5.
Fliedner, T. M. (1998). "The role of blood stem cells in hematopoietic cell renewal." Stem Cells **16**(6): 361-74.
Folkman, J. (1982). "Angiogenesis: initiation and control." Ann N Y Acad Sci **401**: 212-27.
Frampton, M. W., W. A. Pryor, et al. (1999). "Ozone exposure increases aldehydes in epithelial lining fluid in human lung." Am J Respir Crit Care Med **159**(4 Pt 1): 1134-7.
Franzen, B., S. Linder, et al. (1996). "Analysis of polypeptide expression in benign and malignant human breast lesions: down-regulation of cytokeratins." Br J Cancer **74**(10): 1632-8.
Frickel, E. M., R. Riek, et al. (2002). "TROSY-NMR reveals interaction between ERp57 and the tip of the calreticulin P-domain." Proc Natl Acad Sci U S A **99**(4): 1954-9.
Futagami, S., T. Hamamoto, et al. (2010). "Celecoxib inhibits CD133-positive cell migration via reduction of CCR2 in Helicobacter pylori-infected Mongolian gerbils." Digestion **81**(3): 193-203.
Gardai, S. J., K. A. McPhillips, et al. (2005). "Cell-surface calreticulin initiates clearance of viable or apoptotic cells through trans-activation of LRP on the phagocyte." Cell **123**(2): 321-34.
Gardai, S. J., Y. Q. Xiao, et al. (2003). "By binding SIRPalpha or calreticulin/CD91, lung collectins act as dual function surveillance molecules to suppress or enhance inflammation." Cell **115**(1): 13-23.
Geick, A., P. Redecker, et al. (2001). "Uteroglobin promoter-targeted c-MYC expression in transgenic mice cause hyperplasia of Clara cells and malignant transformation of T-lymphoblasts and tubular epithelial cells." Transgenic Res **10**(6): 501-11.
Gelebart, P., M. Opas, et al. (2005). "Calreticulin, a Ca2+-binding chaperone of the endoplasmic reticulum." Int J Biochem Cell Biol **37**(2): 260-6.
Gething, M. J. (1999). "Role and regulation of the ER chaperone BiP." Semin Cell Dev Biol **10**(5): 465-72.
Ghiran, I., L. B. Klickstein, et al. (2003). "Calreticulin is at the surface of circulating neutrophils and uses CD59 as an adaptor molecule." J Biol Chem **278**(23): 21024-31.
Giangreco, A., S. D. Reynolds, et al. (2002). "Terminal bronchioles harbor a unique airway stem cell population that localizes to the bronchoalveolar duct junction." Am J Pathol **161**(1): 173-82.
Ginsberg, M. S. (2005). "Epidemiology of lung cancer." Semin Roentgenol **40**(2): 83-9.
Glasser, S. W., T. R. Korfhagen, et al. (1991). "Genetic element from human surfactant protein SP-C gene confers bronchiolar-alveolar cell specificity in transgenic mice." Am J Physiol **261**(4 Pt 1): L349-56.
Goicoechea, S., A. W. Orr, et al. (2000). "Thrombospondin mediates focal adhesion disassembly through interactions with cell surface calreticulin." J Biol Chem **275**(46): 36358-68.

Goicoechea, S., M. A. Pallero, et al. (2002). "The anti-adhesive activity of thrombospondin is mediated by the N-terminal domain of cell surface calreticulin." J Biol Chem **277**(40): 37219-28.
Gold, L. I., M. Rahman, et al. (2006). "Overview of the role for calreticulin in the enhancement of wound healing through multiple biological effects." J Investig Dermatol Symp Proc **11**(1): 57-65.
Goldberg, R. M., H. I. Hurwitz, et al. (2005). "Angiogenesis inhibition in the treatment of colorectal cancer Part 3 of a 3-part series: targeting VEGF--current and future research directions." Clin Adv Hematol Oncol **3**(12): 1-10; quiz 11.
Goldman, E. (1907). "The growth of malignant disease in man and the lower animals with special reference to the vascular system." Lancet **2**: 236-1240.
Goldman, R., L. Enewold, et al. (2001). "Smoking increases carcinogenic polycyclic aromatic hydrocarbons in human lung tissue." Cancer Res **61**(17): 6367-71.
Gomperts, B. N., J. A. Belperio, et al. (2006). "Circulating progenitor epithelial cells traffic via CXCR4/CXCL12 in response to airway injury." J Immunol **176**(3): 1916-27.
Gory, S., M. Vernet, et al. (1999). "The vascular endothelial-cadherin promoter directs endothelial-specific expression in transgenic mice." Blood **93**(1): 184-92.
Gotzmann, J., M. Mikula, et al. (2004). "Molecular aspects of epithelial cell plasticity: implications for local tumor invasion and metastasis." Mutat Res **566**(1): 9-20.
Greenblatt, M. S., W. P. Bennett, et al. (1994). "Mutations in the p53 tumor suppressor gene: clues to cancer etiology and molecular pathogenesis." Cancer Res **54**(18): 4855-78.
Greenwood, J. A., M. A. Pallero, et al. (1998). "Thrombospondin signaling of focal adhesion disassembly requires activation of phosphoinositide 3-kinase." J Biol Chem **273**(3): 1755-63.
Grunewald, M., I. Avraham, et al. (2006). "VEGF-induced adult neovascularization: recruitment, retention, and role of accessory cells." Cell **124**(1): 175-89.
Gu, H., Y. R. Zou, et al. (1993). "Independent control of immunoglobulin switch recombination at individual switch regions evidenced through Cre-loxP-mediated gene targeting." Cell **73**(6): 1155-64.
Guo, L., J. Groenendyk, et al. (2003). "Identification of an N-domain histidine essential for chaperone function in calreticulin." J Biol Chem **278**(50): 50645-53.
Haematology., I. C. f. S. i. (1993). "Procedures for the classification of acute leukaemias." Leukemia and Lymphoma. **11:37.**
Hanahan, D. and J. Folkman (1996). "Patterns and emerging mechanisms of the angiogenic switch during tumorigenesis." Cell **86**(3): 353-64.
Hangai, M., Y. S. Moon, et al. (2001). "Systemically expressed soluble Tie2 inhibits intraocular neovascularization." Hum Gene Ther **12**(10): 1311-21.
Hann, C. L. and C. M. Rudin (2008). "Management of small-cell lung cancer: incremental changes but hope for the future." Oncology (Williston Park) **22**(13): 1486-92.
Harper, J. W., G. R. Adami, et al. (1993). "The p21 Cdk-interacting protein Cip1 is a potent inhibitor of G1 cyclin-dependent kinases." Cell **75**(4): 805-16.

Harris, M. R., Y. Y. Yu, et al. (1998). "Calreticulin and calnexin interact with different protein and glycan determinants during the assembly of MHC class I." J Immunol **160**(11): 5404-9.
Haupt, Y., R. Maya, et al. (1997). "Mdm2 promotes the rapid degradation of p53." Nature **387**(6630): 296-9.
Hawinkels, L. J., K. Zuidwijk, et al. (2008). "VEGF release by MMP-9 mediated heparan sulphate cleavage induces colorectal cancer angiogenesis." Eur J Cancer **44**(13): 1904-13.
Hayashi, E., Y. Kuramitsu, et al. (2005). "Proteomic profiling for cancer progression: Differential display analysis for the expression of intracellular proteins between regressive and progressive cancer cell lines." Proteomics **5**(4): 1024-32.
Hayashida, Y., Y. Urata, et al. (2006). "Calreticulin represses E-cadherin gene expression in MDCK cells via slug." J Biol Chem.
Haylock, D. N. and S. K. Nilsson (2005). "Stem cell regulation by the hematopoietic stem cell niche." Cell Cycle **4**(10): 1353-5.
Heissig, B., et al. (2002). "Recruitment of stem and progenitor cells from the bone marrow niche requires MMP-9 mediated release of kit-ligand." Cell **109**: 625–637.
Hemenway, C. S. and J. Heitman (1999). "Calcineurin. Structure, function, and inhibition." Cell Biochem Biophys **30**(1): 115-51.
Hemmati, H. D., I. Nakano, et al. (2003). "Cancerous stem cells can arise from pediatric brain tumors." Proc Natl Acad Sci U S A **100**(25): 15178-83.
Heppner, G. H. (1984). "Tumor heterogeneity." Cancer Res **44**(6): 2259-65.
Herzog, E. L., J. Van Arnam, et al. (2007). "Lung-specific nuclear reprogramming is accompanied by heterokaryon formation and Y chromosome loss following bone marrow transplantation and secondary inflammation." Faseb J **21**(10): 2592-601.
Hong, S. H., D. E. Misek, et al. (2004). "An autoantibody-mediated immune response to calreticulin isoforms in pancreatic cancer." Cancer Res **64**(15): 5504-10.
Horowitz, D., J. F. Callahan, et al. (2002). "Inhibition of hematopoietic progenitor cell growth by Tyr-MIF, an endogenous opiate modulator, and its degradation products." Int Immunopharmacol **2**(5): 721-30.
Hotz, B., A. Visekruna, et al. (2009). "Beyond Epithelial to Mesenchymal Transition: A Novel Role for the Transcription Factor Snail in Inflammation and Wound Healing." J Gastrointest Surg.
Houghton, J., C. Stoicov, et al. (2004). "Gastric cancer originating from bone marrow-derived cells." Science **306**(5701): 1568-71.
Hsu, W. M., F. J. Hsieh, et al. (2005). "Calreticulin expression in neuroblastoma--a novel independent prognostic factor." Ann Oncol **16**(2): 314-321.
Huber, M. A., N. Kraut, et al. (2005). "Molecular requirements for epithelial-mesenchymal transition during tumor progression." Curr Opin Cell Biol **17**(5): 548-58.
Huber, R. M. (2007). "Is lung cancer in never-smokers a different disease?--Back to the figures." J Thorac Oncol **2**(9): 787-8.
Hudson, J. D., M. A. Shoaibi, et al. (1999). "A proinflammatory cytokine inhibits p53 tumor suppressor activity." J Exp Med **190**(10): 1375-82.

Humphries, J. D., P. Wang, et al. (2007). "Vinculin controls focal adhesion formation by direct interactions with talin and actin." J Cell Biol **179**(5): 1043-57.
Ihara, Y., Y. Urata, et al. (2006). "Role of calreticulin in the sensitivity of myocardiac H9c2 cells to oxidative stress caused by hydrogen peroxide." Am J Physiol Cell Physiol **290**(1): C208-21.
Imrich, A., Y. Ning, et al. (2007). "Alveolar macrophage cytokine response to air pollution particles: oxidant mechanisms." Toxicol Appl Pharmacol **218**(3): 256-64.
Inoue, M., J. H. Hager, et al. (2002). "VEGF-A has a critical, nonredundant role in angiogenic switching and pancreatic beta cell carcinogenesis." Cancer Cell **1**(2): 193-202.
Inoue, T., M. Sata, et al. (2007). "Mobilization of CD34-positive bone marrow-derived cells after coronary stent implantation: impact on restenosis." Circulation **115**(5): 553-61.
Ishizawa, K., H. Kubo, et al. (2004). "Bone marrow-derived cells contribute to lung regeneration after elastase-induced pulmonary emphysema." FEBS Lett **556**(1-3): 249-52.
Iwama, A., I. Hamaguchi, et al. (1993). "Molecular cloning and characterization of mouse TIE and TEK receptor tyrosine kinase genes and their expression in hematopoietic stem cells." Biochem Biophys Res Commun **195**(1): 301-9.
Iwanaga, K., Y. Yang, et al. (2008). "Pten inactivation accelerates oncogenic K-ras-initiated tumorigenesis in a mouse model of lung cancer." Cancer Res **68**(4): 1119-27.
Jabbur, J. R., A. D. Tabor, et al. (2002). "Mdm-2 binding and TAF(II)31 recruitment is regulated by hydrogen bond disruption between the p53 residues Thr18 and Asp21." Oncogene **21**(46): 7100-13.
Jackson, E. L., N. Willis, et al. (2001). "Analysis of lung tumor initiation and progression using conditional expression of oncogenic K-ras." Genes Dev. **15**(24): 3243-3248.
Jalali, S., M. Aghasi, et al. (2008). "Calreticulin regulates insulin receptor expression and its downstream PI3 Kinase/Akt signalling pathway." Biochim Biophys Acta **1783**(12): 2344-51.
Jang, Y. Y., M. I. Collector, et al. (2004). "Hematopoietic stem cells convert into liver cells within days without fusion." Nat Cell Biol **6**(6): 532-9.
Janin, A., H. Murata, et al. (2009). "Donor-derived oral squamous cell carcinoma after allogeneic bone marrow transplantation." Blood **113**(8): 1834-40.
Jazii, F. R., Z. Najafi, et al. (2006). "Identification of squamous cell carcinoma associated proteins by proteomics and loss of beta tropomyosin expression in esophageal cancer." World J Gastroenterol **12**(44): 7104-12.
Jemal, A., R. Siegel, et al. (2009). "Cancer statistics, 2009." CA Cancer J Clin **59**(4): 225-49.
Jin, D. K., K. Shido, et al. (2006). "Cytokine-mediated deployment of SDF-1 induces revascularization through recruitment of CXCR4+ hemangiocytes." Nat Med **12**(5): 557-67.
Johnson, R. J., N. Liu, et al. (1998). "Increased calreticulin stability in differentiated NG-108-15 cells correlates with resistance to apoptosis induced by antisense treatment." Brain Res Mol Brain Res **53**(1-2): 104-11.

Johnson, S., M. Michalak, et al. (2001). "The ins and outs of calreticulin: from the ER lumen to the extracellular space." Trends Cell Biol **11**(3): 122-9.
Jones, N., K. Iljin, et al. (2001). "Tie receptors: new modulators of angiogenic and lymphangiogenic responses." Nat Rev Mol Cell Biol **2**(4): 257-67.
Jones, N., D. Voskas, et al. (2001). "Rescue of the early vascular defects in Tek/Tie2 null mice reveals an essential survival function." EMBO Rep **2**(5): 438-45.
Jordan, C. T. (2004). "Cancer stem cell biology: from leukemia to solid tumors." Curr Opin Cell Biol **16**(6): 708-12.
Jung, K. W., Y. J. Won, et al. (2009). "Cancer statistics in Korea: incidence, mortality and survival in 2005." J Korean Med Sci **24**(6): 995-1003.
Kageyama, K., Y. Ihara, et al. (2002). "Overexpression of calreticulin modulates protein kinase B/Akt signaling to promote apoptosis during cardiac differentiation of cardiomyoblast H9c2 cells." J Biol Chem **277**(22): 19255-64.
Kageyama, S., T. Isono, et al. (2004). "Identification by proteomic analysis of calreticulin as a marker for bladder cancer and evaluation of the diagnostic accuracy of its detection in urine." Clin Chem **50**(5): 857-66.
Kageyama, S., T. Isono, et al. (2009). "Urinary calreticulin in the diagnosis of bladder urothelial carcinoma." Int J Urol **16**(5): 481-6.
Kajstura, J., M. Rota, et al. (2005). "Bone marrow cells differentiate in cardiac cell lineages after infarction independently of cell fusion." Circ Res **96**(1): 127-37.
Kalemkerian, G. P. (2008). "Progress and pitfalls in small-cell lung cancer." Oncology (Williston Park) **22**(13): 1498-500, 1506.
Kalemkerian, G. P., W. Akerley, et al. (2008). "Small cell lung cancer." J Natl Compr Canc Netw **6**(3): 294-314.
Kandioler-Eckersberger, D., S. Kappel, et al. (1999). "The TP53 genotype but not immunohistochemical result is predictive of response to cisplatin-based neoadjuvant therapy in stage III non-small cell lung cancer." J Thorac Cardiovasc Surg **117**(4): 744-50.
Kapoor, M., L. Ellgaard, et al. (2004). "Mutational analysis provides molecular insight into the carbohydrate-binding region of calreticulin: pivotal roles of tyrosine-109 and aspartate-135 in carbohydrate recognition." Biochemistry **43**(1): 97-106.
Kastan, M. B., O. Onyekwere, et al. (1991). "Participation of p53 protein in the cellular response to DNA damage." Cancer Res **51**(23 Pt 1): 6304-11.
Katayama, Y., A. Hidalgo, et al. (2003). "PSGL-1 participates in E-selectin-mediated progenitor homing to bone marrow: evidence for cooperation between E-selectin ligands and alpha4 integrin." Blood **102**(6): 2060-7.
Kerr, J. F., A. H. Wyllie, et al. (1972). "Apoptosis: a basic biological phenomenon with wide-ranging implications in tissue kinetics." Br J Cancer **26**(4): 239-57.
Khalil, N., C. Whitman, et al. (1993). "Regulation of alveolar macrophage transforming growth factor-beta secretion by corticosteroids in bleomycin-induced pulmonary inflammation in the rat." J Clin Invest **92**(4): 1812-8.
Kiel, M. J., O. H. Yilmaz, et al. (2005). "SLAM family receptors distinguish hematopoietic stem and progenitor cells and reveal endothelial niches for stem cells." Cell **121**(7): 1109-21.
Kim, C. F. B., E. L. Jackson, et al. (2005). "Identification of Bronchioalveolar Stem Cells in Normal Lung and Lung Cancer." Cell **121**(6): 823-835.

Kim, H. S., J. W. Kim, et al. (2006). "The farnesyltransferase inhibitor, LB42708, inhibits growth and induces apoptosis irreversibly in H-ras and K-ras-transformed rat intestinal epithelial cells." Toxicol Appl Pharmacol **215**(3): 317-29.
Kim, I., H. G. Kim, et al. (2000). "Angiopoietin-1 regulates endothelial cell survival through the phosphatidylinositol 3'-Kinase/Akt signal transduction pathway." Circ Res **86**(1): 24-9.
Kisanuki, Y. Y., R. E. Hammer, et al. (2001). "Tie2-Cre transgenic mice: a new model for endothelial cell-lineage analysis in vivo." Dev Biol **230**(2): 230-42.
Klebanoff, S. J. (1999). "Myeloperoxidase." Proc Assoc Am Physicians **111**(5): 383-9.
Klebanoff, S. J., A. M. Waltersdorph, et al. (1984). "Antimicrobial activity of myeloperoxidase." Methods Enzymol **105**: 399-403.
Klimenko, N. A. and E. A. Pavlova (1999). "[The role of leukocytes in the increased vessel permeability in inflammation]." Biull Eksp Biol Med **127**(8): 165-7.
Kopp, H. G., S. T. Avecilla, et al. (2005). "The bone marrow vascular niche: home of HSC differentiation and mobilization." Physiology (Bethesda) **20**: 349-56.
Kortesidis, A., A. Zannettino, et al. (2005). "Stromal-derived factor-1 promotes the growth, survival, and development of human bone marrow stromal stem cells." Blood **105**(10): 3793-801.
Kotton, D. N., B. Y. Ma, et al. (2001). "Bone marrow-derived cells as progenitors of lung alveolar epithelium." Development **128**(24): 5181-8.
Krause, D. S. (2008). "Bone marrow-derived cells and stem cells in lung repair." Proc Am Thorac Soc **5**(3): 323-7.
Krysan, K., J. M. Lee, et al. (2008). "Inflammation, epithelial to mesenchymal transition, and epidermal growth factor receptor tyrosine kinase inhibitor resistance." J Thorac Oncol **3**(2): 107-10.
Krysko, D. V., T. Vanden Berghe, et al. (2008). "Methods for distinguishing apoptotic from necrotic cells and measuring their clearance." Methods Enzymol **442**: 307-41.
Kucia, M., J. Ratajczak, et al. (2005). "Bone marrow as a source of circulating CXCR4+ tissue-committed stem cells." Biol Cell **97**(2): 133-46.
Kucia, M., R. Reca, et al. (2005). "Bone marrow as a home of heterogenous populations of nonhematopoietic stem cells." Leukemia **19**(7): 1118-27.
Kukk, E., U. Wartiovaara, et al. (1997). "Analysis of Tie receptor tyrosine kinase in haemopoietic progenitor and leukaemia cells." Br J Haematol **98**(1): 195-203.
Kuraishi, T., J. Manaka, et al. (2007). "Identification of calreticulin as a marker for phagocytosis of apoptotic cells in Drosophila." Exp Cell Res **313**(3): 500-10.
Kyd, J. M., A. R. Foxwell, et al. (2001). "Mucosal immunity in the lung and upper airway." Vaccine **19**(17-19): 2527-33.
Lagasse, E., H. Connors, et al. (2000). "Purified hematopoietic stem cells can differentiate into hepatocytes in vivo." Nat Med **6**(11): 1229-34.
Lam, W. K., N. W. White, et al. (2004). "Lung cancer epidemiology and risk factors in Asia and Africa." Int J Tuberc Lung Dis **8**(9): 1045-57.
Lapidot, T., A. Dar, et al. (2005). "How do stem cells find their way home?" Blood **106**(6): 1901-10.
Lauber, K., E. Bohn, et al. (2003). "Apoptotic cells induce migration of phagocytes via caspase-3-mediated release of a lipid attraction signal." Cell **113**(6): 717-30.

Leach, M. R. and D. B. Williams (2004). "Lectin-deficient calnexin is capable of binding class I histocompatibility molecules in vivo and preventing their degradation." J Biol Chem **279**(10): 9072-9.
Lee, G., T. C. Walser, et al. (2009). "Chronic inflammation, chronic obstructive pulmonary disease, and lung cancer." Curr Opin Pulm Med.
Leung-Hagesteijn, C. Y., K. Milankov, et al. (1994). "Cell attachment to extracellular matrix substrates is inhibited upon downregulation of expression of calreticulin, an intracellular integrin alpha-subunit-binding protein." J Cell Sci **107 (Pt 3)**: 589-600.
Lewandoski, M. (2001). "Conditional control of gene expression in the mouse." Nat Rev Genet **2**(10): 743-55.
Li, L., Y. Z. Yuan, et al. (2006). "Treatment of pancreatic carcinoma by adenoviral mediated gene transfer of vasostatin in mice." Gut **55**(2): 259-65.
Li, W., S. A. Johnson, et al. (2004). "Hematopoietic stem cell repopulating ability can be maintained in vitro by some primary endothelial cells." Exp Hematol **32**(12): 1226-37.
Lim, S., W. Chang, et al. (2008). "Enhanced calreticulin expression promotes calcium-dependent apoptosis in postnatal cardiomyocytes." Mol Cells **25**(3): 390-6.
Lin, P., J. A. Buxton, et al. (1998). "Antiangiogenic gene therapy targeting the endothelium-specific receptor tyrosine kinase Tie2." Proc Natl Acad Sci U S A **95**(15): 8829-34.
Lin, P., P. Polverini, et al. (1997). "Inhibition of tumor angiogenesis using a soluble receptor establishes a role for Tie2 in pathologic vascular growth." J Clin Invest **100**(8): 2072-8.
Linnoila, R. I., B. Zhao, et al. (2000). "Constitutive achaete-scute homologue-1 promotes airway dysplasia and lung neuroendocrine tumors in transgenic mice." Cancer Res **60**(15): 4005-9.
Lipskaia, L. and A. M. Lompre (2004). "Alteration in temporal kinetics of Ca2+ signaling and control of growth and proliferation." Biol Cell **96**(1): 55-68.
Little, C. D., M. M. Nau, et al. (1983). "Amplification and expression of the c-myc oncogene in human lung cancer cell lines." Nature **306**(5939): 194-6.
Liu, C., Z. Chen, et al. (2006). "Multiple tumor types may originate from bone marrow-derived cells." Neoplasia **8**(9): 716-24.
Liu, M., H. Imam, et al. (2005). "Gene transfer of vasostatin, a calreticulin fragment, into neuroendocrine tumor cells results in enhanced malignant behavior." Neuroendocrinology **82**(1): 1-10.
Liu, X., X. Wu, et al. (2008). "Calreticulin downregulation is associated with FGF-2-induced angiogenesis through calcineurin pathway in ischemic myocardium." Shock **29**(1): 140-8.
Lodish, H. F. and N. Kong (1990). "Perturbation of cellular calcium blocks exit of secretory proteins from the rough endoplasmic reticulum." J Biol Chem **265**(19): 10893-9.
Loges, S., G. Heil, et al. (2005). "Analysis of concerted expression of angiogenic growth factors in acute myeloid leukemia: expression of angiopoietin-2 represents an independent prognostic factor for overall survival." J Clin Oncol **23**(6): 1109-17.

Lu, H., W. Ouyang, et al. (2006). "Inflammation, a key event in cancer development." Mol Cancer Res **4**(4): 221-33.
MacPherson, H., P. A. Keir, et al. (2006). "Following damage, the majority of bone marrow-derived airway cells express an epithelial marker." Respir Res **7**: 145.
Magdaleno, S. M., G. Wang, et al. (1997). "Cyclin-dependent kinase inhibitor expression in pulmonary Clara cells transformed with SV40 large T antigen in transgenic mice." Cell Growth Differ **8**(2): 145-55.
Maggio-Price, L., P. Treuting, et al. (2006). "Helicobacter infection is required for inflammation and colon cancer in SMAD3-deficient mice." Cancer Res **66**(2): 828-38.
Maisonpierre, P. C., C. Suri, et al. (1997). "Angiopoietin-2, a natural antagonist for Tie2 that disrupts in vivo angiogenesis." Science **277**(5322): 55-60.
Maita, K., M. Hirano, et al. (1988). "Mortality, major cause of moribundity, and spontaneous tumors in CD-1 mice." Toxicol Pathol **16**(3): 340-9.
Malkinson, A. M. (2004). "Evidence that inflammation encourages pulmonary adenocarcinoma formation in mice: clinical implications." Chest **125**(5 Suppl): 154S-5S.
Malkinson, A. M. (2005). "Role of inflammation in mouse lung tumorigenesis: a review." Exp Lung Res **31**(1): 57-82.
Malumbres, M. and M. Barbacid (2003). "RAS oncogenes: the first 30 years." Nat Rev Cancer **3**(6): 459-65.
Mamaeva, O. A., J. Kim, et al. (2009). "Calcium/calmodulin-dependent kinase II regulates notch-1 signaling in prostate cancer cells." J Cell Biochem **106**(1): 25-32.
Manenti, G., F. Galbiati, et al. (2003). "Outbred CD-1 mice carry the susceptibility allele at the pulmonary adenoma susceptibility 1 (Pas1) locus." Carcinogenesis **24**(6): 1143-1148.
Mani, S. A., W. Guo, et al. (2008). "The epithelial-mesenchymal transition generates cells with properties of stem cells." Cell **133**(4): 704-15.
Manzer, R., C. A. Dinarello, et al. (2008). "Ozone Exposure of Macrophages Induces an Alveolar Epithelial Chemokine Response through IL-1{alpha}." Am. J. Respir. Cell Mol. Biol. **38**(3): 318-323.
Mao, W., S. Fukuoka, et al. (2007). "Cardiomyocyte apoptosis in autoimmune cardiomyopathy: mediated via endoplasmic reticulum stress and exaggerated by norepinephrine
10.1152/ajpheart.01377.2006." Am J Physiol Heart Circ Physiol **293**(3): H1636-1645.
Marsden, V. S., L. O'Connor, et al. (2002). "Apoptosis initiated by Bcl-2-regulated caspase activation independently of the cytochrome c/Apaf-1/caspase-9 apoptosome." Nature **419**(6907): 634-7.
Martin, V., J. Groenendyk, et al. (2006). "Identification by mutational analysis of amino acid residues essential in the chaperone function of calreticulin." J Biol Chem **281**(4): 2338-46.
Marx, J. (1994). "A challenge to p16 gene as a major tumor suppressor." Science **264**(5167): 1846.
Mason, R. J. (2006). "Biology of alveolar type II cells." Respirology **11 Suppl**: S12-5.
Mason, R. J., M. Kalina, et al. (2000). "Surfactant protein C expression in urethane-induced murine pulmonary tumors." Am J Pathol **156**(1): 175-82.

Matsuzoe, D., T. Hideshima, et al. (1999). "p53 mutations predict non-small cell lung carcinoma response to radiotherapy." Cancer Lett **135**(2): 189-94.
Mayack, S. R. and A. J. Wagers (2008). "Osteolineage niche cells initiate hematopoietic stem cell mobilization." Blood **112**(3): 519-31.
McDonnell, J. M., G. E. Jones, et al. (1996). "Calreticulin binding affinity for glycosylated laminin." J Biol Chem **271**(14): 7891-4.
McGreal, E. and P. Gasque (2002). "Structure-function studies of the receptors for complement C1q." Biochem Soc Trans **30**(Pt 6): 1010-4.
McIntosh, J. C., A. H. Swyers, et al. (1996). "Surfactant proteins A and D increase in response to intratracheal lipopolysaccharide." Am J Respir Cell Mol Biol **15**(4): 509-19.
McKeown, D. J., D. J. Brown, et al. (2004). "The relationship between circulating concentrations of C-reactive protein, inflammatory cytokines and cytokine receptors in patients with non-small-cell lung cancer." Br J Cancer **91**(12): 1993-5.
Mery, L., N. Mesaeli, et al. (1996). "Overexpression of calreticulin increases intracellular Ca2+ storage and decreases store-operated Ca2+ influx." J Biol Chem **271**(16): 9332-9.
Mesaeli, N., K. Nakamura, et al. (1999). "Calreticulin is essential for cardiac development." J Cell Biol **144**(5): 857-68.
Mesaeli, N. and C. Phillipson (2004). "Impaired p53 expression, function, and nuclear localization in calreticulin-deficient cells." Mol Biol Cell **15**(4): 1862-70.
Meuwissen, R. and A. Berns (2005). "Mouse models for human lung cancer." Genes Dev. **19**(6): 643-664.
Meuwissen, R., S. C. Linn, et al. (2001). "Mouse model for lung tumorigenesis through Cre/lox controlled sporadic activation of the K-Ras oncogene." Oncogene **20**(45): 6551-8.
Mezey, E., S. Key, et al. (2003). "Transplanted bone marrow generates new neurons in human brains." Proc Natl Acad Sci U S A **100**: 1364-9.
Michalak, M., E. F. Corbett, et al. (1999). "Calreticulin: one protein, one gene, many functions." Biochem J **344 Pt 2**: 281-92.
Michalak, M., J. M. Robert Parker, et al. (2002). "Ca2+ signaling and calcium binding chaperones of the endoplasmic reticulum." Cell Calcium **32**(5-6): 269-78.
Migaldi, M., E. Zunarelli, et al. (1996). "The changing histopathology of primitive lung cancer." Pathologica **88**(4): 297-302.
Milner, R. E., S. Baksh, et al. (1991). "Calreticulin, and not calsequestrin, is the major calcium binding protein of smooth muscle sarcoplasmic reticulum and liver endoplasmic reticulum." J Biol Chem **266**(11): 7155-65.
Minami, K., Y. Saito, et al. (2002). "Prognostic significance of p53, Ki-67, VEGF and Glut-1 in resected stage I adenocarcinoma of the lung." Lung Cancer **38**(1): 51-7.
Mitsudomi, T., S. M. Steinberg, et al. (1991). "ras gene mutations in non-small cell lung cancers are associated with shortened survival irrespective of treatment intent." Cancer Res **51**(18): 4999-5002.
Morel, A. P., M. Lievre, et al. (2008). "Generation of breast cancer stem cells through epithelial-mesenchymal transition." PLoS One **3**(8): e2888.

Morimoto, K., H. Amano, et al. (2001). "Alveolar Macrophages that Phagocytose Apoptotic Neutrophils Produce Hepatocyte Growth Factor during Bacterial Pneumonia in Mice." Am. J. Respir. Cell Mol. Biol. **24**(5): 608-615.
Morkin, E. (2000). "Control of cardiac myosin heavy chain gene expression." Microsc Res Tech **50**(6): 522-31.
Mountain, C. F. (1997). "Revisions in the International System for Staging Lung Cancer." Chest **111**(6): 1710-7.
Mountain, C. F. and K. E. Hermes (2003). "Surgical treatment of lung cancer. Past and present." Methods Mol Med **75**: 453-87.
Muguruma, Y., T. Yahata, et al. (2006). "Reconstitution of the functional human hematopoietic microenvironment derived from human mesenchymal stem cells in the murine bone marrow compartment." Blood **107**(5): 1878-87.
Muller, A., K. Lange, et al. (2002). "Expression of angiopoietin-1 and its receptor TEK in hematopoietic cells from patients with myeloid leukemia." Leuk Res **26**(2): 163-8.
Mullin, J. M., K. V. Laughlin, et al. (2000). "Increased tight junction permeability can result from protein kinase C activation/translocation and act as a tumor promotional event in epithelial cancers." Ann N Y Acad Sci **915**: 231-6.
Murry, C. E., M. H. Soonpaa, et al. (2004). "Haematopoietic stem cells do not transdifferentiate into cardiac myocytes in myocardial infarcts." Nature **428**(6983): 664-8.
Muscat, J. E. and E. L. Wynder (1995). "Lung cancer pathology in smokers, ex-smokers and never smokers." Cancer Lett **88**(1): 1-5.
Nagamachi, Y., M. Tani, et al. (1998). "Orthotopic growth and metastasis of human non-small cell lung carcinoma cell injected into the pleural cavity of nude mice." Cancer Lett **127**(1-2): 203-9.
Nakamura, K., E. Bossy-Wetzel, et al. (2000). "Changes in endoplasmic reticulum luminal environment affect cell sensitivity to apoptosis." J Cell Biol **150**(4): 731-40.
Nakamura, K., M. Robertson, et al. (2001). "Complete heart block and sudden death in mice overexpressing calreticulin." J Clin Invest **107**(10): 1245-53.
Nakamura, K., A. Zuppini, et al. (2001). "Functional specialization of calreticulin domains." J Cell Biol **154**(5): 961-72.
Nau, M. M., B. J. Brooks, et al. (1985). "L-myc, a new myc-related gene amplified and expressed in human small cell lung cancer." Nature **318**(6041): 69-73.
Naugler, W. E. and M. Karin (2008). "NF-kappaB and cancer-identifying targets and mechanisms." Curr Opin Genet Dev **18**(1): 19-26.
Nauseef, W. M., S. J. McCormick, et al. (1995). "Calreticulin functions as a molecular chaperone in the biosynthesis of myeloperoxidase." J Biol Chem **270**(9): 4741-7.
Nauseef, W. M., S. J. McCormick, et al. (1998). "Coordinated participation of calreticulin and calnexin in the biosynthesis of myeloperoxidase." J Biol Chem **273**(12): 7107-11.
Neal, J. W. and N. A. Clipstone (2003). "A constitutively active NFATc1 mutant induces a transformed phenotype in 3T3-L1 fibroblasts." J Biol Chem **278**(19): 17246-54.

Neiva, K., Y. X. Sun, et al. (2005). "The role of osteoblasts in regulating hematopoietic stem cell activity and tumor metastasis." Braz J Med Biol Res **38**(10): 1449-54.
Nettesheim, P. and A. S. Hammons (1971). "Induction of squamous cell carcinoma in the respiratory tract of mice." J Natl Cancer Inst **47**(3): 697-701.
Nicchitta, C. V. (1998). "Biochemical, cell biological and immunological issues surrounding the endoplasmic reticulum chaperone GRP94/gp96." Curr Opin Immunol **10**(1): 103-9.
Nishio, M., T. Koshikawa, et al. (1996). "Prognostic significance of abnormal p53 accumulation in primary, resected non-small-cell lung cancers." J Clin Oncol **14**(2): 497-502.
Noorman, F., E. A. Braat, et al. (1997). "Monoclonal antibodies against the human mannose receptor as a specific marker in flow cytometry and immunohistochemistry for macrophages." J Leukoc Biol **61**(1): 63-72.
Nygren, J. M., S. Jovinge, et al. (2004). "Bone marrow-derived hematopoietic cells generate cardiomyocytes at a low frequency through cell fusion, but not transdifferentiation." Nat Med **10**(5): 494-501.
Obeid, M., T. Panaretakis, et al. (2007). "Calreticulin exposure is required for the immunogenicity of gamma-irradiation and UVC light-induced apoptosis." Cell Death Differ **14**(10): 1848-50.
Obeid, M., A. Tesniere, et al. (2007). "Calreticulin exposure dictates the immunogenicity of cancer cell death." Nat Med **13**(1): 54-61.
Ogden, C. A., A. deCathelineau, et al. (2001). "C1q and mannose binding lectin engagement of cell surface calreticulin and CD91 initiates macropinocytosis and uptake of apoptotic cells." J Exp Med **194**(6): 781-95.
Ohsaki, Y., S. Tanno, et al. (2000). "Epidermal growth factor receptor expression correlates with poor prognosis in non-small cell lung cancer patients with p53 overexpression." Oncol Rep **7**(3): 603-7.
Okunaga, T., Y. Urata, et al. (2006). "Calreticulin, a Molecular Chaperone in the Endoplasmic Reticulum, Modulates Radiosensitivity of Human Glioblastoma U251MG Cells." Cancer Res **66**(17): 8662-71.
Oliver, J. D., H. L. Roderick, et al. (1999). "ERp57 functions as a subunit of specific complexes formed with the ER lectins calreticulin and calnexin." Mol Biol Cell **10**(8): 2573-82.
Omer, C. A. and N. E. Kohl (1997). "CA1A2X-competitive inhibitors of farnesyltransferase as anti-cancer agents." Trends Pharmacol Sci **18**(11): 437-44.
Opas, M., M. Szewczenko-Pawlikowski, et al. (1996). "Calreticulin modulates cell adhesiveness via regulation of vinculin expression." J Cell Biol **135**(6 Pt 2): 1913-23.
Orazi, A., M. Kahsai, et al. (1996). "p53 overexpression in myeloid leukemic disorders is associated with increased apoptosis of hematopoietic marrow cells and ineffective hematopoiesis." Mod Pathol **9**(1): 48-52.
Orlic, D., J. Kajstura, et al. (2001). "Bone marrow cells regenerate infarcted myocardium." Nature **410**(6829): 701-5.

Orr, A. W., C. A. Elzie, et al. (2003). "Thrombospondin signaling through the calreticulin/LDL receptor-related protein co-complex stimulates random and directed cell migration." J Cell Sci **116**(Pt 14): 2917-27.
Orr, A. W., C. E. Pedraza, et al. (2003). "Low density lipoprotein receptor-related protein is a calreticulin coreceptor that signals focal adhesion disassembly." J Cell Biol **161**(6): 1179-89.
Orrenius, S., B. Zhivotovsky, et al. (2003). "Regulation of cell death: the calcium-apoptosis link." Nat Rev Mol Cell Biol **4**(7): 552-65.
Ostwald, T. J. and D. H. MacLennan (1974). "Isolation of a high affinity calcium-binding protein from sarcoplasmic reticulum." J Biol Chem **249**(3): 974-9.
Otto, W. R. (2002). "Lung epithelial stem cells." J. Pathol **197**: 527–535.
Owonikoko, T. and S. Ramalingam (2008). "Minimal progress, potential promise in small-cell lung cancer." Oncology (Williston Park) **22**(13): 1495-6.
Oyadomari, S., K. Takeda, et al. (2001). "Nitric oxide-induced apoptosis in pancreatic beta cells is mediated by the endoplasmic reticulum stress pathway." Proc Natl Acad Sci U S A **98**(19): 10845-50.
Page, C., M. Huang, et al. (2000). "Elevated phosphorylation of AKT and Stat3 in prostate, breast, and cervical cancer cells." Int J Oncol **17**(1): 23-8.
Pallero, M. A., C. A. Elzie, et al. (2008). "Thrombospondin 1 binding to calreticulin-LRP1 signals resistance to anoikis." Faseb J.
Panaretakis, T., O. Kepp, et al. (2009). "Mechanisms of pre-apoptotic calreticulin exposure in immunogenic cell death." Embo J **28**(5): 578-90.
Panigrahi, A. R., S. E. Pinder, et al. (2004). "The role of PTEN and its signalling pathways, including AKT, in breast cancer; an assessment of relationships with other prognostic factors and with outcome." J Pathol **204**(1): 93-100.
Pao, W., V. A. Miller, et al. (2005). "Acquired resistance of lung adenocarcinomas to gefitinib or erlotinib is associated with a second mutation in the EGFR kinase domain." PLoS Med **2**(3): e73.
Papp, S., M. P. Fadel, et al. (2007). "Calreticulin affects fibronectin-based cell-substratum adhesion via the regulation of c-Src activity." J Biol Chem **282**(22): 16585-98.
Papp, S., E. Szabo, et al. (2008). "Kinase-dependent adhesion to fibronectin: regulation by calreticulin." Exp Cell Res **314**(6): 1313-26.
Parkin, D. M., F. Bray, et al. (2001). "Estimating the world cancer burden: Globocan 2000." Int J Cancer **94**(2): 153-6.
Parkin, D. M., F. Bray, et al. (2005). "Global cancer statistics, 2002." CA Cancer J Clin **55**(2): 74-108.
Parsonnet, J. (1997). "Molecular mechanisms for inflammation-promoted pathogenesis of cancer--The Sixteenth International Symposium of the Sapporo Cancer Seminar." Cancer Res **57**(16): 3620-4.
Partanen, J., E. Armstrong, et al. (1992). "A novel endothelial cell surface receptor tyrosine kinase with extracellular epidermal growth factor homology domains." Mol Cell Biol **12**(4): 1698-707.
Partanen, J., T. P. Makela, et al. (1990). "Putative tyrosine kinases expressed in K-562 human leukemia cells." Proc Natl Acad Sci U S A **87**(22): 8913-7.
Pattle, R. E. (1955). "Properties, function and origin of the lining layer." Nature **175**: 1125–1126.

Patz, E. F., Jr. (2000). "Imaging bronchogenic carcinoma." Chest **117**(4 Suppl 1): 90S-95S.
Pavelic, Z. P., H. K. Slocum, et al. (1980). "Growth of Cell Colonies in Soft Agar from Biopsies of Different Human Solid Tumors." Cancer Res **40**(11): 4151-4158.
Peled, A., V. Grabovsky, et al. (1999). "The chemokine SDF-1 stimulates integrin-mediated arrest of CD34(+) cells on vascular endothelium under shear flow." J Clin Invest **104**(9): 1199-211.
Pelham, H. R. (1988). "Evidence that luminal ER proteins are sorted from secreted proteins in a post-ER compartment." Embo J **7**(4): 913-8.
Perez-Moreno, M., W. Song, et al. (2008). "Loss of p120 catenin and links to mitotic alterations, inflammation, and skin cancer." Proc Natl Acad Sci U S A **105**(40): 15399-404.
Perkins, R. C., R. K. Scheule, et al. (1993). "Human alveolar macrophage cytokine release in response to in vitro and in vivo asbestos exposure." Exp Lung Res **19**(1): 55-65.
Peters, K. G., A. Coogan, et al. (1998). "Expression of Tie2/Tek in breast tumour vasculature provides a new marker for evaluation of tumour angiogenesis." Br J Cancer **77**(1): 51-6.
Petersen, B. E., W. C. Bowen, et al. (1999). "Bone marrow as a potential source of hepatic oval cells." Science **284**(5417): 1168-70.
Petit, I., M. Szyper-Kravitz, et al. (2002). "G-CSF induces stem cell mobilization by decreasing bone marrow SDF-1 and up-regulating CXCR4." Nat Immunol **3**(7): 687-94.
Pfister, D. G., D. H. Johnson, et al. (2004). "American Society of Clinical Oncology Treatment of Unresectable Non-Small-Cell Lung Cancer Guideline." J Clin Oncol **22**(2): 330-353.
Pike, S. E., L. Yao, et al. (1998). "Vasostatin, a calreticulin fragment, inhibits angiogenesis and suppresses tumor growth." J Exp Med **188**(12): 2349-56.
Pike, S. E., L. Yao, et al. (1999). "Calreticulin and calreticulin fragments are endothelial cell inhibitors that suppress tumor growth." Blood **94**(7): 2461-8.
Pisters, K. M., W. K. Evans, et al. (2007). "Cancer Care Ontario and American Society of Clinical Oncology adjuvant chemotherapy and adjuvant radiation therapy for stages I-IIIA resectable non small-cell lung cancer guideline." J Clin Oncol **25**(34): 5506-18.
Pizzi, C., L. Panico, et al. (2002). "p53 expression is decreased in primary breast carcinomas with microsatellite instability." Breast Cancer Res Treat **73**(3): 257-66.
Plopper, C. G., S. J. Nishio, et al. (1992). "The role of the nonciliated bronchiolar epithelial (Clara) cell as the progenitor cell during bronchiolar epithelial differentiation in the perinatal rabbit lung." Am J Respir Cell Mol Biol **7**(6): 606-13.
Ponti, D., A. Costa, et al. (2005). "Isolation and in vitro propagation of tumorigenic breast cancer cells with stem/progenitor cell properties." Cancer Res **65**(13): 5506-11.
Proescholdt, M. A., J. D. Heiss, et al. (1999). "Vascular endothelial growth factor (VEGF) modulates vascular permeability and inflammation in rat brain." J Neuropathol Exp Neurol **58**(6): 613-27.

Prophet, E., B. Mills, et al. (1994). "Laboratory Methods in Histotechnology."
Prudkin, L., D. D. Liu, et al. (2009). "Epithelial-to-mesenchymal transition in the development and progression of adenocarcinoma and squamous cell carcinoma of the lung." Mod Pathol **22**(5): 668-78.
Radisky, D. C., D. D. Levy, et al. (2005). "Rac1b and reactive oxygen species mediate MMP-3-induced EMT and genomic instability." Nature **436**(7047): 123-7.
Ramos, R. R., A. J. Swanson, et al. (2007). "Calreticulin and Hsp90 stabilize the human insulin receptor and promote its mobility in the endoplasmic reticulum." Proc Natl Acad Sci U S A **104**(25): 10470-5.
Rauch, F., J. Prud'homme, et al. (2000). "Heart, brain, and body wall defects in mice lacking calreticulin." Exp Cell Res **256**(1): 105-11.
Ray, M. K., S. W. Magdaleno, et al. (1995). "cis-acting elements involved in the regulation of mouse Clara cell-specific 10-kDa protein gene. In vitro and in vivo analysis." J Biol Chem **270**(6): 2689-94.
Ray, M. K., G. Wang, et al. (1996). "Immunohistochemical localization of mouse Clara cell 10-KD protein using antibodies raised against the recombinant protein." J Histochem Cytochem **44**(8): 919-27.
Raz, D. J., B. He, et al. (2006). "Bronchioloalveolar carcinoma: a review." Clin Lung Cancer **7**(5): 313-22.
Reddy, R., S. Buckley, et al. (2004). "Isolation of a putative progenitor subpopulation of alveolar epithelial type 2 cells." Am J Physiol Lung Cell Mol Physiol **286**(4): L658-67.
Rehm, S., D. E. Devor, et al. (1991). "Origin of spontaneous and transplacentally induced mouse lung tumors from alveolar type II cells." Exp Lung Res **17**(2): 181-95.
Reissmann, P. T., H. Koga, et al. (1999). "Amplification and overexpression of the cyclin D1 and epidermal growth factor receptor genes in non-small-cell lung cancer. Lung Cancer Study Group." J Cancer Res Clin Oncol **125**(2): 61-70.
Restrepo, C. I., Q. Dong, et al. (1999). "Surfactant protein D stimulates phagocytosis of Pseudomonas aeruginosa by alveolar macrophages." Am J Respir Cell Mol Biol **21**(5): 576-85.
Reynolds, P. R., M. G. Cosio, et al. (2006). "Cigarette smoke-induced Egr-1 upregulates proinflammatory cytokines in pulmonary epithelial cells." Am J Respir Cell Mol Biol **35**(3): 314-9.
Reynolds, S. D., A. Giangreco, et al. (2000). "Neuroepithelial Bodies of Pulmonary Airways Serve as a Reservoir of Progenitor Cells Capable of Epithelial Regeneration." Am J Pathol **156**(1): 269-278.
Ricci-Vitiani, L., D. G. Lombardi, et al. (2007). "Identification and expansion of human colon-cancer-initiating cells." Nature **445**(7123): 111-5.
Richardson, G. E. and B. E. Johnson (1993). "The biology of lung cancer." Semin Oncol **20**(2): 105-27.
Rojas, M., J. Xu, et al. (2005). "Bone marrow-derived mesenchymal stem cells in repair of the injured lung." Am J Respir Cell Mol Biol **33**(2): 145-52.
Rojiani, M. V., B. B. Finlay, et al. (1991). "In vitro interaction of a polypeptide homologous to human Ro/SS-A antigen (calreticulin) with a highly conserved amino acid sequence in the cytoplasmic domain of integrin alpha subunits." Biochemistry **30**(41): 9859-66.

Rosti, G., G. Bevilacqua, et al. (2006). "Small cell lung cancer." Ann Oncol **17**(suppl_2): ii5-10.
Rusch, V., D. Klimstra, et al. (1997). "Overexpression of the epidermal growth factor receptor and its ligand transforming growth factor alpha is frequent in resectable non-small cell lung cancer but does not predict tumor progression." Clin Cancer Res **3**(4): 515-22.
Saito, Y., Y. Ihara, et al. (1999). "Calreticulin functions in vitro as a molecular chaperone for both glycosylated and non-glycosylated proteins." Embo J **18**(23): 6718-29.
Salgia, R. and A. T. Skarin (1998). "Molecular abnormalities in lung cancer." J Clin Oncol **16**(3): 1207-17.
Sarvaiya, H. A., J. H. Yoon, et al. (2006). "Proteome profile of the MCF7 cancer cell line: a mass spectrometric evaluation." Rapid Commun Mass Spectrom **20**(20): 3039-55.
Sata, M., A. Saiura, et al. (2002). "Hematopoietic stem cells differentiate into vascular cells that participate in the pathogenesis of atherosclerosis." Nat Med **8**(4): 403-9.
Sato, K., H. Tomioka, et al. (2002). "Type II alveolar cells play roles in macrophage-mediated host innate resistance to pulmonary mycobacterial infections by producing proinflammatory cytokines." J Infect Dis **185**(8): 1139-47.
Sato, M., D. S. Shames, et al. (2007). "A translational view of the molecular pathogenesis of lung cancer." J Thorac Oncol **2**(4): 327-43.
Sato, T. N., Y. Qin, et al. (1993). "Tie-1 and tie-2 define another class of putative receptor tyrosine kinase genes expressed in early embryonic vascular system." Proc Natl Acad Sci U S A **90**(20): 9355-8.
Sato, T. N., Y. Tozawa, et al. (1995). "Distinct roles of the receptor tyrosine kinases Tie-1 and Tie-2 in blood vessel formation." Nature **376**(6535): 70-4.
Schlaeger, T. M., S. Bartunkova, et al. (1997). "Uniform vascular-endothelial-cell-specific gene expression in both embryonic and adult transgenic mice." Proc Natl Acad Sci U S A **94**(7): 3058-63.
Schliemann, C., R. Bieker, et al. (2006). "Expression of angiopoietins and their receptor Tie2 in the bone marrow of patients with acute myeloid leukemia." Haematologica **91**(9): 1203-11.
Schrag, J. D., J. J. Bergeron, et al. (2001). "The Structure of calnexin, an ER chaperone involved in quality control of protein folding." Mol Cell **8**(3): 633-44.
Schreinemachers, D. M. and R. B. Everson (1994). "Aspirin use and lung, colon, and breast cancer incidence in a prospective study." Epidemiology **5**(2): 138-46.
Semerad, C. L., M. J. Christopher, et al. (2005). "G-CSF potently inhibits osteoblast activity and CXCL12 mRNA expression in the bone marrow." Blood **106**(9): 3020-7.
Shao, J., T. Fujiwara, et al. (2000). "Overexpression of the wild-type p53 gene inhibits NF-kappaB activity and synergizes with aspirin to induce apoptosis in human colon cancer cells." Oncogene **19**(6): 726-36.
Shaw, J. P., R. Basch, et al. (2004). "Hematopoietic stem cells and endothelial cell precursors express Tie-2, CD31 and CD45." Blood Cells Mol Dis **32**(1): 168-75.

Shaw, P., R. Bovey, et al. (1992). "Induction of apoptosis by wild-type p53 in a human colon tumor-derived cell line." Proc Natl Acad Sci U S A **89**(10): 4495-9.
Sherr, C. J. (1996). "Cancer cell cycles." Science **274**(5293): 1672-7.
Shimkin, M. B. (1955). "Pulmonary tumors in experimental animals." Adv Cancer Res **3**: 223-67.
Shimkin, M. B. and G. D. Stoner (1975). "Lung tumors in mice: application to carcinogenesis bioassay." Adv Cancer Res **21**: 1-58.
Shin, M. K., M. K. Kim, et al. (2008). "A novel collagen-binding peptide promotes osteogenic differentiation via Ca2+/calmodulin-dependent protein kinase II/ERK/AP-1 signaling pathway in human bone marrow-derived mesenchymal stem cells." Cell Signal **20**(4): 613-24.
Shiojima, I. and K. Walsh (2002). "Role of Akt signaling in vascular homeostasis and angiogenesis." Circ Res **90**(12): 1243-50.
Shirakawa, K., M. Shibuya, et al. (2002). "Tumor-infiltrating endothelial cells and endothelial precursor cells in inflammatory breast cancer." Int J Cancer **99**(3): 344-51.
Sidransky, D. and M. Hollstein (1996). "Clinical implications of the p53 gene." Annu Rev Med **47**: 285-301.
Siemeister, G., M. Schirner, et al. (1999). "Two independent mechanisms essential for tumor angiogenesis: inhibition of human melanoma xenograft growth by interfering with either the vascular endothelial growth factor receptor pathway or the Tie-2 pathway." Cancer Res **59**(13): 3185-91.
Sin, D. D., S. F. Man, et al. (2006). "Progression of airway dysplasia and C-reactive protein in smokers at high risk of lung cancer." Am J Respir Crit Care Med **173**(5): 535-9.
Singh, S. K., I. D. Clarke, et al. (2003). "Identification of a cancer stem cell in human brain tumors." Cancer Res **63**(18): 5821-8.
Skliris, G. P., F. Hube, et al. (2008). "Expression of small breast epithelial mucin (SBEM) protein in tissue microarrays (TMAs) of primary invasive breast cancers." Histopathology **52**(3): 355-69.
Slack, J. M. n. W. (2000). "Stem Cells in Epithelial Tissues." Science **287**(5457): 1431-1433.
Slebos, R. J., R. E. Kibbelaar, et al. (1990). "K-ras oncogene activation as a prognostic marker in adenocarcinoma of the lung." N Engl J Med **323**(9): 561-5.
Slebos, R. J. and S. Rodenhuis (1992). "The ras gene family in human non-small-cell lung cancer." J Natl Cancer Inst Monogr(13): 23-9.
Socinski, M. A., D. E. Morris, et al. (2003). "Chemotherapeutic Management of Stage IV Non-small Cell Lung Cancer*
10.1378/chest.123.1_suppl.226S." Chest **123**(1 suppl): 226S-243S.
Soga, M., Y. Kishimoto, et al. (2003). "Spontaneous development of hepatocellular carcinomas in the FLS mice with hereditary fatty liver." Cancer Lett **196**(1): 43-8.
Soltermann, A., V. Tischler, et al. (2008). "Prognostic significance of epithelial-mesenchymal and mesenchymal-epithelial transition protein expression in non-small cell lung cancer." Clin Cancer Res **14**(22): 7430-7.

Song, D. E., S. J. Jang, et al. (2007). "Mucinous bronchioloalveolar carcinoma of lung with a rhabdoid component--report of a case and review of the literature." Histopathology **51**(3): 427-30.
Soria, J. C., H. Y. Lee, et al. (2002). "Lack of PTEN expression in non-small cell lung cancer could be related to promoter methylation." Clin Cancer Res **8**(5): 1178-84.
Sounni, N. E., L. Devy, et al. (2002). "MT1-MMP expression promotes tumor growth and angiogenesis through an up-regulation of vascular endothelial growth factor expression." Faseb J **16**(6): 555-64.
Spira, A., J. Beane, et al. (2004). "Effects of cigarette smoke on the human airway epithelial cell transcriptome." Proc Natl Acad Sci U S A **101**(27): 10143-8.
Spira, A., J. E. Beane, et al. (2007). "Airway epithelial gene expression in the diagnostic evaluation of smokers with suspect lung cancer." Nat Med **13**(3): 361-6.
Srinivasan, S., M. Ohsugi, et al. (2005). "Endoplasmic Reticulum Stress-Induced Apoptosis Is Partly Mediated by Reduced Insulin Signaling Through Phosphatidylinositol 3-Kinase/Akt and Increased Glycogen Synthase Kinase-3{beta} in Mouse Insulinoma Cells
10.2337/diabetes.54.4.968." Diabetes **54**(4): 968-975.
Stadnyk, A. (1994). "Cytokine production by epithelial cells." FASEB J. **8**(13): 1041-1047.
Stripp, B. R., P. L. Sawaya, et al. (1992). "cis-acting elements that confer lung epithelial cell expression of the CC10 gene." J Biol Chem **267**(21): 14703-12.
Stuppia, L., G. Calabrese, et al. (1997). "p53 loss and point mutations are associated with suppression of apoptosis and progression of CML into myeloid blastic crisis." Cancer Genet Cytogenet **98**(1): 28-35.
Subramanian, J. and R. Govindan (2007). "Lung cancer in never smokers: a review." J Clin Oncol **25**(5): 561-70.
Sun, S., J. H. Schiller, et al. (2007). "Lung cancer in never smokers--a different disease." Nat Rev Cancer **7**(10): 778-90.
Sunday, M. E., K. J. Haley, et al. (1999). "Calcitonin driven v-Ha-ras induces multilineage pulmonary epithelial hyperplasias and neoplasms." Oncogene **18**(30): 4336-47.
Suri, C., P. F. Jones, et al. (1996). "Requisite role of angiopoietin-1, a ligand for the TIE2 receptor, during embryonic angiogenesis." Cell **87**(7): 1171-80.
Szabo, E., T. Feng, et al. (2009). "Cell Adhesion and Spreading Affect Adipogenesis From ES Cells: The Role of Calreticulin." Stem Cells.
Takahama, M., M. Tsutsumi, et al. (1999). "Enhanced expression of Tie2, its ligand angiopoietin-1, vascular endothelial growth factor, and CD31 in human non-small cell lung carcinomas." Clin Cancer Res **5**(9): 2506-10.
Takemura, Y., N. Ouchi, et al. (2007). "Adiponectin modulates inflammatory reactions via calreticulin receptor-dependent clearance of early apoptotic bodies." J Clin Invest **117**(2): 375-86.
Takizawa, H. and M. G. Manz (2007). "Macrophage tolerance: CD47-SIRP-[alpha]-mediated signals matter." **8**(12): 1287-1289.

Tanaka, I., O. Matsubara, et al. (1988). "Increasing incidence and changing histopathology of primary lung cancer in Japan. A review of 282 autopsied cases." Cancer **62**(5): 1035-9.
Tanaka, S., K. Sugimachi, et al. (2002). "Tie2 vascular endothelial receptor expression and function in hepatocellular carcinoma." Hepatology **35**(4): 861-7.
Taylor, G., M. S. Lehrer, et al. (2000). "Involvement of follicular stem cells in forming not only the follicle but also the epidermis." Cell **102**(4): 451-61.
Taylor, P. R., A. Carugati, et al. (2000). "A hierarchical role for classical pathway complement proteins in the clearance of apoptotic cells in vivo." J Exp Med **192**(3): 359-66.
Tchou-Wong, K. M., Y. Jiang, et al. (2002). "Lung-specific expression of dominant-negative mutant p53 in transgenic mice increases spontaneous and benzo(a)pyrene-induced lung cancer." Am J Respir Cell Mol Biol **27**(2): 186-93.
Theise, N. D., O. Henegariu, et al. (2002). "Radiation pneumonitis in mice: a severe injury model for pneumocyte engraftment from bone marrow." Exp Hematol **30**(11): 1333-8.
Theise, N. D., M. Nimmakayalu, et al. (2000). "Liver from bone marrow in humans." Hepatology **32**(1): 11-6.
Thiery, J. P. and J. P. Sleeman (2006). "Complex networks orchestrate epithelial-mesenchymal transitions." Nat Rev Mol Cell Biol **7**(2): 131-42.
Timmerman, L. A., N. A. Clipstone, et al. (1996). "Rapid shuttling of NF-AT in discrimination of Ca2+ signals and immunosuppression." Nature **383**(6603): 837-40.
Tirino, V., R. Camerlingo, et al. (2009). "The role of CD133 in the identification and characterisation of tumour-initiating cells in non-small-cell lung cancer." Eur J Cardiothorac Surg **36**(3): 446-53.
Toquet, C., A. Jarry, et al. (2007). "Altered Calreticulin expression in human colon cancer: maintenance of Calreticulin expression is associated with mucinous differentiation." Oncol Rep **17**(5): 1101-7.
Travis, W. D. (2002). "Pathology of lung cancer." Clin Chest Med **23**(1): 65-81, viii.
Travis, W. D., L. B. Travis, et al. (1995). "Lung cancer." Cancer **75**(1 Suppl): 191-202.
Trombetta, E. S. (2003). "The contribution of N-glycans and their processing in the endoplasmic reticulum to glycoprotein biosynthesis." Glycobiology **13**(9): 77R-91R.
Tu, S., G. Bhagat, et al. (2008). "Overexpression of interleukin-1beta induces gastric inflammation and cancer and mobilizes myeloid-derived suppressor cells in mice." Cancer Cell **14**(5): 408-19.
Uvarov, A. V. and N. Mesaeli (2008). "Enhanced ubiquitin-proteasome activity in calreticulin deficient cells: a compensatory mechanism for cell survival." Biochim Biophys Acta **1783**(6): 1237-47.
Valenzuela, D. M., J. A. Griffiths, et al. (1999). "Angiopoietins 3 and 4: diverging gene counterparts in mice and humans." Proc Natl Acad Sci U S A **96**(5): 1904-9.
Van der Wal, F. J., J. D. Oliver, et al. (1998). "The transient association of ERp57 with N-glycosylated proteins is regulated by glucose trimming." Eur J Biochem **256**(1): 51-9.

Van Dyke, A. L., M. L. Cote, et al. (2008). "Regular Adult Aspirin Use Decreases the Risk of Non-Small Cell Lung Cancer among Women." Cancer Epidemiol Biomarkers Prev **17**(1): 148-157.
Vandivier, R. W., C. A. Ogden, et al. (2002). "Role of surfactant proteins A, D, and C1q in the clearance of apoptotic cells in vivo and in vitro: calreticulin and CD91 as a common collectin receptor complex." J Immunol **169**(7): 3978-86.
Vassilopoulos, G., P. R. Wang, et al. (2003). "Transplanted bone marrow regenerates liver by cell fusion." Nature **422**(6934): 901-4.
Vincent, R., S. G. Bjarnason, et al. (1997). "Acute pulmonary toxicity of urban particulate matter and ozone." Am J Pathol **151**(6): 1563-70.
Vincent, R. G., J. W. Pickren, et al. (1977). "The changing histopathology of lung cancer: a review of 1682 cases." Cancer **39**(4): 1647-55.
Virchow, R. (1863). "Cellular Pathology As Based Upon Physiological And Pathological Histology." Philadelphia, JB Lippincott.
Visvader, J. E. and G. J. Lindeman (2008). "Cancer stem cells in solid tumours: accumulating evidence and unresolved questions." Nat Rev Cancer **8**(10): 755-68.
Vogelstein, B. and K. W. Kinzler (1992). "p53 function and dysfunction." Cell **70**(4): 523-6.
Vougas, K., E. Gaitanarou, et al. (2008). "Two-dimensional electrophoresis and immunohistochemical study of calreticulin in colorectal adenocarcinoma and mirror biopsies." J Buon **13**(1): 101-7.
Voynow, J. A., B. M. Fischer, et al. (2004). "Neutrophil elastase induces mucus cell metaplasia in mouse lung." Am J Physiol Lung Cell Mol Physiol **287**(6): L1293-302.
Vu, T. H., J. M. Shipley, et al. (1998). "MMP-9/gelatinase B is a key regulator of growth plate angiogenesis and apoptosis of hypertrophic chondrocytes." Cell **93**(3): 411-22.
Wagers, A. J., R. I. Sherwood, et al. (2002). "Little evidence for developmental plasticity of adult hematopoietic stem cells." Science **297**(5590): 2256-9.
Wakamatsu, N., T. R. Devereux, et al. (2007). "Overview of the molecular carcinogenesis of mouse lung tumor models of human lung cancer." Toxicol Pathol **35**(1): 75-80.
Walker, S. R., M. C. Williams, et al. (1986). "Immunocytochemical localization of the major surfactant apoproteins in type II cells, Clara cells, and alveolar macrophages of rat lungs." J. Histochem. Cytochem. **34**: 1137–1148.
Walser, T., X. Cui, et al. (2008). "Smoking and lung cancer: the role of inflammation." Proc Am Thorac Soc **5**(8): 811-5.
Wang, J., K. Wu, et al. (2005). "Expressions and clinical significances of angiopoietin-1, -2 and Tie2 in human gastric cancer." Biochem Biophys Res Commun **337**(1): 386-93.
Wang, W., H. Y. Wang, et al. (2007). "[Expression of CD133 in bone marrow cells of patients with leukemia and myelodysplastic syndrome]." Zhongguo Shi Yan Xue Ye Xue Za Zhi **15**(3): 470-3.
Wang, Y., Z. Zhang, et al. (2006). "A mouse model for tumor progression of lung cancer in ras and p53 transgenic mice." Oncogene **25**: 1277–1280.

Ward, D. G., N. Suggett, et al. (2006). "Identification of serum biomarkers for colon cancer by proteomic analysis." Br J Cancer **94**(12): 1898-905.
Ware, L. B., Matthay, M.A. (2002). "Keratinocyte and hepatocyte growth factors in the lung: roles in lung development, inflammation, and repair." Am. J. Physiol. Lung Cell. Mol.Physiol. **282**: L924–40.
Waterhouse, N. J. and M. J. Pinkoski (2007). "Calreticulin: raising awareness of apoptosis." Apoptosis **12**(4): 631-4.
Weihua, Z., R. Tsan, et al. (2005). "Apoptotic cells initiate endothelial cell sprouting via electrostatic signaling." Cancer Res **65**(24): 11529-35.
Weiss, S. J. and A. Slivka (1982). "Monocyte and granulocyte-mediated tumor cell destruction. A role for the hydrogen peroxide-myeloperoxidase-chloride system." J Clin Invest **69**(2): 255-62.
Wert, S. E., S. W. Glasser, et al. (1993). "Transcriptional elements from the human SP-C gene direct expression in the primordial respiratory epithelium of transgenic mice." Dev Biol **156**(2): 426-43.
White, T. K., Q. Zhu, et al. (1995). "Cell surface calreticulin is a putative mannoside lectin which triggers mouse melanoma cell spreading." J Biol Chem **270**(27): 15926-9.
Whitsett, J. A., S. W. Glasser, et al. (2001). "Transgenic models for study of lung morphogenesis and repair: Parker B. Francis lecture." Chest **120**(1 Suppl): 27S-30S.
Wikenheiser, K. A., J. C. Clark, et al. (1992). "Simian virus 40 large T antigen directed by transcriptional elements of the human surfactant protein C gene produces pulmonary adenocarcinomas in transgenic mice." Cancer Res **52**(19): 5342-52.
Wikenheiser, K. A. and J. A. Whitsett (1997). "Tumor progression and cellular differentiation of pulmonary adenocarcinomas in SV40 large T antigen transgenic mice." Am J Respir Cell Mol Biol **16**(6): 713-23.
Wilhelm, D. L. (1973). "Mechanisms responsible for increased vascular permeability in acute inflammation." Agents Actions **3**(5): 297-306.
Wistuba, II (2007). "Genetics of preneoplasia: lessons from lung cancer." Curr Mol Med **7**(1): 3-14.
Wistuba, II, J. Berry, et al. (2000). "Molecular changes in the bronchial epithelium of patients with small cell lung cancer." Clin Cancer Res **6**(7): 2604-10.
Wistuba, II, S. Lam, et al. (1997). "Molecular damage in the bronchial epithelium of current and former smokers." J Natl Cancer Inst **89**(18): 1366-73.
Wong, C. J., J. Akiyama, et al. (1996). "Localization and developmental expression of surfactant proteins D and A in the respiratory tract of the mouse." Pediatr. Res **39**: 930–937.
Worthley, D. L., A. Ruszkiewicz, et al. (2009). "Human gastrointestinal neoplasia-associated myofibroblasts can develop from bone marrow-derived cells following allogeneic stem cell transplantation." Stem Cells **27**(6): 1463-8.
Wright, D. E., A. J. Wagers, et al. (2001). "Physiological migration of hematopoietic stem and progenitor cells." Science **294**(5548): 1933-6.
Wright, J. R. (2003). "Pulmonary surfactant: a front line of lung host defense." J Clin Invest **111**(10): 1453-5.
Wright, J. R. (2004). "Immunoregulatory function of surfactant proteins." Nature **5**: 58-68.

Wu, M., H. Massaeli, et al. (2007). "Differential expression and activity of matrix metalloproteinase-2 and -9 in the calreticulin deficient cells." Matrix Biol **26**(6): 463-72.
Wu, Y., J. Deng, et al. (2009). "Stabilization of snail by NF-kappaB is required for inflammation-induced cell migration and invasion." Cancer Cell **15**(5): 416-28.
Wynder, E. L. and E. A. Graham (1950). "Tobacco smoking as a possible etiologic factor in bronchiogenic carcinoma; a study of 684 proved cases." J Am Med Assoc **143**(4): 329-36.
Xiao, F., Y. Wei, et al. (2002). "A gene therapy for cancer based on the angiogenesis inhibitor, vasostatin." Gene Ther **9**(18): 1207-13.
Xiao, G., T. F. Chung, et al. (1999). "Calreticulin is transported to the surface of NG108-15 cells where it forms surface patches and is partially degraded in an acidic compartment." J Neurosci Res **58**(5): 652-62.
Xiao, G., T. F. Chung, et al. (1999). "KDEL proteins are found on the surface of NG108-15 cells." Brain Res Mol Brain Res **72**(2): 121-8.
Xu, M., E. Bruno, et al. (2005). "Constitutive mobilization of CD34+ cells into the peripheral blood in idiopathic myelofibrosis may be due to the action of a number of proteases." Blood **105**(11): 4508-15.
Yamada, M., H. Kubo, et al. (2004). "Bone marrow-derived progenitor cells are important for lung repair after lipopolysaccharide-induced lung injury." J Immunol **172**(2): 1266-72.
Yanagi, S., H. Kishimoto, et al. (2007). "Pten controls lung morphogenesis, bronchioalveolar stem cells, and onset of lung adenocarcinomas in mice." J Clin Invest **117**(10): 2929-40.
Yao, L., S. E. Pike, et al. (2002). "Laminin binding to the calreticulin fragment vasostatin regulates endothelial cell function." J Leukoc Biol **71**(1): 47-53.
Yasuda, H., N. Shima, et al. (1998). "Osteoclast differentiation factor is a ligand for osteoprotegerin/osteoclastogenesis-inhibitory factor and is identical to TRANCE/RANKL." Proc Natl Acad Sci U S A **95**(7): 3597-602.
Yin, A. H., S. Miraglia, et al. (1997). "AC133, a novel marker for human hematopoietic stem and progenitor cells." Blood **90**(12): 5002-12.
Yonish-Rouach, E., D. Resnitzky, et al. (1991). "Wild-type p53 induces apoptosis of myeloid leukaemic cells that is inhibited by interleukin-6." Nature **352**(6333): 345-7.
Yoon, G.-S., H. Lee, et al. (2000). "Nuclear Matrix of Calreticulin in Hepatocellular Carcinoma." Cancer Res **60**(4): 1117-1120.
You, M. and G. Bergman (1998). "Preclinical and clinical models of lung cancer chemoprevention." Hematol Oncol Clin North Am **12**(5): 1037-53.
You, M., Y. Wang, et al. (1992). "Parental bias of Ki-ras oncogenes detected in lung tumors from mouse hybrids." Proc Natl Acad Sci U S A **89**(13): 5804-8.
Yu, L. R., R. Zeng, et al. (2000). "Identification of differentially expressed proteins between human hepatoma and normal liver cell lines by two-dimensional electrophoresis and liquid chromatography-ion trap mass spectrometry." Electrophoresis **21**(14): 3058-68.
Yu, Y., J. Varughese, et al. (2001). "Increased Tie2 expression, enhanced response to angiopoietin-1, and dysregulated angiopoietin-2 expression in hemangioma-derived endothelial cells." Am J Pathol **159**(6): 2271-80.

Zadeh, G., B. Qian, et al. (2004). "Targeting the Tie2/Tek receptor in astrocytomas." Am J Pathol **164**(2): 467-76.
Zakowski, M. F. (2003). "Pathology of small cell carcinoma of the lung." Semin Oncol **30**(1): 3-8.
Zhang, J., C. Niu, et al. (2003). "Identification of the haematopoietic stem cell niche and control of the niche size." Nature **425**(6960): 836-41.
Zhang, K., N. Li, et al. (2007). "High expression of nuclear factor of activated T cells in Chinese primary non-small cell lung cancer tissues." Int J Biol Markers **22**(3): 221-5.
Zhao, M., B. Song, et al. (2006). "Electrical signals control wound healing through phosphatidylinositol-3-OH kinase-gamma and PTEN." Nature **442**(7101): 457-60.
Zheng, D., A. M. Bode, et al. (2008). "The cannabinoid receptors are required for ultraviolet-induced inflammation and skin cancer development." Cancer Res **68**(10): 3992-8.
Zhou, G., H. Li, et al. (2005). "Proteomic analysis of global alteration of protein expression in squamous cell carcinoma of the esophagus." Proteomics **5**(14): 3814-21.
Zhu, N., E. B. Pewitt, et al. (1998). "Calreticulin: an intracellular Ca++-binding protein abundantly expressed and regulated by androgen in prostatic epithelial cells." Endocrinology **139**(10): 4337-44.
Zhu, N. and Z. Wang (1999). "Calreticulin expression is associated with androgen regulation of the sensitivity to calcium ionophore-induced apoptosis in LNCaP prostate cancer cells." Cancer Res **59**(8): 1896-902.